

**From human genetics to radiobiology:
in vitro radiosensitivity in individuals with a germline
defect in DNA damage response genes.**

Annelot BAERT

2017

Promotor: Prof. dr. Anne Vral

Co-promotor: Prof. dr. Ir. Kathleen Claes

**Thesis submitted in fulfilment of the requirement for the degree of
DOCTOR IN HEALTH SCIENCES**

**Department of Basic Medical Sciences
Faculty of Medicine and Health Sciences**

Cover Picture: Picture of the majestic spiral staircase with impressive light fixture at Heal's
(Tottenham Court Road, London, UK) © Simon Syon – Simon & His Camera

Ghent University

Faculty of Medicine and Health Sciences
Department of Basic Medical Sciences
Research group: Radiobiology

Supervisors

Prof. dr. Anne Vral

Prof. dr. Ir. Kathleen Claes

Prof. dr. Hubert Thierens

dr. Kim De Leeneer

Examination Board

Chairman: Prof. dr. Elfride De Baere¹

Prof. dr. Ir. Ans Baeyens¹

dr. Elke Decrock¹

Dr. Filomeen Haerynck¹

Prof. Dr. Jacques De Greve²

Dr. Ir. Rien Blok³

dr. Roel Quintens⁴

¹Ghent University, Ghent, Belgium

²University Hospital Brussel, Jette, Belgium

³Maastricht University medical hospital,
Maastricht, The Netherlands

⁴Belgian Nuclear Research Centre, Mol, Belgium

Research institute

Ghent University
Faculty of Medicine and Health Sciences
Department of Basic Medical Sciences
De Pintelaan 185, 6B3
B-9000 Ghent
Tel: 09 332 51 35



DANKWOORD

Het is zover, mijn doctoraatsdagen zijn geteld!

Het was een unieke beproeving en eerlijkheid gebied mij te bekennen dat ik deze bijzondere uitdaging enkel tot een goed einde kon brengen dankzij vele helpende handen en een grote portie onvoorwaardelijke steun.

Vooreerst gaat mijn dankbaarheid uit naar *Professor Vral*. Anne, je gaf me de mogelijkheid te doctoreren en stond geduldig aan mijn zijde gedurende het hele proces. Bedankt voor jouw wetenschappelijke inbreng en bedankt om mijn papers en thesis talloze keren na te lezen. Jouw deur stond steeds open en ik ben menigmaal binnen gevallen met vragen.

Professor Claes, Kathleen, dankzij jouw samenwerking met Anne kon ik werken aan een boeiend project dat mijn interesse voor genetica en straling combineert. Bedankt om mijn enthousiasme voor de genetica verder te stimuleren en bedankt voor jouw input in de vergaderingen, de papers en de thesis.

Ook de leden van de begeleidingscommissie wil ik bedanken. *Professor Thierens*, bedankt om uw grenzeloze vakkennis met mij te delen. Kim, je wist me telkens weer uit te dagen om het onderzoek nog beter aan te pakken en de papers nog sterker te schrijven. Bedankt – ook al durfde ik er weleens om te vloeken, maar dat hoeft je niet persoonlijk te nemen!

Dit onderzoek was niet mogelijk zonder de talloze bloeddonaties, zowel van gezonde vrijwilligers als *test-individuen*. Mijn oprechte dank gaat uit naar iedereen die een bloedstaaltje doneerde in naam van de wetenschap. Daarbij wil ik ook het team van artsen, verpleegkundigen en administratieve medewerkers van het CMGG bedanken.

Julie, strijdgenoot van het eerste uur. Bedankt om mij de kneepjes van het wetenschappelijke werk bij te brengen. Bedankt om steeds met me mee te denken over nieuwe experimenten en niet de andere kant uit te kijken wanneer ik hulp nodig had om bestralingen op een ontielig vroeg uur af te werken. Maar vooral, bedankt voor de vele babbels tussendoor en de onvergetelijke ervaringen op congressen. Het was een plezier met jou samen te werken!

Veerle en Charlot, elk op jullie manier – was het aan het begin of op het einde – hebben jullie je steentje bijgedragen aan mijn doctoraat. Bedankt om me de nuances van wetenschappelijk onderzoek bij te brengen. Charlot, samen met Julie beleefden we een wetenschappelijk en cultureel hoogtepunt op congres in Kyoto, Japan. Bedankt om mij te vergezellen tijdens dit avontuur.

Mattias, Jeroen, Greet, Flavia, Annelies, Charlot, Lise, Bram en Stefanie, mijn bondgenoten. Bedankt om me scherp te houden, maar ook bedankt voor *peptalks* en de *off topic* gesprekken – de boog kan immers niet steeds gespannen staan. Zoals jullie al weten, of nog zullen ontdekken, is het doctoraatschap een rollercoaster en ik wens jullie veel succes bij wat komen zal!

Leen, Johanna, Greet, Toke en Ilse, vele handen maken licht werk... Bedankt voor het bijspringen bij tal van experimenten, het opsnorren van data en de vele leuke babbels.

Heidi, Chris, Ans en Ria, bedankt voor jullie interesse in mijn onderzoek en de luchtige conversaties tijdens de lunch.

Ans, bedankt voor jouw input tijdens de vele *radiobiologische* vergaderingen.

Gedurende dit onderzoek heb ik met veel plezier master en bachelor studenten begeleid en geïntroduceerd in de wondere wereld van wetenschappelijk onderzoek. Joske, Dieter, Tessa, Sara en Fede, bedankt voor jullie hulp bij het vele labowerk. Ik was bijwijlen streng, maar leerde tegelijkertijd ook bij door jullie input en vragen.

Aan mijn vrienden: bedankt om steeds oprecht geïnteresseerd te vragen hoe het met mijn doctoraat gaat, maar vooral bedankt om me te laten beseffen dat er ook buiten dit doctoraat een hele wereld te ontdekken valt.

Aan de treinmadammen: bedankt om telkens weer mijn frustraties te aanhoren en deze te counteren met een luchtige noot!

Een bijzonder woord van dank gaat uit naar mijn familie en schoonfamilie. Bedankt voor jullie interesse in mijn werk. En ook al hadden sommige onder jullie niet echt een concreet idee van hoe ik mijn dagen in het labo spendeerde, ik kon steeds op jullie steun rekenen.

Bedankt mama en papa, jullie hebben me steeds gesteund bij mijn studies en in deze uitdaging. Ook op het einde, wanneer de loodjes het zwaarst wegen, kon ik op jullie enthousiasme rekenen voor het regelen van de receptie.

Bedankt ook aan mijn grootouders, jullie hebben me mee grootgebracht tot de persoon die ik nu ben.

Mijn laatste woord van dank gaat uit naar Jens.

Eén huis, één verlovingsring, één kat, één hond en één doctoraatstitel later sta je nog steeds aan mijn zijde. Liefje, je bent mijn rustpunt en weet me ook steeds aan het lachen te brengen. Ik had dit doctoraat nooit tot een goed einde kunnen brengen zonder jouw onvoorwaardelijke steun. Weet dat ik fier ben jouw verloofde te zijn!

Op naar het volgende avontuur!

Annelot

7 mei 2017

PS. Liefje, ik heb het nogal druk gehad de laatste tijd, maar ik beloof plechtig meer tijd voor jou vrij te maken en zal het woord *doctoraat* een maand lang niet meer uitspreken.

SUMMARY	4
SAMENVATTING	6
ACRONYMS	8
PART I: INTRODUCTION	11
1 BREAST CANCER	12
1.1 BREAST TISSUE AND BREAST CANCER	12
1.2 INCIDENCE AND MORTALITY – ALARMING FIGURES	13
1.3 RISK FACTORS	15
1.4 HEREDITARY BREAST CANCER DUE TO GERMLINE MUTATION IN “BREAST CANCER GENES”	17
1.4.1 High risk breast cancer genes	18
1.4.1.1 <i>BRCA1</i>	18
1.4.1.2 <i>BRCA2</i>	20
1.4.1.3 <i>PALB2</i>	20
1.4.1.4 Associated risks	20
1.4.1.5 Risk reducing surgeries in high risk individuals	22
1.4.2 Moderate risk genes - ATM as an example	23
1.4.3 Breast cancer gene panels	24
1.4.4 Deleterious germline mutations versus Variants of Unknown Clinical Significance	25
1.5 BREAST CANCER SCREENING	28
1.5.1 Population screening	29
1.5.2 Breast cancer screening in individuals at high risk	29
1.6 BREAST CANCER TREATMENT	31
2 IONIZING RADIATION	33
2.1 WHAT IS IONIZING RADIATION?	33
2.2 RADIATION-INDUCED DAMAGE	34
2.3 HEALTH EFFECTS OF EXPOSURE TO IONIZING RADIATION	36
2.3.1 Exposure to ionizing radiation	36
2.3.2 Health effects of ionizing radiation	36
2.3.3 Radiosensitivity	39

3	DNA DAMAGE RESPONSE	41
3.1	DNA DAMAGE RESPONSE	41
3.2	CELL CYCLE & CELL CYCLE CHECKPOINTS	42
3.2.1	The cell cycle	42
3.2.2	Cell cycle checkpoints	45
3.2.3	BRCA1 in cell cycle checkpoint arrest	48
3.3	REPAIR OF RADIATION-INDUCED DSB	48
3.3.1	Detection and signaling of a DNA double strand break	48
3.3.2	Pathways for the repair of radiation-induced DSB	50
3.3.2.1	Non-homologous end- joining	50
3.3.2.2	Homologous recombination	51
3.3.2.3	Alternative DSB repair pathways	54
3.3.2.4	PARP activity and inhibition – A breast cancer targeted therapy	57
3.3.3	Pathway choice for repair of radiation-induced DSB	60
3.3.3.1	Cell cycle phase	60
3.3.3.2	Complexity of the DSB	62
3.3.3.3	Chromatin structure	63
3.4	EXTENSIVE DNA DAMAGE AND CELL DEATH	63
4	RADIOSENSITIVITY OF <i>BRCA1</i> AND <i>BRCA2</i> MUTATION CARRIERS	66
4.1	CLINICAL STUDIES	66
4.2	IN VITRO RADIOSENSITIVITY TESTING	67
4.2.1	Chromosomal radiosensitivity	67
4.2.2	Homologous recombination testing	68
5	ASSAYS TO MEASURE RADIATION-INDUCED DNA DAMAGE	69
5.1	MICRONUCLEUS ASSAY	69
5.1.1	What are MN?	69
5.1.2	The cytokinesis block micronucleus assay and its applications	70
5.1.2.1	The G0 CBMN assay for lymphocytes	71
5.1.2.2	The G2 CBMN assay for lymphocytes	72
5.2	RAD51 FOCI ASSAY	73
6	AIM OF THIS THESIS	75
7	REFERENCES	77

PART II: ORIGINAL RESEARCH	87
OUTLINE OF THE RESEARCH	88
PAPER I: VARIANT ATAXIA TELANGIECTASIA: CLINICAL AND MOLECULAR FINDINGS AND EVALUATION OF RADIOSENSITIVE PHENOTYPES IN A PATIENT AND RELATIVES	92
PAPER II: INCREASED CHROMOSOMAL RADIOSENSITIVITY IN ASYMPTOMATIC CARRIERS OF A HETEROZYGOUS <i>BRCA1</i> MUTATION	116
PAPER III: ANALYSIS OF CHROMOSOMAL RADIOSENSITIVITY OF HEALTHY <i>BRCA2</i> MUTATION CARRIERS AND NON-CARRIERS IN <i>BRCA</i> FAMILIES WITH THE G2 MICRONUCLEUS ASSAY.	144
PAPER IV: THE RAD51 FOCI ASSAY FOR THE DETECTION OF IMPAIRED HOMOLOGOUS RECOMBINATION IN SYNCHRONIZED AND IRRADIATED MCF10A CELLS WITH A <i>BRCA1</i> OR <i>BRCA2</i> KNOCKDOWN	162
PAPER V: THOROUGH <i>IN SILICO</i> AND <i>IN VITRO</i> cDNA ANALYSIS OF 21 PUTATIVE <i>BRCA1/2</i> SPLICE VARIANTS AND IDENTIFICATION OF ACTIVATED CRYPTIC SPLICE DONOR SITES IN EXON 11 OF <i>BRCA2</i>	182
PART III: GENERAL DISCUSSION	211
1 RADIOSENSITIVITY TESTING	212
1.1 THE G2 MICRONUCLEUS ASSAY	212
1.1.1 Development of the G2 micronucleus assay	212
1.1.2 Validation of the G2 MN assay in an AT patient and its application in heterozygous ATM mutation carriers	217
1.1.3 Chromosomal radiosensitivity measured by the G2 MN assay in a cohort of <i>BRCA1</i> and <i>BRCA2</i> mutation carriers	218
1.1.4 Chromosomal radiosensitivity measured by the G2 MN assay in non-carriers	224
1.1.5 G2 MN assay for individual assessment of radiosensitivity	225
1.2 THE RAD51 FOCI ASSAY TO ASSESS RADIOSENSITIVITY IN CELLS WITH REDUCED <i>BRCA1</i> AND <i>BRCA2</i> PROTEIN LEVELS	228
1.3 THE CARCINOGENIC RISK OF MEDICAL EXPOSURE TO IR OF <i>BRCA1</i> AND <i>BRCA2</i> MUTATION CARRIERS	232
1.4 CHOOSING THE APPROPRIATE ASSAY TO EVALUATE INDIVIDUAL RADIOSENSITIVITY	237
1.5 LIMITATION OF THE USE OF LYMPHOCYTES FOR ANALYSIS OF INDIVIDUAL RADIOSENSITIVITY	238
2 cDNA ANALYSIS OF PUTATIVE SPLICE SITE VARIANTS	240
2.1 ABERRANT SPLICING AND ACCURACY OF <i>IN SILICO</i> PREDICTION TOOLS	240
2.2 ABERRANT SPLICING, PATHOGENICITY ASSESSMENT AND FUNCTIONAL ANALYSIS	241
3 GENERAL CONCLUSION	245
4 REFERENCES	246

SUMMARY

All currently known high to intermediate risk “breast cancer genes”, including *BRCA1* and *BRCA2*, are involved in the DNA damage response pathway. Heterozygous germline mutations in these genes predispose to breast and ovarian cancer. In addition, such mutations may also result in enhanced radiosensitivity mediated by chromosomal instability after exposure to ionizing radiation, leading to a higher risk to develop radiation-induced breast cancer. However, results of currently available clinical studies evaluating carcinogenesis and *in vitro* studies comparing chromosomal radiosensitivity in mutation carriers and non-carriers are inconclusive. Nevertheless, insights into the radiosensitive phenotype of healthy tissues of mutation carriers is of the utmost importance for the safe use of ionizing radiation for diagnostic purposes or radiotherapy treatment. In this thesis, we evaluated *in vitro* radiosensitivity in carriers of a mutation in DNA damage response genes by means of two different assays.

The first assay, the G2 micronucleus assay, is a cytogenetic assay in which MN are analyzed in cells irradiated in the G2 phase of the cell cycle. This assay was developed to evaluate radiosensitivity in cells with a heterozygous *BRCA1* or *BRCA2* mutation. *BRCA1* and *BRCA2* have a function in homologous recombination (HR), the main DNA double strand break repair pathway activated in late S and G2 phase of the cell cycle. Furthermore, *BRCA1* is also involved in the G2/M cell cycle checkpoint. The G2 micronucleus assay allows evaluation of both functions by means of two distinct endpoints: (1) the radiation-induced micronucleus yield, which reflects DNA double strand break repair capacity and (2) the G2/M checkpoint efficiency ratio, which allows evaluation of the G2 arrest capacity.

Before applying the G2 micronucleus assay on *BRCA* mutation carriers, the assay was validated in a patient with Ataxia Telangiectasia (AT). AT patients are characterized by a manifest increased radiosensitivity. AT patients show biallelic inactivation of *ATM*, involved in both DNA double strand break repair by means of HR and G2/M checkpoint activation. We demonstrated a severely increased radiosensitivity with both endpoints when applying the G2 micronucleus assay in lymphocytes of this AT patient. In lymphocytes of healthy relatives with a heterozygous *ATM* mutation the radiosensitivity observed with this assay was intermediate between the AT patient and the control cohort.

When applying the G2 micronucleus assay on lymphocytes of healthy *BRCA1/2* mutation carriers, we demonstrated significantly enhanced radiation-induced MN yields in both *BRCA1* and *BRCA2* germline mutation carriers, pointing to an impaired DNA double strand break repair capacity in both groups. Furthermore, an impaired G2 arrest capacity was observed in *BRCA1* mutation carriers. In healthy relatives who did not inherit the familial mutation, no enhanced radiosensitivity was observed. Although a significantly enhanced radiosensitivity was demonstrated for the cohort of *BRCA1* and *BRCA2* mutation carriers compared to the

control cohort, individual radiosensitivity evaluation was less straightforward due to overlap in micronucleus yields between both cohorts. Therefore, a scoring system to evaluate individual radiosensitivity was implemented.

As both *BRCA1* and *BRCA2* are involved in HR, we evaluated if the accumulation of RAD51, a key protein involved in this pathway, at the double strand break site can be used to assess HR functionality and radiosensitivity. To this end, a radiation-induced RAD51 foci assay was optimized in a breast epithelial cell line (MCF10A) expressing $\pm 50\%$ reduced *BRCA1* and *BRCA2* protein levels, obtained by RNA interference. RAD51 foci were analyzed in cells synchronized in S phase by aphidicolin as HR is upregulated during this phase of the cell cycle. We demonstrated significantly reduced RAD51 foci formation, and thus impaired HR capacity, in response to the induction of radiation-induced double strand breaks in the *BRCA* knockdown cells compared to control cells. As no overlap in RAD51 foci distribution is observed between knockdown and control cells, we think that this assay could better differentiate between normal cells and cells with a heterozygous *BRCA1* or *BRCA2* mutation than the G2 micronucleus assay. This will be further explored in synchronized lymphocytes of heterozygous germline mutation carriers.

In addition to the detection of unequivocal deleterious mutations in *BRCA1* and *BRCA2*, , variants of unknown clinical significance (VUS) are detected during diagnostic screening. The associated breast cancer risk is unknown, which creates a challenge for genetic counselling. mRNA analysis to assess variants that might impair proper RNA splicing, a highly regulated process, are widely used. We evaluated the outcome at cDNA level of 21 putative splicing variants in *BRCA1* and *BRCA2* and demonstrated aberrant splicing for 12 variants, suggesting that these are likely pathogenic. Furthermore, we demonstrated that *in silico* prediction tools might assist in the evaluation of these putative splicing variants. However, further optimization is warranted to allow reliable application outside the highly conserved consensus splice sites.

The results obtained in this thesis may indicate that care should be taken when applying ionizing radiation for diagnostic or therapeutic purposes in individuals with a germline mutation in *BRCA1* or *BRCA2* as they may be at higher risk of developing radiation-induced breast cancer.

SAMENVATTING

Alle tot op heden gekende borstkanker predispositie genen, inclusief *BRCA1* en *BRCA2*, zijn betrokken bij het herstel van DNA schade. Individuen met een kiembaan mutatie in deze genen hebben dus niet alleen een hoger risico op het ontwikkelen van borstkanker, ze worden mogelijks ook gekenmerkt door een verhoogde stralingsgevoeligheid gelinkt aan chromosomale instabiliteit; daardoor is de kans op het ontwikkelen van een stralingsgeïnduceerde tumor voor deze individuen eventueel groter. Echter, klinische studies die carcinogenese evalueren in mutatie dragers of *in vitro* studies die de chromosomale stralingsgevoeligheid in de aanwezigheid van een mutatie nagaan na blootstelling aan ioniserende straling kunnen dit niet éénduidig bevestigen of weerleggen. Het is evenwel cruciaal om de stralingsgevoeligheid van gezonde weefsels in mutatiedragers te evalueren voor het veilig gebruik van ioniserende straling in diagnostische of therapeutische setting. In deze thesis wordt de *in vitro* stralingsgevoeligheid van mutatiedragers in kaart gebracht aan de hand van twee verschillende testen.

De eerste test, de G2 micronucleus assay, is een cytogenetische test waarbij micronuclei worden geanalyseerd in cellen bestraald in de G2 fase van de celcyclus. Deze test werd ontwikkeld voor de evaluatie van de stralingsgevoeligheid in lymfocyten met een heterozygote, inactiverende mutatie in *BRCA1* of *BRCA2*. *BRCA1* en *BRCA2* zijn immers beiden betrokken in homologe recombinatie (HR), een belangrijke pathway voor het herstellen van DNA dubbelstrengbreuken. Deze pathway is vooral actief in de late S en G2 fase van de celcyclus. Daarenboven is *BRCA1* ook betrokken in de activatie van de G2/M celcyclus checkpoint. De G2 micronucleus assay maakt het mogelijk om beide functies te evalueren door middel van 2 unieke eindpunten: (1) de stralingsgeïnduceerde micronucleus opbrengst, dewelke de DNA dubbelstrengbreuk herstelcapaciteit in kaart brengt en (2) de G2/M checkpoint efficiëntie ratio, een ratio die de G2 arrest capaciteit reflecteert.

Alvorens deze assay werd toegepast op lymfocyten van *BRCA* mutatiedragers, werd de assay gevalideerd in een patiënt met Ataxia Telangiectasia (AT). AT patiënten worden immers gekenmerkt worden door een uitgesproken verhoogde stralingsgevoeligheid. Daarenboven is *ATM*, het gen gemuteerd in deze patiënten, net als *BRCA1* en *BRCA2*, betrokken in DNA dubbelstrengbreuk herstel en G2/M checkpoint activatie. Bij de AT patiënt werd een sterk verhoogde stralingsgevoeligheid waargenomen met beide eindpunten van de G2 micronucleus assay. Verder werd ook vastgesteld met deze test dat familieleden met een heterozygote *ATM* mutatie een verhoogde stralingsgevoeligheid vertoonden, intermediair tussen de AT patiënt en de controle groep.

Wanneer de G2 micronucleus assay werd toegepast op lymfocyten van gezonde *BRCA* mutatiedragers, werd een significant verhoogde micronucleus waarde gedetecteerd, wat wijst op een verminderde DNA dubbelstrengbreuk herstel capaciteit voor zowel *BRCA1* als

BRCA2 mutatie dragers. Daarnaast, werd ook aangetoond dat lymfocyten van *BRCA1* mutatie dragers een verminderde G2 arrest capaciteit bezitten. Familieleden die de familiale mutatie niet dragen, vertoonden geen verhoogde stralingsgevoeligheid. Hoewel een significante verhoogde stralingsgevoeligheid voor mutatie dragers ten opzichte van een controlegroep werd bevestigd, bleek het niet mogelijk om op individueel niveau stralingsgevoeligheid bij *BRCA1* als *BRCA2* mutatie dragers eenduidig te evalueren door overlap in micronucleus waarden tussen beide groepen. Daarom werd een scoring systeem ontwikkeld voor de bepaling van de individuele stralingsgevoeligheid.

Aangezien zowel *BRCA1* en *BRCA2* betrokken zijn in HR, werd nagegaan of de accumulatie van RAD51, een belangrijk eiwit voor deze pathway, ter hoogte van de DNA dubbelstrengbreuken gebruikt kan worden om HR activatie en stralingsgevoeligheid te evalueren. Hiervoor werd een stralingsgeïnduceerde RAD51 foci assay geoptimaliseerd in een borstepitheel cellijn (MCF10A) met $\pm 50\%$ gereduceerde *BRCA1* en *BRCA2* eiwit niveaus. RAD51 foci werden geanalyseerd in cellen gesynchroniseerd in S fase. We demonstreerden dat gesynchroniseerde MCF10A cellen met een gereduceerd *BRCA1* of *BRCA2* eiwit niveau een significant lager aantal stralingsgeïnduceerde RAD51 foci vertoonden in vergelijking met de controle cellijn, wat wijst op een gedaalde HR functionaliteit. Daarenboven werd geen overlap geobserveerd tussen de distributies van RAD51 foci in controle cellen en cellen met een reductie in *BRCA1* of *BRCA2* eiwit. Dit laat vermoeden dat deze assay een betere discriminatie tussen normale cellen en cellen met een heterozygote *BRCA1/2* mutatie zou kunnen toelaten in vergelijking met de G2 micronucleustest. Dit zal verder onderzocht worden in gesynchroniseerde lymfocyten van heterozygote kiembaan mutatie dragers.

Naast de identificatie van pathogene mutaties in *BRCA1* en *BRCA2*, die aanleiding geven tot een verhoogd risico op borstkanker, worden er tijdens mutatie screening ook varianten van ongekende significantie gedetecteerd. Aangezien het onduidelijk is of deze varianten geassocieerd zijn met een verhoogd borstkanker risico wordt adequate genetische counseling in personen met zo'n variant sterk bemoeilijkt. mRNA analyse om de impact van deze varianten op correcte mRNA splicing, een sterk geconserveerd proces, na te gaan, is een strategie om de pathogeniciteit van deze varianten te evalueren. In deze thesis werd het effect op cDNA niveau van 21 potentiële splice site varianten in *BRCA1* en *BRCA2* nagegaan. Voor 12 varianten werd aberrante splicing – en dus een potentieel pathogeen effect – bewezen. Verder toonden we aan dat *in silico* predictie tools, verdere optimalisatie vergen om deze adequaat te kunnen aanwenden om het effect op splicing van varianten gelegen buiten de sterk geconserveerde splice sites adequaat te kunnen voorspellen.

De resultaten voorgesteld in deze thesis tonen aan dat er best omzichtig wordt omgesprongen met de blootstelling van *BRCA1* en *BRCA2* mutatie dragers aan ioniserende straling voor diagnostische en therapeutische doeleinden.

ACRONYMS

53BP1	tumor suppressor p53-binding protein 1
AA	amino acid
alt-EJ	alternative end joining
AT	ataxia telangiectasia
ATM	ataxia telangiectasia mutated
ATR	ataxia telangiectasia related
b-NHEJ	backup non-homologous end joining
BARD1	BRCA1 associated RING domain 1
BER	base excision repair
BIR	break-induced replication
BLM	bloom syndrome protein
BN	binucleated
BRCA1	breast cancer early onset 1
BRCA2	breast cancer early onset 2
c-NHEJ	classical non-homologous end joining
CDC	cell-division cycle protein
CDK	cyclin dependent kinase
cDNA	complementary DNA
CI	confidence interval
CHEK2	checkpoint kinase 2 (gene)
CHK2	checkpoint kinase 2 (protein)
CtIP	ctPB-interacting protein
Cyto B	cytochalasin B
DDR	DNA damage response
DNA	deoxyribonucleic acid
DNA-PKcs	DNA-dependent protein kinase, catalytic subunit
DSB	double strand break
DSBR	double strand break repair
DSE	single-ended DSB
EMA	European Medicines Agency
ER	estrogen receptor
ERR	excess relative risk
ESE	exonic splicing enhancer
ESS	exonic splicing silencer
Exo	exonuclease
FA	fanconi anemia
FANC	fanconi anemia complementary group
FDA	American food and drugs administration
FISH	fluorescent in situ hybridization
Gy	gray

H2AX	H2A histone family member X
HER2	human epidermal growth factor receptor type 2
HR	homologous recombination
IARC	International Agency for Research on Cancer
IR	Ionizing Radiation
KAP	KRAB-associated protein 1
KCE	Federaal Kenniscentrum voor de Gezondheid
kDa	kilo dalton
kV	kilo volt
LC	lethal concentration
LCL	lymphoblastoid cell line
LET	linear energy transfer
LNT	linear no treshold
LSS	life span study
M/I	mortality to incidence ratio
MDC1	mediator of DNA damage checkpoint protein 1
MMEJ	micro-homology end joining
MN	micronucleus
MOMP	mitochondrial outer membrane
MRI	magnetic resonance imaging
MRN	Mre11-RAD50-NBS1 complex
mRNA	messenger RNA
NAD	nicotinamide adenine dinucleotide
NBS	nibrin
NER	nucleotide excision repair
NMD	nonsense-mediated decay
Nt	nucleotide
P16	tumor protein 16
P21	tumor protein 21
P53	tumor protein 53
PALB2	partner and localizer of BRCA2
PARP	poly ADP ribose polymerase
PARPi	PARP inhibition
PARylation	poly ADP ribosylation
PAXX	paralog of XRCC4 and XLF
PHA	phytohaemagglutinin
(DNA-) POL...	(DNA) polymerase ...
PR	progesterone receptor
Pre-mRNA	primary mRNA
PTM	posttranslational modification

RB	retinoblastoma protein
RBE	relative biological effectiveness
RC	replication complex
RIP	receptor interacting protein
RIND	radiosensitivity indicator
RNA	ribonucleic acid
RPA	replication protein A
RR	relative risk
RS	radiosensitivity
snRNP	small nuclear ribonucleoproteins
SDSA	synthesis-dependent strand annealing
SSA	single strand annealing
SSB	single strand break
ssDNA	single stranded DNA
Sv	sievert
Tdt	terminal deoxynucleotidyl transferase
TMEJ	theta-mediated end joining
TNBC	triple negative breast cancer
TNM	tumor node metastasis grading system
TS	template switching
UZ Gent	Universitair Ziekenhuis Gent (University Hospital Ghent)
VUS	variants of unknown clinical significance
WHO	World Health Organisation
WSR	world standard population; age-standardized rate
XLF	XRCC4-like factor
XRCC	X-ray repair cross-complementing protei

PART I: INTRODUCTION

1 BREAST CANCER

1.1 Breast tissue and breast cancer

The breast consists predominantly of adipose tissue, connective tissue and mammary glands. However, composition evolves pending on age and hormones. The mammary glands are modified sweat glands present in both sexes but only functional in lactating females. Each gland consists of 15 to 25 lobes and each lobe consists of smaller units, called lobules containing alveoli (see Figure 1.1). These alveoli are lined with cuboidal epithelium cells, capable of producing milk. Furthermore, the breast tissue holds a system of lymph vessels which drain into the axillary lymph nodes in the armpit (see Figure 1.1) (Marieb et al. 2008).

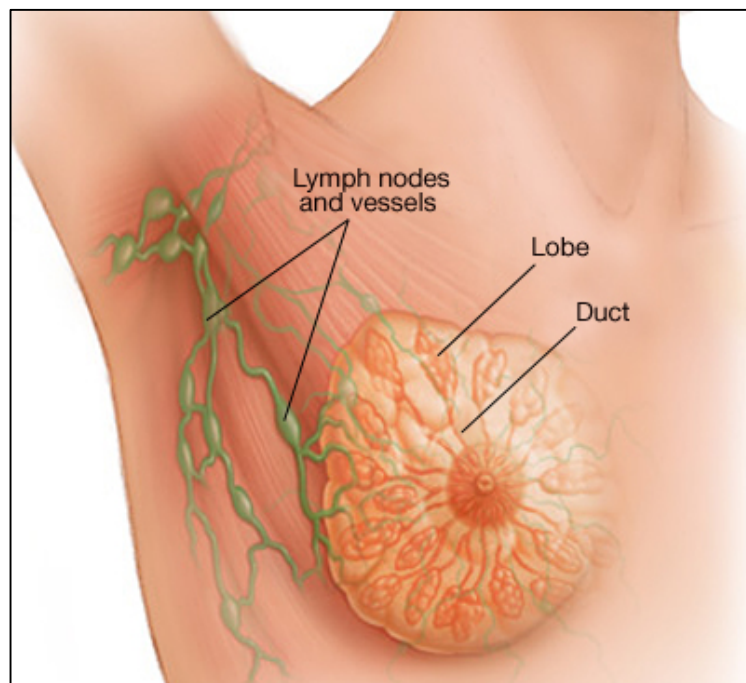


Figure 1.1: Breast anatomy ©Mayo foundation

Breast cancer is usually derived from the epithelial cells lining the ducts and lobules. Approximately 85% of all carcinoma arise in the ducts, referred to as ductal carcinoma. A minority is formed in the lobule itself (lobular carcinoma). Furthermore, the carcinoma can remain in situ, meaning that it remains restricted to the particular tissue compartment. The tumor can also penetrate the surrounding tissue (invasive carcinoma), which can eventually lead to invasion of the lymph nodes and metastasis (Marieb et al. 2008). Breast cancer is divided in five stages, using the Tumor Node Metastasis (TNM) system. This staging is based

on three characteristics: the tumor size (T), the invasion of the lymph nodes (N) and the presence of metastases (M) (Gannon et al. 2013; Senkus et al. 2015). Additionally, breast tumors can be divided in five categories, depending on their receptor status (Gannon et al. 2013). Assessment of estrogen receptor (ER), progesterone receptor (PR) and HER2 provides prognostic data and guides treatment selection (see chapter 1.6: Breast cancer treatment). If the tumor cells do not express any of these three receptors, they are referred to as being triple-negative (Gannon et al. 2013). Triple negative breast cancer (TNBC) accounts for 20% of all breast cancers worldwide (Mirzania 2016).

1.2 Incidence and mortality – Alarming figures

Breast cancer is worldwide the most common cancer and in the Western world, one in eight females will develop breast cancer in their lifetime (WHO). In Belgium, breast cancer is the most frequent tumor in females with 35% of all female malignancies developing in the breast. In 2013, 10.695 females were diagnosed with breast cancer (see Figure 1.2).

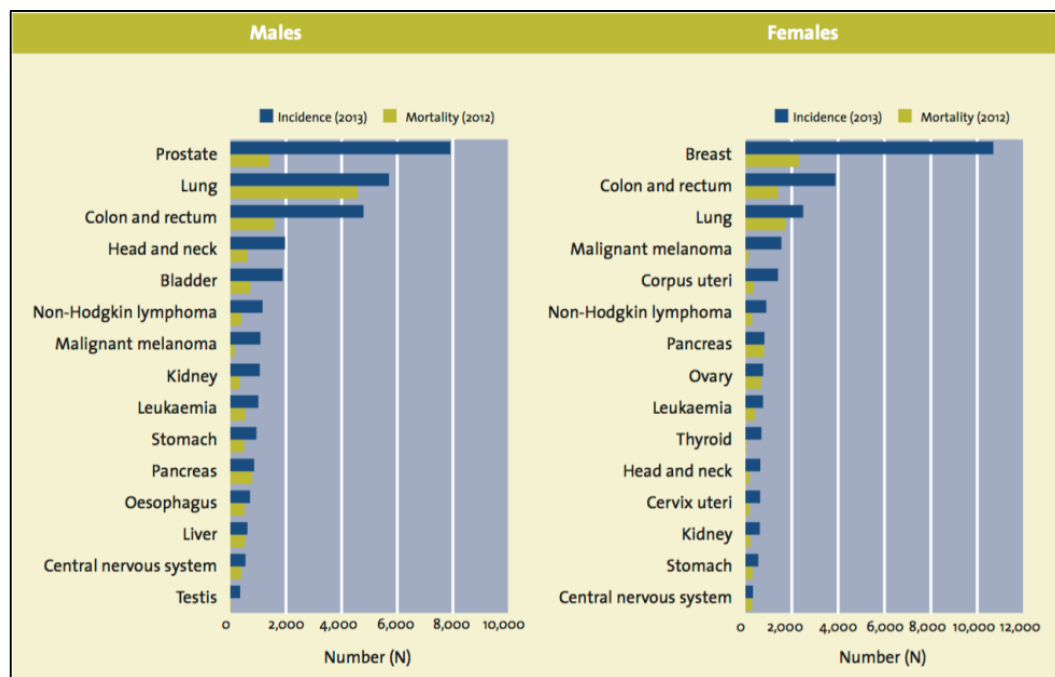


Figure 1.2: Incidence (2013) and mortality (2012) for the 15 most frequently diagnosed malignancies (excluding non-melanoma skin cancer) in males and females in Belgium (Belgian Cancer Registry 2015).

Belgium has the highest incidence of female breast cancer of all European countries, with an age standardized rate of 109,8 per 100 000 (see Figure 1.3). Moreover, Belgium has the highest rate of breast cancer worldwide (WCRF 2012).

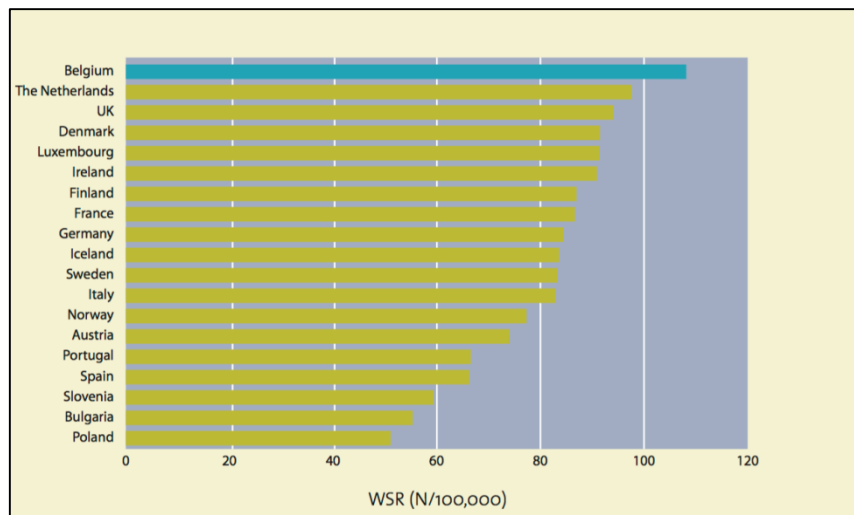


Figure 1.3: Comparison of age-standardized breast cancer incidence rates using the World Standard Population (WSR) (per 100 000) in Belgium and a selection of European registry data (Belgian Cancer Registry 2015).

The risk pattern for breast cancer is age related, with the highest incidence observed in the age group 50-69 years (see Figure 1.4).

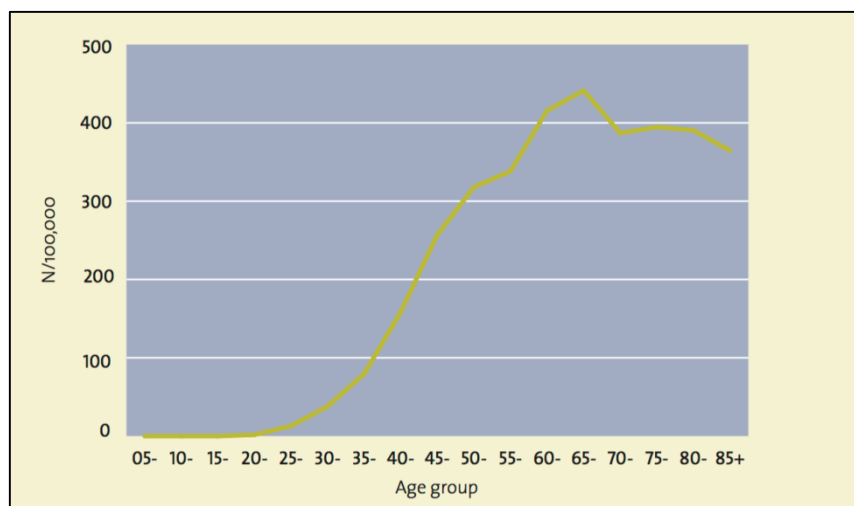


Figure 1.4: Age-specific incidence breast cancer rates (per 100 000) in females in Belgium 2009-2013 (Belgian Cancer Registry 2015).

Breast cancer is responsible for 20% of cancer deaths in females. In 2012, 2.312 women died as a consequence of breast cancer in Belgium (see Figure 1.2). Mortality to incidence (M/I) ratio is 21%. This is relatively low which may be due to intensified screening programs (see chapter 1.5: Breast cancer screening), as reflected in the fact that the majority of female breast cancer (up to 80%) is diagnosed in the prognostic more favorable stages I and II. In addition, extensive treatment options result in a high 5-year relative survival rate of 89,6%. For comparison, the M/I ratio for the third most common cancer in females, lung cancer, is 77% and the 5-year relative survival rate is merely 20% (Belgian Cancer Registry 2015).

Breast cancer in males is very rare with only 83 new diagnoses in 2013 and 22 deaths in 2012 in Belgium. Prognosis is more or less comparable to female breast cancer with a 5-year relative survival of 83.1% (Belgian Cancer Registry 2015).

1.3 Risk factors

Different factors are known to increase the risk of breast cancer. The best known risk factor, besides gender, is having a familial history of breast cancer. Breast cancer risk increases with the number of affected relatives and decreases with increasing age of diagnosis. Twin studies estimate the effect of hereditary factors to be around 31% for breast cancer (Mucci et al. 2016). However, a mere 5 to 10 % of all breast cancers have a strong inherited background and only a fraction of all breast cancers (5 %) are due to high penetrance genes, referred to as “breast cancer genes”, discussed in the next chapter 1.4: Hereditary breast cancer (Lalloo & Evans 2012).

Another risk factor is breast density. Breast density is evaluated by means of mammography imaging and scored according to different systems (e.g. Wolfe grade and BIRADS). Basically, dense breasts contain a high percentage of glandular and connective tissue whereas less dense breast contain a higher portion of fat. The meta-analysis by McCormack demonstrated that increasing breast density is associated with an increased breast cancer risk, which is as high as 4.64-fold (95% confidence interval (CI): 3.64 – 5.91) for the most dense (>75% glandular and connective tissue) compared to the least dense category (<5% glandular and connective tissue) (McCormack et al. 2006).

A couple of life style related risk factors have also been identified. One of those factors is the use of alcohol. The International Agency for Research on Cancer (IARC) classifies alcohol as a group 1 carcinogen for breast and other types of cancer, meaning that there is sufficient evidence that the compound is carcinogenic to humans (IARC 2016). Repetitive moderate (approx. one drink/day) or high (> one drink/day) alcohol intake confers in an elevated risk of breast cancer (Relative risk (RR) = 1.3 (95% CI: 1.1 – 1.7) and RR = 1.6 (95%CI: 1.3 – 2.0 respectively)) (Rice et al. 2016). Another life style factor influencing breast cancer risk is body weight. Interestingly, childhood and adolescent obesity is associated with a lower pre- and postmenopausal breast cancer risk (WCRF/AICR 2007; Rice et al. 2016). On the contrary, postmenopausal weight gain is associated with an increased breast cancer risk at a ratio of 8% increase per 5 kg/m² weight gain (WCRF/AICR 2007).

Another well documented risk factor is the lifetime exposure to estrogen. An early menarche, late natural menopause, late first pregnancy (after the age of 30) or no child bearing result in an increased breast cancer risk (WCRF/AICR 2007). Furthermore exposure to exogenous hormones, by means of oral contraceptives and post-menopausal hormonal therapy (both estrogen and/or progestin), is also associated with an increased risk of breast cancer (e.g. RR for oral contraceptives = 1.33 (95%CI= 1.03-1.73)) (Rice et al. 2016).

A last well documented risk factor – also classified as group 1 carcinogen – is exposure to ionizing radiation (IARC 2016). A valuable cohort to evaluate the effect of exposure to ionizing radiation are the atomic bomb survivors. The Hiroshima and Nagasaki survivors and a fixed group of non-exposed Japanese controls are combined in the Life Span Study (LSS) to evaluate late health effects of ionizing radiation. The cohort follow-up between 1950 to 2003, demonstrated a significant increase in mortality in both females and males as a consequence of breast cancer with an excess relative risk (ERR) of 1.5 (95% CI = 0.91 – 2.3) and 9.1 (95%CI = 0.51 -128) per gray (Gy) respectively (Ozasa et al. 2012). In addition to the Atomic bomb survivors, a lot can be learned from follow-up of individuals exposed to ionizing radiation in a medical setting. After all, these studies provide data in a non-Japanese cohort and demonstrate the effect of various organs receiving various doses. Furthermore, organ specific doses can be as high as 50Gy or more. Exposure to ionizing radiation from medical applications, e.g. X-ray based chest fluoroscopies, also result in an increased breast cancer

incidence as reviewed by Gilbert (2009). However, a clear influence of age at exposure could be distinguished. Exposure to ionizing radiation at a younger age implies a higher risk of radiation-induced breast cancer compared to exposures later in life (e.g. after the age of 50) (Gilbert 2009).

1.4 Hereditary breast cancer due to germline mutation in “breast cancer genes”

By far the strongest risk factor is the genetic predisposition. To date, several genes have been identified as “genes associated with an increased risk for breast cancer”. Germline mutations in these genes result in a raised breast cancer risk compared to the population risk, which is approximately 13% (World Health Organization). The level of this increase is inherent to the gene in which the germline mutation occurred and, in some particular cases, the mutation itself. The best known highly penetrant breast cancer genes are *BRCA1* and *BRCA2* (breast cancer susceptibility gene 1 and 2). Mutations in these genes are rare, but are highly penetrant (see Figure 1.5) (Foulkes & Shuen 2013). More recently, *PALB2* was identified as a hereditary breast cancer gene (Antoniou et al. 2014).

Germline mutations in other genes were shown to be associated with a moderate increase of breast cancer risk such as Ataxia Telangiectasia mutated (*ATM*) and *CHEK2* (see Figure 1.5) (Lalloo & Evans 2012). Finally, a high number of low-risk common alleles have been identified through genome wide association studies (see Figure 1.5) (Figuerola et al. 2011; Darabi et al. 2016; Michailidou et al. 2014).

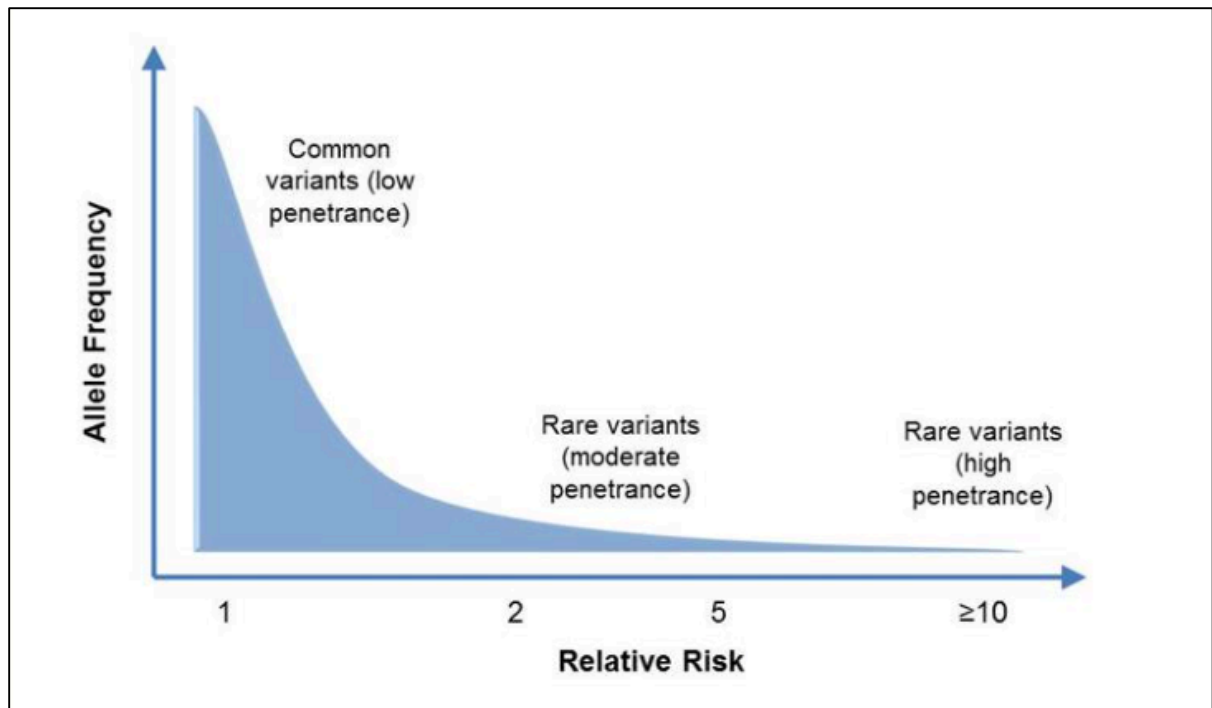


Figure 1.5: Genetic architecture of cancer risk: relative risk (x-axis) compared to minor allele frequency (y-axis) for breast cancer. Three distinct groups can be observed, see text for further details (www.cancer.gov/ 2016).

1.4.1 High risk breast cancer genes

1.4.1.1 *BRCA1*

BRCA1 was the first gene in which DNA alterations were associated with an increased risk of breast cancer. It was discovered in 1990, when Hall et al. linked the gene on chromosome 17q21 with inherited breast cancer in families with early-onset disease (Hall et al. 1990). In 1994, the gene was cloned for the first time (Miki et al. 1994).

BRCA1 is a large gene containing 24 exons. It codes for a 2843 amino acid (AA) or 220 kDa protein. It is a pleiotropic DNA damage response protein important for DNA double strand break (DSB) repair and cell cycle checkpoint activation. It has several functional domains and numerous binding partners to fulfill its many functions as a caretaker gene (Foulkes & Shuen 2013; Roy et al. 2012). An overview of the functional domains, binding partners and functions is provided in Figure 1.6 and Table I. The role of *BRCA1* in the cell cycle checkpoints and DSB repair will be discussed in detail in chapter 3: DNA damage response.

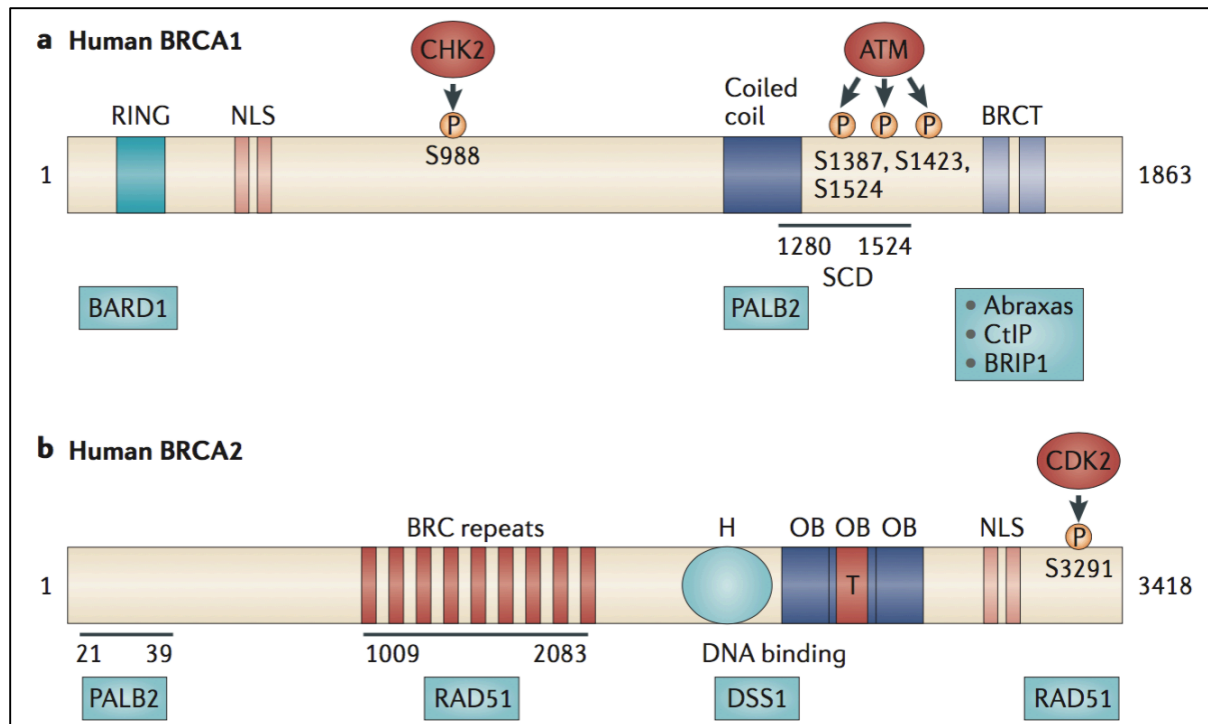


Figure 1.6: Overview of the functional domains of BRCA1 (a) and BRCA2 (b) and their interaction partners (Roy et al. 2012).

Table I: Overview of the functions, functional domains and interaction partners of BRCA1 and BRCA2 (Roy et al. 2012).

Function	Domain	Direct binding	Indirect binding
BRCA1			
Recruitment to DNA damage sites	BRCT	Abraxas	RAP80
DNA end resection	BRCT and RING?	CtIP	MRN complex
G2/M checkpoint	BRCT	Abraxas	RAP80
	BRCT	CtIP	MRN complex
	SCD (S1423 and S1524 phosphorylation)	ATM	MRN complex
S-phase checkpoint	SCD (S1387 phosphorylation)	ATM	MRN complex
	BRCT	BRIP1	TOPBP1
Repair during DNA replication	BRCT	BRIP1	TOPBP1
HR	Coiled-coil and S988 phosphorylation	PALB2	BRCA2
BRCA2			
HR	BRC	RAD51	
	DBD	DSS1	
	N terminus	PALB2	BRCA1
	C terminus	RAD51	CDK2

1.4.1.2 *BRCA2*

BRCA2 (BRCA2) was discovered in 1994 by Wooster et al. and cloned by the same research group a year later (Wooster et al. 1994; Wooster et al. 1995). Mutations in *BRCA2* account for approximately 10% of all familial breast cancers (Lalloo & Evans 2012).

BRCA2 is a very large protein containing 3416 AA (390kDa) for which the gene is located on chromosome 13q13 (Strachan & Read 2011). Compared to BRCA1, BRCA2 holds less preserved domains, despite being a larger protein. In addition, BRCA2 has fewer interaction partners and is predominantly involved in homologous recombination (HR), a specific DSB repair pathway (Roy et al. 2012; Narod & Foulkes 2004). An overview of functional domains and interaction partners is provided in Figure 1.6 and Table I. The role of BRCA2 in HR is discussed in chapter 3: DNA damage response.

1.4.1.3 *PALB2*

A more recently discovered 'breast cancer gene' is *PALB2* (partner and localizer of BRCA2) (Antoniou et al. 2014). *PALB2* is located on chromosome 16 and encodes a 131kDa (1186 AA) protein containing two distinct functional domains being an amino-terminal coiled-coil structure and a carboxy-terminal WD40-repeat domain. The former domain enables interaction with BRCA1 while the latter is necessary for BRCA2 binding. Via these interactions, *PALB2* mediates HR-specific DSB repair (see chapter 3: DNA damage response) (Zhang et al. 2009; Park et al. 2014).

1.4.1.4 Associated risks

Mutations in *BRCA1* account for 7 to 10% of familial breast cancer (Lalloo & Evans 2012). Heterozygous pathogenic mutations in *BRCA1* result in a lifetime breast cancer risk of 70 to 80%. Furthermore, *BRCA1* mutation carriers are at high risk of ovarian cancer with a lifetime risk up to 50% (Roy et al. 2012). Individual variations in breast or ovarian cancer incidence in mutation carriers can be explained by differences in genotype, genetic modifiers and environmental factors (Levy-Lahad & Friedman 2007). *BRCA1* mutation associated breast cancers are characterized by an early age of onset, originate predominantly from the duct epithelial cells and are defective for HR. Furthermore, the percentage of triple negative breast

cancers is considerably higher in mutation carriers (71%) than in the general population (17%) (Peshkin et al. 2010) and in approximately 10% of patients with triple negative breast cancer, a germline *BRCA1* was identified (Severson et al. 2015).

Heterozygous pathogenic mutations in *BRCA2* result in a life time breast cancer risk of 50 to 60%. Furthermore, mutations in *BRCA2* incline a life time ovarian cancer risk of up to 30%. Again, individual variation is observed which can be explained by differences in genotype, genetic modifiers and environmental background. For example, mutations in the central part of the gene (nucleotide c.3035 – c.6629 of exon 11) are linked with a high ovarian cancer risk (RR=1.88; 95% CI: 1.08-3.33) (Levy-Lahad & Friedman 2007). *BRCA2* mutations are also linked with a higher than average male breast cancer risk demonstrated by a cumulative risk of approximately 7% (Tai et al. 2007). The percentage triple negative breast cancers in *BRCA2* mutation carriers is comparable to the population incidence. Furthermore, lobular cancer is as frequent as in sporadic breast cancers (Peshkin et al. 2010; Roy et al. 2012).

Heterozygous loss of function mutations in *PALB2* result in an increased breast cancer risk. The cumulative risk of female mutation carriers is just short of 50% by the age of 70. This increase is comparable to that associated with mutation in *BRCA2*. However, mutation in *PALB2* are less frequent and so far, no link with ovarian cancer is reported (Antoniou et al. 2014; Zhang et al. 2009; Kleibl & Kristensen 2016; Flanagan et al. 2015).

Individuals harboring a germline mutation are not only at high risk, they also tend to develop breast cancer at younger age compared to the control cohort. Firstly described by Knudson in retinoblastoma, the formation of the tumor is based on two mutational events. Given that the first event is already present in mutation carriers, only a second event is needed to induce carcinogenesis (Knudson 1971). Moreover, for these breast cancer predisposing genes, the first event occurs in key DSB repair genes, known as tumor suppressor genes. Previous studies have demonstrated that *BRCA1* and *BRCA2* haploinsufficiency is sufficient to compromise genome instability. This facilitates additional genetic alterations and accounts for the increased risk of cancer promoting mutations (Cousineau & Belmaaza 2014). This accelerates breast carcinogenesis, resulting in a young age at time of diagnosis and an overall high lifetime cancer risk (Konishi et al. 2011; Venkitaraman 2014; Nikkilä et al. 2013; Salmena & Narod

2012; Cousineau & Belmaaza 2014). The inactivation of the wild type allele is not necessarily due to a second mutation but might also be the result of alternative mechanisms such as promotor methylation and miRNA deregulation (Luzi et al. 2012; Pronina et al. 2017).

Biallelic germline mutation in either three genes result in fanconi anemia. Fanconi anemia is an autosomal recessive disorder caused by mutation in several genes, called FANC genes, to date mutation in 19 different genes have been described. The majority of their respective proteins form a core protein, which is necessary for DNA crosslink repair. Other proteins, from genes such as *FANCS (BRCA1)*, *FANCD1 (BRCA2)* and *FANCN (PALB2)*, are important for DNA double strand break (DSB) repair through HR. Both repair pathways interact and mutations in these genes lead to impaired DNA damage repair and a diverse phenotype, including short stature, developmental delay and cancer. Identification of this disorder is performed by mutation analyses and by detection of cross linking sensitivity (e.g. mytomycin C assay) (Sawyer et al. 2015; Strachan & Read 2011; Dong et al. 2015).

1.4.1.5 Risk reducing surgeries in high risk individuals

Woman at high risk because of the presence of a mutation in *BRCA1* or *BRCA2* may consider reducing this risk by prophylactic mastectomy and/or salpingo-oophorectomy (Domchek et al. 2010). Prophylactic mastectomy reduces the risk of breast cancer by 90% or more. Risk reducing salpingo-oophorectomy is usually performed between the ages of 35 to 40 and after childbearing has been completed. This results in a reduction of ovarian cancer risk of 80% in *BRCA1* and *BRCA2* carriers. Furthermore, the salpingo-oophorectomy might also reduce breast cancer risk by approximately 50% when performed before menopause (Longo et al. 2016).

A couple of years ago, actress Angelina Jolie – carrier of a *BRCA1* mutation – wrote an opinion piece in the New York Times titled '*my medical choice*' about her choice to perform a mastectomy, thereby creating awareness for genetic testing and the surgery (Jolie 2013).

1.4.2 Moderate risk genes - *ATM* as an example

Over the years, numerous intermediate risk genes (see Figure 1.5) have been identified including CHEK2 and ATM (Lalloo & Evans 2012). Furthermore, specific mutation in high risk genes such as R1699Q in BRCA1 were classified as moderate penetrant (Spurdle et al. 2012).

In the frame of this thesis, *ATM* will be discussed elaborately. *ATM* (ataxia telangiectasia mutated) is located on chromosome 11q23 and encodes a 3056 AA long (350kDa) serine/threonine kinase responsible for the detection and signaling of DSB (Taylor et al. 2015; Strachan & Read 2011).

Heterozygous mutations in *ATM*, a known DNA damage response gene, result in an increase in breast cancer risk. Estimated relative breast cancer risk for individuals with a heterozygous *ATM* mutation vary across different studies. Van Os et al. combined all published data in a recent review. The lifetime risk of developing breast cancer for female carriers is 38%, compared to 13% in the general population. Furthermore, for young female carriers, the cumulative risk reaches 16% at the age of 50, compared to 2.3% in an age matched general population. One particular *ATM* mutation, c.7271T>G, results in an estimated lifetime breast cancer risk of up to 69% in heterozygous carriers. This is comparable to the risk of *BRCA1* and *BRCA2* mutation carriers. Furthermore, *ATM* carriers are also at higher risk for cancers of the digestive tract (van Os et al. 2016).

Ataxia Telangiectasia

Biallelic inactivation of this gene result in Ataxia Telangiectasia (AT). AT is a rare autosomal recessive disorder. This neurodegenerative disease with early onset is characterized by a range of neurological signs including progressive cerebellar ataxia, oculomotor abnormalities and cognitive dysfunction. The syndrome is furthermore associated with multiple symptoms including immunodeficiency, an extreme radiosensitivity due to DSB repair defects and cancer predisposition, predominantly from lymphoid origin (Teive et al. 2015; Taylor et al. 2015; Kühne et al. 2004). AT is also linked with an increased serum α -fetoprotein level, which is used in diagnostic testing (Schieving et al. 2014). Incidence is estimated to be between one in 40 000 to one in 200 000 births depending on the population (Shiloh & Lederman 2017).

Unfortunately, no cure is available. Current treatment is limited to a multidisciplinary, symptom-based approach (Lavin et al. 2007).

AT presents as a very heterogeneous disease. Usually, it is diagnosed in its classical, severe form, due to frameshift mutations in *ATM* and a complete loss of ATM protein. This is linked with a younger age at time of diagnosis (median age = 5.9 years) and a young mean survival age (median age = 15.9 years). However, patients with at least one missense mutation or a leaky splice site mutation, resulting in a residual level of ATM protein, present a milder variant of the disease. These patients are typically a few years older at time of diagnosis (median age = 8.0 years), tend to live longer (median age = 20.4 years) and develop tumors at a later age compared to patients with a complete absence of ATM. Several mild founder mutations have been reported in Europe (Taylor et al. 2015; Micol et al. 2011).

1.4.3 Breast cancer gene panels

“Multiple sequencing panels, or gene panels, are an important tool to evaluate genetic variation that may be associated with an increased risk of breast cancer. Given the recent efforts to improve its cost-effectiveness, the use has grown exponentially. However, their clinical validity – whether the test result correctly predicts the high cancer risk – and clinical utility – whether the test result enables better patient care and outcome – must be evaluated (Kurian et al. 2016). To date, breast cancer risk is established for a number of genes, however, reliable estimates of risk are lacking for the majority as this is challenging, especially for rare mutations. For instance, many studies on pleiotropic tumor syndromes (like Li Fraumeni, Cowden syndrome neurofibromatosis type 1, etc.) in which breast cancer is only one feature, are subject to ascertainment bias and may therefore overestimate the associated risk. Furthermore, there are problems of publication bias, in which negative studies are not published. Many gene-discovery studies oversample for early-onset cases of disease or cases with a family history. This leads to seriously biased risk estimates unless the ascertainment is allowed for in the analysis. Moreover, risk estimates based on data from highly selected families may not reflect the true “average” risk for all carriers of pathogenic variants.

In Belgium, currently a panel of five genes is offered to patients with a presumed predisposition for breast cancer. This panel includes genes associated with a high to moderate

increased risk of breast cancer (BRCA1, BRCA2, TP53, PALB2 and CHEK2). But discussions are going on to expand the panel to other genes involved in HR, like BARD1, ATM, etc. Especially in patients with ovarian cancer evidence is emerging to include also genes like RAD51C, RAD51D and BRIP1 (personal communication). However, exact risk assessments are not available. Recently, NCCN published recommendations for genetic testing and counseling for hereditary breast/ovarian cancer syndromes and risk management recommendations for patients who are diagnosed with a syndrome. The authors stress that insights are still changing and will be subject of regular updates (Daly et al. 2017).

This was recently illustrated for mutations in BRIP1. Whereas the gene is incorporated in numerous commercially available gene panels for breast cancer (Easton et al. 2015), a recent study demonstrated that truncating variants in BRIP1 are not associated with an increased risk of breast cancer (OR=0.90, 95%CI:0.48-1.7)(Easton et al. 2016).

Expanded testing will provide better insight in the associated breast and ovarian cancer risk, but as risks associated with different mutations in these genes are still unclear, genetic counseling is a challenge. In order to achieve risk assessments for these genes in large cohorts, multicenter studies have been started. Results of those studies will either confirm or rule out their use in multiple sequencing panels and will aid patient counseling (van Marcke et al. 2016). At the moment family history remains an important tool for genetic counselling and patient management (van Marcke et al. 2016).

In addition to the challenge created by genes included in gene panels for which breast cancer risk is unclear or not unequivocally established, variants of unknown significance (VUS) – detected at high rate – pose another problem (van Marcke et al. 2016)."

1.4.4 Deleterious germline mutations versus Variants of Unknown Clinical Significance

For all above discussed high risk genes, risk assessment is based on the presence of deleterious mutations. These incline the loss of function of one allele, either due to frameshift mutations or nonsense mutations, both leading to a premature termination codon and degradation of the mRNA due to nonsense-mediated decay (NMD). On the other hand, the mutant allele might still be present, but deleterious missense mutation or (small) in-frame

insertions or deletions may affect a functional domain, thereby inhibiting proper functionality of the protein (Strachan & Read 2011).

However, due to an evolution in sequencing technologies, the number of individuals undergoing screening drastically increased and led to a significant rise in the number of VUS (Kraus et al. 2017). The detection of a VUS is a challenge for health care providers as the impact on breast or ovarian cancer risk is unclear. For missense variants, a large number of functional tests have been proposed (Milot et al. 2012; Hendriks et al. 2014) but the implementation on a large scale in a clinical diagnostic setting is not feasible. Messenger RNA (mRNA) analyses to investigate intronic and exonic variants that might impair proper RNA splicing, are more widely used.

During RNA splicing, the intervening intronic sequences are removed from the primary mRNA (pre-mRNA), thereby linking the exonic sequences to generate a mature mRNA. It is a highly regulated process orchestrated by the spliceosome, which is a complex formed by small nuclear ribonucleoproteins (snRNP), each composed of small nuclear RNA and associated proteins (see Figure 1.7). Accurate splicing relies on conserved areas in the intron and exon. The best-defined regions necessary for accurate splicing are the highly conserved dinucleotides at the splice donor and acceptor sites situated at the intron boundaries. Splicing is furthermore guided by the conserved adjacent sequences and the branch point. Finally, splicing is influenced by exonic splicing regulatory elements, both enhancers (ESE) and silencers (ESS) (Strachan & Read 2010).

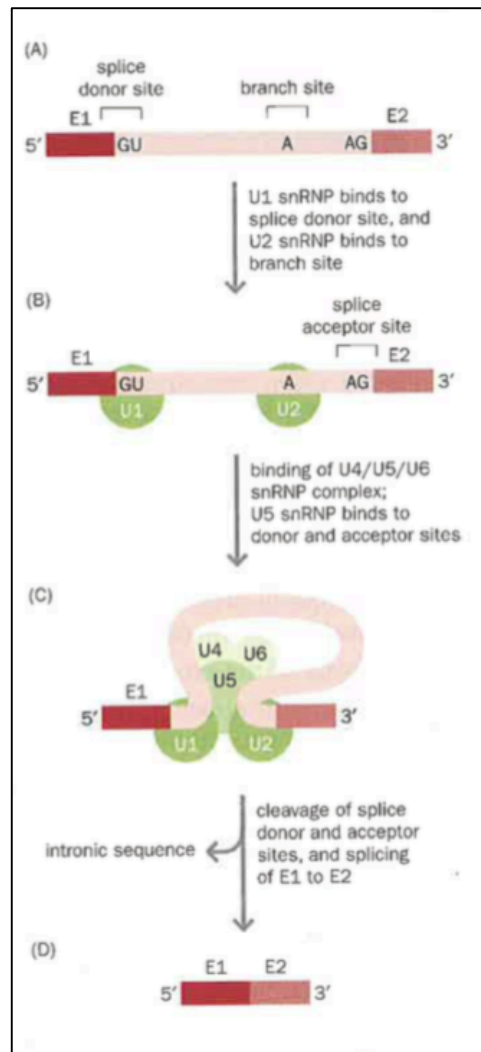


Figure 1.7: Schematic representation of pre-mRNA splicing (Strachan & Read 2010).

Variants in these highly conserved regions may lead to aberrant splicing and be pathogenic if this results in a truncated protein or in complete loss of one allele if a premature termination codon leads to NMD. Aberrant splicing of putative variants can be evaluated *in silico*, by means of numerous prediction tools. However, mRNA analysis, e.g. in *in vitro* cultured peripheral blood lymphocytes of an individual with the variant of interest, is the designated approach to assess the effect of a variant on mRNA splicing (Strachan & Read 2010; Houdayer et al. 2012; Spurdle et al. 2008; Colombo et al. 2013).

1.5 Breast cancer screening

Breast cancer screening is predominantly performed by mammography screening. Mammography screening uses low energy X-rays, typically 28-30kV, to image the breasts. Usually, two images are taken from each breast resulting in a mean glandular dose between 3.7 and 4.7 mGy. Digitalization of mammography screening tends to result in lower doses (Gillet et al. 2011; Hendrick 2010). The screening enables physicians to detect breast cancer before clinical symptoms appear (see Figure 1.8), thus allowing an early treatment and a good survival rate. However, one has to take into account the disadvantages of this screening method. Disadvantages include, but are not limited to, the false positive and false negative results, treatment of tumors that would not progress in life threatening cancer and the possibility that the ionizing radiation-based screening method can result in radiation-induced tumors. In order to justify the use of mammography screening, the gain derived from the number of detected tumors must outweigh the number of induced tumors excessively (Gillet et al. 2011).



Figure 1.8: Mammogram of breast with breast cancer (indicated with arrows), visible as a white, dense mass. ©Bakerstmd (Wikipedia)

Other screening methods such as ultrasound and magnetic resonance imaging (MRI) avoid the use of ionizing radiation and are usually offered to women at high risk. The use of ultrasound usually results in high number of false positives and often accompany mammography screening. However, the application in breast cancer screening is not recommended (Gillet et al. 2011). MRI has proven to be a high sensitivity screening tool for women at high risk and is implemented in breast cancer screening, often in addition to mammography screening, in these individuals, despite being an expensive procedure (Enriquez & Listinsky 2009).

1.5.1 Population screening

In Flanders, Belgium, all woman between the age of 50 and 69 years are offered a 2-yearly mammography screening to allow detection of breast cancer in an early stage. In 2014, 47% of all eligible woman responded to this initiative, another 18% arranged screening on own initiative (CvKO n.d.). Population screening is limited to this particular age group as the highest breast cancer incidence is observed between the ages of 50 and 69 (see chapter 1.2: Incidence and mortality, Figure 1.4). Contemplating to the principal “foremost, do no harm (primum non nocere)” and taking into account the limited beneficial effect on survival, an expansion of this program to include women between the ages of 40 to 49 (Mambourg et al. 2010) or older than 70 is advised against (Mambourg et al. 2010; Mambourg et al. 2012).

1.5.2 Breast cancer screening in individuals at high risk

The Belgian *Federaal Kenniscentrum voor de Gezondheid* (KCE) issued guidelines for breast cancer screening in individuals at high risk in KCE report 172A. Proper screening management of these individuals is necessary as they are not only more prone to breast cancer, but develop tumors at a younger age (Gillet et al. 2011).

Individuals are divided in three risk classes based, predominantly, on familial anamnesis (Gillet et al. 2011):

Average Risk

- No or one first- or second-degree relative with breast cancer diagnosed after the age of 40 (see chapter 1.5.1: Population screening)

Raised Risk (lifetime risk of 17-30%)

- One first-degree relative with breast cancer diagnosed before the age of 40
- Two first- or second-degree relatives with breast cancer diagnosed before the age of 50
- Three first- or second-degree relatives with breast cancer diagnosed before the age of 60

High Risk (lifetime risk of 30% and higher)

- Two first- or second-degree relatives with breast cancer before the mean age of 50, of which at least one first degree relative.
- Three first- or second-degree relatives with breast cancer before the mean age of 60, of which at least one first-degree relative
- Four relatives diagnosed with breast cancer at any age, of which at least on first-degree relative.
- Jewish decent
- One of the following criteria in the familial anamneses
 - o Bilateral breast cancer
 - o Breast cancer in men
 - o Ovarian cancer
 - o Sarcoma before the age of 45
 - o Glioma or adrenal cortical carcinoma during childhood
 - o Multiple carcinoma at young age
 - o Strong indication in the paternal pedigree

This risk assessment does not directly take into account the presence of a familial mutation. Individuals of Jewish decent are classified as being at high risk because of the presence of three founder mutations in *BRCA1* and *BRCA2* in this population (McClain et al. 2005). Individuals with a raised risk are offered a yearly mammogram between the ages of 40-49 and a two-yearly mammogram between 50 and 69 years (see Figure 1.9). Individuals at high risk are offered yearly mammography screening and MRI starting at the age of 30 or 5 years

before the age of diagnoses of the youngest diagnosed family member (but not before the age of 25) (see Figure 1.9) (Gillet et al. 2011). In UZ Gent and several other Belgian hospitals, the consensus is to commence screening with yearly MRI and only offer regular mammography after the age of 50 (personal communication). However, this gentle use of ionizing radiation based screening is not applied worldwide. For example, current guidelines in the US involve an annual MRI (or mammography if MRI is unavailable) between the ages of 25 to 29 and annual MRI and mammography screening between 30 and 75 years for individuals with a *BRCA* mutation (NCCN 2016). This annual screening approach starting at 30, results in a relatively high cumulative burden in these individuals, increasing the chance to develop a radiation-induced tumor.

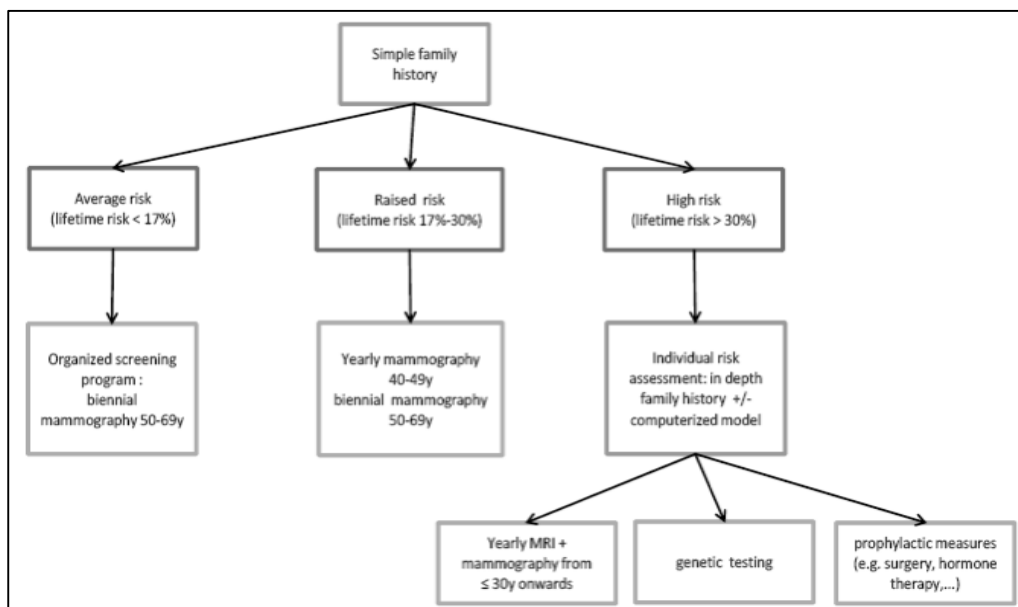


Figure 1.9: KCE guidelines for breast cancer screening in all three risk groups (Gillet et al. 2011).

1.6 Breast cancer treatment

The best option for breast cancer treatment depends on several factors including: breast cancer type, tumor size, the possible invasion of lymph nodes, the presence of metastasis and the presence of hormonal receptors on the tumor cell surface. Treatment strategies include systemic treatment or a more local approach. Local treatment options comprise surgery and/or radiotherapy. The goal of radiotherapy is to deliver a sufficiently high dose of ionizing radiation at the tumor site to eliminate the tumor cells whilst preserving the surrounding healthy tissue. Unfortunately, ionizing radiation will also interact with all surrounding healthy

tissues and organs without specificity for the tumor cells resulting in normal tissue effects as well as tumor cell killing. In order to achieve maximal tumor response while protecting normal tissue, high total doses (50Gy or more) are delivered in small daily fractions of 2Gy over a long period of time (La Torre Travis 1989; Löbrich & Jeggo 2007).

Systemic treatment consists of a general chemotherapy or a more specific approach, such as hormonal therapy in case of ER and PR positive status. Additionally, targeted therapies, which can be selected if the tumor exhibits certain features are a possibility. One well-known target is HER2 status. Overexpression of HER2 is correlated with a more aggressive breast cancer and poor outcome. Several compounds specifically targeting HER2, yield good responses and improve survival rates (Rutqvist 2004; Gradishar 2012). Another of these characteristics is HR deficiency, which is frequently observed in tumors of *BRCA1* and *BRCA2* mutation carriers (Lord & Ashworth 2016). HR and the targeted therapy using PARP inhibitors, will be discussed in chapter 3.3.2.2 and 3.3.2.4 respectively.

2 IONIZING RADIATION

2.1 What is ionizing radiation?

Ionizing radiation is radiation that carries sufficient energy to ionize atoms or molecules by ejecting one or more orbital electrons. It is characterized by a localized release of a large amount of energy and the dose to biological material is defined by the amount of energy absorbed per unit of mass, expressed in Gray (Gy). Besides ionizations, ionizing energy also possesses sufficient energy to excite atoms by displacing an orbital electron. Two types of ionizing radiation are described.

- (1) particle irradiation consists of subatomic particles, ions or atoms travelling at high speed and can be described by mass and charge.
- (2) electromagnetic waves are photons which have no mass or charge. X-rays and γ -rays are the best known examples (La Torre Travis 1989; Lehnert 2008).

In order to quantify energy deposits in the tissue, Linear Energy Transfer (LET) was introduced. LET is the ratio between energy deposition and the corresponding path length in units of keV/microm. It depends on several parameters including velocity of the particle. Low-LET radiation includes electrons and electromagnetic waves such as X-rays and γ -rays and produces a limited number of ionizations and/or excitations throughout the cell (See Figure 1.10). High-LET radiation includes α -particles and other large ion particles generated by accelerators. High-LET irradiation results in a dense ionization and excitation deposit along the track of the particle (see Figure 1.10) (Pouget & Mather 2001). Because of differences in energy deposits in the tissue, equal doses of different LET radiation will not produce the same biological effect. To evaluate the biological effect of a certain type of ionizing radiation in the cell, the relative biological efficiency (RBE) is determined. RBE is defined as the ratio of a dose of test radiation to a dose of reference radiation (e.g. 250kV X-rays) that produces the same biological effect (La Torre Travis 1989).

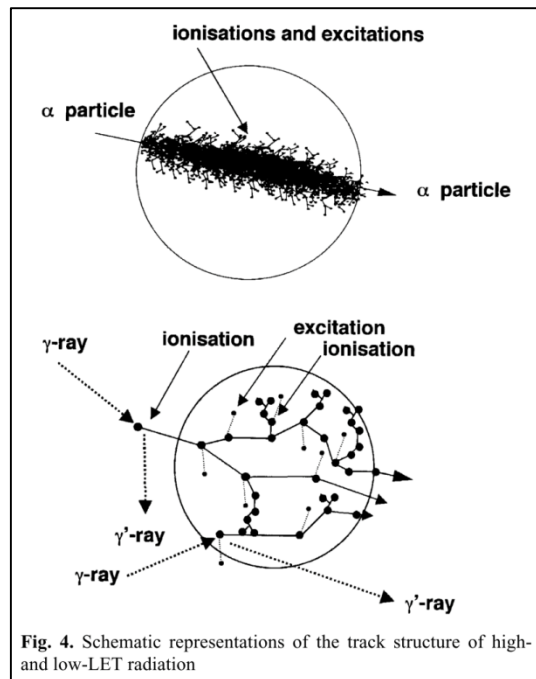


Figure 1.10: Schematic visualization of ionizations and excitations by high-LET (α -particle) and low-LET (γ -ray) ionizing radiation (Pouget & Mather 2001).

2.2 Radiation-induced damage

When ionizing radiation interacts with cells, the nucleus and its DNA are the most vulnerable parts (Pouget & Mather 2001). Damage to the DNA may be induced directly, in which case an ejected electron interacts directly with the DNA (see Figure 1.11). Damage may also be inflicted in an indirect manner. In this process, the ejected electron interacts with a water molecule producing a free radical (e.g. reactive oxygen species) which damages the DNA (see Figure 1.11). As 80% of the cell consists of water, indirect damage to the DNA is much more likely to occur than direct damage. Furthermore, the ratio direct/indirect damage also depends on the type of radiation used. High-LET ionizing radiation will result in more direct damage compared to low-LET radiation. Besides damage to the DNA caused by ionizing radiation, the DNA is continuously exposed to endogenous damaging agents which are also capable of producing highly reactive radicals (Pouget & Mather 2001; Lehnert 2008; La Torre Travis 1989).

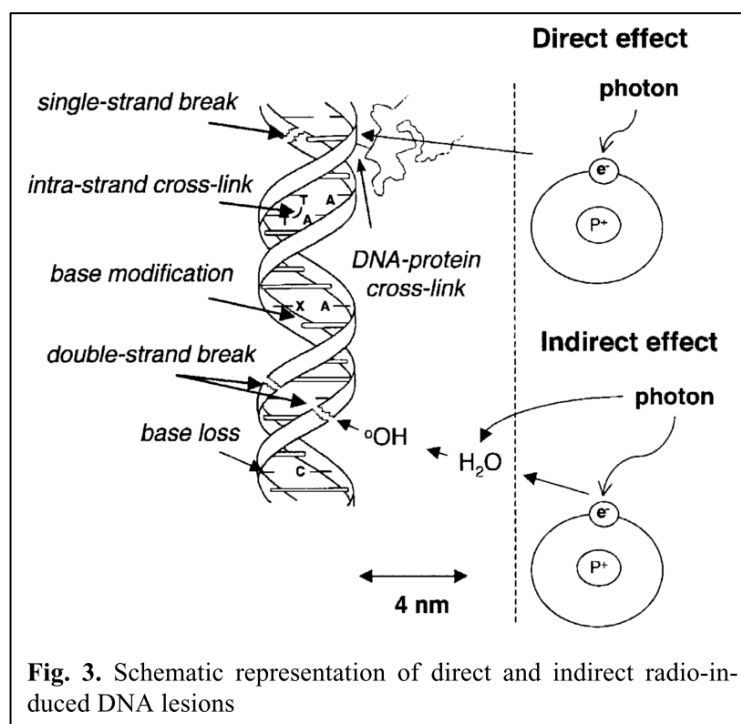


Figure 1.11: Schematic visualization of direct and indirect induced DNA lesions by ionizing radiation (Pouget & Mather 2001).

DNA damage occurs in many forms and includes base damage, crosslinks and DNA strand breaks (see Figure 1.11). Base damage occurs at high rate in the cell upon exposure to ionizing radiation and includes either loss or modification of the base. DNA-protein and DNA intra-strand crosslinks are produced when DNA radicals interact with DNA or protein radicals. DNA strand breaks are the result of a breakage in the sugar-phosphate bond of the DNA. Strand breaks include both single and double strand breaks. Breaks in only one strand of the DNA (single strand breaks) are relatively easy to repair with limited long term consequences for the cell as the proper DNA sequence remains available on the complementary DNA strand. However, DNA double strands pose a larger threat to the cell. A DNA double strand break comprises of two single strand breaks on opposite strands in close proximity (within 20 basepairs). Repair is more difficult and maintenance of the correct DNA sequence might be impaired (La Torre Travis 1989; Pouget & Mather 2001). DSB and the repair mechanisms are discussed in chapter 3: DNA damage response.

Furthermore, ionizing radiation also causes damage to other parts of the cell and impairs, amongst others, the integrity of the cell membrane (reviewed by (Corre et al. 2010)).

2.3 Health effects of exposure to ionizing radiation

2.3.1 Exposure to ionizing radiation

Exposure to ionizing radiation predominantly occurs from background radiation or via ionizing radiation-based medical applications. Daily background levels are limited to approximately 5 μSv . Doses of exposure to X-rays from diagnostic tools, such as, mammography screening, thorax X-rays and CT scans vary between 1 and 30 mSv (see Figure 1.12) (Brenner et al. 2003; Löbrich & Jeggo 2007). Another medical application of ionizing radiation is radiotherapy (see chapter 1.6: Breast cancer treatment). Radiotherapy delivers high doses of ionizing radiation in a fractionated pattern. Cumulative doses of radiotherapy can be as high as 50 Sv (see Figure 1.12) (La Torre Travis 1989; Löbrich & Jeggo 2007).

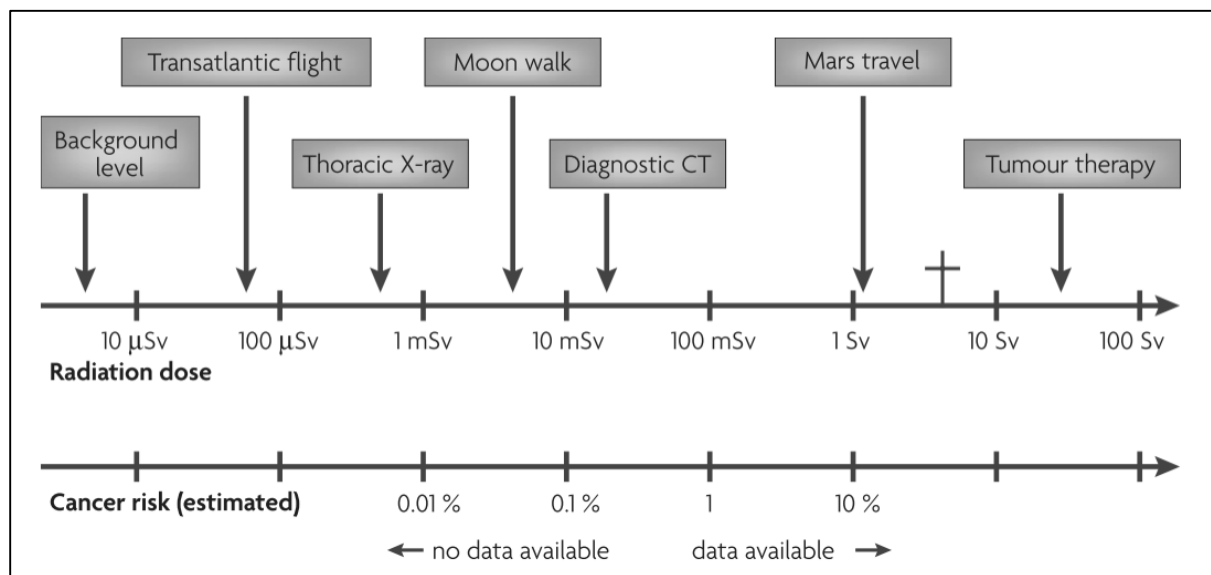


Figure 1.12: Exposure to ionizing radiation and cancer risk estimation. For reference, a transatlantic flight, moon walk and Mars travel are indicated. Whole body exposure of 5Sv is lethal (Löbrich & Jeggo 2007). (Note: Sievert represents the equivalent biological effect of the deposit of a joule of radiation energy in a kilogram of human tissue and is used to express the health effect of ionizing radiation in the human body. For whole body exposures with X-rays, 1Sv equal to 1Gy (Löbrich & Jeggo 2007)).

2.3.2 Health effects of ionizing radiation

Health consequences of exposure to ionizing radiation due to cellular damage can be divided in two main categories. The first category is the deterministic effect. Deterministic effects are adverse effects observed after exposure to higher doses (usually acute doses in excess of 500 mGy) and severity is directly linked to the dose. These effects and the dose threshold are related to the irradiated tissue. Deterministic effects are due to cell death in the exposed tissues and tend to appear shortly after irradiation, however, some deterministic effects may

take several months to develop. Examples include infertility, skin damage and cataract (La Torre Travis 1989; HPA 2013).

The second category is the stochastic effect. The best known and most studied stochastic effect is cancer. There is no dose limit for this effect and it only appears several years after the original exposure. Furthermore, the risk, but not the severity, is linked with increasing doses. Cancer risk is well documented for doses above 100 mGy (see Figure 1.12) and follows a linear regression (Averbeck 2009; La Torre Travis 1989; Löbrich & Jeggo 2007). Data for these higher dose ranges are predominantly obtained from the LSS cohort of Atomic bomb survivors and patients exposed to ionizing radiation for medical purposes (e.g. radiotherapy or multiple X-ray examinations) (Mattsson & Nilsson 2015). In the higher dose range, a total body dose of 2-3 Sv (or 2-3 Gy in case of exposure to X-rays) results in a doubling of cancer risk (Löbrich & Jeggo 2007). The risk of breast cancer upon exposure to ionizing radiation was previously discussed in chapter 1.3: Risk factors.

Evaluation of the stochastic risk after exposure to low doses (below 100 mGy) and very low doses (below 10 mGy) of ionizing radiation remains difficult. However, understanding the impact of (very) low doses of ionizing radiation is important as exposure to ionizing radiation for diagnostic purposes is situated mainly in this (very) low dose range (see Figure 1.12). Although the effect of low dose exposure as used in diagnostic X-rays might be small, it could still result in a large impact when applied to a large cohort (e.g. population screening with mammography) (Brenner et al. 2003). Unfortunately, epidemiological data are not strong enough to identify a small increase in risk as an extremely high number of exposed individuals would be necessary to achieve sufficient power (Brenner et al. 2003).

To estimate the risk effect of low doses of ionizing radiation, data of high doses of ionizing radiation are extrapolated to the low dose ranges. The standard for extrapolation is the linear no threshold model (see Figure 1.13). This model is based on a linear increase of cancer risk with increasing doses of ionizing radiation. However, whereas the linear no threshold model has proven its application for doses above 100 mSv, its usage for dose < 100 mSv is challenged by recent developments and new insights (Averbeck 2009).

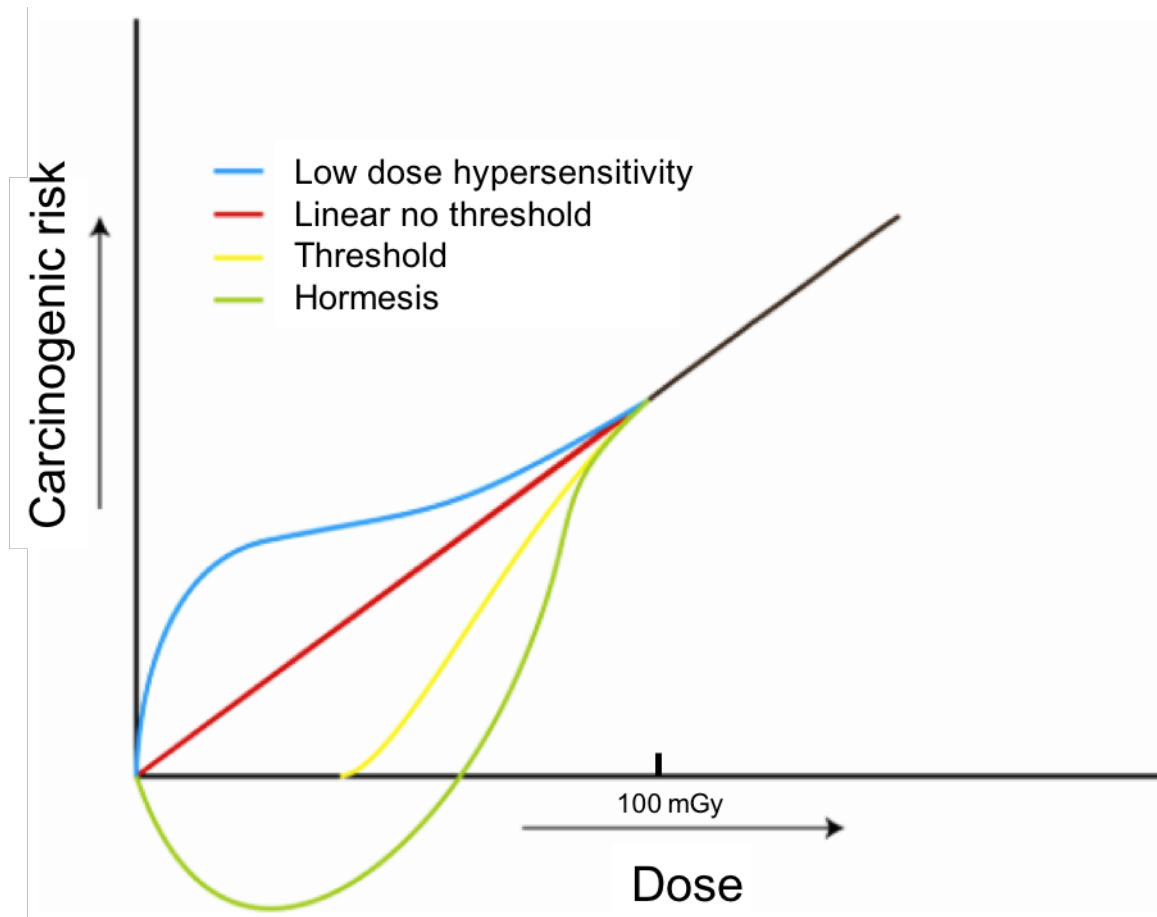


Figure 1.13: Schematic representation of possible extrapolations of high-dose data to low and very low doses (Robertson et al. 2013).

Nowadays, it is known that cells and tissues act differently in response to low doses of ionizing radiation compared to high doses. These effects might either be beneficial or detrimental for cells or tissue. One effect to take into account when investigating the effect of low dose radiation exposure is low dose hypersensitivity (see Figure 1.13). This phenomenon might be caused by the bystander effect, which is based on the induction of ionizing radiation-linked effects in non-targeted cells and involves intercellular communication via intercellular gap junctions or release of cellular mediators in the medium. It is only relevant at lower doses, as not all cells will be hit by the ionizing radiation directly. On the other hand, low dose hypersensitivity might also be the result of increased cell lethality at very low doses as a threshold of induced damage is needed to activate DNA damage response and repair. A reduced DNA damage repair after low dose exposure could subsequently result in a higher than expected cell lethality. Low dose hypersensitivity would imply an underestimation of the risks after exposure to low doses of ionizing radiation by the linear no threshold model. Its

counterparts, namely radioadaptation, threshold hypothesis and beneficial low-level radiation effects (hormesis), imply an overestimation by the linear no threshold risk extrapolation model. Radioadaptation suggests that small doses of ionizing radiation (below 20 mGy) prepare the cells for higher doses. Hormesis (see Figure 1.13) proposes that low doses of ionizing radiation may have beneficial effects for cells or tissue. Finally, the threshold hypothesis (see Figure 1.13) implies that below a certain dose, no risk exists for a particular endpoint (Brenner et al. 2003; Averbeck 2009).

2.3.3 *Radiosensitivity*

Consequences of exposure to ionizing radiation depend on the radiation dose but will also depend on the sensitivity to ionizing radiation which is important for proper risk assessment. Radiosensitivity – sensitivity to ionizing radiation – can be evaluated at several levels using different endpoints. It is therefore essential that, whenever discussing radiosensitivity, the precise parameters are defined. Radiosensitivity can be defined on a cellular level, in regard to specific tissues or for a complete organism. End points include cancer formation, cell death and chromosomal damage (see Table II) (HPA 2013).

Table II: Summary of frequently applied radiosensitivity forms and assays (HPA 2013).

Whole tissue radiosensitivity	Measured by assays such as LC50/30, which refers to the radiation dose required to kill 50% of a given population within 30 days of exposure.
Normal tissue radiosensitivity	Generally used in the context of the reaction/damage to non-target tissues as a consequence of radiotherapy for cancer and other conditions. They are assessed by clinical evaluation of tissue damage using a variety of scoring schemes. The main tissues of concern include skin (burning), lung and connective tissue (fibrosis).
Susceptibility to radiation carcinogenesis	Refers to differences in susceptibility amongst individuals to radiation-induced cancer in specific tissues. It is measured in epidemiological (human) studies or experimental animal carcinogenesis studies. Generally, this is considered in terms of yield of tumors (in a specific tissue) per unit of absorbed dose.
Tissue radiosensitivity (for cancer)	Refers to the difference in sensitivity of individual tissues in organisms to radiation-associated carcinogenesis. Most information for this comes from epidemiological studies and is generally considered in terms of yield of tumors (in a specific tissue) per unit absorbed dose. Tissue radiosensitivity can also refer to differences in response to radiotherapy of tissues in terms of their function or structure.
Cellular radiosensitivity	Refers to a wide range of phenomena measured at the cellular level where response to radiation can vary between individuals or cell types. Endpoints can be cell killing, chromosomal damage, damage/repair to DNA, cell cycle endpoints, apoptosis and others. It is measured in yield of the endpoint per unit absorbed dose or parameters derived from dose-response relationships.

3 DNA DAMAGE RESPONSE

3.1 DNA damage response

As the cell, and especially the DNA, are vulnerable to damage caused by both endogenous and exogenous agents, proper DNA damage response is crucial. Despite differences pending on the type of DNA damage, a general pattern can be identified. This pattern inclines the detection and signaling of the damage, followed by a cellular response (see Figure 1.14) (Pouget & Mather 2001; Jackson & Bartek 2010; Matt & Hofmann 2016).

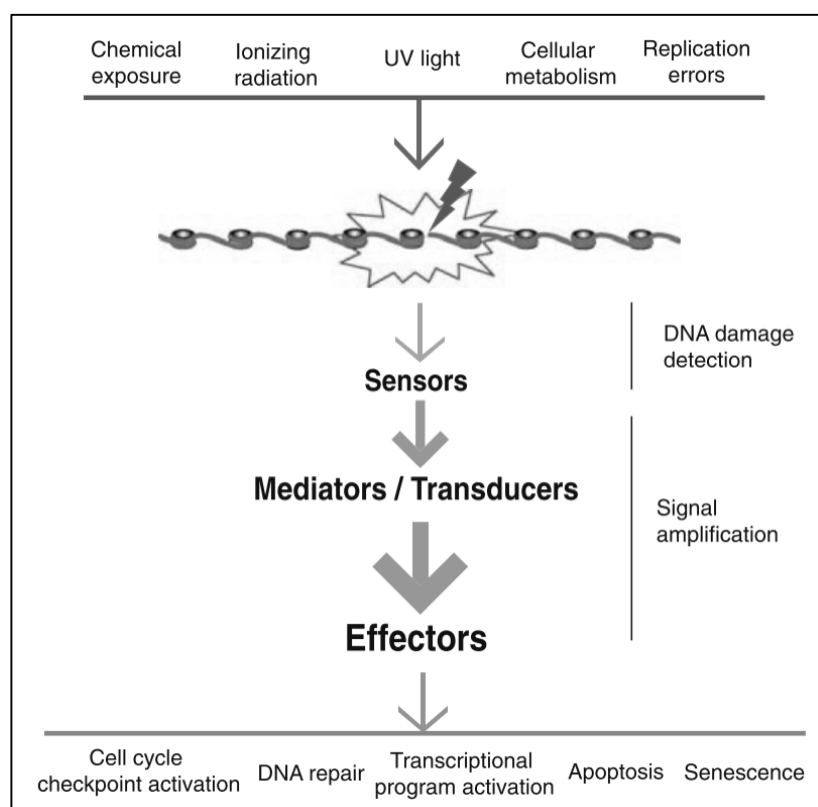


Figure 1.14: The DNA damage response. DNA damage caused by endogenous or exogenous sources is recognized by sensor proteins (detectors) which activate a signaling cascade. The signal is amplified by mediators/transducers and finally reaches the effector proteins, which are involved in triggering the cellular responses to DNA damage (Rupnik et al. 2010).

The DNA damage response will be discussed in regard to radiation-induced DSB as this type of DNA damage is the main focus of this research. The DNA double strand break is the most toxic type of DNA damage induced by ionizing radiation. The formation of local clustered lesions due to radiation-induced double strand breaks combined with single strand breaks and base damage within a small region of ten to 20 bp further complicates the repair. This

type of lesions is more common after exposure to more densely ionizing forms of radiation (Rothkamm & Lobrich 2002; Borgmann et al. 2016; Mladenov et al. 2016).

Detection of the DSB involves the activation of MRN complex, ATM and/or ATR (See chapter 3.3.1) (Matt & Hofmann 2016; Awasthi et al. 2015; Rupnik et al. 2010). The subsequent signaling cascade will determine the ultimate cellular response. The cellular response includes, but is not limited to, repair of the induced DNA damage via appropriate repair mechanisms (discussed in chapter 3.3.2), activation of checkpoints to delay cell cycle progression to allow repair (discussed in chapter 3.2.2) and controlled cell death or proliferation arrest if the damage is too extensive for repair (discussed in chapter 3.5) (Jackson & Bartek 2010; Matt & Hofmann 2016).

3.2 Cell cycle & cell cycle checkpoints

3.2.1 *The cell cycle*

In order to discuss cell cycle checkpoint arrest and DNA damage repair, insight in the cell cycle is necessary. During cell proliferation the cell passes four phases: G1 phase, S phase, G2 phase and mitosis (or M phase) (see Figure 1.15). Besides engaging in cell proliferation, the cell may enter a quiescent and often reversible G0 phase instead (Weinberg 2007). The first phase of the cell cycle is the G1 phase. During G1 phase, growth-regulating factors present in the extracellular environment might influence the decision-making process. At this point, the cell decides whether conditions are favorable to continue cell division or whether an arrest in G1 phase or progress in G0 phase is necessary. Once committed to cell division - indicated by passing the R-point of G1 phase -, the cell prepares itself to complete the cell cycle consisting of the S phase, followed by the G2 phase and mitosis. Progression through these phases of the cell cycle is highly regulated by cyclins and cyclin dependent kinases (see Figure 1.15) (Weinberg 2007; Strachan & Read 2011).

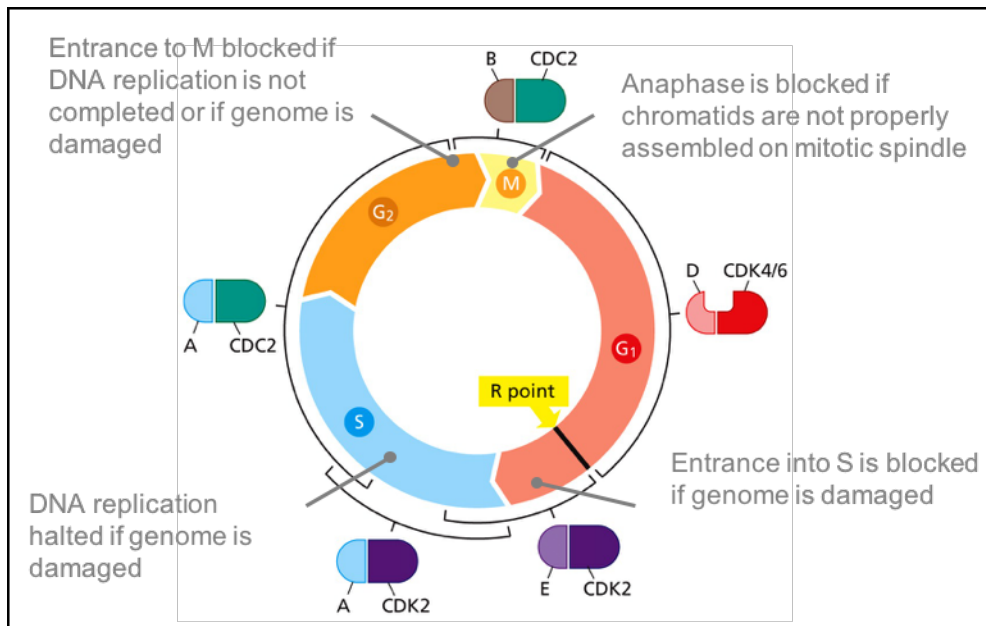


Figure 1.15: Scheduled rise, decline and (de)phosphorylation of certain cyclins and cyclin dependent kinases (CDK) in function of the cell cycle phases result in a tight interplay between these proteins and the cell cycle progression. During G₁ phase of the cell cycle, CDK4 and CDK6 interact with D-type cyclins. Once past the R point, E-type cyclins will associate with CDK2. Whilst progressing to the S-phase, A-type cyclins replace the E-type cyclins. Towards mid/end S-phase and during G₂ phase, A-type cyclins interact with CDC2 (also known as CDK1). Finally, CDC2 will interact with B-type cyclins in preparation of Mitosis (M-phase). Immediately after M phase, B-type cyclin levels drop due to protein degradation and the scheme repeats itself. The cell also possesses four cell cycle checkpoints, one in every phase of the cell cycle. The checkpoints and its purpose are indicated in grey. Adapted from (Weinberg 2007).

The main goal of the S-phase is a complete and accurate DNA replication. This is an enormous challenge as the genome contains an estimated 3.2 billion base pairs. In order to duplicate the genome within an acceptable time frame, replication starts at several 100 to 1000 replication origins. At each site, a pre-replicative complex (pre-RC) initiates unwinding of the DNA double helix by means of helicases at the replication origin (see Figure 1.16). Furthermore, the pre-RC recruits B-family DNA polymerases to the site. This results in the formation of replication forks (Takeda & Dutta 2005; Lodish et al. 2007). The DNA replication fork is in essence the unwound DNA complete with all necessary proteins of the replication machinery (see Figure 1.16). The replication fork always proceeds from 5' to 3' along the leading strand for which duplication can progress continuously, starting from one RNA primer, by DNA polymerase. The lagging strand is duplicated in smaller, discontinuous segments, called Okazaki fragments. Each fragment is formed by an RNA primer (created by primase) and subsequently elongated by DNA polymerase. RNA primer fragments are subsequently

replaced with DNA by the DNA polymerase of the adjacent fragment and subsequent ligation to the neighboring fragment. While duplication takes place, RPA (replication protein A) protects the single stranded DNA (Lodish et al. 2007).

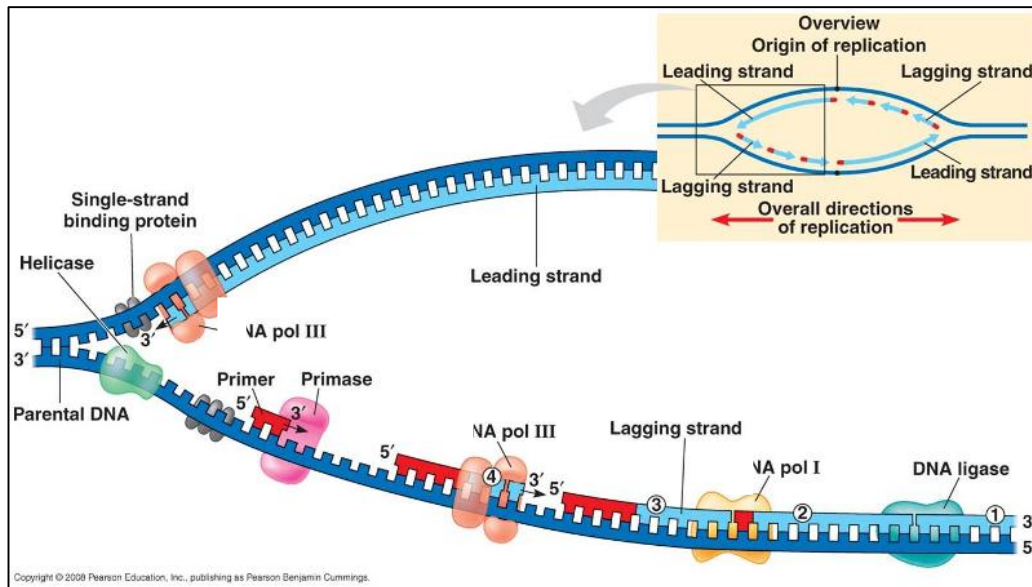


Figure 1.16: Overview of the origin of replication and the replication fork (see text). Adapted Figure. Copyright © 2008 Pearson Education, Inc. Pearson Benjamin Cummings.

In order to avoid extensive induction of errors during duplication, DNA polymerase δ – the dominant replication polymerase in humans – possesses proofreading capacity and the ability to correct errors. Still, the process is not completely error free and on average one mistake will be made every billion nucleotides (Lodish et al. 2007; Takeda & Dutta 2005).

Not only proper DNA duplication itself is a challenge for the replication machinery, also unresolved DNA damages form a challenge. These obstacles lead to slowing or stalling of the replication fork, also referred to as replication stress. The cell has the possibility to rely on other replication origins to finish replication or can activate replication-stress-response proteins (amongst which ATM and ATR) to maintain fork stability, overcome replication obstacles and complete DNA duplication under stress. However, stalled replication forks can also lead to formation of double strand breaks upon natural collapse (passive breakage) or due to endonuclease activity in an attempt to resolve the stalled replication fork (Lim & Kaldis 2013; Zeman & Cimprich 2014). Once a cell surpasses all challenges and completes DNA replication, the S phase is finalized and the cell can progression to G2 phase of the cell cycle (Takeda & Dutta 2005).

In the G₂ phase of the cell cycle the cell contains a double DNA content. This phase is characterized by rapid cell growth and protein synthesis in preparation of the mitosis (Weinberg 2007; Strachan & Read 2010).

During M phase or mitosis, the duplicated DNA – in the form of chromosomes each consisting of two sister chromatids – is divided amongst the two daughter cells. The mitosis is divided in four stages (prophase, metaphase, anaphase and telophase) and ends with the cytokinesis, which is the division of the cytoplasm and the formation of two new daughter cells (Weinberg 2007; Lodish et al. 2007).

A complete cell cycle varies in time pending on, amongst others, the cell type. Usually, a complete cell division in *in vitro* circumstances takes 20-30 hours (Strachan & Read 2011). However, in highly proliferating cells, the cycle is shorter and takes between 10 to 20 hours (Lodish et al. 2007) and extremely fast proliferating cells in embryos may do so even more rapidly (Weinberg 2007).

The position of the cell in the cell cycle at time of irradiation has an influence on the cellular response. In general, cells are most radiosensitive in G₂ and M phase of the cell cycle as a double DNA content is present. On the contrary, they are most radioresistant in S phase, at time of DNA duplication, due to activated DNA repair mechanisms for supervision of the replication process (La Torre Travis 1989).

3.2.2 *Cell cycle checkpoints*

In order to prevent DNA damage transmission to the daughter cells, a cell possesses monitoring mechanisms, called checkpoints. Throughout the cell cycle, four checkpoints aid in the maintenance of genomic stability (see Figure 1.15). They act on cell cycle progression through inactivation of several cyclins and cyclin dependent kinases, either via induction of transcription of certain inhibitory proteins or through posttranslational modifications (PTM) of mediator proteins. Checkpoint arrest through PTM of mediators is generally considered to be a fast process whereas induction of arrest by means of transcription induction is relatively slow. Removal of the PTM by specific enzymes or degradation of transcribed proteins

ultimately results in checkpoint silencing and completion of the cell cycle (Weinberg 2007; Lodish et al. 2007; Shaltiel et al. 2015).

The G1/S checkpoint prevents cells from starting DNA synthesis when DNA damage is detected. Upon detection by MRN and ATM of the DSB in the G1 phase, a fast p53-independent and a slower p53-dependent pathway result in the inactivation of the cyclin E/CDK2 complex in order to prevent transition to S phase (Shaltiel et al. 2015). The ATM-dependent G1/S phase checkpoint is highly sensitive and is activated after the detection of a single double strand break (see Figure 1.17) (Deckbar et al. 2011).

The mid S phase checkpoint, prevents CDC2 activation and progression to G2 phase and mitosis before completion of DNA duplication. In addition, this checkpoint responds to double strand breaks by the activation of both ATM (detection of a double strand break) and ATR (Ataxia telangiectasia and Rad3 related) (detection of single strand DNA due to end resection). The p53-dependant pathway loses its importance as downstream p21 is degraded in S phase. The p53 independent ATM pathway and the activation of ATR ultimately results in cyclin A/CDK2 inactivation and arrest in S phase (see Figure 1.17) (Shaltiel et al. 2015).

The G2/M checkpoint prevents cells with an incomplete or damaged genome to enter mitosis. ATM activation upon detection of a double strand break in G2 phase of the cell cycle leads to a similar response as in the G1 phase. Furthermore, ATR activation due to DNA end resection results in an additional reinforcing pathway. All activated pathways target cyclin A/CDK2 and cyclin B/CDK1 (or CDC2) activity to prevent entering of the mitoses and provide sufficient time for double strand break repair (Shaltiel et al. 2015). The G2/M checkpoint is less sensitive than the G1/S checkpoint. As much as ten to 20 double strand breaks would be necessary to arrest (highly damaged) cells in G2 phase (see Figure 1.17) (Deckbar et al. 2011; Löbrich & Jeggo 2007).

The M phase checkpoint is important for proper execution of the mitosis rather than detection and signaling of DNA damage. M phase arrest is activated by improper chromosome/mitotic spindle organization (Weinberg 2007; Lodish et al. 2007). Detection of a double strand break does not result in checkpoint activation as downstream factors are not activated (see Figure 1.17) (Shaltiel et al. 2015).

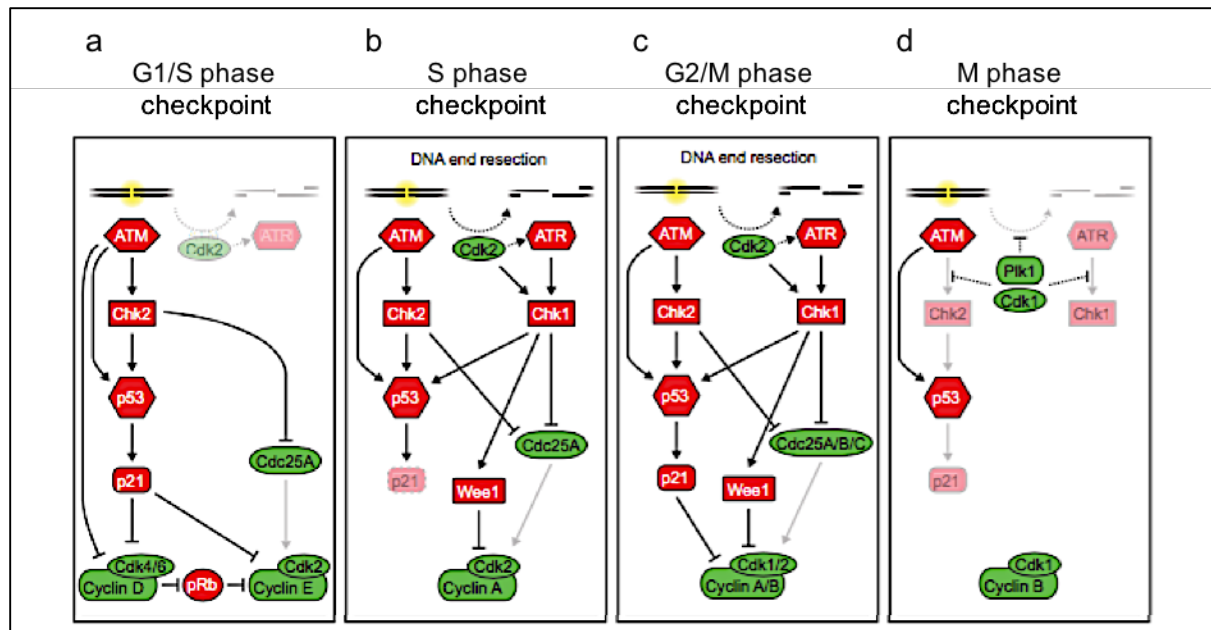


Figure 1.17: DNA damage signaling after double strand break induction

a. the presence of a double strand break in the G1 phase of the cell cycle results in the activation of ATM. ATM subsequently activates Chk2 (checkpoint kinase 2), a kinase which, together with ATM stabilizes p53. P53 leads to transcription of p21 which in turn inhibits Cyclin E/CDK2 in prevention of progression to S phase. In addition, Chk2 phosphorylates Cdc25A (cell division cycle protein), which leads to its inactivation. Absence of the phosphatase activity of Cdc25A keeps the Cyclin E/CDK2 complex in its phosphorylated form, unable to activate cell cycle progression to S phase.

b. In S phase, a double strand break undergoes end resection due to CDK2 phosphorylation of CtIP and Exo1 leading to single strand fragments. The double strand break activates ATM, whereas the single strand DNA results in ATR activation. ATM activates chk2 and results in Cdc25 phosphorylation. However, downstream accumulation of p21 via p53 is interrupted by ubiquitin ligase. ATR on the other hand activates Chk1, leading to both Cdc25A inhibition (phosphatase) and Wee1 (kinase) activation. As during G1 phase, inactive phosphatase cdc25A results in phosphorylated CDK2. In addition, activated Wee1 phosphorylates CDK2. Both pathways lead to the inactivation of the Cyclin A/CDK2 and S phase arrest.

c. In G2 phase, ATM inhibits cell cycle progression in a similar manner as during G1 phase. In addition, end resection results in ATR activation and the inhibition and activation of Cdc25 and Wee1 respectively. The net result is the inactivation of both Cyclin A/CDK1 (or Cdc2) and Cyclin B/CDK1 (Cdc2) to arrest the cell in G2 phase of the cell cycle.

d. During mitosis, Plk1 (Polo-like kinase 3) and CDK1 (Cdc2) inhibit activation of Chk1 and Chk2 respectively. Furthermore, both proteins phosphorylate several DNA repair proteins. This results in the inhibition of double strand break repair and checkpoint arrest.

Adapted (Shaltiel et al. 2015).

3.2.3 *BRCA1 in cell cycle checkpoint arrest*

BRCA1 is necessary for both G1/S and G2/M checkpoint activation through signaling of DNA damage (Löbrich & Jeggo 2007). Its effect on the G2/M checkpoint could be dual. Yarden et al. demonstrated an activation of Chk1 by BRCA1, subsequently leading to Cdc25 inhibition and Wee1 activation. Another possibility is direct ubiquitination of Cdc25 and Cyclin B. This would be achieved by heterodimer formation and subsequent activation of E3 ubiquitin ligase activity with BARD1 (BRCA1 associated RING domain 1) through RING domains on both proteins. All pathways eventually result in inactivation of the Cyclin B/Cdc2 (CDK1) complex and G2 arrest (Yarden et al. 2002; Shabbeer et al. 2013).

3.3 Repair of radiation-induced DSB

3.3.1 *Detection and signaling of a DNA double strand break*

Activation of the DNA damage response begins with the detection of the DNA damage. Pending on the type of DNA damage, specific proteins will detect and signal its presence to activate a multitude of cellular responses. For DNA DSB breaks, two major sensors are identified.

The first sensor is the MRN complex, reviewed by Rupnik et al. (Rupnik et al. 2010).

The MRN complex is composed of RAD50, NBS1 (Nibrin) and MRE11. MRE11 nuclease forms a homodimer and catalyzes the basic MRN function of DNA binding. The MRE11 homodimer interacts with RAD50 and NBS1 by means of a C- and N-terminal domain respectively (Williams et al. 2008). RAD50 plays a role in DNA binding, the unwinding and/or tethering of the DNA break ends (de Jager et al. 2002). NBS1 serves as a regulator protein. It does not possess any enzymatic activities, but is essential for the nuclear localization of both MRE11 and RAD50 (Cerosaletti et al. 2000). It also catalyzes the focal assembly of the complex (Lee & Paull 2004) and finally, it stimulates the activities of both MRE11 and RAD50 (Lee et al. 2003).

Recruitment of MRN to the DSB site results in activation of DNA checkpoint kinase ATM (see Figure 1.18). The inactive ATM dimers undergo autophosphorylation at Ser residue 1981, which result in active monomers. In order to achieve ATM activation at DSB sites, blunt ends

or short overhangs are needed. Presence of long overhangs (25 nucleotides and more), inhibits ATM activation and initiates ATR activation (Matt & Hofmann 2016; Paull 2015). Activated ATM subsequently activates an array of proteins needed for, amongst others, DNA repair and cell cycle arrest (Paull 2015). Upon its activation, ATM phosphorylates histone variant H2AX at serine residue 139, referred to as γ H2AX. Phosphorylated H2AX subsequently serves as a binding substrate for MDC1. Binding and activation of MDC1 protects γ H2AX from dephosphorylation and enhances ATM recruitment and binding at the DSB site. This further promotes the total γ H2AX signal and leads to an amplification loop (Paull 2015; Matt & Hofmann 2016). Besides coordination of the DNA repair, ATM is also directly involved in the initiation of HR (see chapter 3.3.2.2) (Matt & Hofmann 2016).

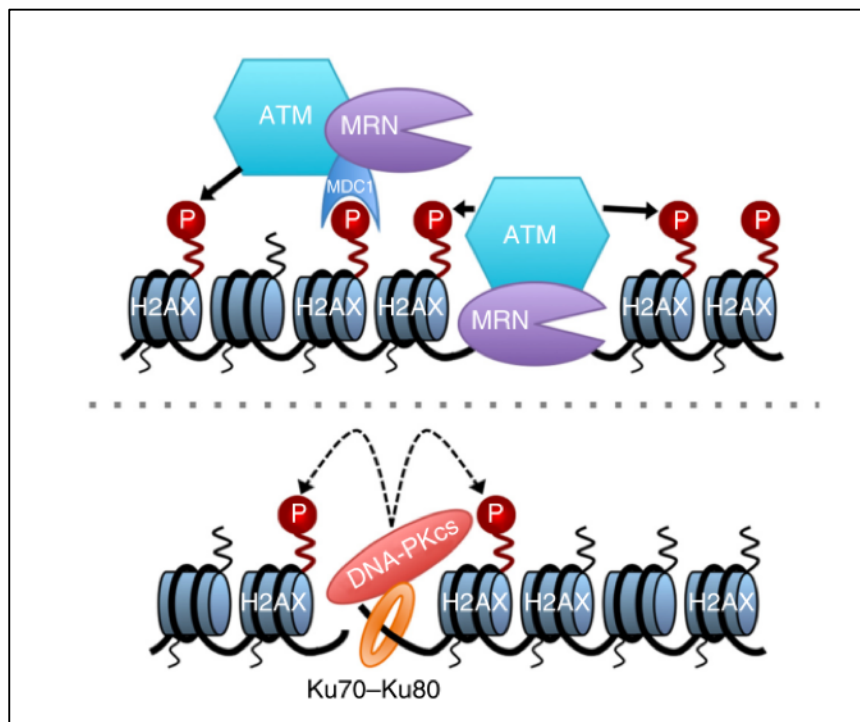


Figure 1.18: DNA damage detection and signaling by means of MRN and ATM (top) or Ku70/Ku80 and DNA-PKcs (bottom) (Hartlerode et al. 2015).

Besides activation of the MRN complex/ATM and subsequent initiation of DNA repair and cell cycle arrest, DNA DSBs are also detected by the Ku70/Ku80 heterodimer which binds blunt free DNA ends (Hartlerode et al. 2015) (see Figure 1.18). This second sensor relocates to the DSB site independently of the MRN complex. Ku70/Ku80 is activated upon DNA binding and recruits DNA-PKcs (DNA-dependent protein kinase; catalytic subunit) to the damage site.

DNA-PKcs subsequently coordinates non-homologous end-joining (discussed in chapter 3.3.2.1) and is furthermore also capable of phosphorylating H2AX (Matt & Hofmann 2016; Hartlerode et al. 2015). Both the Ku heterodimer and MRN are recruited within half a minute to the DSB site (Hartlerode et al. 2015).

3.3.2 *Pathways for the repair of radiation-induced DSB*

3.3.2.1 Non-homologous end- joining

Classical non-homologous end-joining (c-NHEJ) is the dominant repair pathway for radiation-induced DSB (DSB) in mammalian cells. NHEJ is active in all phases of the cell cycle except for mitosis as there is no repair in this particular phase (Heijink et al. 2013). The initial steps of c-NHEJ are the binding of the Ku70/Ku80 heterodimer to the DSB site and recruitment and activation of the catalytic subunit of DNA-dependent protein kinase (DNA-PKcs) (Walker et al. 2001) (see Figure 1.19). DNA-PKcs undergoes autophosphorylation and subsequently phosphorylates an array of DDR proteins, thereby regulating c-NHEJ (Chan & Chen 2002). It recruits and phosphorylates Artemis nuclease to resolve damaged DNA ends of complex breaks, for example induced by ionizing irradiation (Deriano & Roth 2013). Furthermore, DNA-PKcs recruits several polymerases (e.g. pol μ and λ) and Terminal deoxynucleotidyl Transferase (TdT). DNA polymerase λ stabilizes the DNA ends. Polymerase μ is able to add nucleotides to a blunt end and TdT catalyzes the addition of multiple nucleotides without a DNA template. These three DNA end-processing activities create compatible DNA ends for ligation. Finally, PAXX (Paralog of XRCC4 and XLF) is recruited to the DSB site by Ku70/Ku80 to complete DNA ligation; assisted by Ligase4, XRCC4 (X-ray repair cross-complementing protein 4) and XLF (XRCC4-like factor) for stabilization of the DNA ends (Borgmann et al. 2016; Mladenov et al. 2016; Rodgers & Mcvey 2016 (and references herein)).

As c-NHEJ restores DSB without a template, it can be associated with the induction of small DNA alterations (Rodgers & Mcvey 2016), but can also result in larger chromosomal rearrangement, particularly translocations (Mladenov et al. 2016).

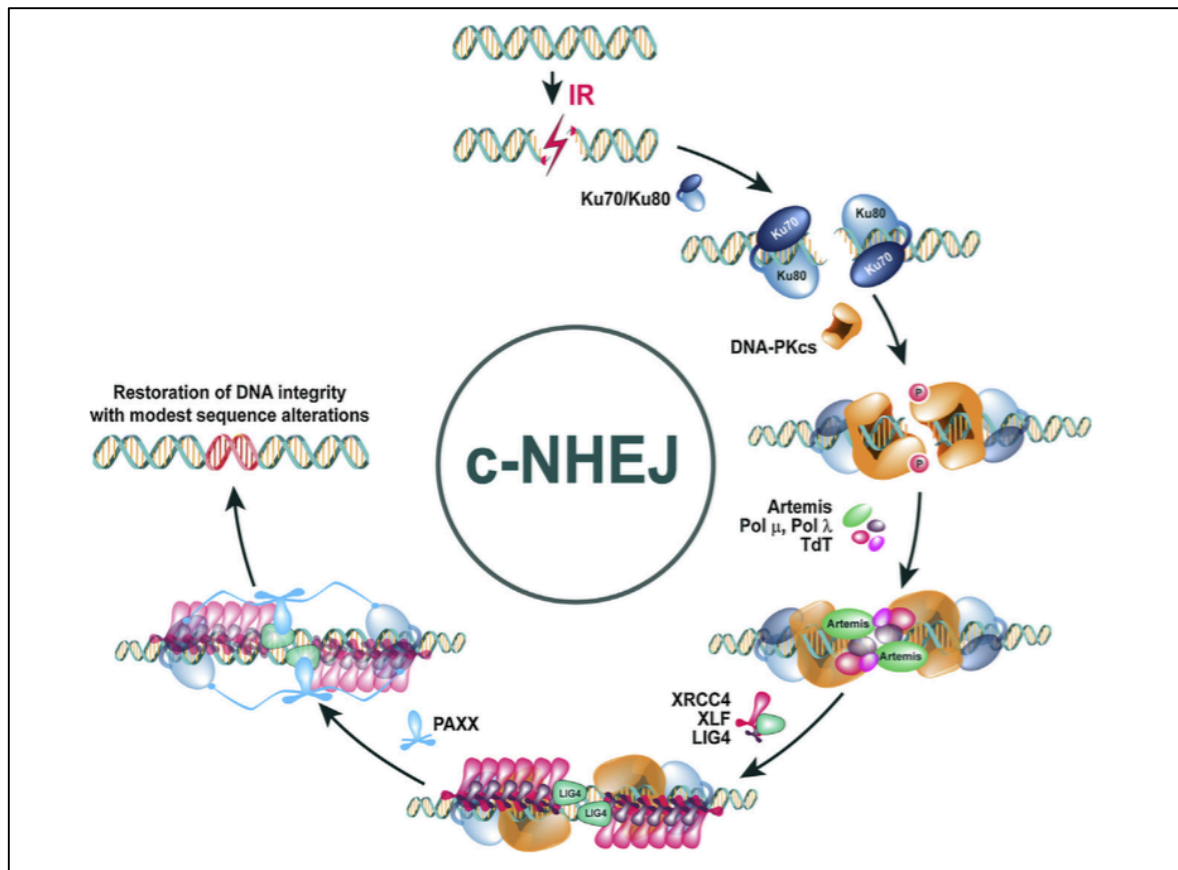


Figure 1.19: Schematic visualization of c-NHEJ (see text) (Mladenov et al. 2016).

3.3.2.2 Homologous recombination

HR is a pathway which relies on the sister chromatid available during the S and G2 phase of the cell cycle for DSB repair and can therefore only be activated when DSB are induced in these particular phases of the cell cycle. As it relies on a template, repair is largely error-free. However, the complex pathway results in a relatively slow repair and can take up to 7 hours (Mladenov et al. 2016; Mao et al. 2008a). Upon detection of the DSB by the MRN complex and signaling by ATM, HR relies on the MRN complex and the recruited CtIP for the initiation of the 5' to 3' end resection. Therefore, CtIP redirects the MRN complex role at the site of the DSB from DSB sensor to resection activator (You & Bailis 2010; Sartori et al. 2007). In a second phase, Exo1 (exonuclease 1) and Dna2/BLM (Bloom syndrome protein) are recruited to the DSB site for additional end resection. Exo1 binds the double stranded DNA with recessed 5' ends as produced by CtIP (CtBP-interacting protein) and MRN end resection. BLM, associated in a complex with Dna2 helicase, assists in the unwinding of the 3' DNA. Dna2 on the other hand is necessary for its endonuclease activity in the DNA resection (Liu & Huang 2016). The

resection-induced single stranded DNA is subsequently coated with RPA for stabilization. The RPA coated ssDNA is in essence a substrate for other repair proteins (Zou et al. 2006). One of those proteins is BRCA1. BRCA1 subsequently coordinates recruitment of BRCA2 and its binding partner PALB2 to the DSB site. BRCA2, assisted by RAD52, PALB2 and BRCA1, mediates HR by loading of RAD51 on the ssDNA, thus replacing RPA (Liu et al. 2010; Mladenov et al. 2016; Rodgers & Mcvey 2016). RAD51 is the key recombinase of HR and acts in a microfilament with its paralogs (see Figure 1.20). Accumulation of BRCA2, RAD51 and RAD51 paralogs at the DSB initiate the search for the homologous sequence and strand invasion (see Figure 1.21) (Mladenov et al. 2016; Rodgers & Mcvey 2016; McIlwraith et al. 2000).

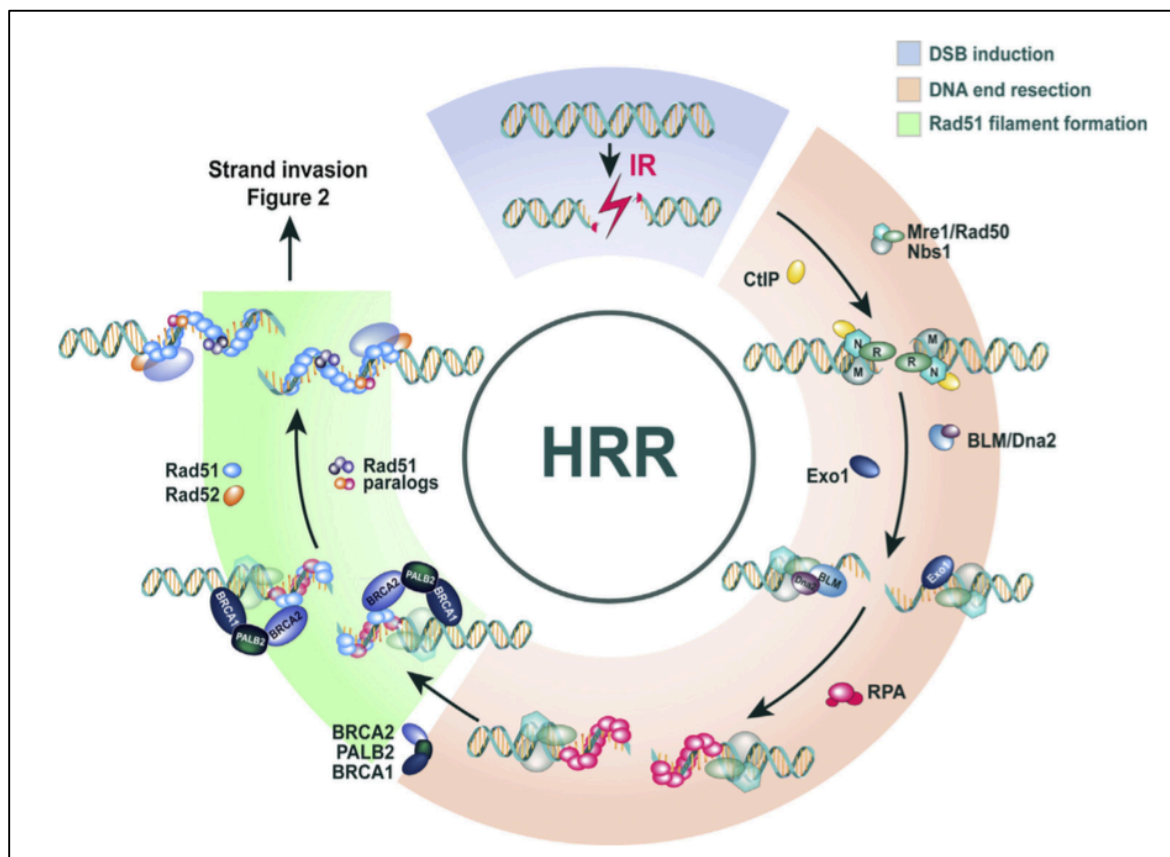


Figure 1.20: Schematic visualization of HR (see text) (Mladenov et al. 2016).

After RAD51 filament formation, the search for the homologous sequence and strand invasion, three different pathways can be initiated to allow DSB repair.

The first pathway, double-strand break repair (DSBR) (see Figure 1.21 middle panel), results in a displacement loop (D-loop) after strand invasion, in which the 3' end of the broken DNA aligns with the invaded strand. DNA polymerases subsequently elongate the DNA, thereby extending the D-loop. The extended D-loop results in the alignment of the displaced strand

with the 3' single strand tail, with the formation of a double holiday junction. Upon successful elongation and ligation of the DNA, this holiday junction is resolved by endonucleases, more specifically, resolvases. This results in formation of either crossover or non-crossover products. Despite being perceived as largely error-free because of the use of a DNA template, DSBR can induce errors due to the use of an error-prone polymerase (polymerase ζ) and the instability of large stretches of ssDNA (Mladenov et al. 2016; Rodgers & Mcvey 2016; Li & Xu 2016).

The second pathway, synthesis-dependent strand annealing (SDSA) (see Figure 1.21 left panel), initially follows the DSBR pathway. However, the extension of the D loop leads to unwinding of this loop, re-annealing to the other 3' end of the broken strand and filling of the gaps. SDSA never results in crossover products. SDSA could be perceived as more conservative as the template DNA remains intact. However, as the D-loop unwinds, the newly formed DNA has the possibility to align with sequences other than the other end of the DSB, which could result in mutagenesis (Mladenov et al. 2016; Rodgers & Mcvey 2016).

A third, alternative option is break-induced replication (BIR) (see Figure 1.21 right panel). BIR, in essence a specific pathway for repair of one-ended DSB, relies on the synthesis of large sections of DNA (as large as 100 kb). However, BIR is also described as backup for SDSA and DSBR. BIR completes repair by initiation of a replication fork and relies on common replication factors and on a few specific polymerases (Pol32/PolD3). DNA repair starts with invasion of the template DNA and synthesis following the leading strand. DNA synthesis of the lagging strand completes BIR. BIR is also perceived as being a more error-prone type of HR DSB repair because of occurrence of template switching. BIR can even result in complex chromosomal translocations if multiple template switches occur (Mladenov et al. 2016; Rodgers & Mcvey 2016).

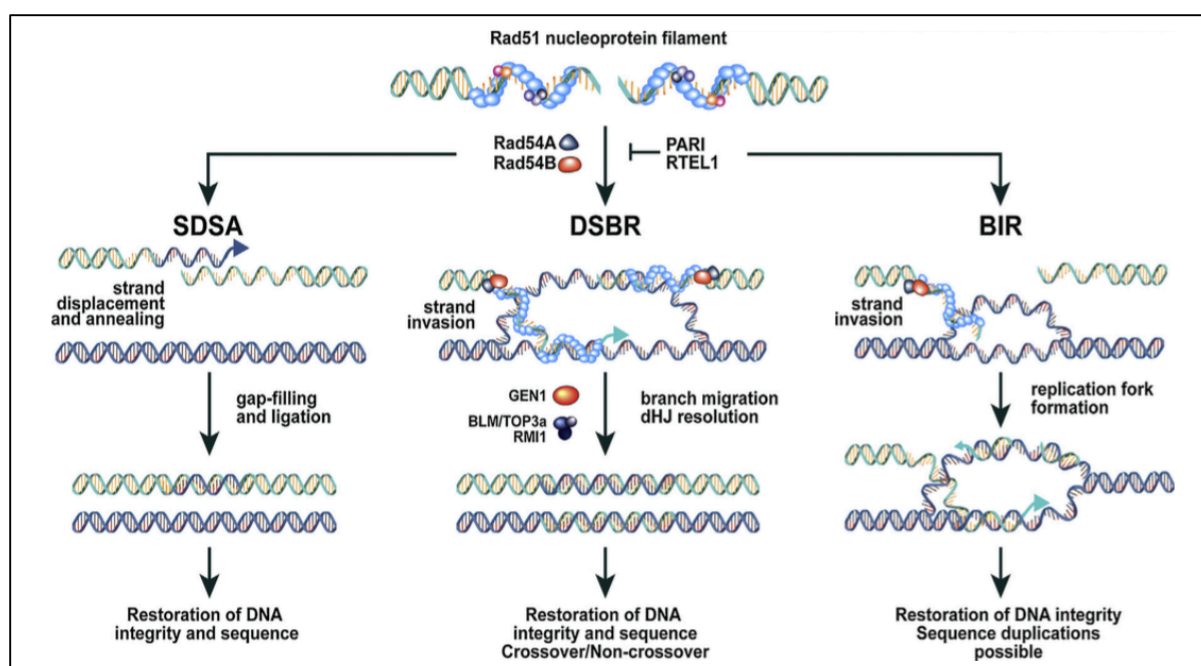


Figure 1.21: Schematic visualization of the three different pathways for repair of the DSB by HR (see text) (Mladenov et al. 2016).

3.3.2.3 Alternative DSB repair pathways

Besides the previously discussed c-NHEJ and HR, the cell also resorts to backup mechanisms to repair radiation-induced DSB. To date, there are three main alternative pathways described: Alternative NHEJ (Alt-EJ) (also referred to as theta-mediated end joining (TMEJ) or backup NHEJ (B-NHEJ)), microhomology-mediated end-joining (MMEJ) and single strand annealing (SSA). All these backup mechanisms lead to erroneous repair of the DSB, however, the different pathways are not always fully understood (Mladenov et al. 2016; Rodgers & Mcvey 2016; Deriano & Roth 2013).

Alternative end-joining (Alt-EJ) starts with the binding of PARP1 (poly (ADP-ribose) polymerase 1) to the DSB site where it competes with the Ku70/Ku80 heterodimer. The subsequent binding of CtIP and MRN results in DNA end resection. Polymerase θ (POLQ) subsequently interacts with the resected DNA and initiates elongation of the DNA ends using the opposite ssDNA sequence as template. Finally, ligase 1 and 3 ligate the DSB ends, either in absence or presence of XRCC1 (see Figure 1.22) (Mladenov et al. 2016; Soni et al. 2014). Repair by Alt-EJ is more error-prone than c-NHEJ. Not only are small deletions and/or insertions of DNA observed after repair, alt-EJ also results in a higher number of chromosomal

translocations. This increase could be due to the absence of Ku-heterodimer binding at the DSB site in alt-NHEJ, which stabilizes the ends of the DSB, and the slower repair kinetics, allowing for exchange at sites with multiple DSB close to each other and resulting in chromosomal translocations (Deriano & Roth 2013; Rodgers & Mcvey 2016).

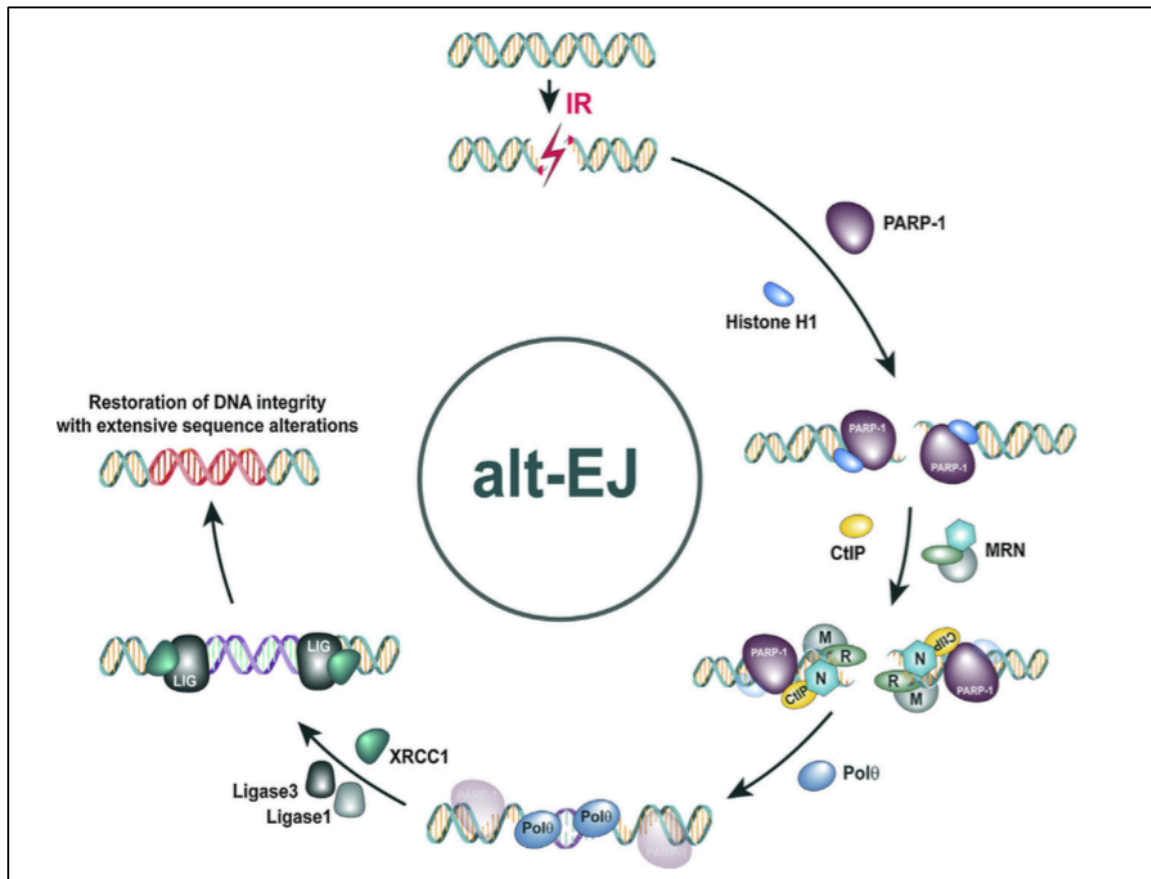


Figure 1.22: Schematic visualization of alternative end joining (see text) (Mladenov et al. 2016).

Alternative end-joining may rely partly or completely on microhomology. This is possible due to end resection by CtIP and MRN, and would rely on the use of a small number of nucleotides (usually 2-4 nt) for DNA alignment, possibly catalyzed by polymerase θ , and subsequent ligation. Microhomology-mediated end-joining (MMEJ) has also been described as a backup repair pathway and demonstrates large resemblance with microhomology-driven alt-EJ. MMEJ would require larger homologous fractions, typically six to 20 nucleotides, but it also relies on DNA end resection and proteins such as PARP1, ligase 1 and ligase 3. Whereas MMEJ relies on end resection for unveiling of microhomologous fragments, alt-EJ can resort to activation of polymerase θ for (template dependent or independent) synthesis of new DNA,

which could mediate as microhomologous sequences. In this regard, Alt-EJ could be referred to as synthesis-mediated MMEJ (SM-MMEJ) (Mladenov et al. 2016; Rodgers & Mcvey 2016; Yu & McVey 2010).

Single Strand annealing (SSA) is often described as an extreme version of MMEJ or alt-EJ (or SM-MMEJ). However, it also shows similarities to HR (Mladenov et al. 2016; Rodgers & Mcvey 2016). SSA typically occurs when the DSB is induced in genomic loci with extensive homology. It relies on extensive end resection to reveal complementary DNA ends with the length of the complementary sequences varying between 25 nt and multiple kilobases. SSA relies on CtIP for end resection and RPA for stabilization of the ssDNA. RAD52 mediates annealing of the homologous DNA and DNA ligase 1 ligates the DNA sequences. ERCC1 and XPF nucleases foresee in trimming of the created DNA tails. Repair of DSB via SSA results in deletion of DNA sequences of variable length, but could, in specific situations, also result in translocations (see Figure 1.23) (Mladenov et al. 2016; Rodgers & Mcvey 2016; Bhargava et al. 2016)



Figure 1.23: Schematic visualization of single strand annealing (Mladenov et al. 2016).

3.3.2.4 PARP activity and inhibition – A breast cancer targeted therapy

PARP function

PARP1 catalyzes poly(ADP-ribosyl)ation (PARylation), a post translational modification, of several proteins including DNA damage repair proteins. It was initially identified as necessary for efficient repair of single strand breaks by means of base excision repair (BER) but also appears to be involved in nucleotide excision repair and DSB repair (Khodyreva & Lavrik 2016). Both PARP1 and PARP2 are necessary for SSB repair by BER. The proteins have an overlapping function, but differences in their substrate preferences are noticeable (Langelier et al. 2014). In short, the detection of a SSB and binding of PARP1/2, results in its activation. This activation results in autoPARylation with NAD^+ as substrate and subsequent dissociation of PARP at the SSB. This allows access of other repair factors, such as XRCC1 to bind and repair the SSB (see Figure 1.24, left panel (A-D)) (Pommier et al. 2016).

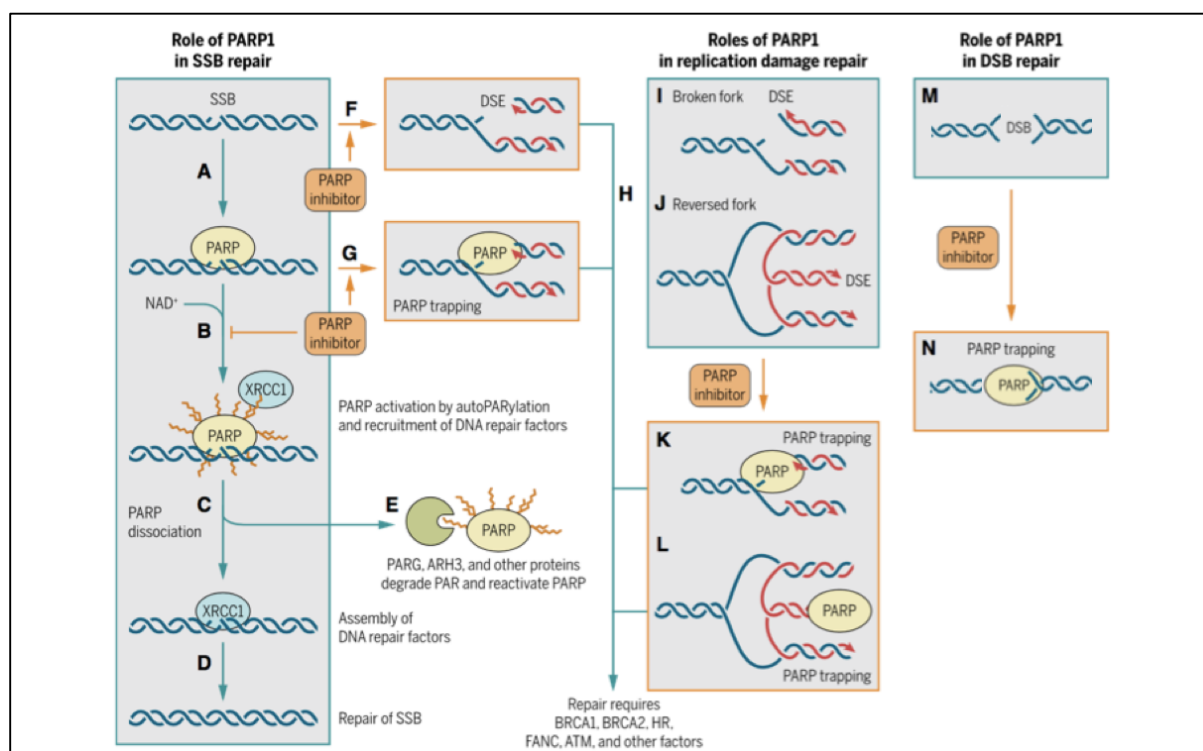


Figure 1.24: DNA repair by PARP1 and the effects of PARP inhibitors (see text) (Pommier et al. 2016) (adapted). DSE = single-ended DSB

In addition to its role in SSB repair, PARP1 is also involved in (single-ended) DSB repair (see Figure 1.24 M). PARP1 competes with the Ku70/80 heterodimer for binding of DSB ends. Binding of the Ku heterodimer results in NHEJ. During NHEJ, PARP1 binds to DNA-PKcs and

PARylates its catalytic subunit, thus increasing its kinase activity. On the other hand, binding of PARP1 instead of Ku70/Ku80 to the DSB promotes alt-EJ or HR. Furthermore, PARP1 is involved in the resolution of stalled replication forks (see Figure 1.24 I & J). PARP1 binds to stalled replication forks where it aids in recruitment of the MRN complex and initiations of HR (Khodyreva & Lavrik 2016; Pommier et al. 2016). Finally, PARP1 also has a role in nucleotide excision repair (NER), a repair pathway for bulky adducts, induced by short-wavelength UV light (Khodyreva & Lavrik 2016).

PARP inhibition

PARP inhibition is a targeted therapy which exploits HR deficiency in tumor cells. This characteristic is predominantly observed in *BRCA1* and *BRCA2* mutation carriers, as the second, still functional allele is lost in tumor cells (loss of heterozygosity). However, tumors who exhibit a HR deficiency without the germinal mutation in *BRCA1* or *BRCA2*, so called 'BRCAness', may also benefit from this treatment. Impaired HR activation may be due to inactivating mutations or epigenetic alterations in other genes involved in HR (see Table III) (Lord & Ashworth 2016).

Table III. Overview of all cancer-associated alterations in BRCAness genes (Lord & Ashworth 2016).

Gene	Tumour types with somatic alterations (mutations, gene deletions and promoter hypermethylation)	Tumour types and syndromes with germline mutations
ATM	T-PLL, breast cancer, GBM, ccRCC, lung adenocarcinoma, sarcoma, and prostate, gastric, bladder, colorectal, uterine and pancreatic cancer	Leukaemia, lymphoma, medulloblastoma, glioma and ataxia telangiectasia
ATR	Breast, colorectal, head and neck, gastric and uterine cancer	Oropharyngeal cancer and familial cutaneous telangiectasia and cancer syndrome
BAP1	ccRCC, cholangiosarcoma, liver cancer and uveal melanoma	Mesothelioma and uveal melanoma
BRCA1	TNBC, HGS-OvCa, lung cancer, prostate cancer, mCRPC and PDAC	TNBC, HGS-OvCa and PDAC
BRCA2	Breast cancer, HGS-OvCa, PDAC, prostate cancer, mCRPC, gastric, bladder and lung cancer, DLBCL and sarcoma	Breast cancer, HGS-OvCa, PDAC and leukaemia
CDK12	HGS-OvCa?, mCRPC and gastric cancer	
CHEK2 (CHK2)	Uterine cancer and HGS-OvCa	Breast cancer
FANCA	HGS-OvCa and lung adenocarcinoma	AML, leukaemia and Fanconi anaemia
FANCC		AML, leukaemia and Fanconi anaemia
FANCD2	ccRCC	AML, leukaemia and Fanconi anaemia
FANCE		AML, leukaemia and Fanconi anaemia
FANCF		AML, leukaemia and Fanconi anaemia
PALB2	Gastric cancer and HGS-OvCa	Wilms tumour, medulloblastoma, AML, Fanconi anaemia, breast cancer, PDAC and HGS-OvCa
NBS1 (NBN)	Gastric and uterine cancer	
WRN	HGS-OvCa, mCRPC, lung adenocarcinoma and uterine cancer	Werner syndrome
RAD51C	HGS-OvCa	Breast cancer and HGS-OvCa
RAD51D		Breast cancer and HGS-OvCa
MRE11A	Colorectal cancer	
CHEK1 (CHK1)	PDAC and sarcoma	
BLM		Bloom syndrome
RAD51B	HGS-OvCa	
BRIP1	HGS-OvCa	

In 2014, Olaparib (commercially available as Lynparza, AstraZeneca, UK) was the first PARP inhibitor to be approved by the American Food and Drug administration (FDA) and European Medicines Agency (EMA) for treatment of advanced ovarian cancer due to a germline or somatic *BRCA1* or *BRCA2* mutation carriers (Brown et al. 2016; Kim et al. 2015). However, several other promising PARP inhibitors are currently tested in different clinical trials, including rucaparib, niraparib and veliparib. In June 2016, the FDA accepted the submission of rucaparib (Clovis Oncology, USA) for accelerated approval (Businesswire 2016).

The activity of a PARP inhibitor, such as Olaparib, is dual. On the one hand, it inhibits repair of single strand breaks by inhibition of both PARP1 and PARP2 (see Figure 1.24 F). On the other hand, it traps PARP at the DNA damage site resulting in toxic PARP-DNA complexes (see Figure 1.24 G, K, L and N). PARP trapping is only partially understood, but may be the result

of direct interactions of the inhibitor with the PARP NAD⁺ binding site (Murai et al. 2012; Pommier et al. 2016).

The failure to repair SSB results in a stalled replication fork during synthesis. This unstable complex might subsequently collapse, resulting in a single-ended DSB (DSE). In addition, a DSE can also be induced to resolve blocked replication forks. The cell subsequently relies on factors such as BRCA1 and BRCA2 and HR to resolve these induced DSE (see Figure 1.24 F) (Pommier et al. 2016; Zeman & Cimprich 2014; Lim & Kaldis 2013). PARP trapping is considered more deleterious than the non-repaired SSB. However, the mechanisms are not fully understood. One possibility is the collision of the replication fork at the PARP-DNA complexes. This subsequently results in the collapse of the replication fork and the formation of a DSE. Again, the cell must rely on BRCA1/BRCA2 mediated HR for repair (Pommier et al. 2016). However, HR deficient tumor cells struggle to cope with the induced damage while heterozygous cells still express BRCA1 and BRCA2 and therefore, HR can be initiated. This ultimately leads to tumor-specific cell death and is referred to as synthetic lethality as only the combination of BRCA1/2 protein loss in the tumor cell and PARP inhibition is lethal (Pommier et al. 2016; Murai et al. 2012; Lord & Ashworth 2016).

3.3.3 *Pathway choice for repair of radiation-induced DSB*

3.3.3.1 Cell cycle phase

Pathway choice relies on a complex interplay of proteins and is not completely understood. The phase of the cell cycle determines, to a great degree, the choice of DSB repair pathway. Classically, c-NHEJ is presented as the pathway of first choice and its activity is predominant throughout all phases of the cell cycle, except for mitosis. During S and G2 phase, the presence of the homologous sister chromatid allows HR. However, studies demonstrated that HR is predominantly upregulated in S-phase, as it is important in replication-induced DSB repair. The use of this repair pathway declines again during G2 phase in favor of NHEJ (Mao et al. 2008b; Li & Xu 2016; Mladenov et al. 2016). Besides these two traditional repair pathways, the cell also has a selection of backup repair pathways which may be activated in different phases of the cell cycle (Mladenov et al. 2016).

In essence, DSB end resection is the divergent step in the DSB repair pathway choice (Li & Xu 2016). In first instance, the cell relies on c-NHEJ, however, failure of the Ku heterodimer to detect or bind to the DSB or failure of DNA-PKcs to initiate c-NHEJ allows for end resection of the DSB, guiding the repair towards SSA, MMEJ, alt-EJ or HR (Kakarougkas & Jeggo 2014; Mladenov et al. 2016). End resection is upregulated during S and G2 phase of the cell cycle, allowing for an upregulation of HR in these phases of the cell cycle, in addition to SSA, MMEJ and alt-EJ. This upregulation is predominantly associated with CtIP activity in S and G2 phase of the cell cycle due to CDK2 and BRCA1 modifications (Ceccaldi et al. 2016; You & Bailis 2010).

53BP1 (p53-binding protein 1), on the other hand, promotes c-NHEJ during G1 phase of the cell cycle as it restricts end resection (Li & Xu 2016; Mladenov et al. 2016). 53BP1 interaction at the DSB is mutually exclusive with BRCA1. The presence of 53BP1 results in c-NHEJ, while binding of BRCA1 guides repair towards HR during S and G2 phase of the cell cycle (Panier & Boulton 2014; Li & Xu 2016). However, as discussed previously, the underlying 'decision process' is not completely understood. Recent studies demonstrated that 53BP1 also promotes MMEJ during G1 phase of the cell cycle. End resection for MMEJ would involve the activation of the MRN complex and CtIP appears to be BRCA1 dependent (Xiong et al. 2015). Furthermore, alt-EJ is also active in G1 phase of the cell cycle as backup mechanism (Mladenov et al. 2016). In addition, BRCA1 might act in a cell cycle dependent manner according to Saha and Davis (2016). They propose a key role for BRCA1 in promotion of precise DSB repair as it induces c-NHEJ in G1 phase and HR in S and G2 phase (see Figure 1.25). Pathways known to be relatively error-free compared to their backup mechanisms (Saha & Davis 2016).

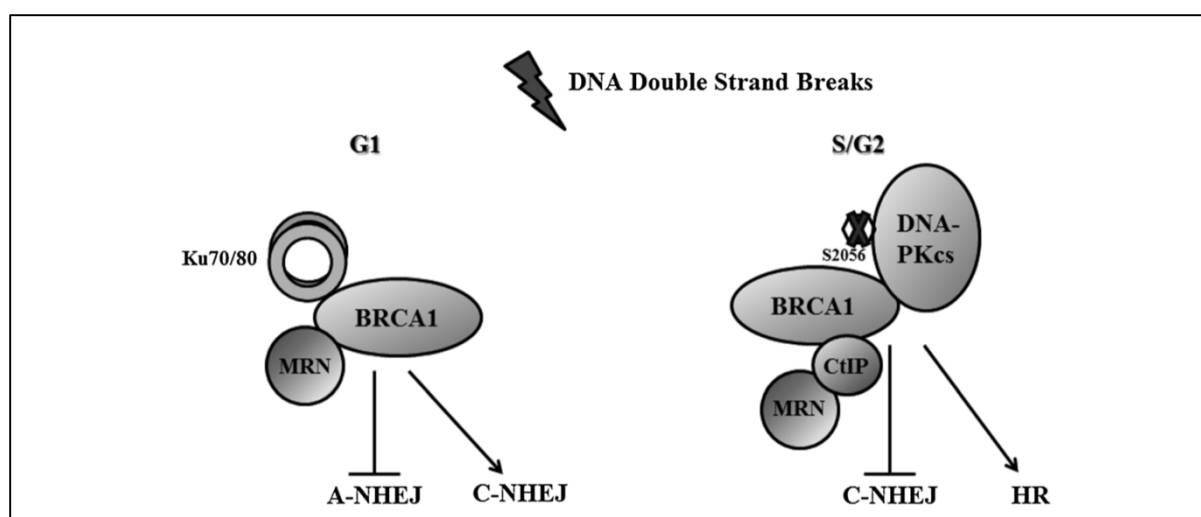


Figure 1.25: BRCA1 interactions during G1 and S/G2 phase for repair of radiation-induced DSB (see text) (Saha & Davis 2016). A-NHEJ = Alt-EJ

During mitosis, DSB are not actively repaired as certain parts of the DDR are blocked despite ATM signaling. DSB are rather marked for repair after completion of mitosis, during G1 phase of the cell cycle (Heijink et al. 2013).

3.3.3.2 Complexity of the DSB

Another factor influencing DSB repair is the complexity of the lesion. High-LET ionizing radiation gives rise to complex DSB lesions containing multiple DSB, SSB and base damage. Whereas more simple DSB induced by low-LET radiation are usually rejoined within a matter of hours, high-LET DSB lesions are more persistent, indicating a repair failure (Lorat et al. 2016). Okayasu's mini-review concerning DNA repair upon one specific high-LET radiation quality, heavy ion irradiation, provides insights in DNA repair pathways, repair kinetics and misrepair. As these complex lesions are more difficult to repair, the slower repair kinetics may subsequently cause an increase in misrepair of DSB and chromosome breaks in cells exposed to heavy ions (Okayasu 2012). Several studies revealed that c-NHEJ is not the pathway of choice for repair of high-LET DSB and demonstrated that the damaged cell rather relies on HR, MMEJ and alt-EJ for repair. All these pathways demand DSB end resection, which partially explains the slower repair kinetics (Lorat et al. 2016; Okayasu 2012; Wang et al. 2008; Taleei & Nikjoo 2013).

3.3.3.3 Chromatin structure

DSB repair is furthermore complicated by the chromatin structure. Variation in chromatin structure does not necessarily influence the pathway choice, but it affects the repair kinetics (Taleei & Nikjoo 2013). DNA undergoes several levels of compaction to fit the nucleus. In order to achieve this compaction, DNA is complexed with various proteins, histones, and subjected to coiling and supercoiling to form chromatin. Chromatin occurs in two different degrees of compaction. Euchromatin is an active and more extended state of DNA condensation which allows for transcription of genes. Euchromatin allows for variations in gene expression pending on cell type or functional requirements. Heterochromatin, on the other hand, is highly condensed. Genes located in heterochromatin are typically not expressed (Strachan & Read 2011). Because of its high compaction, DSB in heterochromatin are difficult to access for DDR proteins and require relaxation mediated by KAP1 (KRAB-associated protein 1), which results in a slower repair kinetic. Chromatin remodeling by KAP1 is initiated by ATM activation after which the DSB will be repaired by c-NHEJ in G1 phase and c-NHEJ or HR in S/G2 phase. DNA repair in function of chromatin condensation is reviewed by Goodarzi et al. (Goodarzi & Jeggo 2012; Matt & Hofmann 2016; Hartlerode et al. 2015; Taleei & Nikjoo 2013).

3.4 Extensive DNA damage and cell death

If the DNA damage is too extensive and/or damage is irreparable, the cell can trigger proliferation arrest or cell death instead of repair. Apoptosis is a highly regulated form of cell death which results in the destruction and removal of the damaged cell in order to protect the organism. Alterations in the control of apoptosis contributes to cancer formation. Cell death can also occur in a mitosis-linked form, the mitotic catastrophe, which is the result of premature mitosis-entry. Senescence on the other hand inclines a permanent arrest of the cell cycle. However, this mechanism can be overrun. Furthermore, the cell remains active and is able to secrete pro-inflammatory cytokines. Whereas apoptosis and necrosis create a permanent solution, damaged senescent cells keep posing a source of danger (Baumann et al. 2009; Matt & Hofmann 2016). Additionally, cells, such as hematopoietic stem cells can resort to differentiation upon detection of extensive DNA damage to prevent the transfer of damage DNA to daughter cells (Wingert & Rieger 2016).

Apoptosis is a highly organized cell death pathway. This pathway results in the efficient removal of damaged cells either due to intrinsic or extrinsic damage (Matt & Hofmann 2016). Both pathways ultimately result in caspase activation and the formation of apoptotic bodies, the first step of the orchestrated cell degradation. A dominant player in these apoptosis pathways is p53, which is activated upon ATM signaling of the DNA damage results (Matt & Hofmann 2016; Sullivan et al. 2012). P53 is not only necessary for apoptosis, but its activation upon detection of DNA damage also results in a multitude of effects including cell cycle arrest (discussed in chapter: 3.2.2 Cell cycle checkpoints). The fine-tuning of these different outcomes is not well understood. However, posttranslational modification and differences in accessibility and sensitivity of response elements for cell cycle arrest and apoptosis might play a role. Furthermore, cell type and stimulus specific factors might have an influence (Matt & Hofmann 2016; Sullivan et al. 2012). In addition to the p53-dependent apoptosis, the cell can also initiate a p53-independent apoptosis pathway. This pathway relies on chk1/chk2 activation by ATM/ATR and the increased expression of pro-apoptotic factors (Roos & Kaina 2006).

While apoptosis is a highly regulated form of cell death, necrosis is a disorganized and unregulated variant of cell destruction. Necrosis is the result of profound cellular damage including membrane disruption, organelle degradation and cellular swelling. Necrosis can be induced following exposure to high doses of ionizing radiation, for example radiotherapy (Lehnert 2008; Baumann et al. 2009). However, Vandenabeele and his research group demonstrated the existence of a controlled necrosis (Vercammen et al. 1998), later defined as necroptosis. Induction of necroptosis relies on the activation of RIP1 and 3 (receptor interacting protein kinase 1 and 3), mediated by PARP1, and results in active disintegration of mitochondrial, lysosomal and plasma membranes (Vandenabeele et al. 2010).

Recently, Nehs et al. demonstrated a role for necroptosis in radiation-induced cell death in endocrine cancers (Nehs et al. 2011). As evasion of programmed cell death is a hallmark of cancer which results in treatment resistance, (radiation-induced) necroptosis might form an interesting novel target for therapeutic intervention (Fulda 2014).

Mitotic catastrophe is a delayed cell death process in which cell death occurs during mitosis. Mitotic catastrophe is the result of either premature entry of this cell cycle phase due to a

failure of the G2/M cell cycle checkpoint or centrosome hyperamplification (Eriksson & Stigbrand 2010). Radiation-induced mitotic catastrophe occurs several days after exposure to ionizing radiation and is usually the result of failed G2/M arrest capacity. Activation of the mitotic checkpoint stops cell progression and induces caspase activation, predominantly caspase 2, and mitochondrial damage. This ultimately leads to “delayed” apoptosis in metaphase (Castedo et al. 2004; Eriksson & Stigbrand 2010).

Senescence is a controlled form of growth arrest. The best-known type of senescence is replicative senescence, which is the result of telomere attrition by repeated cell divisions. DNA damage induced senescence is triggered by ATM and ATR activation, promoting p53 signaling. This subsequently leads to p21 activation and inhibition of CDK2 and CDK4 inhibition. Inhibition of these kinases results in the dephosphorylation of RB (retinoblastoma protein). Furthermore, irreparable DNA damage leads to p16 upregulation. The induction of RB and p16 result in G0 arrest (Burton & Faragher 2015; Baumann et al. 2009).

4 RADIOSENSITIVITY OF *BRCA1* AND *BRCA2* MUTATION CARRIERS

It is known that exposure to ionizing radiation results in an increased risk of cancer development, including breast cancer (see chapter 1.3 Risk factors). However, exposure to ionizing radiation of *BRCA1* and *BRCA2* mutation carriers is counterintuitive because these individuals might be characterized by an elevated radiosensitivity compared to non-carriers as both *BRCA1* and *BRCA2* are caretaker genes involved in the DNA damage response. *BRCA1* has a more pleiotropic role in DNA damage repair as it is involved in repair pathway selection, HR and cell cycle arrest. *BRCA2* on the other hand has a more limited, though essential, role in the HR pathway (Roy et al. 2012). An inadequate response to radiation-induced DNA damage in mutation carriers might result in an elevated radiosensitivity for these individuals. The possible enhanced radiosensitive phenotype of *BRCA1* and *BRCA2* mutation carriers compared to non-carriers has been the subject of extensive research as it may have important consequences regarding exposure to ionizing radiation for diagnostic (e.g. mammography screening) or therapeutic purposes (e.g. radiotherapy).

4.1 Clinical studies

The evaluation of contralateral breast cancer induction in *BRCA1* and *BRCA2* mutation carriers compared to non-carriers due to radiotherapy for a primary breast tumor, can be used to evaluate if there is a difference in carcinogenic risk for both cohorts. However, results of such studies are not univocal. Bernstein and colleagues demonstrated that the increased risk of contralateral breast cancer incidence in *BRCA1* and *BRCA2* mutation carriers observed after radiotherapy is merely due to the mutation status and could not be linked to the exposure to ionizing radiation. Indeed, mutation carriers not treated with radiotherapy are also at high risk of contralateral breast cancer (Bernstein et al. 2013). Broeks et al., on the other hand, did demonstrate a link between mutations in DNA damage response genes (*BRCA1*, *BRCA2*, *CHEK2* and *ATM*) and radiotherapy on the incidence of contralateral breast cancer. Unfortunately, they did not evaluate this link for *BRCA1* and *BRCA2* mutation carriers separately (Broeks et al. 2007).

A similar indistinct result is observed when evaluating breast cancer induction in mutation carriers versus non-carriers upon exposure to diagnostic ionizing radiation. Numerous studies

were conducted to evaluate the effect of a mutation in either *BRCA1* or *BRCA2* on carcinogenic risk after mammography screenings or diagnostic chest X-rays. Several studies demonstrate a significant increased breast cancer risk in mutation carriers compared to non-carriers (Pijpe et al. 2012; Lecarpentier et al. 2011; Gronwald et al. 2008; Andrieu et al. 2006). However, other studies could not detect a positive correlation between mutation status, ionizing radiation and carcinogenesis (John et al. 2013; Giannakeas et al. 2014; Narod et al. 2006; Goldfrank et al. 2006).

At present, an increased carcinogenic risk in *BRCA1* and *BRCA2* mutation carriers compared to non-carriers cannot be excluded based on the contradictory data obtained in clinical studies evaluating the effect of diagnostic or therapeutic exposure to ionizing radiation. The observed variation can be attributed to differences in inclusion criteria, differences in follow-up and limited power due to small cohorts. As proper studies are difficult to set-up and unethical, *in vitro* assays may aid to establish if *BRCA1* and *BRCA2* mutation carriers are characterized by an enhanced radiosensitive phenotype.

4.2 In vitro radiosensitivity testing

4.2.1 Chromosomal radiosensitivity

In vitro chromosome aberration assays are effective tools to investigate radiosensitivity. These assays are generally performed on peripheral blood lymphocytes which are a grateful source of patient-own material to test individual radiosensitivity. Chromosomal radiosensitivity testing on lymphocytes from *BRCA1* and *BRCA2* mutation carriers has been performed with techniques such as the G0 micronucleus assay (see chapter 5.1) and the G2 assay for chromatid breaks (Baeyens et al. 2004; Gutiérrez-Enríquez et al. 2011; Trenz et al. 2002; Ernestos et al. 2010; Becker et al. 2012; Bolognesi et al. 2014; Barwell et al. 2007; Buchholz et al. 2002; Kote-Jarai et al. 2006; Frankenberg-Schwager & Gregus 2012). However, in several of these studies, it was unclear if the heterozygote mutation carriers were healthy individuals or breast cancer patients. Furthermore, differences in experimental set-up make comparisons between studies difficult (Cardinale et al. 2012). Despite these differences, most studies could detect an elevated chromosomal radiosensitivity in breast cancer patients with a germline mutation compared to healthy control individuals (Gutiérrez-Enríquez et al. 2011;

Ernestos et al. 2010; Baeyens et al. 2004). Unfortunately, comparison with radiosensitivity of sporadic breast cancer patients was not always performed. The study of Baeyens et al. previously demonstrated enhanced radiosensitivity in both breast cancer patients with a *BRCA1/2* mutation and sporadic breast cancer patients, suggesting that the enhanced radiosensitivity might not be the result of the mutation but might be inherent to the cancer status (Baeyens et al. 2004). Chromosomal radiosensitivity testing with different assays in lymphocytes of healthy *BRCA1* and *BRCA2* mutation carriers versus healthy control individuals without a germline mutation yielded no univocal results (Barwell et al. 2007; Becker et al. 2012; Gutiérrez-Enríquez et al. 2011; Ernestos et al. 2010; Baeyens et al. 2004).

4.2.2 Homologous recombination testing

Another – relatively new – assay to study *in vitro* radiosensitivity in *BRCA1* and *BRCA2* mutation carriers might be the RAD51 foci assay (see chapter 5.2: RAD51 foci assay). This assay has previously been performed on fresh biopsy samples of cancer patients, irradiated *ex vivo*, to evaluate HR deficiency due to defects in proteins involved in the HR pathway such as *BRCA1* and *BRCA2* (Willers et al. 2009; Naipal et al. 2014; AlHilli et al. 2016; Mukhopadhyay et al. 2010; Shah et al. 2014).

A few studies have also investigated radiation-induced RAD51 foci formation in non-tumor cells with a *BRCA1* or *BRCA2* mutation. Sioftanos et al. detected a significantly reduced RAD51 foci formation in *BRCA1* and *BRCA2* heterozygous mice embryonic stem cells after doses varying between 2 and 4 Gy X-rays (Sioftanos et al. 2010). Warren et al. evaluated RAD51 foci formation in the chicken B cell line DT40 with a heterozygous *BRCA2* mutation after exposure to a dose of 6 Gy X-rays. Foci formation was significantly impaired in mutant cells compared to control cells (Warren et al. 2003). Vaclova et al. could demonstrate a significantly increased γ H2AX foci intensity, an indication of more radiation-induced DSBs, in human lymphoblastoid cell lines of heterozygous *BRCA1* mutation carriers compared to controls after exposure to 10 Gy. However, no similar induction of RAD51 foci could be observed, pointing towards an impaired RAD51 foci formation (Vaclová et al. 2015).

5 ASSAYS TO MEASURE RADIATION-INDUCED DNA DAMAGE

Radiation-induced DNA damage can be evaluated in different ways. These assays allow the evaluation of DNA damage induction, repair and cellular outcome. In this thesis, the G2 MN assay was used to evaluate chromosomal rearrangements and the RAD51 foci assay, was applied to evaluate HR-mediated DSB repair after exposure to ionizing radiation.

5.1 Micronucleus assay

5.1.1 What are MN?

Exposure to ionizing radiation may result in chromosome or chromatid rearrangements. These rearrangements are the result of mis- or unrepaired DSB which can either occur within the same chromosome (intra-) or between different chromosomes (interchanges) (Pouget & Mather 2001). These mis- or unrepaired DSB may result in acentric fragments which lack a centromere. Therefore, they will fail to attach to the mitotic spindle during division and remain in the cytoplasm, where they will be enveloped by a nuclear membrane and form a MN (see Figure 1.26) (Vral et al. 2016).















						INTRACHANGES	Chromatid aberrations		
normal		gap		fragment					
								INTERCHANGES	Chromosome aberrations
normal				exchanges					
						INTRACHANGES	Chromosome aberrations		
normal	terminal deletion	inversion	interstitial deletion	centric or acentric Rings and fragments					
								INTERCHANGES	Chromosome aberrations
normal			dicentric and fragments		interchanges				

Figure 1.26: Relation between chromosome/chromatid aberrations and MN. Acentric fragment that result in MN are indicate in red (Pouget & Mather 2001).

Whether chromosome or chromatid aberrations are formed depends on the cell cycle phase during which the damage was induced. Generally, exposure to ionizing irradiation before S phase results in chromosome aberrations as failure to repair the lesion before DNA replication results in damage of both chromatids. Exposure to ionizing radiation after S phase yields chromatid aberrations and exposure during S phase leads to a mix of both aberrations. Symmetric aberrations such as an inversion or translocation are more stable and can be passed on to the daughter nuclei during mitosis. However, these aberrations can result in overexpression of oncogenes or loss of tumor suppressor gene activity and genome instability can eventually lead to tumorigenesis. Asymmetric aberrations are predominantly the result of misrepair rather than terminal deletions and will result in a MN after cell division. The loss of genetic information will eventually lead to mitotic cell death (Pouget & Mather 2001).

5.1.2 *The cytokinesis block micronucleus assay and its applications*

For evaluation of the MN in the first interphase after cell division, the cytokinesis block MN (CBMN) assay, developed by Fenech, is used (Fenech 2007). In this assay, cytochalasine B (cyto B) is added to the cell cultures to block cytokinesis. This results in binucleated (BN) cells in which MN are evaluated. The CBMN assay can be performed in every cell type which can be stimulated to divide. However, as lymphocytes are easy to obtain by means of a simple blood withdrawal, they are the preferred cell type to analyze.

MN can be the result of exposure to various clastogenic agents, including ionizing radiation and can therefore be used as a biomarker for the analysis of radiation-induced DNA damage. With regard to ionizing radiation, the CBMN assay can be used for biological dosimetry, during which occupational, medical or accidental (and thus *in vivo*) exposure to ionizing radiation of individuals is evaluated in blood samples. On the other hand, the assay can be used to evaluate individual radiosensitivity and cancer susceptibility, by *in vitro* exposure of blood samples of a test cohort to ionizing radiation (El-Zein et al. 2011). The use of a CBMN assay offers several advantages compared to other cytogenetic assays. These advantages include the speed and ease of analysis and the reliable identification of cells that have completed one nuclear division (El-Zein et al. 2011).

Radiation-induced MN contain mainly acentric fragments that are the result of mis- or unrepaired DNA DSB (see Figure 1.26 and 1.27). Besides acentric fragments, MN may also contain whole chromosomes which also failed to bind to the mitotic spindle. These MN are referred to as a spontaneous MN (see Figure 1.27). MN containing whole chromosomes can also be the result of exposure to aneugenic agents (Melo et al. 2014). One drawback of the CBMN assay is the relatively high and inter-individual variable frequency of spontaneous MN (ranging from 2 to 36 per 1000 BN cells). The variation in spontaneous MN can be attributed to diet, exposure to environmental mutagens, age and gender (Vral et al. 2011). Due to this variable background, the detection limit is about 0.2 Gy X or γ -rays. One can distinguish between spontaneous and radiation-induced MN by means of a fluorescent in situ hybridization (FISH) using pan-centromeric probes. MN-centromere analysis is especially useful in the low dose area, where it results in a lowering of the dose detection limit to 0.05-0.1 Gy with the MN-centromere assay (Baeyens et al. 2011).

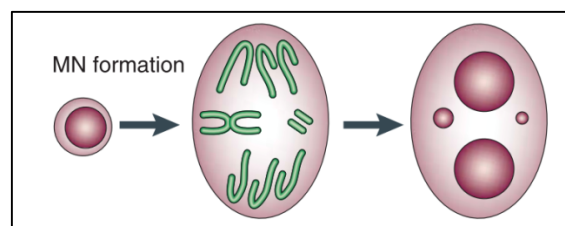


Figure 1.27: Schematic visualization of MN formation in cells during nuclear division. The binucleated cell shown on this figure, obtained by blocking cytokinesis through addition of cytochalasin B, holds both a spontaneous MN (left) and a radiation-induced MN which is the result of a mis- or unrepaired DSB, leading to an acentric fragment (right), adapted from (Fenech 2007).

5.1.2.1 The G0 CBMN assay for lymphocytes

In the classical micronucleus assay, the G0 micronucleus assay, peripheral blood lymphocytes are exposed to ionizing radiation in G0 phase of the cell cycle. Samples are subsequently stimulated to divide by the addition of phytohemagglutinin (PHA). After an initial incubation period of 23 h, cyto B is added to inhibit cytokinesis. The lymphocytes are subsequently allowed an additional incubation period to become binucleated. After a total incubation period of 70 h, the cells are harvested, fixed, transferred to slides and analyzed (Baeyens et al. 2002).

MN slides can be stained with giemsa for light microscopy or DAPI (4',6-diamidino-2-phenylindole) staining for fluorescence microscopy analysis. MN scoring can be performed manually or by automated software (eg. MSearch software, Metasystems, Germany) (see Figure 1.28). In general, MN are scored per 1000 BN cells. MN induced by low-LET radiation typically follow a linear-quadratic dose response. An *in vitro* MN dose response obtained in a reference cohort can be used to assess radiosensitivity of an individual or cohort of interest (Willems et al. 2010; Rastkhah et al. 2016).

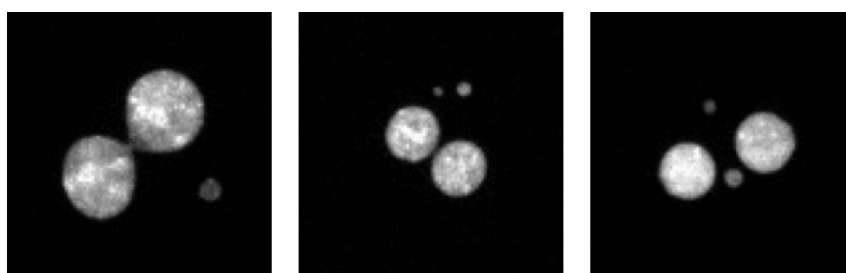


Figure 1.28: DAPI-stained binucleated (BN) cells with one (left) or two (middle and right panel) micronuclei (MN) (image by Metafer 4, Metasystems).

5.1.2.2 The G2 CBMN assay for lymphocytes

The G2 micronucleus assay is a variant of the G0 micronucleus assay and has been developed to evaluate chromosomal radiosensitivity of cells irradiated in S and G2 phase of the cell cycle (Claes et al. 2013). The adapted protocol for lymphocytes requires an initial incubation period of 3 days in the presence of PHA to obtain proliferating lymphocytes. As G0 lymphocytes start cycling at different time points after PHA stimulation, a heterogeneous population of lymphocytes will be obtained at the moment of irradiation. The proliferating lymphocytes are exposed to ionizing radiation and cyto B is added to the cultures immediately after exposure to ionizing radiation. Cells are subsequently allowed a short post-irradiation incubation period of 8 h for repair of the radiation-induced DNA damage and BN formation. This short incubation period limits the number of G1 phase cells becoming BN, resulting in the analysis of MN in BN cells predominantly originating from cells irradiated in S and G2 of the cell cycle. The number of radiation-induced MN is a first endpoint of the G2 micronucleus assay.

In order to test the G2/M checkpoint capacity of the lymphocytes, caffeine is added to a subset of cultures. The addition of caffeine results in an overruling of the G2/M checkpoint by ATM inhibition. Subsequently, the ratio of the number of MN in 1000 BN cells in the

presence of caffeine over the number of MN in 1000 BN cells in the absence of caffeine indicates the checkpoint efficiency. This is the second endpoint of the G2 micronucleus assay. A higher ratio, indicate a more potent checkpoint capacity. G2/M checkpoint analysis has previously been evaluated by means of the G2 chromatid break assay. If activation is completely impaired, which is the case in AT patients without functional ATM, a ratio of one is observed (Terzoudi 2009; Pantelias & Terzoudi 2011).

5.2 RAD51 foci assay

DNA damage response foci can be observed at the DNA damage site upon recruitment of DNA damage proteins. This accumulation of proteins at the damage site, for example at the site of a DSB, can be visualized by means of immunostaining. This technique was first described for the phosphorylated histone variant H2AX (γ H2AX), one of the earliest events in the DNA damage response activated by DSB (see 3.3.1: DNA damage detection and signaling). Given that the phosphorylation is restricted to the DSB site and expands over several 100 to 1000 histones, the DSB can be microscopically detected as a γ H2AX focus after specific immunostaining. Using a fluorescent labelled antibody, these foci can be quantified in DAPI-stained nuclei. This can be done in a manual or automated modus, for example by means of the Metafer 4 automated scanning platform and Metacyte software (Metasystems, Germany). The initial induction of γ H2AX foci after exposure to ionizing radiation and the subsequent foci disappearance over time can be used to assess radiation-induced DSB and repair kinetics (Rothkamm et al. 2015; Rogakou et al. 1999).

Whereas the γ H2AX foci is a DSB signaling protein, one can also evaluate recruitment of DSB repair proteins to the DNA damage site. One of those proteins, specific for HR, is RAD51 (see chapter 3.3.2.2: Homologous recombination). In short, HR relies on RAD51 filament formation for complementary strand invasion and repair of the DSB. RAD51 protein recruitment to the DSB site is mediated by BRCA1 and BRCA2 and can be detected as nuclear foci upon immunostaining (see Figure 1.29) (Mladenov et al. 2016; Rothkamm et al. 2015). Radiation-induced RAD51 foci formation, has been shown to be useful for the evaluation of HR efficiency in different cell types. Also, PARP inhibitors, in combination with the RAD51 foci assay, can be used to analyze HR efficiency (Willers et al. 2015). In contrast to the γ H2AX foci, for which a

DSB-induced specific modification (phosphorylation) is exploited, the RAD51 foci assay merely relies on the accumulation of the RAD51 protein at the DSB site.

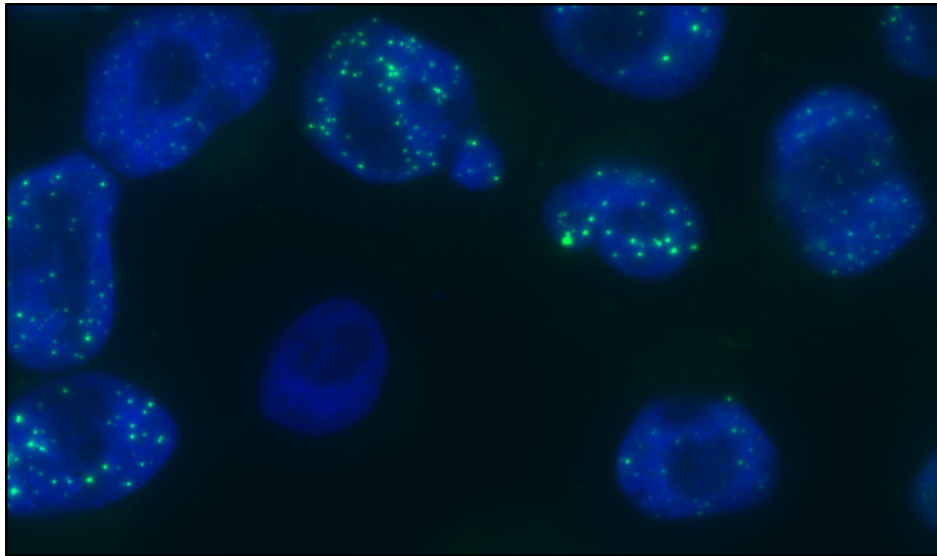


Figure 1.29: RAD51 foci (green) in DAPI-stained nuclei (blue) of MCF10A cells after exposure to ionizing radiation (5Gy 220 kV X-rays) (image by Metafer 4, Metasystems).

6 AIM OF THIS THESIS

To date, all known high to intermediate risk “breast cancer genes” are involved in the DNA damage response pathway. Therefore, heterozygous mutation carriers may show enhanced radiosensitivity associated with an increased carcinogenic risk after exposure to ionizing radiation. Results obtained in clinical studies evaluating the effect of medical exposure to ionizing radiation are however inconclusive and cannot exclude a possible increased cancer-induction risk for mutation carriers. Also, studies analyzing *in vitro* chromosomal radiosensitivity in lymphocytes of healthy heterozygous mutations yielded inconsistent results. Because of these indecisive results, more empirical studies are needed to determine the radiosensitivity phenotype of individuals carrying germline mutations in breast cancer predisposing genes. Better insights into the radiosensitive phenotype of healthy tissues of mutation carriers is of the utmost importance for the safe use of ionizing radiation for diagnostic purposes or radiotherapy treatment.

The first aim of this thesis was to evaluate cellular *in vitro* chromosomal radiosensitivity of healthy mutation carriers. In order to assess chromosomal aberrations in the proper phase of the cell cycle, a G2 micronucleus assay has been developed and applied on peripheral blood lymphocytes of mutation carriers. The classical G0 micronucleus assay is not well designed to evaluate radiosensitivity in cells with a *BRCA1* or *BRCA2* germline mutation as these proteins are mainly involved in HR, a repair pathway activated in S/G2 phase of the cell cycle. In a first phase of our study, the G2 MN assay has been optimized in an AT patient with a mild representation of the disease, who is compound heterozygous for two *ATM* germline mutations (paper I). We also evaluated the *in vitro* chromosomal radiosensitivity in several healthy relatives, who were heterozygous carriers of an *ATM* mutation. In a second phase of our study, the optimized G2 MN assay has been applied on a cohort of healthy *BRCA1* (paper II) and *BRCA2* (paper III) mutation carriers. Furthermore, radiosensitivity has also been evaluated in healthy non-carrier relatives (paper III). Also, we evaluated if there was a link between the individual radiosensitive phenotype of *BRCA1* mutation carriers and NMD (paper II).

The second aim was to evaluate the effect of reduced protein levels of BRCA1 and BRCA2 on radiosensitivity and the functionality of HR in breast epithelial cells. To this end, a radiation-induced RAD51 foci assay was optimized in a breast epithelial cell line (MCF10A) expressing different BRCA1 and BRCA2 protein levels, obtained by RNA interference (paper IV). RAD51 foci were analyzed in cells synchronized in S phase by aphidicolin, this to obtain a maximum number of cells in S phase of the cell cycle, during which HR is active. Also, experiments with a PARP inhibitor were set up to evaluate if the combined use of IR and PARP inhibition result in a more distinct discrimination between the BRCA1 and BRCA2 knockdown cell lines, partially deficient in HR, and the control cell line.

The third aim focusses on the evaluation of the effect on mRNA splicing of Variants of Unknown clinical Significance (VUS). It is known that breast cancer risk increases drastically in individuals carrying a deleterious *BRCA1* or *BRCA2* mutation. However, *BRCA1* and *BRCA2* diagnostic screenings also results in the identification of VUS at a high rate, which is reflected in the large number of VUS reported in the ClinVar database (NCBI). Variants that have not been classified are individually rare and segregation analysis might be impossible due to small families or interpretation may be complicated by the occurrence of phenocopies. VUS are a true challenge for health care providers as the impact of these variants on breast/ovarian cancer risk is unclear. mRNA analysis to investigate intronic and exonic variants that might impair proper RNA splicing, a highly regulated process, are widely used. Here, we assessed splicing of *BRCA1* and *BRCA2* VUS by means of both *in silico* prediction and mRNA analyses in lymphocytes of mutation carriers (paper V).

7 References

- AlHilli, M.M. et al., 2016. In vivo anti-tumor activity of the PARP inhibitor niraparib in homologous recombination deficient and proficient ovarian carcinoma. *Gynecologic Oncology*, pp.1–10.
- Andrieu, N. et al., 2006. Effect of Chest X-Rays on the Risk of Breast Cancer Among BRCA1 / 2 Mutation Carriers in the International BRCA1 / 2 Carrier Cohort Study : A Report from the EMBRACE , GENEPSO , GEO-HEBON , and IBCCS Collaborators ' Group. *Journal of Clinical Oncology*, 24(21), pp.3361–3366.
- Antoniou, A.C. et al., 2014. Breast-cancer risk in families with mutations in PALB2. *The New England journal of medicine*, 371(6), pp.497–506.
- Averbeck, D., 2009. Does scientific evidence support a change from the LNT model for low-dose radiation risk extrapolation? *Health physics*, 97(5), pp.493–504.
- Awasthi, P. et al., 2015. ATM and ATR signaling at a glance. *Journal of cell science*, 128(23), pp.4255–62.
- Baeyens, A. et al., 2011. A semi-automated micronucleus-centromere assay to assess low-dose radiation exposure in human lymphocytes. *International journal of radiation biology*.
- Baeyens, A. et al., 2004. Chromosomal radiosensitivity in BRCA1 and BRCA2 mutation carriers. *International journal of radiation biology*, 80(10), pp.745–756.
- Baeyens, A. et al., 2002. Chromosomal radiosensitivity in breast cancer patients with a known or putative genetic predisposition. *British journal of cancer*, 87(12), pp.1379–1385.
- Barwell, J. et al., 2007. Lymphocyte radiosensitivity in BRCA1 and BRCA2 mutation carriers and implications for breast cancer susceptibility. *International journal of cancer.*, 121(7), pp.1631–6.
- Baumann, M. et al., 2009. *Basic clinical radiobiology* 4th ed. M. Joiner & A. van der Kogel, eds., Hodder Arnold.
- Becker, A.A. et al., 2012. A 24-color metaphase-based radiation assay discriminates heterozygous BRCA2 mutation carriers from controls by chromosomal radiosensitivity. *Breast Cancer Research and Treatment*, 135(1), pp.167–175.
- Belgian Cancer Registry, 2015. Cancer Burden in Belgium. , p.233.
- Bernstein, J.L. et al., 2013. Contralateral breast cancer after radiotherapy among BRCA1 and BRCA2 mutation carriers: a WECARE study report. *European journal of cancer (Oxford, England : 1990)*, 49(14), pp.2979–85.
- Bhargava, R., Onyango, D.O. & Stark, J.M., 2016. Regulation of Single-Strand Annealing and its Role in Genome Maintenance. *Trends in Genetics*, 32(9), pp.566–575.
- Bolognesi, C. et al., 2014. Clinical application of micronucleus test: A case-control study on the prediction of breast cancer risk/susceptibility. *PLoS ONE*, 9(11), pp.1–18.
- Borgmann, K. et al., 2016. DNA repair. In *Molecular Radio-Oncology*. pp. 1–24.
- Brenner, D.J. et al., 2003. Cancer risks attributable to low doses of ionizing radiation: assessing what we really know. *Proceedings of the National Academy of Sciences of the United States of America*, 100(24), pp.13761–6.
- Broeks, A. et al., 2007. Identification of women with an increased risk of developing radiation-induced breast cancer: a case only study. *Breast cancer research*, 9(2), p.R26.
- Brown, J.S., Kaye, S.B. & Yap, T.A., 2016. PARP inhibitors: the race is on. *British Journal of Cancer*, 114(7), pp.713–715.
- Buchholz, T.A. et al., 2002. Evidence of haplotype insufficiency in human cells containing a germline mutation in BRCA1 or BRCA2. *International Journal of Cancer*, 97, pp.557–561.
- Burton, D.G.A. & Faragher, R.G.A., 2015. Cellular senescence: from growth arrest to immunogenic conversion. *Age*, 37(2), pp.1–19.
- Businesswire, 2016. businesswire.com. Available at:

- <http://www.businesswire.com/news/home/20160823006191/en/FDA-Accepts-Clovis-Oncology's-Drug-Application-Rucaparib>.
- Cardinale, F., Bruzzi, P. & Bolognesi, C., 2012. Role of micronucleus test in predicting breast cancer susceptibility: a systematic review and meta-analysis. *British journal of cancer*, 106(4), pp.780–90.
- Castedo, M. et al., 2004. Mitotic catastrophe constitutes a special case of apoptosis whose suppression entails aneuploidy. *Oncogene*, 23(25), pp.4362–70.
- Ceccaldi, R., Rondinelli, B. & D'Andrea, A.D., 2016. Repair Pathway Choices and Consequences at the Double-Strand Break. *Trends in Cell Biology*, 26(1), pp.52–64.
- Cerosaletti, K. et al., 2000. Retroviral expression of the nbs1 gene in cultured nijmegen breakage syndrome cells restores normal radiation sensitivity and nuclear focus formation. *Mutagenesis*, 15(3), pp.281–286.
- Chan, D.W. & Chen, B.P.C., 2002. Autophosphorylation of the DNA-dependent protein kinase catalytic subunit is required for rejoining of DNA double-strand breaks. *Genes and Development*, 16, pp.2333–2338.
- Claes, K. et al., 2013. Variant Ataxia Telangiectasia: Clinical and Molecular Findings and Evaluation of Radiosensitive Phenotypes in a Patient and Relatives. *Neuromolecular medicine*, 15(3), pp.447–457.
- Colombo, M. et al., 2013. Comparative In Vitro and In Silico Analyses of Variants in Splicing Regions of BRCA1 and BRCA2 Genes and Characterization of Novel Pathogenic Mutations. *PLoS ONE*, 8(2).
- Corre, I., Niaudet, C. & Paris, F., 2010. Plasma membrane signaling induced by ionizing radiation. *Mutation Research - Reviews in Mutation Research*, 704(1–3), pp.61–67.
- Cousineau, I. & Belmaaza, A., 2014. BRCA1 Haploinsufficiency, but not Heterozygosity for a BRCA1-truncating Mutation, Dereglates Homologous Recombination. *Cell Cycle*, 6(8), pp.962–971.
- CvKO, Bevolkingsonderzoek. Available at: www.bevolkingsonderzoek.be.
- Daly, M.B. et al., 2017. Genetic / Familial High-Risk Assessment : Breast and Ovarian , Version 2.2017. *Journal of national comprehensive cancer network*, 15(1), pp.9–20.
- Darabi, H. et al., 2016. Fine scale mapping of the 17q22 breast cancer locus using dense SNPs, genotyped within the Collaborative Oncological Gene-Environment Study (COGs). *Scientific reports*, 6(August), p.32512.
- Deckbar, D., Jeggo, P. a & Löbrich, M., 2011. Understanding the limitations of radiation-induced cell cycle checkpoints. *Critical reviews in biochemistry and molecular biology*, 46(4), pp.271–283.
- Deriano, L. & Roth, D.B., 2013. Modernizing the nonhomologous end-joining repertoire: alternative and classical NHEJ share the stage. *Annual review of genetics*, 47, pp.433–55.
- Domchek, S.M. et al., 2010. Association of Risk-Reducing Surgery in BRCA1 or BRCA2 Mutation Carriers with Cancer Risk and Mortality. *Jama*, 304(9), pp.967–975.
- Dong, H. et al., 2015. Update of the human and mouse Fanconi anemia genes. *Human genomics*, 9, p.32.
- Easton, D.F. et al., 2015. Gene-Panel Sequencing and the Prediction of Breast-Cancer Risk. *The new england journal of medicine*.
- Easton, D.F. et al., 2016. No evidence that protein truncating variants in BRIP1 are associated with breast cancer risk: implications for gene panel testing. *Journal of medical genetics*, pp.1–12.
- El-Zein, R., Vral, A. & Etzel, C.J., 2011. Cytokinesis-blocked micronucleus assay and cancer risk assessment. *Mutagenesis*, 26(1), pp.101–106.
- Enriquez, L. & Listinsky, J., 2009. Role of MRI in breast cancer management. *Cleveland Clinic*

- Journal of Medicine*, 76(9), pp.525–532.
- Eriksson, D. & Stigbrand, T., 2010. Radiation-induced cell death mechanisms. *Tumor Biology*, 31(4), pp.363–372.
- Ernestos, B. et al., 2010. Increased chromosomal radiosensitivity in women carrying BRCA1/BRCA2 mutations assessed with the G2 assay. *International journal of radiation oncology, biology, physics*, 76(4), pp.1199–205.
- Fenech, M., 2007. Cytokinesis-block micronucleus cytome assay. *Nature protocols*, 2(5), pp.1084–1104.
- Figueroa, J.D. et al., 2011. Associations of common variants at 1p11.2 and 14q24.1 (RAD51I1) with breast cancer risk and heterogeneity by tumor subtype: Findings from the Breast Cancer Association Consortium. *Human Molecular Genetics*, 20(23), pp.4693–4706.
- Flanagan, E.P. et al., 2015. PALB2, CHEK2 and ATM rare variants and cancer risk: data from COGS. *Journal of medical genetics*, 72(1), pp.81–87.
- Foulkes, W.D. & Shuen, A.Y., 2013. In Brief: BRCA1 and BRCA2. *The Journal of Pathology*, 230(4), pp.347–349.
- Frankenberg-Schwager, M. & Gregus, A., 2012. Chromosomal instability induced by mammography X-rays in primary human fibroblasts from BRCA1 and BRCA2 mutation carriers. *International Journal of Radiation Biology*, 88(11), pp.846–857.
- Fulda, S., 2014. Therapeutic exploitation of necroptosis for cancer therapy. *Seminars in Cell and Developmental Biology*, 35, pp.51–56.
- Gannon, L.M., Cotter, M.B. & Quinn, C.M., 2013. The classification of invasive carcinoma of the breast. *Expert review of anticancer therapy*, 13(8), pp.941–54.
- Giannakeas, V. et al., 2014. Mammography screening and the risk of breast cancer in BRCA1 and BRCA2 mutation carriers: a prospective study. *Breast cancer research and treatment*, 147(1), pp.113–8.
- Gilbert, E.S., 2009. Ionising radiation and cancer risks: what have we learned from epidemiology? *International journal of radiation biology*, 85(6), pp.467–82.
- Gillet, P. et al., 2011. Borstkanker screening : hoe vrouwen met een verhoogd risico identificeren - welke beeldvorming gebruiken ? Good Clinical Practice (GCP). *Federaal Kenniscentrum voor Gezondheidszorg (KCE)*, KCE Report(D/2011/10.273/90).
- Goldfrank, D. et al., 2006. Effect of mammography on breast cancer risk in women with mutations in BRCA1 or BRCA2. *Cancer epidemiology, biomarkers & prevention : a publication of the American Association for Cancer Research, cosponsored by the American Society of Preventive Oncology*, 15(11), pp.2311–2313.
- Goodarzi, A.A. & Jeggo, P.A., 2012. The heterochromatic barrier to DNA double strand break repair: How to get the entry visa. *International Journal of Molecular Sciences*, 13(9), pp.11844–11860.
- Gradishar, W.J., 2012. HER2 Therapy — An Abundance of Riches. *The New England journal of medicine*, 366(2), pp.176–178.
- Gronwald, J. et al., 2008. Early radiation exposures and BRCA1-associated breast cancer in young women from Poland. *Breast cancer research and treatment*, 112(3), pp.581–4.
- Gutiérrez-Enríquez, S. et al., 2011. Ionizing radiation or mitomycin-induced micronuclei in lymphocytes of BRCA1 or BRCA2 mutation carriers. *Breast cancer research and treatment*, 127(3), pp.611–22.
- Hall, J.M. et al., 1990. Linkage of early-onset familial breast cancer to chromosome 17q21. *Science*, 250(4988), pp.1684–1689.
- Hartlerode, A.J. et al., 2015. Recruitment and activation of the ATM kinase in the absence of DNA-damage sensors. *Nature Structural & Molecular Biology*, 22(9), pp.736–743.
- Heijink, A.M., Krajewska, M. & Van Vugt, M.A.T.M., 2013. The DNA damage response during

- mitosis. *Mutation Research - Fundamental and Molecular Mechanisms of Mutagenesis*, 750(1–2), pp.45–55.
- Hendrick, R.E., 2010. Radiation doses and cancer risks from breast imaging studies. *Radiology*, 257(1), pp.246–53.
- Hendriks, G. et al., 2014. An efficient pipeline for the generation and functional analysis of human BRCA2 variants of uncertain significance. *Human Mutation*, 35(11), pp.1382–1391.
- Houdayer, C. et al., 2012. Guidelines for splicing analysis in molecular diagnosis derived from a set of 327 combined in silico/in vitro studies on BRCA1 and BRCA2 variants. *Human Mutation*, 33(8), pp.1228–1238.
- HPA, 2013. *Human Radiosensitivity. Report of the independent advisory group on ionising radiation*,
- IARC, 2016. <http://monographs.iarc.fr/ENG/Classification/>.
- Jackson, S.P. & Bartek, J., 2010. The DNA-damage response in human biology and disease. *Nature*, 461(7267), pp.1071–1078.
- de Jager, M. et al., 2002. DNA end-binding specificity of human Rad50 / Mre11 is influenced by ATP. *Nucleic Acids Research*, 30(20), pp.4425–4431.
- John, E.M. et al., 2013. Diagnostic chest X-rays and breast cancer risk before age 50 years for BRCA1 and BRCA2 mutation carriers. *Cancer epidemiology, biomarkers & prevention : a publication of the American Association for Cancer Research, cosponsored by the American Society of Preventive Oncology*, 22(9), pp.1547–56.
- Jolie, A., 2013. My Medical Choice. Available at: http://www.nytimes.com/2013/05/14/opinion/my-medical-choice.html?_r=0.
- Kakarougkas, A. & Jeggo, P.A., 2014. DNA DSB repair pathway choice: An orchestrated handover mechanism. *British Journal of Radiology*, 87(1035).
- Khodyreva, S.N. & Lavrik, O.I., 2016. Poly(ADP-Ribose) polymerase 1 as a key regulator of DNA repair. *Molecular Biology*, 50(4), pp.580–595.
- Kim, G. et al., 2015. FDA approval summary: Olaparib monotherapy in patients with deleterious germline BRCA-mutated advanced ovarian cancer treated with three or more lines of chemotherapy. *Clinical Cancer Research*, 21(19), pp.4257–4261.
- Kleibl, Z. & Kristensen, V.N., 2016. Women at high risk of breast cancer: Molecular characteristics, clinical presentation and management. *The Breast*, 28(2016), pp.136–144.
- Knudson, A.G., 1971. Mutation and cancer: statistical study of retinoblastoma. *Proceedings of the National Academy of Sciences of the United States of America*, 68(4), pp.820–3.
- Konishi, H. et al., 2011. Mutation of a single allele of the cancer susceptibility gene BRCA1 leads to genomic instability in human breast epithelial cells. *Proc Natl Acad Sci U S A*, 108(43), pp.17773–17778.
- Kote-Jarai, Z. et al., 2006. Increased level of chromosomal damage after irradiation of lymphocytes from BRCA1 mutation carriers. *British journal of cancer*, 94(2), pp.308–310.
- Kraus, C. et al., 2017. Gene panel sequencing in familial breast/ovarian cancer patients identifies multiple novel mutations also in genes others than BRCA1/2. *International Journal of Cancer*, 140(1), pp.95–102.
- Kühne, M. et al., 2004. A Double-Strand Break Repair Defect in ATM-Deficient Cells Contributes to Radiosensitivity. *Cancer Research*, 64, pp.500–508.
- Kurian, A.W., Antoniou, A.C. & Domchek, S.M., 2016. Refining Breast Cancer Risk Stratification: Additional Genes, Additional Information. *American Society of Clinical Oncology educational book / ASCO. American Society of Clinical Oncology. Meeting*, 35, pp.44–56.
- Laloo, F. & Evans, D.G., 2012. Familial Breast Cancer. *Clinical Genetics*, 82(2), pp.105–114.
- Langelier, M.F., Riccio, A.A. & Pascal, J.M., 2014. PARP-2 and PARP-3 are selectively activated by 5' phosphorylated DNA breaks through an allosteric regulatory mechanism shared with

- PARP-1. *Nucleic Acids Research*, 42(12), pp.7762–7775.
- Lavin, M.F. et al., 2007. Current and potential therapeutic strategies for the treatment of ataxia-telangiectasia. *British Medical Bulletin*, 81–82(1), pp.129–147.
- Lecarpentier, J. et al., 2011. Variation in breast cancer risk with mutation position , smoking , alcohol , and chest X-ray history , in the French National BRCA1 / 2 carrier cohort (GENEPSO). *Breast cancer research and treatment*, 130(3), pp.927–938.
- Lee, J.-H. & Paull, T.T., 2004. Direct activation of the ATM protein kinase by the Mre11/Rad50/Nbs1 complex. *Science*, 304(5667), pp.93–96.
- Lee, J.H. et al., 2003. Regulation of Mre11/Rad50 by Nbs1: Effects on nucleotide-dependent DNA binding and association with ataxiatelangiectasia-like disorder mutant complexes. *Journal of Biological Chemistry*, 278(46), pp.45171–45181.
- Lehnert, S., 2008. *Biomolecular action of ionizing radiation*, Taylor & Francis Group.
- Levy-Lahad, E. & Friedman, E., 2007. Cancer risks among BRCA1 and BRCA2 mutation carriers. *British journal of cancer*, 96(1), pp.11–5.
- Li, J. & Xu, X., 2016. DNA double-strand break repair: a tale of pathway choices. *Acta Biochimica et Biophysica Sinica*, 48(7), pp.641–646.
- Lim, S. & Kaldis, P., 2013. Cdks, cyclins and CKIs: roles beyond cell cycle regulation. *Development*, 140(15), pp.3079–93.
- Liu, J. et al., 2010. Human BRCA2 protein promotes RAD51 filament formation on RPA-covered ssDNA. *Nature structural & molecular biology*, 17(10), pp.1260–1262.
- Liu, T. & Huang, J., 2016. DNA End Resection: Facts and Mechanisms. *Genomics, Proteomics and Bioinformatics*, 14(3), pp.126–130.
- Löbrich, M. & Jeggo, P. a, 2007. The impact of a negligent G2/M checkpoint on genomic stability and cancer induction. *Nature Reviews Cancer*, 7(November), pp.861–870.
- Lodish, H. et al., 2007. *Molecular cell biology* 6th, ed., W.H. Freeman and Company.
- Longo, D.L., Hartmann, L.C. & Lindor, N.M., 2016. The role of risk-reducing surgery in hereditary breast and ovarian cancer. *New England Journal of Medicine*, 374(5), pp.454–468.
- Lorat, Y. et al., 2016. Clustered double-strand breaks in heterochromatin perturb DNA repair after high linear energy transfer irradiation. *Radiotherapy and Oncology*, 121(1), pp.154–161.
- Lord, C.J. & Ashworth, A., 2016. BRCAness revisited. *Nature Reviews Cancer*, 16(2), pp.110–20.
- Luzi, E. et al., 2012. The negative feedback-loop between the Oncomir mir-24-1 and Menin modulates the men1 tumorigenesis by mimicking the “Knudson’s second hit.” *PLoS ONE*, 7(6), pp.1–10.
- Mambourg, F. et al., 2010. Opsporing van borstkanker tussen 40 en 49 jaar. Good Clinical Practice (GCP). *Brussel: Federaal Kenniscentrum voor de gezondheid (KCE)*.
- Mambourg, F., Robays, J. & Gerkens, S., 2012. Opsporing van borstkanker tussen 70 en 74 jaar. *Federaal Kenniscentrum voor Gezondheidszorg (KCE)*.
- Mao, Z. et al., 2008a. Comparison of nonhomologous end joining and homologous recombination in human cells. *DNA Repair*, 7(10), pp.1765–1771.
- Mao, Z. et al., 2008b. DNA repair by nonhomologous end joining and homologous recombination during cell cycle in human cells. *Cell Cycle*, 7(18), pp.2902–2906.
- van Marcke, C. et al., 2016. Routine use of gene panel testing in hereditary breast cancer should be performed with caution. *Critical Reviews in Oncology/Hematology*, 108, pp.33–39.
- Marieb, E.N., Mallatt, J. & Wilhelm, P.B., 2008. *Human Anatomy* 5th Editio., Pearson Benjamin Cummings.
- Matt, S. & Hofmann, T.G., 2016. The DNA damage-induced cell death response: a roadmap to kill cancer cells. *Cellular and Molecular Life Sciences*, 73(15), pp.2829–2850.
- Mattsson, S. & Nilsson, M., 2015. On the estimation of radiation-induced cancer risks from very

- low doses of radiation and how to communicate these risks. *Radiation Protection Dosimetry*, 165(1–4), pp.17–21.
- McClain, M.R. et al., 2005. An evaluation of BRCA1 and BRCA2 founder mutations penetrance estimates for breast cancer among Ashkenazi Jewish women. *Genetics in medicine : official journal of the American College of Medical Genetics*, 7(1), pp.34–39.
- Mccormack, V.A., Dos, I. & Silva, S., 2006. Breast Density and Parenchymal Patterns as Markers of Breast Cancer Risk: A Meta-analysis. *Cancer Epidemiol Biomarkers Prev*, 15(6), pp.1159–69.
- McIlwraith, M.J. et al., 2000. Reconstitution of the strand invasion step of double-strand break repair using human Rad51 Rad52 and RPA proteins. *Journal of molecular biology*, 304(2), pp.151–64.
- Melo, K.M. et al., 2014. FISH in micronucleus test demonstrates aneugenic action of rotenone in a common freshwater fish species, Nile tilapia (*Oreochromis niloticus*). *Mutagenesis*, 29(3), pp.215–219.
- Michailidou, K. et al., 2014. Large-scale genotyping identifies 41 new loci associated with breast cancer risk Kyriaki. *Nature Genetics*, 45(4), pp.353–361.
- Micol, R. et al., 2011. Morbidity and mortality from ataxia-telangiectasia are associated with ATM genotype. *Journal of Allergy and Clinical Immunology*, 128(2), pp.382–390.
- Miki, Y. et al., 1994. A Strong Candidate for the Breast and Ovarian Cancer Susceptibility Gene BRCA1. *Science*, 266(5182), pp.66–71.
- Millot, G. et al., 2012. A guide for Functional Analysis of BRCA1 Variants of Uncertain Significance (VUS). *human mutation*, 33(11), pp.1526–1537.
- Mirzania, M., 2016. Approach to the Triple Negative Breast Cancer in New Drugs Area. *International journa of hematology- oncology and stem cell research*, 10(2).
- Mladenov, E. et al., 2016. DNA double-strand-break repair in higher eukaryotes and its role in genomic instability and cancer: Cell cycle and proliferation-dependent regulation. *Seminars in Cancer Biology*, 37–38(2016), pp.51–64.
- Mucci, L.A. et al., 2016. Familial Risk and Heritability of Cancer Among Twins in Nordic Countries. *Jama*, 315(1), pp.68–76.
- Mukhopadhyay, A. et al., 2010. Development of a functional assay for homologous recombination status in primary cultures of epithelial ovarian tumor and correlation with sensitivity to poly(ADP-ribose) polymerase inhibitors. *Clinical Cancer Research*, 16(8), pp.2344–2351.
- Murai, J. et al., 2012. Trapping of PARP1 and PARP2 by clinical PARP inhibitors. *Cancer Research*, 72(21), pp.5588–5599.
- Naipal, K. a. T. et al., 2014. Functional ex vivo assay to select Homologous Recombination deficient breast tumors for PARP inhibitor treatment. *Clinical cancer research : an official journal of the American Association for Cancer Research*, 20(18), pp.4816–4826.
- Narod, S.A. et al., 2006. Screening mammography and risk of breast cancer in BRCA1 and BRCA2 mutation carriers: a case-control study. *The Lancet. Oncology*, 7(5), pp.402–6.
- Narod, S. a & Foulkes, W.D., 2004. BRCA1 and BRCA2: 1994 and beyond. *Nature Reviews Cancer*, 4(9), pp.665–676.
- NCCN, 2016. Genetic / Familial High-Risk Assessment : Breast and Ovarian cancer.
- Nehs, M.A. et al., 2011. Necroptosis is a novel mechanism of radiation-induced cell death in anaplastic thyroid and adrenocortical cancers. *Surgery*, 150(6), pp.1032–1039.
- Nikkilä, J. et al., 2013. Heterozygous mutations in PALB2 cause DNA replication and damage response defects. *Nature communications*, 4, p.2578.
- Okayasu, R., 2012. Repair of DNA damage induced by accelerated heavy ions-A mini review. *International Journal of Cancer*, 130(5), pp.991–1000.

- van Os, N.J.H. et al., 2016. Health risks for ataxia-telangiectasia mutated heterozygotes: a systematic review, meta-analysis and evidence-based guideline. *Clinical Genetics*, 90(2), pp.105–117.
- Ozasa, K. et al., 2012. Studies of the Mortality of Atomic Bomb Survivors , Report 14 , 1950 – 2003 : An Overview of Cancer and Noncancer Diseases. *Radiation Research*, 243(3), pp.229–243.
- Panier, S. & Boulton, S.J., 2014. Double-strand break repair: 53BP1 comes into focus. *Nature reviews. Molecular cell biology*, 15(1), pp.7–18.
- Pantelias, G.E. & Terzoudi, G.I., 2011. A standardized G2-assay for the prediction of individual radiosensitivity. *Radiotherapy and Oncology*, 101(1), pp.28–34.
- Park, J.Y., Zhang, F. & Andreassen, P.R., 2014. PALB2: The hub of a network of tumor suppressors involved in DNA damage responses. *Biochimica et Biophysica Acta - Reviews on Cancer*, 1846(1), pp.263–275.
- Paull, T.T., 2015. Mechanisms of ATM activation. *Annual Review of Biochemistry*, 84, pp.711–738.
- Peshkin, B., Alabek, M. & Isaacs, C., 2010. BRCA 1/2 Mutations and Triple Negative Breast Cancers. *Breast Disease*, 32(1–2), pp.25–33.
- Pijpe, A. et al., 2012. Exposure to diagnostic radiation and risk of breast cancer among carriers of BRCA1/2 mutations: retrospective cohort study (GENE-RAD-RISK). *BMJ*, 345, p.e5660.
- Pommier, Y., O'Connor, M.J. & de Bono, J., 2016. Laying a trap to kill cancer cells: PARP inhibitors and their mechanisms of action. *Science Translational Medicine*, 8(362), pp.1–8.
- Pouget, J.P. & Mather, S.J., 2001. General aspects of the cellular response to low- and high-LET radiation. *European Journal of Nuclear Medicine*, 28(4), pp.541–561.
- Pronina, I. V. et al., 2017. DNA methylation contributes to deregulation of 12 cancer-associated microRNAs and breast cancer progression. *Gene*, 604(2017), pp.1–8.
- Rastkhah, E. et al., 2016. The cytokinesis-blocked micronucleus assay: dose response calibration curve, background frequency in the population and dose estimation. *Radiation and Environmental Biophysics*, 55(1), pp.41–51.
- Rice, M.S. et al., 2016. Breast cancer research in the nurses' health studies: Exposures across the life course. *American Journal of Public Health*, 106(9), pp.1592–1598.
- Robertson, A. et al., 2013. The cellular and molecular carcinogenic effects of radon exposure: A review. *International Journal of Molecular Sciences*, 14(7), pp.14024–14063.
- Rodgers, K. & Mcvey, M., 2016. Error-Prone Repair of DNA Double-Strand Breaks. *Journal of Cellular Physiology*, 231(1), pp.15–24.
- Rogakou, E.P. et al., 1999. Megabase chromatin domains involved in DNA double-strand breaks in vivo. *Journal of Cell Biology*, 146(5), pp.905–915.
- Roos, W.P. & Kaina, B., 2006. DNA damage-induced cell death by apoptosis. *Trends in Molecular Medicine*, 12(9), pp.440–450.
- Rothkamm, K. et al., 2015. DNA Damga Foci: Meaning and Significance. *Environmental and molecular mutagenesis*, 56, pp.491–504.
- Rothkamm, K. & Lobrich, M., 2002. Misrepair of radiation-induced DNA double-strand breaks and its relevance for tumorigenesis and cancer treatment (review). *International Journal of Oncology*, 21(2), pp.433–440.
- Roy, R., Chun, J. & Powell, S.N., 2012. BRCA1 and BRCA2: different roles in a common pathway of genome protection. *Nature reviews. Cancer*, 12(1), pp.68–78.
- Rupnik, A., Lowndes, N.F. & Grenon, M., 2010. MRN and the race to the break. *Chromosoma*, 119(2), pp.115–135.
- Rutqvist, L.E., 2004. Adjuvant endocrine therapy. *Best practice & research. Clinical endocrinology & metabolism*, 18(1), pp.81–95.

- Saha, J. & Davis, A.J., 2016. Unsolved mystery: the role of BRCA1 in DNA end-joining. *Journal of radiation research*, 57(S1), pp.18–24.
- Salmena, L. & Narod, S., 2012. BRCA1 haploinsufficiency: consequences for breast cancer. *Women's health (London, England)*, 8(2), pp.127–9.
- Sartori, A.A. et al., 2007. Human CtIP promotes DNA end resection. *Nature*, 450(7169), pp.509–514.
- Sawyer, S.L. et al., 2015. Biallelic mutations in BRCA1 cause a new Fanconi anemia subtype. *Cancer Discovery*, 5(2), pp.135–142.
- Schieving, J.H. et al., 2014. Alpha-fetoprotein, a fascinating protein and biomarker in neurology. *European Journal of Paediatric Neurology*, 18(3), pp.243–248.
- Senkus, E. et al., 2015. Primary breast cancer: ESMO Clinical Practice Guidelines for diagnosis, treatment and follow-up. *Annals of Oncology*, 26(Supplement 5), pp.v8–v30.
- Severson, T.M. et al., 2015. BRCA1-like signature in triple negative breast cancer: Molecular and clinical characterization reveals subgroups with therapeutic potential. *Molecular Oncology*, 9(8), pp.1528–1538.
- Shabbeer, S. et al., 2013. BRCA1 targets G2/M cell cycle proteins for ubiquitination and proteasomal degradation. *Oncogene*, 32(42), pp.5005–16.
- Shah, M.M. et al., 2014. An ex vivo assay of XRT-induced Rad51 foci formation predicts response to PARP-inhibition in ovarian cancer. *Gynecologic Oncology*, 134(2), pp.331–337.
- Shaltiel, I.A. et al., 2015. The same, only different - DNA damage checkpoints and their reversal throughout the cell cycle. *Journal of cell science*, 128(4), pp.607–20.
- Shiloh, Y. & Lederman, H.M., 2017. Ataxia-telangiectasia (A-T): An emerging dimension of premature ageing. *Ageing Research Reviews*, 33, pp.76–99.
- Sioftanos, G. et al., 2010. BRCA1 and BRCA2 heterozygosity in embryonic stem cells reduces radiation-induced Rad51 focus formation but is not associated with radiosensitivity. *International journal of radiation biology*, 86(12), pp.1095–105.
- Soni, A. et al., 2014. Requirement for Parp-1 and DNA ligases 1 or 3 but not of Xrcc1 in chromosomal translocation formation by backup end joining. *Nucleic Acids Research*, 42(10), pp.6380–6392.
- Spurdle, A.B. et al., 2012. BRCA1 R1699Q variant displaying ambiguous functional abrogation confers intermediate breast and ovarian cancer risk. *J Med Genet*, 49(8), pp.525–532.
- Spurdle, A.B. et al., 2008. Prediction and assessment of splicing alterations: Implications for clinical testing. *Human Mutation*, 29(11), pp.1304–1313.
- Strachan, T. & Read, A., 2011. *Human Molecular Genetics* 4th Editio., Garland Science, Taylor & Francis Group, LLC.
- Strachan, T. & Read, A., 2010. Nucleic Acid Structure and Gene Expression. In *Human molecular genetics*. Taylor & Francis Group, pp. 1–27.
- Sullivan, K.D. et al., 2012. The p53 circuit board. *Acta Biochimica et Biophysica Sinica*, 1825(2), pp.229–244.
- Tai, Y.C. et al., 2007. Breast cancer risk among male BRCA1 and BRCA2 mutation carriers. *Journal of the National Cancer Institute*, 99(23), pp.1811–1814.
- Takeda, D.Y. & Dutta, A., 2005. DNA replication and progression through S phase. *Oncogene*, 24(17), pp.2827–2843.
- Taleei, R. & Nikjoo, H., 2013. Biochemical DSB-repair model for mammalian cells in G1 and early S phases of the cell cycle. *Mutation Research - Genetic Toxicology and Environmental Mutagenesis*, 756(1–2), pp.206–212.
- Taylor, A.M.R. et al., 2015. Ataxia telangiectasia: More variation at clinical and cellular levels. *Clinical Genetics*, 87(3), pp.199–208.
- Teive, H. a. G. et al., 2015. Ataxia-telangiectasia — A historical review and a proposal for a new

- designation: ATM syndrome. *Journal of the Neurological Sciences*, 355(1–2), pp.3–6.
- Terzoudi, 2009. G2-checkpoint abrogation in irradiated lymphocytes: A new cytogenetic approach to assess individual radiosensitivity and predisposition to cancer. *International Journal of Oncology*, 35(5).
- La Torre Travis, E., 1989. *Primer of medical radiobiology* 2nd ed., Mosby - Year Book.
- Trenz, K. et al., 2002. Mutagen sensitivity of peripheral blood from women carrying a BRCA1 or BRCA2 mutation. *Mutation research*, 500(1–2), pp.89–96.
- Vaclová, T. et al., 2015. DNA repair capacity is impaired in healthy BRCA1 heterozygous mutation carriers. *Breast Cancer Research and Treatment*, 152(2), pp.271–282.
- Vandenabeele, P. et al., 2010. Molecular mechanisms of necroptosis: an ordered cellular explosion. *Nature reviews. Molecular cell biology*, 11(10), pp.700–14.
- Venkitaraman, A.R., 2014. Tumour suppressor mechanisms in the control of chromosome stability: insights from BRCA2. *Molecules and cells*, 37(2), pp.95–9.
- Vercammen, D. et al., 1998. Inhibition of caspases increases the sensitivity of L929 cells to necrosis mediated by tumor necrosis factor. *The Journal of experimental medicine*, 187(9), pp.1477–85.
- Vral, A. et al., 2016. A semi-automated FISH-based micronucleus-centromere assay for biomonitoring of hospital workers exposed to low doses of ionizing radiation. *Molecular Medicine Reports*, pp.103–110.
- Vral, A., Fenech, M. & Thierens, H., 2011. The micronucleus assay as a biological dosimeter of in vivo ionising radiation exposure. *Mutagenesis*, 26(1), pp.11–17.
- Walker, J.R., Corpina, R.A. & Goldberg, J., 2001. Structure of the Ku heterodimer bound to DNA and its implications for double-strand break repair. *Nature*, 412(6847), pp.607–14.
- Wang, H. et al., 2008. The Ku-dependent non-homologous end-joining but not other repair pathway is inhibited by high linear energy transfer ionizing radiation. *DNA Repair*, 7(5), pp.725–733.
- Warren, M. et al., 2003. Phenotypic effects of heterozygosity for a BRCA2 mutation. *Human Molecular Genetics*, 12(20), pp.2645–2656.
- WCRF, 2012. No Title. Available at: <http://www.wcrf.org/int/cancer-facts-figures/data-specific-cancers/breast-cancer-statistics>.
- WCRF/AICR, 2007. *Food, Nutrition, Physical Activity, and the Prevention of Cancer: a Global Perspective.*
- Weinberg, R.A., 2007. *The biology of cancer* 2nd ed., Garland Science, Taylor & Francis Group, LLC.
- Willems, P. et al., 2010. Automated micronucleus (MN) scoring for population triage in case of large scale radiation events. *International journal of radiation biology*, 86(1), pp.2–11.
- Willers, H. et al., 2015. DNA Damage Response Assessments in Human Tumor Samples Provide Functional Biomarkers of Radiosensitivity. *Seminars in Radiation Oncology*, 25(4), pp.237–250.
- Willers, H. et al., 2009. Utility of DNA repair protein foci for the detection of putative BRCA1 pathway defects in breast cancer biopsies. *Molecular cancer research*, 7(8), pp.1304–9.
- Williams, R.S. et al., 2008. Mre11 Dimers Coordinate DNA End Bridging and Nuclease Processing in Double-Strand-Break Repair. *Cell*, 135(1), pp.97–109.
- Wingert, S. & Rieger, M.A., 2016. Terminal differentiation induction as DNA damage response in hematopoietic stem cells by GADD45A. *Experimental Hematology*, 44(7), pp.561–566.
- Wooster, R. et al., 1995. Identification of the breast cancer susceptibility gene BRCA2. *Nature*, 378(6559), pp.789–92.
- Wooster, R. et al., 1994. Localization of a breast cancer susceptibility gene, BRCA2, to chromosome 13q12-13. *Science*, 265, pp.2088–2090.

- www.cancer.gov/, 2016. www.cancer.gov/. Available at: <https://www.cancer.gov/about-cancer/causes-prevention/genetics/overview-pdq%0D>.
- Xiong, X. et al., 2015. 53BP1 promotes microhomology-mediated end-joining in G1-phase cells. *Nucleic Acids Research*, 43(3), pp.1659–1670.
- Yarden, R.I. et al., 2002. BRCA1 regulates the G2/M checkpoint by activating Chk1 kinase upon DNA damage. *Nature genetics*, 30(3), pp.285–9.
- You, Z. & Bailis, J.M., 2010. DNA damage and decisions: CtIP coordinates DNA repair and cell cycle checkpoints. *Trends in Cell Biology*, 20(7), pp.402–409.
- Yu, A.M. & McVey, M., 2010. Synthesis-dependent microhomology-mediated end joining accounts for multiple types of repair junctions. *Nucleic Acids Research*, 38(17), pp.5706–5717.
- Zeman, M.K. & Cimprich, K.A., 2014. Causes and consequences of replication stress. *Nature cell biology*, 16(1), pp.2–9.
- Zhang, F. et al., 2009. PALB2 links BRCA1 and BRCA2 in the DNA-Damage Response. *Current Biology*, 19(6), pp.524–529.
- Zou, Y. et al., 2006. Functions of Human Replication Protein A (RPA): From DNA Replication to DNA Damage and Stress Responses. *Journal of cell physiology*, 208(2), pp.267–273.

PART II: ORIGINAL RESEARCH

OUTLINE OF THE RESEARCH

Paper I: Variant Ataxia Telangiectasia: Clinical and Molecular Findings and Evaluation of Radiosensitive Phenotypes in a Patient and Relatives

Kathleen B.M. Claes, Julie Depuydt, A. Malcolm R. Taylor, James I. Last, Annelot Baert, Peter Schietecatte, Veerle Vandersickel, Bruce Poppe, Kim De Leeneer, Marc D'Hooghe and Anne Vral

Neuromolecular Medicine 2013; 15 (3), 447-457

The genetic data of an AT patient was analyzed and correlated with the mild AT phenotype, data from a kinase assay, and results from two chromosomal radiosensitivity assays. Genotyping revealed compound heterozygosity for *ATM*: c.8122G>A (p.Asp2708Asn) and c.8851-1G>T, leading to an in frame loss of 63 nucleotides at the cDNA level. A kinase assay demonstrated remaining activity of ATM, which is generally absent in classic AT patients. Enhanced radiosensitivity was demonstrated in lymphocytes of the variant AT patient with the G0 micronucleus assay, though less prominent than observed in classic AT patients. The efficiency of the G2 micronucleus assay was evaluated and demonstrated a more pronounced increase in radiation-induced MN yield for the variant AT patient compared to the results of the G0 micronucleus assay. Furthermore, G2/M checkpoint activity of the variant AT patient was evaluated by means of the G2 micronucleus assay and an impaired arrest capacity was demonstrated compared to healthy controls. In addition, the G2 micronucleus assay was applied on lymphocytes of healthy relatives with a heterozygous *ATM* mutation and demonstrated an enhanced radiosensitivity for both radiation-induced MN yield and G2/M checkpoint efficiency, intermediate between the AT patients and controls.

Paper II: Increased chromosomal radiosensitivity in asymptomatic carriers of a heterozygous *BRCA1* mutation

Annelot Baert, Julie Depuydt, Tom Van Maerken, Bruce Poppe, Fransiska Malfait, Katrien Storm, Jenneke van den Ende, Tim Van Damme, Sylvia De Nobele, Gianpaolo Perletti, Kim De Leeneer, Kathleen B. M. Claes and Anne Vral

Breast Cancer Research 2016; 18 (1), 52-63

Radiosensitivity was analyzed by means of the G2 micronucleus assay in a cohort of 18 *BRCA1* mutation carriers and compared with data from 20 healthy volunteers with no known personal or familial breast cancer anamnesis. A significantly radiation-induced MN yield and G2/M checkpoint ratio, could be demonstrated for the cohort of *BRCA1* mutation carriers compared to the healthy volunteers. This points towards an impaired DNA repair and G2 arrest capacity in mutation carriers. In a second phase of this study, a link between increased individual radiosensitivity and the remaining mRNA level of the mutant allele was evaluated. Therefore, individual radiosensitivity of *BRCA1* mutation carriers, expressed as a Radiosensitivity INDicator (RIND) score, taking into account both MN yield and G2/M checkpoint activity, was evaluated. A higher RIND score was observed for *BRCA1* mutations leading to a premature termination codon in the central part of the gene, prone to NMD and thus mRNA degradation, compared to the control cohort. This suggests haploinsufficiency as the mechanism for radiosensitivity. However, the even higher RIND scores observed in individuals with mutations at the 5' end of the gene, which would escape NMD, suggest a possible alternative mechanism, such as a dominant negative effect.

Paper III: Analysis of chromosomal radiosensitivity of healthy *BRCA2* mutation carriers and non-carriers in *BRCA* families with the G2 micronucleus assay.

Annelot Baert, Julie Depuydt, Tom Van Maerken, Bruce Poppe, Fransiska Malfait, Tim Van Damme, Sylvia De Nobele, Gianpaolo Perletti, Kim De Leeneer, Kathleen B.M. Claes and Anne Vral.

Oncology reports 2017; 37, 1379-1386

In this paper, radiosensitivity of a cohort of 18 healthy *BRCA2* mutation carriers and 17 relatives without the familial *BRCA* mutation (non-carrier relatives) was compared with healthy controls, by means of the G2 MN assay. An increased MN yield in the cohort of *BRCA2* carriers compared to the healthy volunteers without a personal or familial history of breast cancer was observed. For the 17 non-carrier relatives of both *BRCA1* (n=9) and *BRCA2* (n=8) families, no increased radiosensitivity was observed compared to the control cohort.

Paper IV: The RAD51 foci assay for the detection of impaired homologous recombination in irradiated MCF10A cells with a *BRCA1* or *BRCA2* knockdown.

Annelot Baert, Maria Federica Palermo, Julie Depuydt, Mattias Van Heetvelde, Bram Verstraete, Jan Phillippé, Anna Sablina, Kathleen Claes and Anne Vral.

Article in preparation for submission to Plos One

In this paper, the suitability of the RAD51 foci assay for the evaluation of HR activity in breast epithelial cell lines (MCF10A) with reduced protein levels of *BRCA1* and *BRCA2*, obtained by RNA interference, was evaluated. MCF10A cells were synchronized in S phase of the cell cycle by aphidicolin for optimal detection of HR capacity. DSB were induced by exposing the cells to ionizing radiation. Recruitment of RAD51, a key HR protein, to the DSB was observed as foci formation and RAD51 foci were visualized by means of an immunostaining. A significant decrease in RAD51 foci was demonstrated in *BRCA1* and *BRCA2* knockdown cell lines compared to the control cell line.

Paper V: Thorough *in silico* and *in vitro* cDNA analysis of 21 putative *BRCA1/2* splice variants and identification of activated cryptic splice donor sites in exon 11 of *BRCA2*

Annelot Baert, Eva Machackova, Ilse Coene, Carol Cremin, Kristin Turner, Cheryl Portigal-Todd, Marie Jill Asrat, Jennifer Nuk, Allison Mindlin, Young Sean, Andree MacMillan, Tom Van Maerken, Martin Trbusek, Wendy C McKinnon, Marie E Wood, William D Foulkes, Marta Santamariña, Miguel de la Hoya, Lenka Foretov, Bruce Poppe, Toon Rosseel, Kim De Leeneer, Anne Vral, Ana Vega, Kathleen BM Claes

Article in preparation for submission to Human Mutation

In silico predictions and mRNA analysis in short-term cultured lymphocytes were performed for 19 putative *BRCA1* and *BRCA2* splice site variants. Aberrant splicing was demonstrated for nine variants suggesting that these variants are likely pathogenic. Furthermore, the effect at the cDNA level of a novel tandem duplication with a 5' breakpoint in intron 4 and a 3' breakpoint in exon 11 of the *BRCA2* gene was studied. This allowed the identification of an actively used cryptic donor site within the large exon 11.

PAPER I: Variant Ataxia Telangiectasia: Clinical and Molecular Findings and Evaluation of Radiosensitive Phenotypes in a Patient and Relatives

Kathleen Claes^{*1}, Julie Depuydt^{*2}, A. Malcolm R Taylor³, James I Last³, Annelot Baert¹⁻², Peter Schietecatte¹, Veerle Vandersickel⁴, Bruce Poppe¹, Kim De Leeneer¹, Marc D'Hooghe^{**5}, Anne Vral^{**2}

¹ Center for Medical Genetics, Ghent University Hospital, De Pintelaan 185, B-9000 Gent, Belgium

² Department of Basic medical Sciences, Ghent University, De Pintelaan 185, B- 9000 Gent, Belgium

³ School of Cancer Sciences, University of Birmingham, Birmingham B15 2TT, United Kingdom

⁴ NRF iThemba LABS, PO Box 722, 7129 Somerset West, South Africa

⁵ Department of Neurology and Child Neurology, AZ St-Jan, B-8000 Brugge, Belgium

* K. Claes and J. Depuydt contributed equally to this work

** M. D'Hooghe and A. Vral contributed equally to this work

Key words: *in vitro* radiosensitivity, S-G2 micronucleus assay, variant ataxia telangiectasia, ATM heterozygous carriers, cDNA analysis, kinase assay

Neuromolecular Medicine, 2013, 15 (3): 447–457
doi: 10.1007/s12017-013-8231-4

Abstract

Research objectives: Variant ataxia telangiectasia (A-T) may be an underdiagnosed entity.

We correlate data from radiosensitivity and kinase assays with clinical and molecular data from a patient with variant A-T and relatives.

Methods: The coding region of *ATM* was sequenced. To evaluate the functional effect of the mutations we performed kinase assays and developed a novel S-G2 micronucleus test.

Results: Our patient presented with mild dystonia, moderately dysarthric speech, increased serum α -fetoprotein but no ataxia nor telangiectasias, no nystagmus or oculomotor dyspraxia. She has a severe IgA deficiency, but does not have recurrent infections. She is compound heterozygote for *ATM* c.8122G>A (p.Asp2708Asn) and c.8851-1G>T, leading to *in frame* loss of 63 nucleotides at the cDNA level. A trace amount of ATM protein is translated from both alleles. Residual kinase activity is derived only from the p.Asp2708Asn allele.

The conventional G0 micronucleus test, based on irradiation of resting lymphocytes, revealed a radiosensitive phenotype for the patient, but not for the heterozygous relatives. As ATM is involved in HR and G2/M cell cycle checkpoint, we optimised an S/G2 micronucleus assay, allowing to evaluate micronuclei in lymphocytes irradiated in the S and G2 phases. This test showed increased radiosensitivity for both the patient and heterozygous carriers. Intriguingly, heterozygous carriers of c.8851-1G>T (mutation associated with absence of kinase activity) showed a stronger radiosensitive phenotype with this assay than heterozygous carriers of p.Asp2708Asn (mutation associated with residual kinase activity).

Significance: The modified S-G2 micronucleus assay provided phenotypic insight to complement the diagnosis of this atypical A-T patient.

Introduction

Ataxia telangiectasia (A-T) (MIM#208900) is a rare autosomal recessive disorder, caused by germline mutations in the *ATM* gene (MIM#607585). A-T features include cerebellar ataxia, oculomotor apraxia, oculocutaneous telangiectasia, immune deficiency, elevated serum α -fetoprotein levels and acquired 7- and 14-chromosome translocations in the lymphocyte karyotype. In addition, A-T is characterized by clinical and cellular hypersensitivity to ionizing radiation (IR), and by an increased risk of cancer (Chen et al. 1978; Lavin 2008).

In recent years, it has become increasingly evident that the clinical phenotype of ataxia telangiectasia varies from a severe, early-onset classic phenotype to a variant form with milder neurological impairment and fewer systemic symptoms (Hiel et al. 2006; Saviozzi et al. 2002; Silvestri et al. 2010; Simonin et al. 2008; Stankovic et al. 1998; Sutton et al. 2004; Verhagen et al. 2009). Especially in patients with milder or atypical presentations, the disease may be more difficult to diagnose.

ATM is transcribed in a broad range of tissues to a mRNA of approximately 13 kb encoding a nuclear protein of 3056 amino acids, belonging to the family of phosphatidylinositol-3-kinase-related protein kinases (Uziel et al. 1996). The severity of the clinical phenotype of A-T patients depends on the presence of the ATM protein and of residual ATM kinase activity. These features are determined by the genotype: severely affected patients generally have truncating mutations resulting in the total absence of ATM kinase activity, while patients with milder phenotypes carry at least one missense or leaky splice site mutation (still producing some normal ATM), resulting in expression of ATM with residual kinase activity (Verhagen et al. 2012). A single study reported that missense mutations associated with A-T may lead to decreased expression of the ATM protein due to abnormal cytoplasmic localization of ATM (Jacquemin et al. 2012).

ATM plays a critical role in regulating cell cycle progression and checkpoint activation in response to DSB, and in the repair of DSB by HR and c-NHEJ (Deckbar et al. 2007; Kuhne et al. 2004; Riballo et al. 2004). These DNA damage response mechanisms are active in maintaining genomic stability in normal cells. When these mechanisms are defective (as in A-T patients) enhanced susceptibility to cancer may occur. DNA DSB can be induced by endogenous or exogenous agents, like ionizing radiation. Since ATM activation plays a crucial role in the response to DSB, A-T patients are also very sensitive to radiation exposure. It has been shown that exposure to ionizing radiation activates ATM kinase. This activation is accompanied by

autophosphorylation of S1981, S367, S893 in ATM (Bakkenist and Kastan 2003; Kozlov et al. 2011; Kozlov et al. 2006), an extensive list of ATM phosphorylation sites can be found at the PhosphoSite database: <http://www.phosphosite.org/proteinAction.do?id=1393&showAllSites=true> and phosphorylation of a large number of downstream targets. ATM is the central component of the signal transduction pathway that leads to cell cycle checkpoint control and DNA repair (Kurz and Lees-Miller 2004). Consequently, A-T cells show cell cycle checkpoint defects following irradiation resulting in a failure of the cells to arrest in G1-S, S or G2-M in order to allow proper repair of DSB. Xu et al. (Xu et al. 2002) showed the existence of 2 distinct G2/M checkpoints, involving different molecular effectors: (i) the “early” G2/M checkpoint, occurring immediately after irradiation, is ATM-dependent, dose-independent and reflects the failure of cells, irradiated in G2, to progress into mitosis, and (ii) a “later” control mechanism, measurable only several hours after IR, which causes G2 accumulation. This latter mechanism is ATM-independent, dose-dependent and accumulates cells that had been exposed to radiation in earlier phases of the cell cycle (Xu, et al., 2002).

Non-repaired or mis-repaired DSB are responsible for the chromosomal aberrations in the daughter cells. An enhanced level of spontaneous chromosomal translocations and a marked increase of chromosomal radiosensitivity are hallmarks of the A-T cellular phenotype. Although an enhanced chromosomal or cellular radiosensitivity is not unique for A-T patients - it is also observed in patients carrying mutations in other DNA damage response genes (e.g. *MRE11*, *NBS1*, *Artemis*, *DNA Lig4*, *FANC* genes)- it can represent a valuable adjunctive phenotypic marker for A-T when complemented with AFP (serum alpha fetoprotein) testing and with clinical signs of the disease (Buck et al. 2006; Gennery 2006; Girard et al. 2000; Sun et al. 2002).

The cytogenetic assays that are mostly used to detect chromosomal radiosensitivity in patients with cancer-prone genetic disorders and in cancer patients are the G0 micronucleus assay and the G2 chromatid break assay (reviewed in: (Baria et al. 2001; Parshad and Sanford 2001; Scott et al. 1999). These cytogenetic assays have the advantage of being directly performed on primary lymphocytes cultured from a blood sample without establishment of lymphoblastoid or fibroblast cell lines, in contrast with colony survival assays (Fernet et al. 2004; Sun et al. 2002; West et al. 1995; Chen et al. 1978).

Although the above mentioned assays can be used as valuable functional tests to phenotypically complement the diagnosis of A-T in “classic” A-T patients (Pantelias and

Terzoudi 2011; Terzoudi et al. 2009; Tchirkov et al. 1997; Vral et al. 1996; Scott et al. 1996; Chen et al. 1994; Sanford et al. 1990), only scant data are available on the suitability/sensitivity of radiosensitivity assays to confirm a diagnosis of A-T in patients showing “milder or atypical” forms of the disease (Jongmans et al. 1998; Gilad et al. 1998; Bartsch et al. 2012).

In the present study we characterized the genetic and phenotypic profile of an atypical case of A-T. To optimally evaluate the radiosensitive phenotype of the A-T pedigree we designed a modified micronucleus assay focusing on the S/G2 phases of the cell cycle, and allowing to detect defects in the HR and G2/M checkpoint pathways, both involving ATM. For molecular confirmation of the clinical diagnosis, mutation analysis of the complete coding region and splice site regions of the *ATM* gene was performed.

Materials and Methods

Blood sampling

For this study EDTA and heparinized blood samples were collected from a patient with a tentative clinical diagnosis of atypical AT and from her family members (see case description in results section). The EDTA samples were used for mutation analysis of the *ATM* gene and for the splicing assays. This study, has been approved by the ethical committee of Ghent University Hospital (registration number B670201111641 d.d. 20/09/2011). All participants signed an informed consent.

The heparinized samples were subjected to radiosensitivity analysis with the conventional G0 micronucleus assay, and with our novel, optimized S-G2 micronucleus assay. Blood samples were taken on different occasions to confirm the obtained results and to exclude random errors. From the A-T patient, blood samples were collected on three different occasions. Both parents were sampled in 2 different occasions. A cousin (paternal niece) of the patient, diagnosed with an embryonal rhabdomyosarcoma at the age of 7, agreed to donate a single blood sample. For each radiation experiment, a blood sample from a healthy volunteer was collected, this to be paired with the samples from the patient or patient’s relatives.

Mutation analysis of the *ATM* gene

Genomic DNA was extracted from EDTA blood samples of the patient and relatives according to manufacturer's protocols (PureGene DNA extraction, Qiagen). The complete coding region and splice site regions of the *ATM* gene were analysed by direct Sanger sequencing. Reference sequence used: NM_000051.3. Large genomic rearrangements at the *ATM* locus were screened by MLPA analysis (MRC Holland, MLPA P041 and MLPA P042).

Furthermore, the effect of the splice site mutation was verified by RNA extracted from short term IL2/PHA stimulated lymphocyte cultures. At day 7, 4–6 h before harvesting the cells, each culture was split evenly and one part was treated with 200 µg/ml of puromycin (Sigma). RT-PCR was performed with primers spanning the relevant exons. Primer sequences can be found in Table 1.

Table 1: primer sequences used for RT-PCR

<i>Name</i>	<i>exon</i>	<i>sequence (5'-3')</i>
F1	61	CAGGGCAAATCCTTCCTACTCC
R1	64	GGGGTCTATGGCCTGCTGTATG
F2	55	CCAGCAGACCAGCCAATTA
R2	63	TTCAAAGGATTCATGGTCCAG

Immunoblotting for *ATM* expression and *ATM* activity assays

For *ATM* protein expression and activity assays, patient-derived lymphoblastoid cells were harvested. The assays were performed as described before (Reiman et al. 2011).

Radiosensitivity testing / AT phenotyping

For the G0 micronucleus assay blood samples of the patient, of the patient's relatives and of healthy volunteers were sham-irradiated or irradiated *in vitro* with 0.5, 1 and 2 Gy doses of ⁶⁰Co-gamma rays. Blood cultures (0.5 ml blood in 4.5 ml RPMI medium containing 10 % FCS) of irradiated/sham-irradiated peripheral blood lymphocytes (PBL) were set up, and cell division was stimulated by addition of 100 µl phytohaemagglutinin (PHA) (Life Technologies). 24 h after irradiation, cytokinesis was blocked by addition of 6 µg/ml cytochalasin B (Sigma Aldrich); 48 h later cells were fixed in methanol-acetic acid. Micronuclei (MN) - small

extranuclear bodies resulting mainly from acentric chromosomal fragments lagging behind during anaphase - were scored in cells that underwent a single cell division. These cells can be identified as binucleated (BN) cells. Fixed cells were spread on a microscope slide and stained with fluorescent DAPI. MN were subsequently scored in 1000 BN cells by an automated image analysis system that allows high throughput analysis (Metafer4, MNscore software module, Metasystems, Germany). Besides scoring MN, the automated software also calculated a binucleation index (BI), to assess the number of once-divided cells.

For the S-G2 micronucleus assay, blood cultures were set up with the addition of PHA, in order to stimulate division of resting PBL prior to *in vitro* irradiation. Immediately after irradiation, cytochalasin B was added to the cultures.

Based on optimization experiments, a dose of 4 Gy and a post-irradiation (PI) time of 8h was selected for detecting DNA damage induced in cells in the S and G2 phases of the cell cycle. Shorter post-irradiation times were not feasible as they resulted in very low yields of BN cells. Fixation, staining, MN and BI scoring procedures were performed as described above (G0 micronucleus assay). To determine the percentage of cells that were in S or G2 phase of the cell cycle at the moment of irradiation, we performed cell cycle analysis by adding 0,01mM 5-bromo-2'-deoxyuridine (BrdU) (Sigma-Aldrich) to the cell cultures at the moment of irradiation. Subsequently, MN slides were subjected to anti-BrdU staining (Dako) to visualize S phase cells. About 48 % of the BN cells were positively stained (and hence in the S-phase) while the remaining BN cells (≈ 52 %) were negative (and hence in the G2 phase, data not shown).

In addition, we added 4mM caffeine (Sigma-Aldrich) to blood cultures of the patient, the patient's relatives and the healthy volunteers just before irradiation. Caffeine is an agent known to radiosensitize cells in S and G2 by abrogating the ATM dependent 'early' G2/M checkpoint, and by decreasing HR (Terzoudi et al. 2009; Wang et al. 2004). The ratio of MN yields obtained in S- and G2-irradiated lymphocytes of the same individual, in the presence or absence of caffeine (ratio MNcaf+:MNcaf-), shows the efficiency of both the G2/M checkpoint and the HR repair system of an individual. This difference is defined as an individual radiosensitivity parameter (IRP). The lower the IRP value the higher the radiosensitivity of the individual.

Results

Case description

The proband, currently 25 years old, was born after 38 weeks of gestation with a birth weight of 2100 g. According to the parents, she showed normal early psychomotor development, except for a 'peculiar' gait. She has always been considered clumsy. The girl is left-handed. From the age of 2 years on there was a suspicion of athetosis. At the age of 2.5 years she underwent strabismus surgery. During childhood and adolescence she suffered from recurrent sinopulmonary infections. A neurological clinical examination at the age of 6-8 years showed choreo-athetosis and dystonia, dysarthria, slight drooling, no ataxia and normal tendon reflexes. EEG and brain MRI were normal. A diagnosis of mild dyskinetic cerebral palsy was made. She had no learning disabilities. At the age of 10 years normal results were obtained from routine and metabolic investigations in blood and urine. Evoked potential examinations (VER, BAER, SSER) and analysis of cerebrospinal fluid, including 5-HIAA en HVA, revealed normal results. A therapeutic trial with L-dopa, baclofen and tetrazepam had no effect. At the age of 16 years a normal cerebral MRI and MR-spectroscopy was obtained. At the age of 18 years psychological problems led to a temporary psychiatric treatment with psychotherapy and psycho-active drugs. In the following years she successfully completed a master's degree. Clinical examination at the age of 23 years revealed no ocular or cutaneous telangiectasias. There was no nystagmus or oculomotor dyspraxia. Her speech remained moderately dysarthric. The generalized mild dystonia was somewhat more prominent in the face and in the neck. There were difficulties with fine motor skills, such as using utensils and handwriting. The finger-nose test and the heel-knee test were normal, except for a slightly less well performed coordination test in the right upper limb compared to the left upper limb. Examination of muscle strength, sensation, deep tendon reflexes and plantar responses was unremarkable. No abnormalities were observed during the stance and gait examination, including the tandem walking test and one-leg hop test.

As a variant form of ataxia-telangiectasia may present with extrapyramidal signs without telangiectasias nor prominent ataxia, diagnostic tests for this disease were performed. An increased value for serum α -fetoprotein (77.8 U/ml; normal value < 5 U/ml) was found. The patient was referred for genetic testing of the *ATM* gene. Karyotyping did not reveal rearrangements in chromosomes 7 and/or 14 by analysis of 100 mitoses. Hematologic investigations showed severe IgA deficiency, unusual in atypical A-T patients (Verhagen et al.

2009; Verhagen et al. 2012). Besides the recurrent sinopulmonary infections she did not suffer excessively from infectious diseases, nor did she developed other immune-related diseases. Both her parents have normal IgA values, ruling out a familial form of IgA deficiency. A detailed overview of the family pedigree is available in Figure 1.

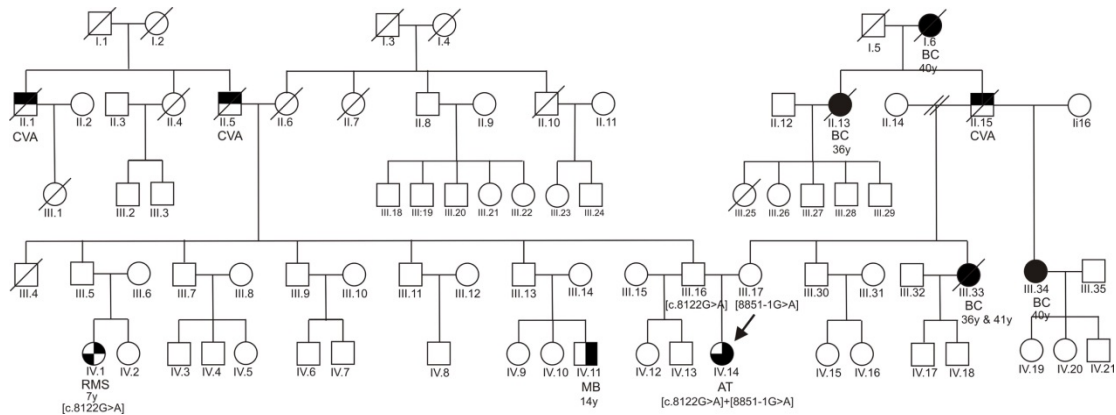


Figure 1. Pedigree of the variant AT patient.

Blood samples were obtained from individuals IV.14 (proband), her parents (III.16 and III.17) and her paternal niece (IV.1) for molecular analysis and analysis of the radiosensitive phenotype.

BC= Breast cancer; CVA=cardiovascular accident; AT= Ataxia telangiectasia like; MB= Medulloblastoma; RMS= embryonal rhabdomyosarcoma

Both parents of the proband are healthy. In the maternal branch of the family a strong burden of breast cancer is evident. In the paternal branch of the family two cousins with childhood tumors are reported. A paternal niece with an embryonal rhabdomyosarcoma at the age of 7 years was treated with chemotherapy and postoperative radiotherapy. A paternal nephew had a medulloblastoma at the age of 14 years, which was surgically resected and postoperatively treated with radiotherapy.

Molecular findings

Sequencing of the complete coding region of the *ATM* gene revealed compound heterozygosity for 2 pathogenic mutations in the proband: a missense mutation in exon 55, c.8122G>A (p.Asp2708Asn), inherited from her father, and a splice site mutation in the acceptor site of exon 63, c.8851-1G>T, inherited from her mother (Figure 2). These findings confirm the diagnosis of a variant form of ataxia-telangiectasia in the proband. In the paternal niece with an embryonal rhabdomyosarcoma at the age of 7 years heterozygosity for the missense mutation *ATM* c.8122G>A (p.Asp2708Asn) was shown.

At the cDNA level, we showed that *ATM* c.8851-1G>T activates a cryptic acceptor site 63 nucleotides downstream of the wild type acceptor (r.8851_8913del; p.Val2951_Gln2971del) (Figure 2). In patients with a variant form of A-T leaky splice site mutations may be the cause

of the milder phenotype (Reiman et al. 2011). However, by amplification with primers located in exon 55 and 63 (Figure 2 - primers F2 and R2, located downstream of *ATM* c.8913 to allow amplification of only the full length allele) we observed only the “A” nucleotide at position c.8122 in exon 56. This indicates that no full length product is transcribed from the mutant allele c.8851-1T (Figure 2).

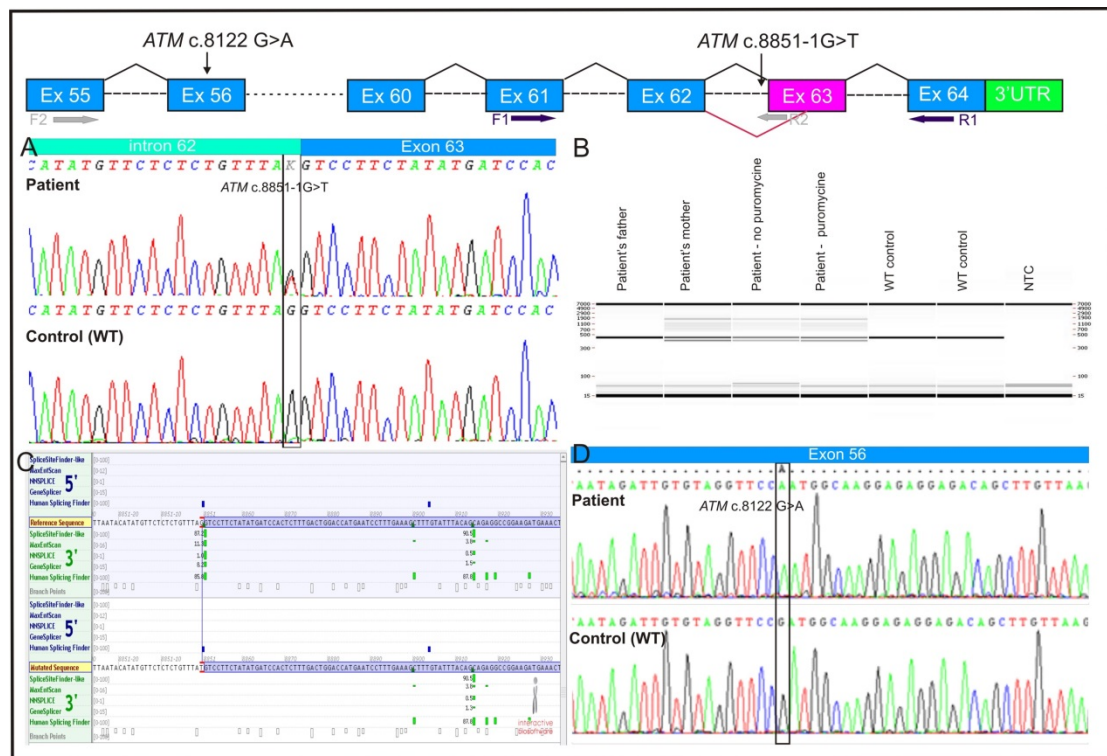


Figure 2: summary molecular results

Direct Sanger sequencing of exon 63 and boundaries (panel A) revealed a heterozygous splice site mutation: *ATM* c.8851-1G>T RT-PCR with primers spanning exon 61-64 (F1-R1)(panel B) revealed that the c.8851-1G>T mutation alters splicing and activates a cryptic acceptor site within exon 63, which was also predicted by splice site prediction programs (panel C). This generates an aberrant transcript with an in frame deletion of the first 63 nucleotides of exon 63 (r.8851_8913del). By amplification of cDNA with primers located in exon 55 and 63 (primers F2 and R2) we observed only the A nucleotide at position c.8122 in exon 56. This indicates that no full length product is transcribed from the mutant allele c.8851-1T.

Protein expression and kinase assays

A strongly reduced level of ATM protein was observed in the patient's cells compared to a negative control (Figure 3). Overexposure of the blot showed trace amounts of 2 different proteins: the largest ATM protein is probably the p.Asp2708Asn from the c.8122G>A

mutation and the lower band is derived from the c.8851-1G>T allele resulting in loss of 21 amino acids from exon 63 (p.Val2951_Gln2971del).

In contrast to the normal control there is a large reduction in kinase activity of the patient's ATM protein. The only activity detectable above the level of the classical A-T patient is with antibodies to KAP-1 ser824, Nbn1 ser343 and CREB ser121 (Figure 3).

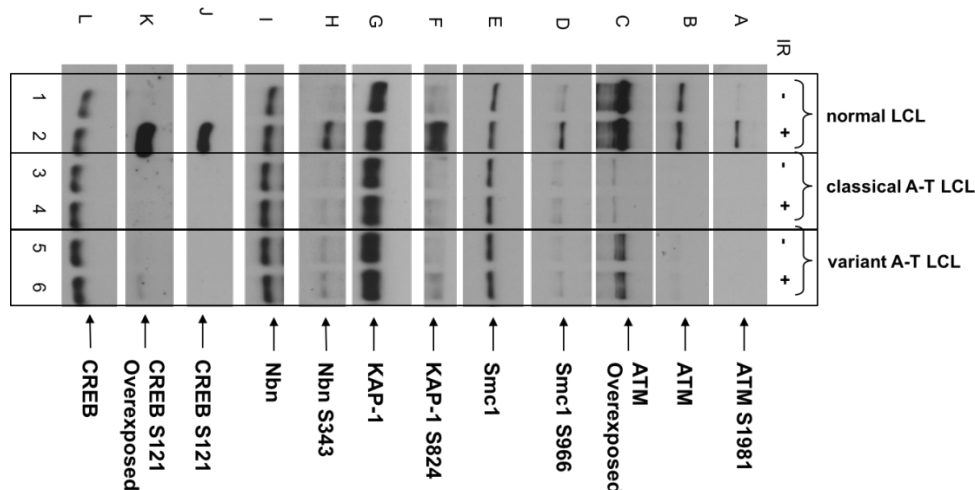


Figure 3: results immunoblots and kinase assays

Whole cell extracts were made from LCLs harvested at 30min post irradiation (2Gy). Blots were probed with phospho antibodies for ATMser1981, SMC1ser966, Nbn1Ser343, Chk2Thr68 and p53Ser15. Blots were also probed with antibodies for ATM, SMC1, Nbn1 and p53 to indicate total levels of these proteins in the lysate. Two lanes per lysate are shown, one unirradiated (-) and one irradiated (+) (activated ATM).

In lanes 1 & 2 are cells from a normal ATM positive control (RB) (panels B & C), showing phosphorylation of the targets SMC1 ser966 (panel D), KAP-1 ser 824 (panel F), Nbn1 ser343 (panel H) and CREB ser121 (panel J & K). There is a strong signal for each of these in lane 2 after activation. The total levels of SMC1, KAP1, Nbn1 and CREB are also shown in panels E, G, I & L respectively.

The negative control is cell lysate from a classical A-T patient (RN) shown in lanes 3 & 4. Here is no phosphorylation of these four targets in this patient's cells in lane 4 – consistent with him having A-T – he has no ATM - (panels B & C).

The cell lysate of our patient with variant A-T is in lanes 5 & 6. Panel B and particularly panel C confirms the reduced level of ATM protein in her cells. With regard to the ATM proteins present, there are three bands. The lowest one is probably non specific (it is seen in the classical A-T with no ATM). The largest ATM protein is probably the p.Asp2708Asn from the c.8122G>A mutation and the middle band from the c.8851-1G>T resulting in loss of 21 amino acids from exon 63. In contrast to the normal control (lane 2) there is a large reduction in activity of ATM protein (lane 6). The only activity detectable (above the level in lane 4 of the classical A-T) is with antibodies to KAP-1 ser824, Nbn1 ser343 and CREB ser121 (overexposed) in lane 6. However, the activity is more than in the lysate from a classical A-T patient (lane 4).

Radiosensitivity assays

G0 micronucleus assay

The data obtained in this study with the G0 micronucleus assay for the patient, the patient's relatives (individuals III.16, III.17, IV.1 from Figure 1) and the healthy volunteers were compared to our reference micronucleus dose response calibration curve (Willems et al. 2010) (Figure 4). In the variant A-T patient, MN values were only obtained after irradiation with doses of 0.5 and 1 Gy. Irradiation with a 2 Gy dose resulted in a very low BN index (< 5%) probably because G0-irradiated lymphocytes (ATM^{-/-}) are irreversibly blocked in G2 (Beamish and Lavin 1994; Xu et al. 2002). In the ATM heterozygous mutation carriers (ATM^{+/-}) and in healthy volunteers higher BN indexes for the 2 Gy dose point were obtained (12% and 17%, respectively), and micronuclei could be scored. The results shown in Figure 4 demonstrate that the conventional G0 micronucleus assay is sensitive enough to identify the variant A-T patient but not the monoallelic ATM mutation carriers. For the variant A-T patient significant, 1.8-fold increases in MN yields were obtained at 0.5 and 1 Gy doses, when compared to the average MN values of our reference curve. In the relatives, heterozygous for an ATM mutation, and in the three healthy donors (data of the healthy donors are not shown in Figure 4 for clarity reasons), the MN values were lying within the 95% confidence limits (UCL, LCL, Figure 4) of the MN reference curve. Although an enhanced radiosensitive phenotype is observed in the variant A-T patient, the observed MN fold-increase of 1.8 is lower than the sensitivity values observed in a previous study from our group, performed on "classic" A-T patients (3 to 5 fold MN increase (Vral et al. 1996)).

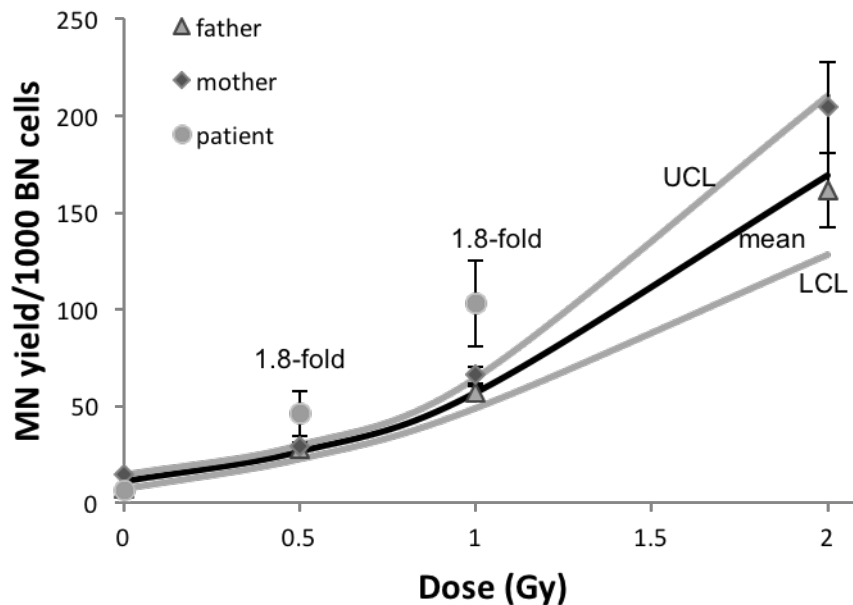


Figure 4: results G0 micronucleus assay

Mean MN values (\pm SD) obtained from the AT patient (3 repeated independent samplings) and from the heterozygous parents (2 repeated independent samplings), plotted against a reference mean MN dose-response curve, and curves for the 95% upper and lower confidence limits (UCL, LCL) (n=10) (adapted from Willems et al. 2010).

S-G2 micronucleus assay

For the modified S-G2 MN assay, the MN yields obtained after exposure to 4 Gy in the variant A-T patient and her relatives were compared with the MN yields from healthy individuals recruited for the present study. The results of the S-G2 MN assay are shown in Figure 5. This figure shows the fold MN increase obtained in repeated, independent samplings in all tested subjects. In the variant A-T patient, a 4-fold increase in the MN yield (mean of three experiments) was observed. This increase in MN yield is more pronounced than the one observed with the G0 micronucleus assay (1.8-fold). The mother of the patient, carrying the *ATM* c.8851-1G>A splice acceptor site mutation, showed a 2.8-fold increase in MN yield (mean of 2 experiments), while the father and the paternal niece, both carrying the *ATM* c.8122G>A (p.Asp2708Asn) missense mutation, showed a similar 1.4-fold MN increase.

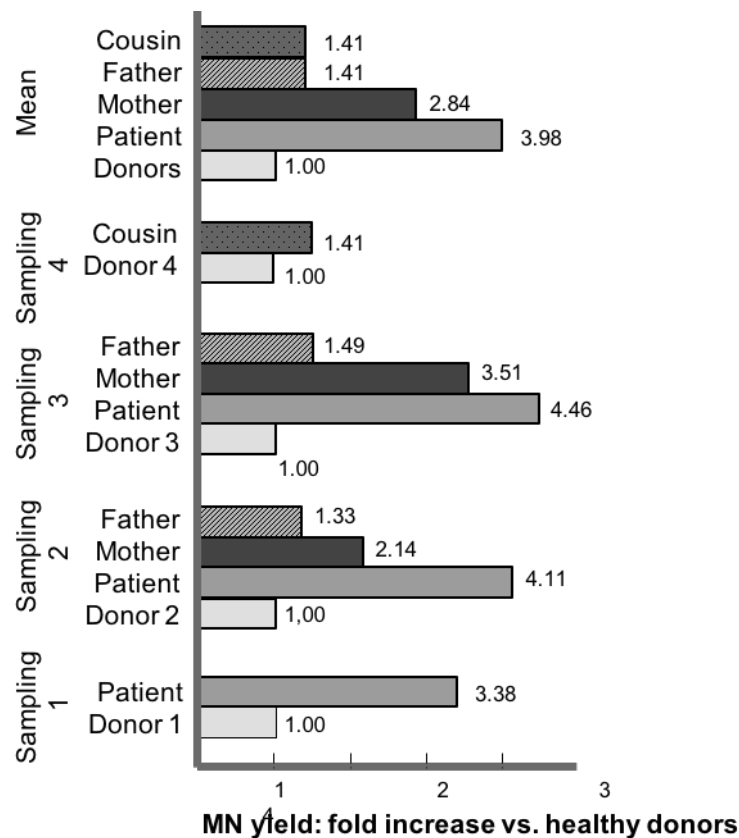


Figure 5: results S-G2 micronucleus assay.

MN yields observed in the tested subjects are expressed as fold increase relative to the MN yields observed in the healthy donors. The average fold increase obtained for the AT patient (3 samplings), the patient's parents (2 samplings) and paternal niece (one sampling) as well as the fold increase observed per single independent sampling are shown in the graph.

S-G2 micronucleus assay with caffeine

IRP values, representing the ratio of MN_{caf+}/MN_{caf-} , are presented in Figure 6. Data obtained from the variant A-T patient, the *ATM* heterozygous family members and seven healthy donors are presented. In healthy donors, a mean IRP value (μ_{IRP}) of 3.86 ± 1.00 (SD) (range IRP values: 2.71-5.39) was obtained. According to Terzoudi et al. (Terzoudi et al. 2009) individuals may be defined "normal" when $IRP = \mu_{IRP} \pm 1SD$, "radiosensitive" when $\mu_{IRP} - 2SD \leq IRP < \mu_{IRP} - 1SD$, and "highly radiosensitive" when $IRP < \mu_{IRP} - 2SD$. Applying this classification system to our data, the variant A-T patient and mother of the patient turned out to be highly radiosensitive ($IRP_{patient} = 1.85$; $IRP_{mother} = 1.6$), while the father and the paternal niece, carrying the same mutation, were found to be radiosensitive ($IRP_{father} = 2.01$; $IRP_{cousin} = 2.6$).

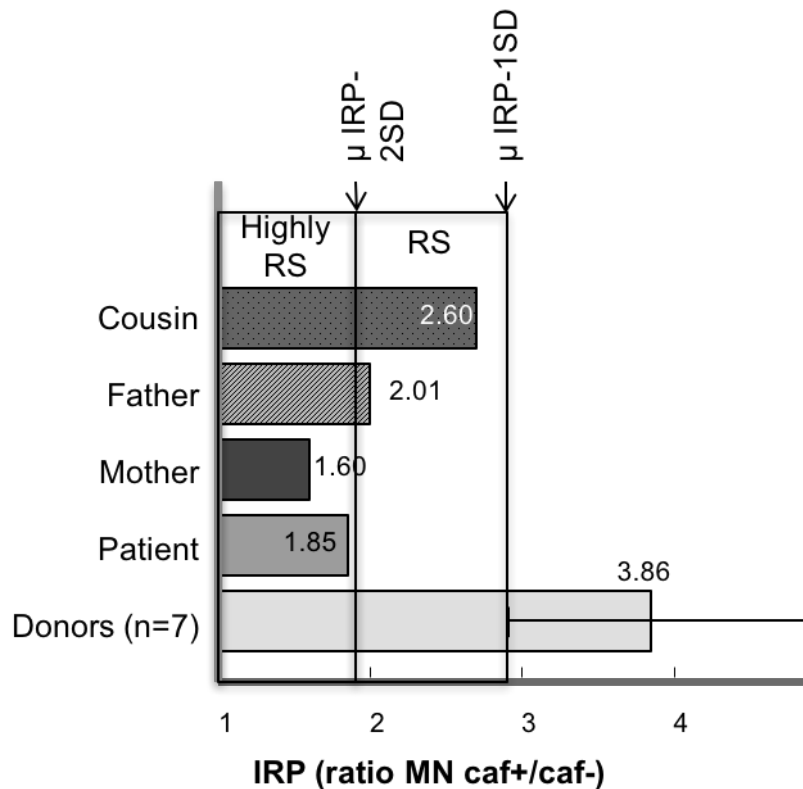


Figure 6: results S-G2 micronucleus assay with the addition of caffeine

Individual Radiosensitivity Parameter (IRP) values, representing the MNcaf+/MNcaf- ratio, i.e. the ratio of micronuclei generated in the presence (MNcaf+) or absence (MNcaf-) of caffeine. IRPs from the A-T patient, from the heterozygous family members and from seven healthy donors are presented. The mean IRP reference value for the healthy donor group ($\mu\text{IRP} \pm 1\text{SD}$) is 3.86 ± 1 . Individuals are defined “normal” when their IRP is equal to $\mu\text{IRP} \pm 1\text{SD}$, “radiosensitive” when their IRP ranges between $\mu\text{IRP}-2\text{SD}$ and $\mu\text{IRP}-1\text{SD}$ ($\mu\text{IRP}-2\text{SD} \leq \text{IRP} < \mu\text{IRP}-1\text{SD}$), and “highly radiosensitive” when their $\text{IRP} < \mu\text{IRP}-2\text{SD}$.

Discussion

Classic ataxia telangiectasia is a severe, childhood-onset disease whose characteristic findings are early-onset cerebellar ataxia, oculocutaneous telangiectasia, and susceptibility to pulmonary disease. These patients have an increased risk of cancer, especially hematologic malignancies.

The long diagnostic delay in the current case exemplifies the difficulties in diagnosing patients with a variant form of A-T. In these cases the ATM protein is still expressed and residual kinase activity of ATM is found. Clinically, these patients have a milder and different neurological phenotype. Extrapyrimal signs (chorea-athetosis, resting tremor, sometimes myoclonus-dystonia) are detected. Telangiectasias are often absent. Ataxia is not an initial symptom, and the later occurring ataxia is of mild-to-moderate degree (Verhagen et al. 2009). These patients

have an extended lifespan. Cancer may occur later in life and generally consists of solid instead of lymphoid malignancies. Serum α -fetoprotein is elevated in both classic and variant A-T (Verhagen et al. 2009; Verhagen et al. 2012), but not in heterozygous carriers (Stray-Pedersen et al. 2007). The patient presented here was found to be immunologically atypical, with a severe IgA deficiency which was not reported in any variant A-T patient described before (Verhagen et al. 2009; Verhagen et al. 2012).

At the age of 25 years the patient has not developed cancer, but as with all A-T patients is at increased risk. The relatives, heterozygous for an *ATM* mutation, have also an increased risk for cancer. In the maternal branch a strong predisposition for breast cancer is evident, while in the paternal branch 2 childhood tumors were reported (Figure 1). The paternal cousin, diagnosed with an embryonal rhabdomyosarcoma, was found to be heterozygous for the *ATM* missense mutation p.Asp2708Asn. Sarcomas are an established entity in the cancer spectrum occurring in classical A-T patients. A further link between *ATM* and rhabdomyosarcoma has previously been established based on the frequent observation of complete loss of *ATM* expression in rhabdomyosarcoma (Zhang et al. 2003).

The finding of a missense and a splice site mutation is compatible with the phenotype of variant ataxia telangiectasia, depending on whether one or both of these results in expression of *ATM* protein with activity. The missense mutation *ATM* c.8122G>A (p.Asp2708Asn) has previously been described in other A-T patients. An Italian A-T patient, was described with a splice site mutation on the second other allele (*ATM* c.2250G>A – in the last nucleotide of exon 14, leading to in frame skipping of this exon at the cDNA level) (Cavalieri et al. 2006). However, the phenotype of this patient was not given. Furthermore, *ATM* c.8122G>A (p.Asp2708Asn) has been reported as a somatic mutation in lung cancer (COSMIC database). A low level of residual kinase activity associated with the *ATM* c.8122G>A (p.Asp2708Asn) mutation has previously been observed in cells from another patient with this mutation (Reiman et al. 2011). Modelling of the mutation and expression of the mutant *ATM* p.Asp2708Asn protein showed it to have some *ATM* kinase activity (Barone et al. 2009). Therefore the confirmation of the low level of *ATM* kinase activity in our patients cells is consistent with the presence of the p.Asp2708Asn mutant protein and diagnosis of variant A-T.

To our knowledge, the substitution c.8851-1G>T in the acceptor site of the penultimate exon of *ATM* has not yet been described in A-T patients but it has previously been reported that heterozygous carriers of this mutation have an increased risk of breast cancer (Goldgar et al. 2011; Tavgigian et al. 2009). Notably, an increased incidence of breast cancer is observed in the maternal branch of the family. Up till now we did not have access to genetic material of any of the maternal relatives affected with breast cancer. The substitution c.8851-1G>T leads to an aberrant transcript with an *in frame* deletion of 21 amino acids (p.Val2951_Gln2971del) from the PI3_PI4_kinase domain (PFAM PF00454, 2711–2962). From the RT-PCR results it is clear that the aberrant transcript is not subjected to NMD and, the shorter protein detected on the immunoblots suggests trace amounts of expression of this protein. However, we have no evidence that p.Val2951_Gln2971del has any residual kinase activity.

The results obtained with the G0 and the S-G2 micronucleus assay, show that the latter was a more powerful assay to demonstrate radiosensitivity in this specific case of variant A-T. The finding of a more pronounced radiosensitive behaviour of lymphocytes with the S-G2 micronucleus assay compared to the G0 micronucleus assay, may indicate that the role of ATM in the DNA damage response is more important when cells are in the S or G2 phases at the moment of irradiation thus resulting in increased chromosomal damage. Our findings in this variant A-T patient of an enhanced micronucleus yield in binucleate cells after irradiation in G2 are in agreement with the enhanced number of chromatid breaks observed in mitotic cells of A-T patients after irradiation in G2 (Pantelias and Terzoudi 2011; Terzoudi et al. 2009; Tchirkov et al. 1997; Scott et al. 1996; Chen et al. 1994; Sanford et al. 1990). The main advantages of the analysis of G2-phase radiation-induced micronuclei compared to chromatid breaks in PHA-stimulated blood lymphocytes, as described in this study, are the high yield of binucleate cells that can be analysed, the easy slide preparation technique and the quick and objective automated scoring procedure (Willems et al. 2010). This makes the S-G2 MN assay very useful in a clinical setting.

We evaluated the effect of the addition of caffeine, an agent known to radiosensitize cells in S and G2 by abrogating the ATM dependent 'early' G2/M checkpoint, for the assessment of individual radiosensitivity in all tested subjects. Although many inhibitors targeting ATM exist (Khalil et al. 2012) our choice for caffeine was based on the studies of Terzoudi et al. (Pantelias

and Terzoudi 2011; Terzoudi et al. 2009) where the cytogenetic G2-assay, combined with caffeine, was applied on blood samples of A-T homozygote and heterozygote patients to investigate radiosensitivity. Our results are in agreement with the evidence shown by this group, who found IRP values pointing to a *highly radiosensitive* phenotype in A-T homozygous patients, while A-T heterozygotes were found to be *radiosensitive*.

Our results show that with the S-G2 micronucleus assay an enhanced radiosensitivity could also be demonstrated in the *ATM* monoallelic mutation carriers (*ATM*+/-). This is in agreement with other studies that reported an intermediate radiosensitivity – compared to “biallelic” A-T – with the G2 chromatid break assay in lymphocytes of heterozygous carriers of *ATM* mutations (Pantelias and Terzoudi 2011; Terzoudi et al. 2009; Tchirkov et al. 1997; Scott et al. 1996; Chen et al. 1994; Sanford et al. 1990).. Interestingly, we found that the extent of the radiosensitive behavior depends on the underlying mutation and may be correlated with the kinase activity. In this study, the splice site mutation *ATM* c.8851-1G>T, segregating in the maternal branch of the family, results in a more radiosensitive phenotype and absence of kinase activity compared to the missense mutation *ATM* p.Asp2708Asn segregating in the paternal branch of the family and associated with some residual kinase activity. The results were consistent between different independent samplings from the same individual and for different individuals carrying the same mutation. As these are preliminary results obtained in a single variant A-T patient and her relatives, they need to be further confirmed in additional A-T patients and relatives carrying a panel of different *ATM* mutations.

Recently Prodosmo et al. reported preliminary results of a newly developed cost-effective and fast functional test to determine mutant *ATM* zygosity based on p53 centrosomal localisation visualised by immunofluorescence staining (Prodosmo et al. 2013).

The development of functional assays allowing the detection of *ATM* heterozygous carriers can also be of clinical importance. Some reports suggest that *ATM* heterozygotes may be over-represented in the proportion of breast cancer cases that show severe normal tissue reactions following radiotherapy (Angele et al. 2003; Meyer et al. 2004). In addition, women who carry rare deleterious *ATM* missense variants and who are treated with radiation have an elevated risk of developing contralateral breast cancer (Bernstein et al. 2010). As the major breast cancer predisposing genes *BRCA1* and *BRCA2* are also involved in the HR repair pathway active in late S and G2 phases and in checkpoint control, the S-G2 MN assay may also represent a functional assay to identify *BRCA1/2* heterozygous mutation carriers.

In all these cases, genetic analysis and phenotypic profiling should go hand-in-hand in order to achieve an optimal characterization of the specific cases and to refine both diagnosis and therapeutic handling of cancer-prone, genomic instability syndromes.

Acknowledgements

This research was supported by grant G.A044.10 from the Fund for Scientific Research Flanders (FWO) to KC, “Emmanuel van der Schueren” grant from the “Vlaamse Liga tegen Kanker” to PS and by the ‘VLIR Own Initiative Programme’ ZEIN2011PR387 between Belgium and South Africa. Bruce Poppe is a senior clinical investigator for the Fund for Scientific Research Flanders (FWO). We would like to thank Mijke Verhagen for her helpful advices. AMRT thanks Cancer Research UK for continued support.

References

- Angele, S., Romestaing, P., Moullan, N., Vuillaume, M., Chapot, B., Friesen, M., et al. (2003). ATM haplotypes and cellular response to DNA damage: association with breast cancer risk and clinical radiosensitivity. *Cancer Res*, 63(24), 8717-8725.
- Bakkenist, C. J., & Kastan, M. B. (2003). DNA damage activates ATM through intermolecular autophosphorylation and dimer dissociation. *Nature*, 421(6922), 499-506, doi:10.1038/nature01368.
- Baria, K., Warren, C., Roberts, S. A., West, C. M., & Scott, D. (2001). Chromosomal radiosensitivity as a marker of predisposition to common cancers? *Br J Cancer*, 84(7), 892-896, doi:10.1054/bjoc.2000.1701.
- Barone, G., Groom, A., Reiman, A., Srinivasan, V., Byrd, P. J., & Taylor, A. M. (2009). Modeling ATM mutant proteins from missense changes confirms retained kinase activity. *Hum Mutat*, 30(8), 1222-1230, doi:10.1002/humu.21034.
- Bartsch, O., Schindler, D., Beyer, V., Gesk, S., van't Slot, R., Feddersen, I., et al. (2012). A girl with an atypical form of ataxia telangiectasia and an additional de novo 3.14 Mb microduplication in region 19q12. *Eur J Med Genet*, 55(1), 49-55, doi:10.1016/j.ejmg.2011.08.001.
- Beamish, H., & Lavin, M. F. (1994). Radiosensitivity in ataxia-telangiectasia: anomalies in radiation-induced cell cycle delay. *Int J Radiat Biol*, 65(2), 175-184.
- Bernstein, J. L., Haile, R. W., Stovall, M., Boice, J. D., Jr., Shore, R. E., Langholz, B., et al. (2010). Radiation exposure, the ATM Gene, and contralateral breast cancer in the women's environmental cancer and radiation epidemiology study. *J Natl Cancer Inst*, 102(7), 475-483, doi:djq055 [pii]10.1093/jnci/djq055.
- Buck, D., Moshous, D., de Chasseval, R., Ma, Y., le Deist, F., Cavazzana-Calvo, M., et al. (2006). Severe combined immunodeficiency and microcephaly in siblings with hypomorphic mutations in DNA ligase IV. *Eur J Immunol*, 36(1), 224-235, doi:10.1002/eji.200535401.
- Cavalieri, S., Funaro, A., Porcedda, P., Turinetto, V., Migone, N., Gatti, R. A., et al. (2006). ATM mutations in Italian families with ataxia telangiectasia include two distinct large genomic deletions. *Hum Mutat*, 27(10), 1061, doi:10.1002/humu.9454.
- Chen, P., Farrell, A., Hobson, K., Girjes, A., & Lavin, M. (1994). Comparative study of radiation-induced G2 phase delay and chromatid damage in families with ataxia-telangiectasia. *Cancer Genet Cytogenet*, 76(1), 43-46.
- Chen, P. C., Lavin, M. F., Kidson, C., & Moss, D. (1978). Identification of ataxia telangiectasia heterozygotes, a cancer prone population. *Nature*, 274(5670), 484-486.
- Deckbar, D., Birraux, J., Krempler, A., Tchouandong, L., Beucher, A., Walker, S., et al. (2007). Chromosome breakage after G2 checkpoint release. *J Cell Biol*, 176(6), 749-755, doi:10.1083/jcb.200612047.
- Fernet, M., Moullan, N., Lauge, A., Stoppa-Lyonnet, D., & Hall, J. (2004). Cellular responses to ionising radiation of AT heterozygotes: differences between missense and truncating mutation carriers. *Br J Cancer*, 90(4), 866-873, doi:10.1038/sj.bjc.6601549.
- Gennery, A. R. (2006). Primary immunodeficiency syndromes associated with defective DNA double-strand break repair. *Br Med Bull*, 77-78, 71-85, doi:10.1093/bmb/ldl006.
- Gilad, S., Chessa, L., Khosravi, R., Russell, P., Galanty, Y., Piane, M., et al. (1998). Genotype-phenotype relationships in ataxia-telangiectasia and variants. *Am J Hum Genet*, 62(3), 551-561, doi:10.1086/301755.

- Girard, P. M., Foray, N., Stumm, M., Waugh, A., Riballo, E., Maser, R. S., et al. (2000). Radiosensitivity in Nijmegen Breakage Syndrome cells is attributable to a repair defect and not cell cycle checkpoint defects. *Cancer Res*, 60(17), 4881-4888.
- Goldgar, D. E., Healey, S., Dowty, J. G., Da Silva, L., Chen, X., Spurdle, A. B., et al. (2011). Rare variants in the ATM gene and risk of breast cancer. *Breast Cancer Res*, 13(4), R73, doi:bcr2919 [pii]10.1186/bcr2919.
- Hiel, J. A., van Engelen, B. G., Weemaes, C. M., Broeks, A., Verrips, A., ter Laak, H., et al. (2006). Distal spinal muscular atrophy as a major feature in adult-onset ataxia telangiectasia. *Neurology*, 67(2), 346-349, doi:67/2/346 [pii]10.1212/01.wnl.0000224878.22821.23.
- Jacquemin, V., Rieunier, G., Jacob, S., Bellanger, D., d'Enghien, C. D., Lauge, A., et al. (2012). Underexpression and abnormal localization of ATM products in ataxia telangiectasia patients bearing ATM missense mutations. *Eur J Hum Genet*, 20(3), 305-312, doi:ejhg2011196 [pii]10.1038/ejhg.2011.196.
- Jongmans, W., Vuillaume, M., Kleijer, W. J., Lakin, N. D., & Hall, J. (1998). The p53-mediated DNA damage response to ionizing radiation in fibroblasts from ataxia-without-telangiectasia patients. *Int J Radiat Biol*, 74(3), 287-295.
- Khalil, H. S., Tummala, H., & Zhelev, N. (2012). ATM in focus: A damage sensor and cancer target. *Biodiscovery*, 5(1), 1-60. doi:10.7750/BioDiscovery.2012.5.1
- Kozlov, S. V., Graham, M. E., Jakob, B., Tobias, F., Kijas, A. W., Tanuji, M., et al. (2011). Autophosphorylation and ATM activation: additional sites add to the complexity. *J Biol Chem*, 286(11), 9107-9119, doi:10.1074/jbc.M110.204065.
- Kozlov, S. V., Graham, M. E., Peng, C., Chen, P., Robinson, P. J., & Lavin, M. F. (2006). Involvement of novel autophosphorylation sites in ATM activation. *EMBO J*, 25(15), 3504-3514, doi:10.1038/sj.emboj.7601231.
- Kuhne, M., Riballo, E., Rief, N., Rothkamm, K., Jeggo, P. A., & Lobrich, M. (2004). A double-strand break repair defect in ATM-deficient cells contributes to radiosensitivity. *Cancer Res*, 64(2), 500-508.
- Kurz, E. U., & Lees-Miller, S. P. (2004). DNA damage-induced activation of ATM and ATM-dependent signaling pathways. *DNA Repair (Amst)*, 3(8-9), 889-900, doi:10.1016/j.dnarep.2004.03.029.
- Lavin, M. F. (2008). Ataxia-telangiectasia: from a rare disorder to a paradigm for cell signalling and cancer. *Nat Rev Mol Cell Biol*, 9(10), 759-769, doi:10.1038/nrm2514.
- Meyer, A., John, E., Dork, T., Sohn, C., Karstens, J. H., & Bremer, M. (2004). Breast cancer in female carriers of ATM gene alterations: outcome of adjuvant radiotherapy. *Radiother Oncol*, 72(3), 319-323, doi:10.1016/j.radonc.2004.07.010.
- Pantelias, G. E., & Terzoudi, G. I. (2011). A standardized G2-assay for the prediction of individual radiosensitivity. *Radiother Oncol*, 101(1), 28-34, doi:10.1016/j.radonc.2011.09.021.
- Parshad, R., & Sanford, K. K. (2001). Radiation-induced chromatid breaks and deficient DNA repair in cancer predisposition. *Crit Rev Oncol Hematol*, 37(2), 87-96.
- Prodosmo, A., De Amicis, A., Nistico, C., Gabriele, M., Di Rocco, G., Monteonofrio, L., et al. (2013). p53 centrosomal localization diagnoses ataxia-telangiectasia homozygotes and heterozygotes. *J Clin Invest*, 123(3), 1335-1342, doi:10.1172/JCI67289.
- Reiman, A., Srinivasan, V., Barone, G., Last, J. I., Wootton, L. L., Davies, E. G., et al. (2011). Lymphoid tumours and breast cancer in ataxia telangiectasia; substantial protective effect of residual ATM kinase activity against childhood tumours. *Br J Cancer*, 105(4), 586-591, doi:10.1038/bjc.2011.266.

- Riballo, E., Kuhne, M., Rief, N., Doherty, A., Smith, G. C., Recio, M. J., et al. (2004). A pathway of double-strand break rejoining dependent upon ATM, Artemis, and proteins locating to gamma-H2AX foci. *Mol Cell*, 16(5), 715-724, doi:10.1016/j.molcel.2004.10.029.
- Sanford, K. K., Parshad, R., Price, F. M., Jones, G. M., Tarone, R. E., Eierman, L., et al. (1990). Enhanced chromatid damage in blood lymphocytes after G2 phase x irradiation, a marker of the ataxia-telangiectasia gene. *J Natl Cancer Inst*, 82(12), 1050-1054.
- Saviozzi, S., Saluto, A., Taylor, A. M., Last, J. I., Trebini, F., Paradiso, M. C., et al. (2002). A late onset variant of ataxia-telangiectasia with a compound heterozygous genotype, A8030G/7481insA. *J Med Genet*, 39(1), 57-61.
- Scott, D., Barber, J. B., Spreadborough, A. R., Burrill, W., & Roberts, S. A. (1999). Increased chromosomal radiosensitivity in breast cancer patients: a comparison of two assays. *Int J Radiat Biol*, 75(1), 1-10.
- Scott, D., Spreadborough, A. R., Jones, L. A., Roberts, S. A., & Moore, C. J. (1996). Chromosomal radiosensitivity in G2-phase lymphocytes as an indicator of cancer predisposition. *Radiat Res*, 145(1), 3-16.
- Silvestri, G., Masciullo, M., Piane, M., Savio, C., Modoni, A., Santoro, M., et al. (2010). Homozygosity for c 6325T>G transition in the ATM gene causes an atypical, late-onset variant form of ataxia-telangiectasia. *J Neurol*, 257(10), 1738-1740, doi:10.1007/s00415-010-5583-7.
- Simonin, C., Devos, D., Vuillaume, I., de Martinville, B., Sablonniere, B., Destee, A., et al. (2008). Attenuated presentation of ataxia-telangiectasia with familial cancer history. *J Neurol*, 255(8), 1261-1263, doi:10.1007/s00415-008-0857-z.
- Stankovic, T., Kidd, A. M., Sutcliffe, A., McGuire, G. M., Robinson, P., Weber, P., et al. (1998). ATM mutations and phenotypes in ataxia-telangiectasia families in the British Isles: expression of mutant ATM and the risk of leukemia, lymphoma, and breast cancer. *Am J Hum Genet*, 62(2), 334-345, doi:S0002-9297(07)63499-5 [pii]10.1086/301706.
- Stray-Pedersen, A., Borresen-Dale, A. L., Paus, E., Lindman, C. R., Burgers, T., & Abrahamsen, T. G. (2007). Alpha fetoprotein is increasing with age in ataxia-telangiectasia. *Eur J Paediatr Neurol*, 11(6), 375-380, doi:10.1016/j.ejpn.2007.04.001.
- Sun, X., Becker-Catania, S. G., Chun, H. H., Hwang, M. J., Huo, Y., Wang, Z., et al. (2002). Early diagnosis of ataxia-telangiectasia using radiosensitivity testing. *J Pediatr*, 140(6), 724-731, doi:10.1067/mpd.2002.123879.
- Sutton, I. J., Last, J. I., Ritchie, S. J., Harrington, H. J., Byrd, P. J., & Taylor, A. M. (2004). Adult-onset ataxia telangiectasia due to ATM 5762ins137 mutation homozygosity. *Ann Neurol*, 55(6), 891-895, doi:10.1002/ana.20139.
- Tavtigian, S. V., Oefner, P. J., Babikyan, D., Hartmann, A., Healey, S., Le Calvez-Kelm, F., et al. (2009). Rare, evolutionarily unlikely missense substitutions in ATM confer increased risk of breast cancer. *Am J Hum Genet*, 85(4), 427-446, doi:S0002-9297(09)00396-6 [pii]10.1016/j.ajhg.2009.08.018.
- Tchirkov, A., Bay, J. O., Pernin, D., Bignon, Y. J., Rio, P., Grancho, M., et al. (1997). Detection of heterozygous carriers of the ataxia-telangiectasia (ATM) gene by G2 phase chromosomal radiosensitivity of peripheral blood lymphocytes. *Hum Genet*, 101(3), 312-316.
- Terzoudi, G. I., Hatzi, V. I., Barszczewska, K., Manola, K. N., Stavropoulou, C., Angelakis, P., et al. (2009). G2-checkpoint abrogation in irradiated lymphocytes: A new cytogenetic approach to assess individual radiosensitivity and predisposition to cancer. *Int J Oncol*, 35(5), 1223-1230.

- Uziel, T., Savitsky, K., Platzer, M., Ziv, Y., Helbitz, T., Nehls, M., et al. (1996). Genomic Organization of the ATM gene. *Genomics*, 33(2), 317-320, doi:S0888-7543(96)90201-3 [pii]10.1006/geno.1996.0201.
- Verhagen, M. M., Abdo, W. F., Willemsen, M. A., Hogervorst, F. B., Smeets, D. F., Hiel, J. A., et al. (2009). Clinical spectrum of ataxia-telangiectasia in adulthood. *Neurology*, 73(6), 430-437, doi:10.1212/WNL.0b013e3181af33bd.
- Verhagen, M. M., Last, J. I., Hogervorst, F. B., Smeets, D. F., Roeleveld, N., Verheijen, F., et al. (2012). Presence of ATM protein and residual kinase activity correlates with the phenotype in ataxia-telangiectasia: a genotype-phenotype study. *Hum Mutat*, 33(3), 561-571, doi:10.1002/humu.22016.
- Vral, A., Thierens, H., & De Ridder, L. (1996). Micronucleus induction by ⁶⁰Co gamma-rays and fast neutrons in ataxia telangiectasia lymphocytes. *Int J Radiat Biol*, 70(2), 171-176.
- Wang, H., Boecker, W., Wang, H., Wang, X., Guan, J., Thompson, L. H., et al. (2004). Caffeine inhibits homology-directed repair of I-SceI-induced DNA double-strand breaks. *Oncogene*, 23(3), 824-834, doi:10.1038/sj.onc.1207168.
- West, C. M., Elyan, S. A., Berry, P., Cowan, R., & Scott, D. (1995). A comparison of the radiosensitivity of lymphocytes from normal donors, cancer patients, individuals with ataxia-telangiectasia (A-T) and A-T heterozygotes. *Int J Radiat Biol*, 68(2), 197-203.
- Willems, P., August, L., Slabbert, J., Romm, H., Oestreicher, U., Thierens, H., et al. (2010). Automated micronucleus (MN) scoring for population triage in case of large scale radiation events. *Int J Radiat Biol*, 86(1), 2-11, doi:10.3109/09553000903264481.
- Xu, B., Kim, S. T., Lim, D. S., & Kastan, M. B. (2002). Two molecularly distinct G(2)/M checkpoints are induced by ionizing irradiation. *Mol Cell Biol*, 22(4), 1049-1059.
- Zhang, P., Bhakta, K. S., Puri, P. L., Newbury, R. O., Feramisco, J. R., & Wang, J. Y. (2003). Association of ataxia telangiectasia mutated (ATM) gene mutation/deletion with rhabdomyosarcoma. *Cancer Biol Ther*, 2(1), 87-91.

PAPER II: Increased chromosomal radiosensitivity in asymptomatic carriers of a heterozygous *BRCA1* mutation

Annelot Baert¹, Julie Depuydt¹, Tom Van Maerken², Bruce Poppe², Fransiska Malfait², Katrien Storm³, Jenneke van den Ende³, Tim Van Damme², Sylvia De Nobele², Gianpaolo Perletti^{1,4}, Kim De Leeneer², Kathleen BM Claes^{2*} and Anne Vral^{1*°}

¹Department of Basic Medical Sciences, Ghent University, Ghent, Belgium, ²Center for Medical Genetics, Ghent University Hospital, Belgium, ³Department of Medical Genetics, University and University Hospital of Antwerp, Antwerp, Belgium, ⁴Biomedical Research Division, Department of Theoretical and Applied Sciences, University of Insubria, Busto A., Italy

* equal contribution

Keywords

BRCA1 mutations

DNA damage repair

Homologous recombination

G2/M cell cycle checkpoint

Ionizing radiation

G2 micronucleus assay

Radiosensitivity indicator

Nonsense-mediated decay

Haploinsufficiency

Breast Cancer Research, 2016, 18 (1): 52
doi: 10.1186/s13058-016-0709-1

Abstract

Introduction: Breast cancer risk increases drastically in individuals carrying a germline *BRCA1* mutation. The exposure to ionizing radiation for diagnostic or therapeutic purposes of *BRCA1* mutation carriers is counterintuitive since *BRCA1* is active in the DNA damage response pathway. The aim of this study was to investigate whether healthy *BRCA1* mutations carriers demonstrate an increased radiosensitivity compared to healthy individuals.

Methods: We defined a novel radiosensitivity indicator (RIND) based on two endpoints measured by the G2 micronucleus assay, reflecting defects in DNA repair and G2 arrest capacity after exposure to doses of 2 or 4Gy. We investigated if a correlation between the RIND score and nonsense-mediated decay (NMD) could be established.

Results: We found significantly increased radiosensitivity in the cohort of healthy *BRCA1* mutation carriers compared to healthy controls. In addition, our analysis show a significantly different distribution over the RIND scores ($p=0.034$, Fisher exact test) for healthy *BRCA1* mutation carriers compared to non-carriers: 72% of mutation carriers show a radiosensitive phenotype (RIND score 1-4) whereas 72% of the healthy volunteers show no radiosensitivity (RIND score 0). Furthermore, 28% of *BRCA1* mutation carriers had a RIND score of 3 or 4 (not observed in controls). The radiosensitive phenotype was similar for relatives within several families but not for unrelated individuals carrying the same mutation. The median RIND score was higher in patients with a mutation leading to a premature termination codon (PTC) located in the central part of the gene than in patients with a germline mutation in the 5' end of the gene.

Conclusion: We show that *BRCA1* mutations are associated with a radiosensitive phenotype related to a compromised DNA repair and G2 arrest capacity after exposure to either 2 or 4Gy. Our study confirms that haploinsufficiency is the mechanism involved in radiosensitivity in patients with a PTC allele, but suggests that further research is needed to evaluate alternative mechanisms for mutations not subjected to NMD.

Introduction

Breast cancer (BC) is the most common malignancy in the Western world (<http://www.who.int/cancer/detection/breastcancer/en/>). Approximately 15% of all BC patients have at least one relative affected by BC. About 15% of all familial BCs can be attributed to a mutation in the *BRCA1* or *BRCA2* genes [1]. Since the discovery of *BRCA1*, many different functions have been attributed to this protein. In its function as tumour suppressor gene, *BRCA1* plays a crucial role in DNA DSB repair pathways (reviewed in: [2, 3]). *BRCA1* is, for instance, important in the homologous recombination (HR), a pathway for repair of DSB in late S and G2 phases of the cell cycle [4–6]. *BRCA1* also plays an important role in the G2/M checkpoint control, allowing the cell to repair DNA damages before proceeding to the next phase of the cell cycle [7].

Carriers of a heterozygous *BRCA1* mutation may show enhanced radiosensitivity, associated with an increased carcinogenic risk after exposure to diagnostic or therapeutic ionizing radiation (IR). Several studies have shown that exposure to diagnostic X-rays may cause cancer in healthy *BRCA1* mutation carriers [8–11], whereas other studies could not detect a positive association between exposure to IR and breast cancer risk in *BRCA1/2* mutation carriers [12–15]. Also, studies analyzing the impact of (adjuvant) radiotherapy on the breast cancer risk in *BRCA1* and *BRCA2* mutation carriers reported no univocal conclusion [16]. The contradictory data obtained in these studies are mainly due to the constraints in the design of the performed studies.

Since long-term studies investigating the effect of exposure to IR in mutation carriers are difficult to setup and are reputed to be unethical, it is clear that more empiric data are needed to determine *in vitro* the radiosensitivity of patients carrying a germline mutation. Research so far yielded contradictory results and lack consistency [17–26].

The G0 micronucleus assay, performed on peripheral blood lymphocytes exposed to *in vitro* doses of 2 to 4 Gy, is frequently used to assess chromosomal radiosensitivity. This assay, however, is not optimized to detect defects in DSB repair activated during G2 phase of the cell cycle or the G2/M checkpoint, two processes in which *BRCA1* plays a major role since irradiation takes place in G0 phase of the cell cycle.

We previously reported a modified micronucleus assay optimized to detect defects in S or G2 phase of the cell cycle. This assay efficiently detected increased radiosensitivity in a patient with a mild form of ataxia telangiectasia (AT) and in heterozygous relatives [27].

In the present study, we applied the G2 micronucleus assay to further elucidate whether healthy *BRCA1* mutation carriers are characterized by an increased *in vitro* radiosensitivity. The endpoints of the study were: 1) micronucleus yields, and 2) G2/M checkpoint efficiency ratio. Both endpoints were assessed after irradiating PHA-stimulated peripheral blood lymphocytes with doses of 2Gy and 4Gy. With this assay, we assessed the mean differences in radiosensitivity for heterozygous *BRCA1* mutation carriers compared to healthy volunteers. We also scored the overall radiosensitivity in each mutation carrier using a 'Radiosensitivity Indicator' (RIND) scoring system. In addition, as our *BRCA1* population consists of individuals carrying different *BRCA1* mutations, we investigated if there is a link between radiosensitivity and the degree of nonsense-mediated decay (NMD) of the specific mutant allele.

Materials and methods

Sample collection

Blood samples were collected from individuals consulting the clinic of the Centre for Medical Genetics, Ghent University Hospital, Belgium (CMGG). Both EDTA and heparin blood samples were collected. EDTA samples were used for mutation analysis at CMGG, whereas the G2 MN assay was performed on heparinized blood samples.

In addition, we collected heparinized blood samples from healthy volunteers (n=20) without a personal or family history of BC, to determine the normal distribution of micronucleus yields in controls.

Lymphocytes were isolated from the blood samples using lymphoprep™ and were preserved in liquid nitrogen for the analysis of the NMD of the mutant allele.

For a number of mutation carriers (n=4) and healthy volunteers (n=7), a second blood sample was taken to determine the reproducibility of the results obtained with the G2 MN assay at different time points.

This study was approved by the ethical committee of the Ghent University Hospital (B670201111641 d.d. 20/09/2011). All study participants (n=18) were counseled by clinical geneticists in the context of a predictive (n=16) or diagnostic test (n=2) for hereditary BC and signed an informed consent. Two of the 18 *BRCA1* mutation carriers had developed BC but

cancer treatment finished more than 2 years ago; these women are both carrier of a substitution affecting the start codon (BC01 and BC02). The mean age of the mutation carriers and healthy volunteers was 40.9 and 35.4, respectively ($p = 0.26$, t-test).

Molecular analysis

All patients selected for this study had a family history of breast/ovarian cancer and a germline *BRCA1* mutation. Targeted analysis for the familial mutation was performed by direct sequencing on 2 independently extracted DNA samples. No molecular analyses were performed in healthy volunteers because of the absence of a personal or familial anamnesis for BC.

The G2 micronucleus assay

For the G2 MN assay, a large blood culture is set up in the presence of the mitogen phytohemagglutinin (PHA). PHA stimulates T-lymphocyte division, resulting in a population of cycling lymphocytes (G1, S1 G2 and M phase) after 3 days of incubation when the blood culture is irradiated. On the contrary, in the G0 MN assay, blood is first irradiated and then cultured in the presence of PHA, resulting in the irradiation of T-lymphocytes in G0 phase. The addition of cytochalasin B (Cyto B), an agent that blocks the cytokinesis, to the blood cultures allows the identification of first division cells as binucleated cells (BN). A non- or misrepaired DSB can result in an acentric chromosomal fragment which is detected as a micronucleus (MN) in the cytoplasm of the BN cell [17, 28].

More precisely, for the G2 MN assay, a 50-ml blood culture was set up using 5 ml heparinized blood, 45 ml cRPMI (RPMI, 1% L-glutamin and 0.5% penicillin/streptomycin) containing 10% Fetal calf serum (FCS) and 1 ml PHA (all Gibco®) in a T75 culture flask [27]. This large culture was set up to avoid inter-culture variation during the first days of incubation. After 3 days, the culture was split and sham-irradiations as well as irradiations with 2 and 4 Gy ^{60}Co γ rays were performed. An overview is shown in Figure 1a. Immediately after irradiation, cyto B (6 $\mu\text{g}/\text{ml}$, sigma-aldrich®) was added. To half of the irradiated cultures, caffeine (CAF, 4 mM, sigma-aldrich®), an agent that abrogates the G2/M checkpoint, was added to determine the G2/M checkpoint efficiency ratio [29, 30]. Based on 5-bromo-2'-deoxyuridine (BrdU) results obtained in our previous study on ATM [27] and new experiments performed for this study, a post-irradiation incubation period of 8 h was selected for detecting DNA damage induced

in cells in G2 phase (Figure 1b). The cultures were then treated with 75 mM KCl, fixed once using a combination of methanol, acetic acid and ringer (9 g NaCl + 0.42 g KCl + 0.24 g CaCl₂ for 1 liter dH₂O) (4/1/5, 4°C) and thrice with methanol and acetic acid (4/1, 4°C). Finally, the cell suspension was concentrated and spread on slides.

After 4',6-diamidino-2-phenylindole (DAPI) staining, the slides were scanned with a Metafer 4 (MNscore software module, Metasystems, Germany). This automated image analysis system selects BN and determines the number of MN per BN cell (see Figure 1a). For each condition, 2 cultures were set up and 2 slides per culture were analysed. A minimum of 600 BN cells was scored on each coded slide for the presence of MN. BN and MN selected in the automated setting were manually checked for false positives and false negatives. To determine the G2/M checkpoint efficiency ratio, the quotient was determined for the MN yield obtained in the presence versus the absence of Caffeine (#MNCaf+/#MNCaf-). The lower this ratio, the more radiosensitive an individual is.

In order to assess the overall radiosensitive phenotype of each patient, a RIND score was calculated. The mean and standard deviation (SD) of the micronucleus yield and the G2/M checkpoint efficiency ratio assessed in the cohort of healthy volunteers served to determine cut-offs to define the radiosensitivity of individual *BRCA1* mutation carriers. An individual value equal or higher than the mean MN yields in controls + 1 SD scored 1 point (color-code orange). A value equal or higher than the mean MN yields of controls + 2SD scored 2 points (color-code red). An individual value lower than the mean of controls + 1SD was scored as naught (color-code white). For the G2/M checkpoint, a similar conversion of the data was performed, with a value lower than mean checkpoint ratio assessed in controls - 1SD scored 1 point (color-code orange), mean – 2 SD scored 2 points (color-code red). An individual value higher than the mean of controls - 1 SD was scored as naught (color-code white). The combined scores from MN yields (0,1 or 2 points) and checkpoint ratios (0,1 or 2 points) were then added to form a single Radiosensitivity Indicator (range: 0 to 4).

Analysis of the cell cycle phase at time of irradiation

5-bromo-2'-deoxyuridine (BrdU) was added to blood cultures of three individuals to analyse the phase of the cell cycle at time of irradiation. BrdU (0.01mM, Sigma Aldrich®) was added to the cultures immediately after irradiation. Binucleated cells that incorporated BrdU during synthesis were in S or G1 phases of the cell cycle at the moment of irradiation, whereas BrdU-negative binucleated cells were irradiated in G2 phase. We corrected for daughter nuclei incorporating BrdU after binucleation by adding BrdU 2 hours before fixation to another subset of cultures. BrdU was visualised by fluorescence immunostaining with a monoclonal BrdU-specific antibody (M0744, Dako).

Analysis of the stability of the mutant allele

For this experiment, 2×10^6 frozen lymphocytes were thawed and cultured in a mix of 1 ml cRPMI, FCS (10%), 2-mercaptoethanol (0.1%, gibco®) and Sodium pyruvate (1%, life technologies™). PHA (10 µl/ml) was added to stimulate cell division. At day 7, whole RNA was extracted using the QIAamp®RNeasy Mini kit (Qiagen) according to manufacturer's instructions. Four hours prior to extraction, all cultures were split in two and to one part puromycin (200 µg/ml, sigma Aldrich®) was added. Puromycin was added to avoid NMD, a pathway responsible for the degradation of aberrant mRNA [31].

The total RNA and purity was measured using the Trinean DropSense96 (VWR). The RNA was converted into cDNA using the iscript™ cDNA Synthesis Kit (Biorad). When RNA was extracted from cultures with puromycin, the converted cDNA is referred to as cDNAp. Prior to this cDNA synthesis, samples were treated with DNase (Heat and run kit, ArcticZymes) to remove any possible remaining genomic DNA (gDNA).

To determine the ratio of the mutant *BRCA1* allele versus the wild type (WT) allele at the mRNA level, we performed PCR amplification and Sanger sequencing of the amplicon harbouring the germline mutation and a heterozygous SNP (c.2311T>C), if present. An overview of the primers used can be found in Additional File 1. Sanger sequencing was performed using the BigDye® Terminator Cycle Sequencing kit (Life Technologies™). PCR was followed by ethanol precipitation and fragments were dissolved in a mix of Hi-Di™ formamide (10 µl, Life Technologies™) and GeneScan™ 500 LIZ™ size standard (0.5 µl, applied biosystems®). The fragments were analysed on the ABI PRISM® 3730KL Genetic Analyzer (Life Technologies™). Results were evaluated using GeneMapper® software (Applied Biosystems®)

for visual inspection and determination of the ratio of the peak heights representing the WT and mutant allele, respectively (Additional File 2 and 3). Data were normalized with a control peak in the near vicinity. To confirm the results, the PCR amplicons were also sequenced with the sequencing by synthesis technology (Illumina) on a MiSeq instrument. The library preparation was performed using an adapted NexteraXT protocol as described by De Leeneer et al. [32]. Reads were mapped with CLC genomic Workbench (Qiagen). The variant allele frequency (VAF) (which reflects the ratio of WT versus mutant allele) of both the mutation and a SNP (if available), were determined in the mutation carriers and in controls without a germline *BRCA1* mutation.

Results

Analysis of the cell cycle phase at time of irradiation

Based on literature data, the cell cycle of proliferating lymphocytes takes between 18 and 22 h. The cell cycle is presented in Figure 1b and the mean length for each phase is indicated [33, 34]. With the BrdU immunostaining experiments, we assessed that a post-irradiation incubation time of 8 h after 2 or 4 Gy irradiation resulted in blood cultures in which 80% ($\pm 13\%$) and 87% ($\pm 3\%$) binucleated cells, respectively, were in G2 phase (negative at BrdU staining) at the time of irradiation. In sham-irradiated samples, the percentage of BrdU-negative binucleated cells was much lower ($56\% \pm 8\%$). These observations suggest that synchronisation of the cells in G2 took place due to radiation-induced G2 arrest. When Caffeine, an agent that abrogates the G2/M checkpoint [29], was added to the cultures, the percentage of cells in G2 decreased (2 Gy: $73\% \pm 6\%$ and 4 Gy: $79\% \pm 2\%$). The high percentage of cells irradiated in G2 indicates that the harvest of BN cells 8 h post-irradiation is optimal.

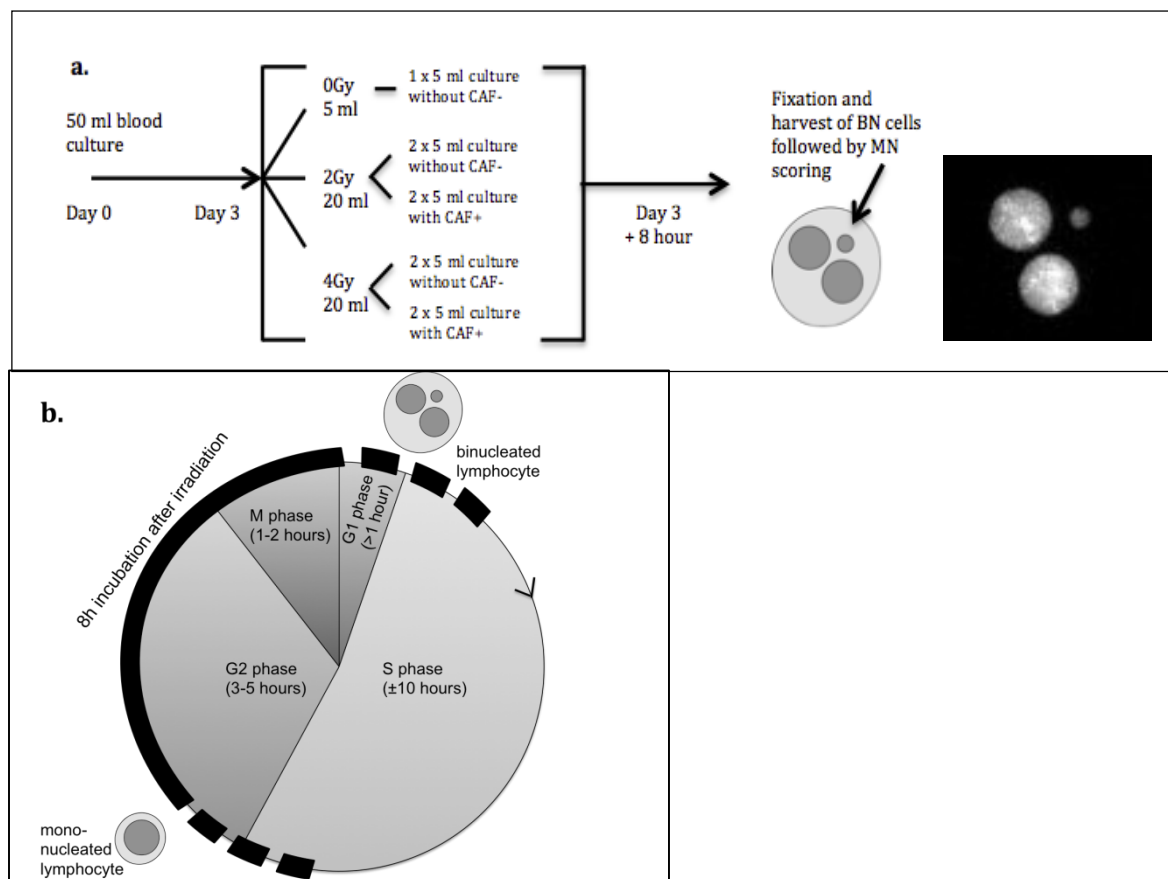


Figure 1. Design of the G2 MN assay and overview of the cell cycle

a. Day 0: set-up of one 50ml large blood culture for every patient. Day 3: division of the cultures and subsequent irradiation. Addition of cyto B and caffeine (if needed) immediately after irradiation, followed by incubation during 8 h before harvesting. Right panel: image of a DAPI stained binucleated cell with micronucleus generated with the Metafer4 (Metasystems).

b. Overview of the cell cycle for proliferating lymphocytes and approximate duration of the different phases with indication of the applied post-irradiation incubation period (black). At the start of the irradiation, all lymphocytes in the blood culture are mononucleated. After 8 h of incubation, the cultures are fixed and BN cells (cells that went through one mitosis) are scored for the presence of MN.

Results of G2 MN assay

The MN yield obtained for the sham-irradiated samples did not show a significantly different mean result between mutation carriers and healthy volunteers (Table 1 and Figure 2). The mean values obtained for the radiosensitivity analysis are shown in Table 1 and Figure 2.

Table 1: Mean MN yields and G2/M checkpoint efficiency ratios obtained with the G2 MN assay

	Micronucleus yield: #MN/1000 BN			G2/M checkpoint efficiency: #MNCAF+/#MNCAF-	
healthy volunteers	0Gy	2Gy	4Gy	2Gy	4Gy
mean	15	61	91	2	3.1
SD	10	21	29	0.5	0.8
SEM	2	5	7	0.1	0.2
BRCA1 mutation carriers	0Gy	2Gy	4Gy	2Gy	4Gy
mean	16	83	128	1.6	2.2
SD	7	31	45	0.5	0.5
SEM	2	7	10	0.1	0.1
p-value (2-sided t-test)	0.83	0.019	0.004	0.01	0.0002

In *BRCA1* mutation carriers, a significantly increased radiosensitivity was observed for both endpoints at both radiation doses of 2 and 4 Gy, compared to healthy volunteers. Our results also show that the 4 Gy dose point is the most discriminative (highest significance based on p-value) for both endpoints. We thus selected this dose to determine the individual overall radiosensitive phenotype. Results of the mutation analysis and individual results obtained for the 2 radiosensitivity endpoints upon 4 Gy irradiation are shown in Table 2. Each value received a colour-code corresponding to a radiosensitivity score from which a RIND score was calculated.

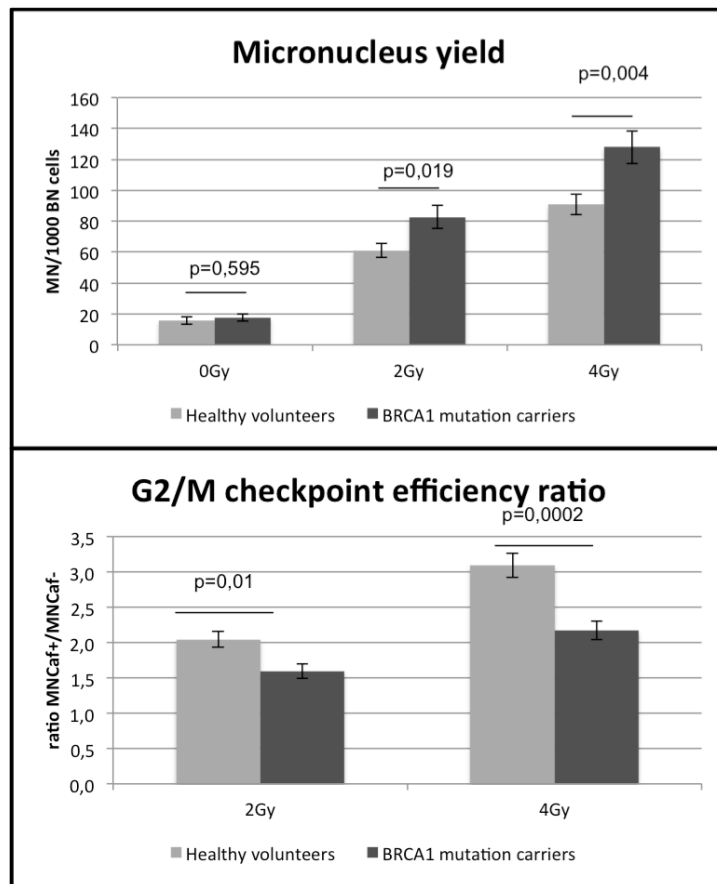


Figure 2. Mean MN yields and G2/M checkpoint efficiency ratios obtained with the G2 MN assay in healthy volunteers and *BRCA1* mutation carriers.

Significance was determined with a 2-sided T-test. P-values for each of the endpoints and dose points are indicated in the graph. Error bars represent the standard error of the mean (SEM).

Significantly different RIND values were found for *BRCA1* mutation carriers (median = 2) and healthy volunteers (median = 0) ($p=0.0076$, Mann Withney). Figure 3 shows the distribution of the *BRCA1* mutation carriers and healthy controls over the five different RIND scores. The distribution amongst the RIND scores between the two groups is significantly different ($p=0.034$, Fisher exact test). The significantly different median and the significantly different distribution over the RIND scores obtained for both groups point towards a difference in response to radiation.

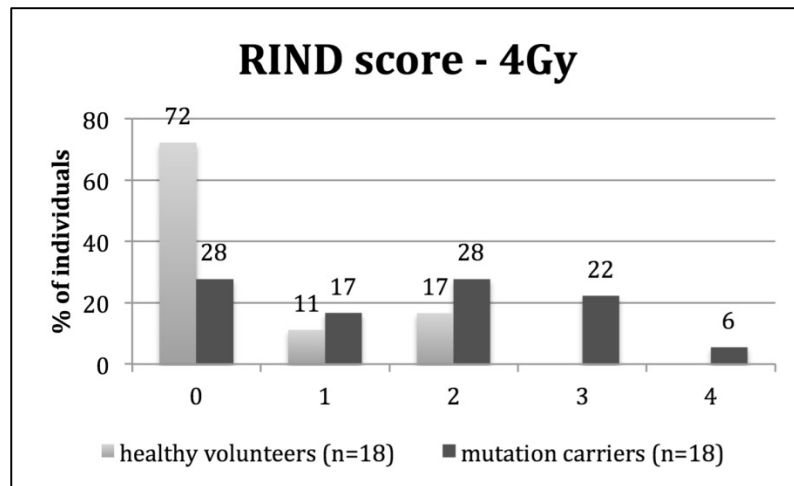


Figure 3. The distribution (%) of healthy volunteers and *BRCA1* mutation carriers over the different RIND scores

Repeated assessments were performed on blood specimens, taken on 2 different occasions, from a random sample of seven healthy volunteers and four mutation carriers, in order to exclude intra-individual variations. Although minor variations were observed, no significant differences were observed between repeated measurements ($P > 0.05$ for both MN yield and G2/M checkpoint efficiency; repeated measures ANOVA).

We also investigated whether relatives of the subjects enrolled in this study, carrying the same mutation, have similar RIND scores. Individuals with the same family ID are known to be related (Table 2). For families BR-32-0196, BR-32-1028 and BR-32-2256, we had access to data and samples of several relatives. Both father and daughter of family BR-32-1028 showed a RIND score of 3. The siblings from family BR-32-2256 show a RIND score of 1 and 2 and for the third degree relatives in family BR-32-0196, we obtained a score of 0 and 1. We thus conclude that there were no major differences in RIND scores within families. However, different RIND scores (ranging from 0-4) were observed between 4 individuals carrying the same mutation (c.2359dup), but unaware of a close relationship.

Table 2. Results of mutation screening and radiosensitivity assessment for each individual

<u>Healthy volunteers</u>		<u>mutation</u>		<u>MN yield</u>	<u>G2/M checkpoint efficiency</u>	<u>Radio-sensitivity indicator (RIND)</u>
sample ID		codon	protein	4 Gy	4 Gy	
D01		N/A	N/A	101	3.9	0
D02		N/A	N/A	67	3.5	0
D03		N/A	N/A	164	2.9	2
D04		N/A	N/A	92	2.1	0
D05		N/A	N/A	84	4.6	0
D06		N/A	N/A	91	3.3	0
D07		N/A	N/A	64	3.1	0
D08		N/A	N/A	84	3.5	0
D09		N/A	N/A	139	1.7	2
D10		N/A	N/A	57	2.6	0
D11		N/A	N/A	90	2.7	0
D12		N/A	N/A	87	3.3	0
D13		N/A	N/A	63	1.6	2
D14		N/A	N/A	94	2.5	0
D15		N/A	N/A	123	3.2	1
D16		N/A	N/A	74	3.3	0
D17		N/A	N/A	97	2.8	0
D18		N/A	N/A	129	3.1	1
<u>BRCA1 mutation carriers</u>		<u>mutation</u>		<u>MN yield</u>	<u>G2/M checkpoint efficiency</u>	<u>Radio-sensitivity indicator (RIND)</u>
sample ID	Family ID	Mutation c.	Mutation p.	4 Gy	4 Gy	
BC01	BR-32-1643	c.1A>G	p.Met1Val	215	1.9	3
BC02	BR-32-3040	c.1A>C	p.Met1Leu	171	2.4	2
BC03	BR-32-1848	c.212+3A>G	N/A	77	1.5	2
BC04	BR-32-2016	c.1961del	p.Lys654fs*47	54	2.5	0
BC05	BR-32-0373	c.2359dup	Glu787fs*3	174	1.7	3
BC06	BR-32-1787	c.2359dup	Glu787fs*3	163	2.9	2
BC07	BR-32-1444	c.2359dup	Glu787fs*3	106	2.5	0
BC08	BR-32-1967	c.2359dup	Glu787fs*3	182	1.3	4
BC09	BR-32-1548	c.3331_3334del	p.Gln111fs*5	104	2	1
BC10	BR-32-2256	c.3481_3491del	pGlu1161fs*3	104	1.6	2
BC11	BR-32-2256	c.3481_3491del	pGlu1161fs*3	85	1.8	1
BC12	BR-32-2256	c.3481_3491del	pGlu1161fs*3	121	2.2	2
BC13	BR-32-0196	c.3661G>T	p.Glu1221*	119	1.7	1
BC14	BR-32-0196	c.3661G>T	p.Glu1221*	112	3.5	0
BC15	BR-32-0305	c.3661G>T	p.Glu1221*	83	2.7	0
BC16	BR-32-1028	c.4327C>T	p.Arg1443*	176	2.1	3
BC17	BR-32-1028	c.4327C>T	p.Arg1443*	164	2.1	3
BC18	BR-32-2212	c.4931_4393delinsTT	p.Pro1464fs*2	94	2.7	0

Analysis of the stability of the mutant allele and correlation with the RIND score

The results of fragment analysis and massive parallel sequencing were comparable (Table 3). All results for cDNA, but not for gDNA, analyses are obtained by in duplo experiments. The results of the MiSeq analysis are expressed as the variant allele frequency (VAF) in %; 50% means equal expression of both alleles. The results of the fragment analysis (fragm. analysis) are shown as a ratio of peak heights mutant/WT allele. A value of 1 equals no loss of expression of the mutant allele. cDNA samples not treated with puromycin were scored as “evidence of NMD” (Table 3) when an average VAF $\leq 31\%$ or a ratio of peak heights < 0.7 were obtained. We observe more variation for deletions/insertions than for substitutions. This can be explained by the more complex mapping of reads containing deletions/duplications. A large deletion and software struggling to map correctly to the reference sequence, explains a VAF lower than 50% for gDNA in some patients (indicated with *, Table 3). Nevertheless, a drop in VAF for cDNA and not for cDNA with puromycin can still be distinguished. For BC02, BC08 and BC15, no lymphocytes were available to perform this assay. However, as we had access to cDNA from other individuals with the same mutation we were able to get an insight in the stability of the mutant mRNA for these three mutation carriers. For BC16, no gDNA data could be obtained; information with regard to mutant mRNA stability for this mutation carrier was obtained via cDNA and BC17.

PTC alleles in the central part of the gene

For all truncating mutations studied in the central part of the gene (7 unique mutations in 15 individuals), we found evidence for NMD. In general, 25-30% residual truncated mRNA was detected in carriers of a PTC mutation. Ten of 15 patients with a truncating allele show a radiosensitive phenotype (RIND score = 1-4, median = 1).

Mutations located in the 5' part of the gene

For mutations in the 5' part of the gene (n=3) we have no evidence for NMD. The effect at the mRNA level for the c.212+3A>G splice site mutation has previously been studied by our group with qPCR. We showed that no full-length transcript is formed, but it leads to a significantly increased expression of an alternative transcript (out of frame skip of 22 last nucleotides of exon 5; r.190_212del), which is not subjected to NMD [35, 36]. As BC03 is not heterozygous for any of the tested common SNPs, results could not be re-analysed with the approach

described in this paper. Our results for BC03 showed a RIND score of 2, which can be attributed to a decreased G2/M checkpoint efficiency. For BC01, carriers of the c.1A>G start codon mutation, no decline of the mutant allele could be detected when analyzing the SNP data (Table 3). This suggests the conservation of the start codon or an alternative one. The mutation itself could not be quantified because of the presence of GC rich areas near the start codon. The introduction of an alternative start codon, could give rise to an aberrant protein with a dominant negative effect [37]. Interestingly, both individuals carrying a mutation affecting the start codon have respectively a RIND score of 3 and 2. A median RIND score of 2 is observed for carriers of a mutation in the 5' part of the gene.

Table 3. Results of the stability of the mutant allele

		Frags. Analysis	MISEQ (VAF)			
Donor	RIND score	ratio peak height (mutant/WT allele)	cDNA	cDNAp	gDNA	Evidence for NMD?
BC01 c.1A>G	3	0.7 (0.6-0.8)	49 (42-55)	52 (51-52)	49 (49-49)	No
BC02 c.1A>C	2	/	/	/	/	No
BC03 c.212+3A>G	2	/	/	/	/	No
BC04 c.1961del	0	0.4 (0.4-0.4)	29 (25-33)	47 (43-51)	47 (47-47)	Yes
BC05 c.2359dup	3	0.6 (0.6-0.6)	28 (25-31)	42 (38-45)	48 (48-48)	Yes
BC06 c.2359dup	2	0.5 (0.5-0.5)	24 (23-25)	44 (41-47)	50 (50-50)	Yes
BC07 c.2359dup	0	0.4 (0.4-0.5)	29 (27-30)	48 (30-67)	57 (55-59)	Yes
BC08 c.2359dup	4	/	/	/	/	Yes
BC09 c.3331_3334del	1	0.4 (0.4-0.4)	25 (18-31)	44 (34-48)	49 (49-49)	Yes
BC10 c.3481_3491del	2	0.4 (0.4-0.4)	23 (16-30)	42 (28-52)	39 (32-46)*	Yes
BC11 c.3481_3491del	1	0.4 (0.3-0.5)	23 (16-32)	41 (23-54)	39 (34-44)*	Yes
BC12 c.3481_3491del	2	0.4 (0.4-0.4)	26 (16-34)	39 (28-50)	42 (35-49)*	Yes
BC13 c.3661G>T	1	0.5 (0.3-0.6)	29 (28-30)	50 (41-57)	50 (46-53)	Yes
BC14 c.3661G>T	0	0.4 (0.3-0.4)	31 (29-32)	52 (52-52)	50 (50-50)	Yes
BC15 c.3661G>T	0	/	/	/	/	Yes
BC16 c.4327C>T	3	0.5 (0.5-0.6)	24 (21-27)	51 (45-56)	/	Yes
BC17 c.4327C>T	3	0.6 (0.4-0.7)	26 (21-30)	48 (44-53)	50 (50-50)	Yes
BC18 c.4931_4393delinsTT	0	0.4 (0.3-0.4)	30 (28-31)	37 (28-47)	52 (52-52)	Yes

Discussion

Our study shows a significantly increased radiosensitivity in the group of healthy *BRCA1* mutation carriers compared to healthy controls for the two endpoints measured by the G2 MN assay for both doses of 2 and 4 Gy. Our results indicate that radiosensitivity in heterozygous *BRCA1* mutation carriers is a complex phenotype linked to defects in DNA damage repair as well as to defective G2 arrest capacity. These results are in agreement with the studies performed by Pantelias and Terzoudi [30]. They applied the G2 chromatid break assay and reported that the G2/M checkpoint efficiency ratio is a good parameter to predict intrinsic radiosensitivity in AT and cancer patients.

In vitro radiosensitivity has previously been investigated in BC patients and *BRCA1* mutation carriers. Cardinale et al. recently published a meta-analysis combining all *in vitro* case-control studies in which the G0 MN assay on peripheral blood lymphocytes was used to analyse *in vitro* radiosensitivity in women with BC or with a known or putative genetic predisposition to BC [17]. Other cytogenetic assays, such as the chromosome aberration and G2 chromatid break assay, or survival assays, have also been applied to determine radiosensitivity in a variety of cell types heterozygous for *BRCA1* mutations using different irradiation protocols [18–26]. It is, however, difficult to correctly compare the results of these studies, as also concluded by Cardinale et al. [17], due to different experimental setups to analyze *in vitro* radiosensitivity. However, despite the heterogeneity of the studies, most of the data generated, including ours, are suggestive of a different radiosensitive phenotype between *BRCA1* heterozygous mutant cells and control cells. Recent studies investigating more specifically the functionality of the HR pathway in *BRCA1* heterozygous cells by means of γ -H2AX and RAD51 foci assays, point towards a less efficient DSB repair by HR. These findings further support the evidence of increased radiosensitivity observed in *BRCA1* heterozygous cells when irradiated in S or G2 phase of the cell cycle and are compatible with haploinsufficiency as underlying mechanism [24, 25, 38]. The strength of our study is that radiosensitivity was analyzed by means of two different endpoints obtained with a G2 specific MN assay, developed by our group [27].

The radiosensitivity results in this study were obtained with doses of 2 and 4 Gy, which is considerably higher than any lifetime cumulative dose received by mammography screening. The average dose delivered to the breast glandular tissue per mammographic screening

session is approximately 4 mGy [39]. Thus, direct extrapolation of our radiosensitivity results towards the risks of mammography is not possible. Despite this limitation, our results may suggest caution in the exposure to IR of healthy tissues of *BRCA1* mutation carriers for diagnostic purposes. It is furthermore noteworthy that recent studies have shown that 30 kV X-rays have a higher relative biological effect (RBE) and are thus more harmful compared to conventional high kV X-rays or ^{60}Co γ -rays, on which current risk assessment is based. This implies that each mammogram may induce more DNA damage than commonly estimated [40, 41]. Several papers suggest that mammography screening might preferably be substituted by MRI in order to avoid IR before the age of 30 [16] or 40 [42] in *BRCA1* mutation carriers. In addition, and more appropriate given the high doses used in this assay, our results suggest caution in the use of adjuvant radiotherapy following breast-conserving surgery. In this respect, there is a need for well designed studies to assess the incidence of second ipsi- or contralateral cancers upon adjuvant radiotherapy in mutation carriers [16].

Since it was our aim to develop a radiosensitivity assay applicable in a clinical setting, we performed the G2 MN assay on peripheral blood samples, which can easily be obtained during a genetic consult. Several studies have demonstrated that radiosensitivity of an individual is also detectable in cells of a type different from cells in which the tumour develops [18, 43, 44]. The scoring system with RIND scores varying between 0 and 4 allowed us to assess the overall radiosensitivity due to both DNA repair and G2 arrest capacity of each mutation carrier (results in Table 2 and Figure 3). With the help of this scoring system, we assessed that 72% of our healthy volunteers showed no radiosensitive phenotype. *BRCA1* mutation carriers, on the contrary, show a distinct pattern towards higher radiosensitivity. Seventy-two percent of all mutation carriers were found to be radiosensitive (RIND score= 1-4). Moreover, 28% of *BRCA1* mutation carriers had RIND scores equal to 3 or 4, scores that were never observed in healthy volunteers. This simple scoring system can be valuable to assist physicians in their decision-making for the clinical follow-up and the refinement of radiotherapy at the individual level.

Since our study is limited in sample size, a larger prospective study with blood samples of *BRCA1* mutation carriers will be undertaken to confirm and prove the importance of an *in vitro* radiosensitivity scoring system to assist clinical management of *BRCA1* mutation carriers.

Haploinsufficiency has been suggested as the main mechanism for hereditary breast carcinogenesis [45]. However, as NMD is not observed for mutations located in the 5' and 3' part of the gene [46], a dominant negative effect can not be excluded whereby the aberrant transcript abolishes the functionality of the WT allele (for a review: [37, 47]). We wanted to evaluate if either or both mechanisms could influence the radiosensitivity score. Information on the stability of the mutant allele at mRNA level was generated by both a fragment analysis and a novel massive parallel sequencing approach. To our knowledge, this is the first time that next generation sequencing is applied to evaluate the level of NMD. The approach we describe here is straightforward and cost-effective to study the relative expression of two alleles in a single individual.

The majority of patients included in this study, are heterozygous for a mutation located in the central part of the gene leading to a premature termination codon (PTC). These PTC inducing mutations result in a truncated mRNA, which can be degraded by NMD. Generally, we observed that the mutated PTC allele was expressed at a ratio of 25-30% of the WT allele at the mRNA level. Our results are consistent with the data of Anczuców et al. and Perrin-Vidoz et al. [46, 47]. Both articles describe a similar reduction of mRNA expression from PTC alleles in the central part of the gene and demonstrate the involvement of NMD in this decrease of mutant mRNA. A radiosensitive phenotype in 10/15 mutation carriers with a PTC allele undergoing NMD suggests haploinsufficiency as mechanism leading to this phenotype in the large majority of the individuals.

Equal expression of the WT and mutant allele at the mRNA level was observed in the patients with the start codon mutation (BC01 and BC02). For the patient with the c.212+3A>G mutation (BC03) equal expression of a full length transcript and a transcript lacking the last 22 nucleotides of exon 5 was observed in previous research by our group and confirmed by others [35, 36]. A higher median RIND score in the individuals carrying a mutation in the 5' part of the gene, for which no NMD could be detected, compared to individuals with a PTC allele may point towards another mechanism involved in the radiosensitive phenotype, like a dominant negative effect. However, current knowledge on translation of mutant alleles not subjected to NMD into proteins is limited. Such detailed studies have not yet been undertaken: in most studies demonstrating a role for haploinsufficiency, *BRCA1* mutation carriers are compared as group to non-carriers (e.g. Vaclova et al; Pathania et al; Sedic et al.

[25, 38, 48]). Our data suggest the need for larger studies involving different types of mutations.

Unique for this radiosensitivity study compared to others is that we had access to material from several individuals from one family and we could also evaluate the radiosensitive phenotype from several unrelated individuals carrying the same mutation. For 4 unrelated carriers of a Belgian founder mutation c.2359dup (p.Glu787fs*3) a large variation for the radiosensitive phenotype based on the RIND score was observed (range: 0-4) (Table 2). Repeated assessments on blood specimens, taken on two different occasions from several individuals, rule out that the different RIND scores are due to experimental variation. Given the smaller variation between related individuals and because of the pleiotropic effect of IR on DNA (for example, strand breaks, fork stalling, base damage, DNA-adducts [49–51]), we are convinced that other genetic factors influence the radiosensitivity. Previous research has, for example, demonstrated the effect of SNPs on individual sensitivity to radiation therapy [52, 53]. In addition, our group has demonstrated the influence of RAD51, Ku70 and Ku80 SNPs as a modulator of *in vitro* radiosensitivity in *BRCA1* mutation carriers and BC patients [54, 55]. A larger study and the inclusion of a control population with relatives not harboring the familial germline mutation could generate important insights.

Conclusion

Our study, using the G2 MN assay, shows that healthy individuals carrying a germline mutation in *BRCA1* are more radiosensitive compared to healthy controls after exposure to doses of 2 and 4 Gy.

Seventy-two percent of the *BRCA1* mutation carriers showed a radiosensitive phenotype and 28% of *BRCA1* mutation carriers had high RIND scores of 3 or 4. Analysis of the mRNA stability of the mutant allele could not demonstrate a clear link between nonsense-mediated decay of the mutant allele and a radiosensitive phenotype. This, combined with the similar radiosensitive phenotype observed for related individuals but not for unrelated individuals carrying the same mutation, is indicative for the fact that additional genetic factors, beside the *BRCA1* mutation, may play a role in the radiation response. Our study emphasizes the need for large prospective studies correlating the *in vitro* findings and exposure to radiation with the risk of developing breast cancer.

Competing interests

The authors have no competing interests to declare.

Acknowledgement

The authors wish to thank all individuals contributing to this study by donating blood samples. We thank Ilse Coene, Brecht Crombez, Céline Debrock, Mattias Van Heetvelde, Greet De Smet, Johanna Aernoudt, Leen Pieters and Toke Thiron for their technical assistance and sharing of their knowledge. We thank Prof. Dr. Thierens for the use of the irradiation facility. This study is funded by the Belgian Foundation against Cancer (*project: 2012-216*).

Corrigendum

In table 1 of this article, a mean based on 20 healthy volunteers, was provided.

In the update version of table 1 (see below), the mean, SD and SEM values, together with the appropriate p-values, of the 18 healthy volunteers presented in table 2 are provided:

Table 1: Mean MN yields and G2/M checkpoint efficiency ratios obtained with the G2 MN assay

	Micronucleus yield: #MN/1000 BN			G2/M checkpoint efficiency: #MNCAF+/#MNCAF-	
	0 Gy	2 Gy	4 Gy	2 Gy	4 Gy
healthy volunteers (n=18)					
mean	16	63	94	2	3.0
SD	11	21	28	0.5	0.7
SEM	3	5	7	0.1	0.2
BRCA1 mutation carriers (n=18)	0 Gy	2 Gy	4 Gy	2 Gy	4 Gy
mean	16	83	128	1.6	2.2
SD	7	31	45	0.5	0.5
SEM	2	7	10	0.1	0.1
p-value (2-sided t-test)	0.83	0.023	0.03	0.016	0.002

A significant increased radiosensitivity remains clear for the *BRCA1* mutation carrier cohort compared to the control cohort for both endpoints and both dose points.

On individual level, the adapted mean and SD values, result in altered RIND scores for D04 and M12, which change from 0 to 1 and 2 to 1 respectively.

A significant difference in RIND values between *BRCA1* mutation carriers and healthy volunteers remains, but with slightly altered median values and p-values (median *BRCA1* mutation carriers = 1.5 versus 2 and p-value = 0.0143 versus 0.0076, Mann Withney). The distribution amongst the different RIND scores (see new Figure 3 below) between the two groups is now borderline significantly different (p-value = 0.069 versus 0.034, Fisher exact test).

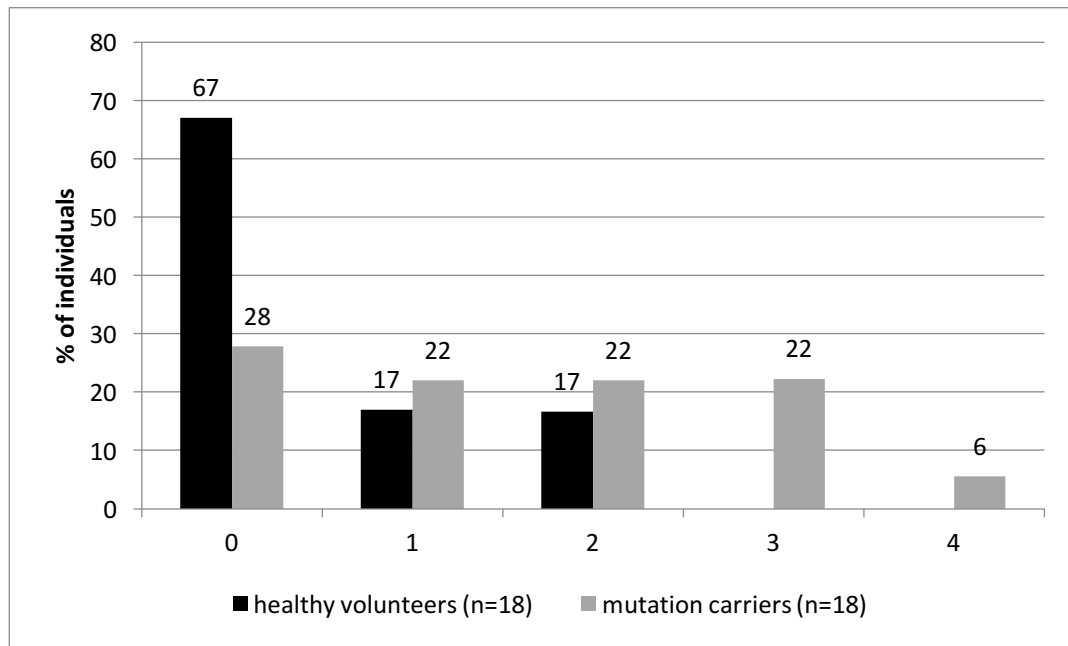


Figure 3. The distribution (%) of healthy volunteers and *BRCA1* mutation carriers over the different RIND scores

We argue that these changes do not affect the general conclusion of this article.

References

1. Couch FJ, Nathanson KL, Offit K (2014) Two decades after BRCA: setting paradigms in personalized cancer care and prevention. *Science* 343:1466–70
2. Caestecker KW, Van de Walle GR (2013) The role of BRCA1 in DNA double-strand repair: past and present. *Exp Cell Res* 319:575–87
3. Roy R, Chun J, Powell SN (2012) BRCA1 and BRCA2: different roles in a common pathway of genome protection. *Nat Rev Cancer* 12:68–78
4. Pfeiffer P, Goedecke W, Kuhfittig-Kulle S, Obe G (2004) Pathways of DNA double-strand break repair and their impact on the prevention and formation of chromosomal aberrations. *Cytogenet Genome Res* 104:7–13
5. Foulkes WD, Shuen AY (2013) In Brief: BRCA1 and BRCA2. *J Pathol* 230:347–349
6. Cousineau I, Abaji C, Belmaaza A (2005) BRCA1 regulates RAD51 function in response to DNA damage and suppresses spontaneous sister chromatid replication slippage: Implications for sister chromatid cohesion, genome stability, and carcinogenesis. *Cancer Res*

65:11384–11391

7. Yarden RI, Pardo-Reoyo S, Sgagias M, Cowan KH, Brody LC (2002) BRCA1 regulates the G2/M checkpoint by activating Chk1 kinase upon DNA damage. *Nat Genet* 30:285–9
8. Pijpe A, Andrieu N, Easton DF, et al (2012) Exposure to diagnostic radiation and risk of breast cancer among carriers of BRCA1/2 mutations: retrospective cohort study (GENE-RAD-RISK). *BMJ* 345:e5660
9. Lecarpentier J, Noguès C, Mouret-Fourme E, et al (2011) Variation in breast cancer risk with mutation position , smoking , alcohol , and chest X-ray history , in the French National BRCA1 / 2 carrier cohort (GENEPSO). *Breast Cancer Res Treat* 130:927–938
10. Andrieu N, Easton DF, Chang-claude J, Rookus MA, Brohet R, Cardis E (2006) Effect of Chest X-Rays on the Risk of Breast Cancer Among BRCA1 / 2 Mutation Carriers in the International BRCA1 / 2 Carrier Cohort Study : A Report from the EMBRACE , GENEPSO , GEO-HEBON , and IBCCS Collaborators ' Group. *J Clin Oncol* 24:3361–3366
11. Gronwald J, Pijpe A, Byrski T, Huzarski T, Stawicka M, Cybulski C, van Leeuwen F, Lubinski J, Narod S a (2008) Early radiation exposures and BRCA1-associated breast cancer in young women from Poland. *Breast Cancer Res Treat* 112:581–4
12. John EM, McGuire V, Thomas D, et al (2013) Diagnostic chest X-rays and breast cancer risk before age 50 years for BRCA1 and BRCA2 mutation carriers. *Cancer Epidemiol Biomarkers Prev* 22:1547–56
13. Narod SA, Lubinski J, Ghadirian P, et al (2006) Screening mammography and risk of breast cancer in BRCA1 and BRCA2 mutation carriers: a case-control study. *Lancet Oncol* 7:402–6
14. Giannakeas V, Lubinski J, Gronwald J, et al (2014) Mammography screening and the risk of breast cancer in BRCA1 and BRCA2 mutation carriers: a prospective study. *Breast Cancer Res Treat* 147:113–8
15. Goldfrank D, Chuai S, Bernstein JL, et al (2006) Effect of mammography on breast cancer risk in women with mutations in BRCA1 or BRCA2. *Cancer Epidemiol Biomarkers Prev* 15:2311–2313
16. Drooger JC, Hooning MJ, Seynaeve CM, Baaijens MH a., Obdeijn IM, Sleijfer S, Jager A (2015) Diagnostic and therapeutic ionizing radiation and the risk of a first and second primary breast cancer, with special attention for BRCA1 and BRCA2 mutation carriers: A critical review of the literature. *Cancer Treat Rev* 41:187–196
17. Cardinale F, Bruzzi P, Bolognesi C (2012) Role of micronucleus test in predicting breast cancer susceptibility: a systematic review and meta-analysis. *Br J Cancer* 106:780–90
18. Kote-Jarai Z, Salmon a, Mengitsu T, et al (2006) Increased level of chromosomal damage after irradiation of lymphocytes from BRCA1 mutation carriers. *Br J Cancer* 94:308–310
19. Frankenberg-Schwager M, Gregus A (2012) Chromosomal instability induced by mammography X-rays in primary human fibroblasts from BRCA1 and BRCA2 mutation carriers. *Int J Radiat Biol* 88:846–857
20. Ernestos B, Nikolaos P, Koulis G, Eleni R, Konstantinos B, Alexandra G, Michael K (2010) Increased chromosomal radiosensitivity in women carrying BRCA1/BRCA2 mutations assessed with the G2 assay. *Int J Radiat Oncol Biol Phys* 76:1199–205
21. Barwell J, Pagon L, Georgiou A, et al (2007) Lymphocyte radiosensitivity in BRCA1 and BRCA2 mutation carriers and implications for breast cancer susceptibility. *Int J Cancer* 121:1631–6
22. A. Buchholz T, Xifeng W, Abu H, Tucker SL, Mills GB, Haffty B, Bergh S, Story M, Geara

- FB, Brock WA (2002) Evidence of haplotype insufficiency in human cells containing a germline mutation in BRCA1 or BRCA2. *Int J Cancer* 561:557–561
23. Hair JM, Terzoudi GI, Hatzi VI, Lehouck K a., Srivastava D, Wang W, Pantelias GE, Georgakilas AG (2010) BRCA1 role in the mitigation of radiotoxicity and chromosomal instability through repair of clustered DNA lesions. *Chem Biol Interact* 188:350–358
24. Sioftanos G, Ismail A, Föhse L, Shanley S, Worku M, Short SC (2010) BRCA1 and BRCA2 heterozygosity in embryonic stem cells reduces radiation-induced Rad51 focus formation but is not associated with radiosensitivity. *Int J Radiat Biol* 86:1095–105
25. Pathania S, Bade S, Le Guillou M, et al (2014) BRCA1 haploinsufficiency for replication stress suppression in primary cells. *Nat Commun* 5:5496
26. Febrer E, Mestres M, Caballín MR, Barrios L, Ribas M, Gutiérrez-Enríquez S, Alonso C, Ramón y Cajal T, Francesc Barquiner J (2008) Mitotic delay in lymphocytes from BRCA1 heterozygotes unable to reduce the radiation-induced chromosomal damage. *DNA Repair (Amst)* 7:1907–11
27. Claes K, Depuydt J, Taylor AMR, et al (2013) Variant Ataxia Telangiectasia: Clinical and Molecular Findings and Evaluation of Radiosensitive Phenotypes in a Patient and Relatives. *Neuromolecular Med* 15:447–457
28. Gutiérrez-Enríquez S, Ramón Y Cajal T, Alonso C, Corral A, Carrasco P, Cornet M, Sanz J, Ribas M, Baiget M, Diez O (2011) Ionizing radiation or mitomycin-induced micronuclei in lymphocytes of BRCA1 or BRCA2 mutation carriers. *Breast Cancer Res Treat* 127:611–22
29. Li N, Zhang H, Wang Y, Hao J (2010) BRCA1 and its phosphorylation involved in caffeine-inhibitable event upstream of G2 checkpoint. *Sci China Physics, Mech Astron* 53:1281–1285
30. Pantelias GE, Terzoudi GI (2011) A standardized G2-assay for the prediction of individual radiosensitivity. *Radiother Oncol* 101:28–34
31. Claes K, Poppe B, Machackova E, Coene I, Foretova L, De Paepe A, Messiaen L (2003) Differentiating pathogenic mutations from polymorphic alterations in the splice sites of BRCA1 and BRCA2. *Genes Chromosom Cancer* 37:314–320
32. De Leeneer K, Hellemans J, Steyaert W, et al (2015) Flexible, Scalable, and Efficient Targeted Resequencing on a Benchtop Sequencer for Variant Detection in Clinical Practice. *Hum Mutat* 36:379–387
33. Sasaki MS, Norman A (1966) Proliferation of human lymphocytes in culture. *Nature* 1–2
34. Bernheim JL, Dorian RE, Mendelsohn J (1978) DAN Synthesis and Proliferation of Human Lymphocytes in Vitro : I . Cell Kinetics of Response to Phytohemagglutinin LYMPHOCYTES I N VITRO I . Cell Kinetics of R e s p o n s e t o P h y t o h e m a g g l u t i n i n 1.
35. Claes K, Vandesompele J, Poppe B, Dahan K, Coene I, De Paepe A, Messiaen L (2002) Pathological splice mutations outside the invariant AG/GT splice sites of BRCA1 exon 5 increase alternative transcript levels in the 5' end of the BRCA1 gene. *Oncogene* 21:4171–5
36. Théry JC, Krieger S, Gaildrat P, et al (2011) Contribution of bioinformatics predictions and functional splicing assays to the interpretation of unclassified variants of the BRCA genes. *Eur J Hum Genet* 19:1052–8
37. Linger RJ, Kruk P a. (2010) BRCA1 16 years later: Risk-associated BRCA1 mutations and their functional implications. *FEBS J* 277:3086–3096
38. Vaclová T, Gómez-López G, Setién F, Bueno JMG, Macías JA, Barroso A, Urioste M, Esteller M, Benítez J, Osorio A (2015) DNA repair capacity is impaired in healthy BRCA1 heterozygous mutation carriers. *Breast Cancer Res Treat*. doi: 10.1007/s10549-015-3459-3

39. Pauwels EKJ, Foray N, Bourguignon MH (2015) Breast Cancer Induced by X- Ray Mammography Screening? A Review Based on Recent Understanding of Low-Dose Radiobiology. *Med Princ Pract*. doi: 10.1159/000442442
40. Heyes GJ, Mill a J, Charles MW (2009) Mammography-oncogenecity at low doses. *J Radiol Prot* 29:A123–A132
41. Depuydt J, Baert A, Vandersickel V, Thierens H, Vral A (2013) Relative biological effectiveness of mammography X-rays at the level of DNA and chromosomes in lymphocytes. *Int J Radiat Biol* 89:532–8
42. Obdeijn I-M, Winter-Warnars G a O, Mann RM, Hoening MJ, Hunink MGM, Tilanus-Linthorst MM a (2014) Should we screen BRCA1 mutation carriers only with MRI? A multicenter study. *Breast Cancer Res Treat* 144:577–82
43. Rieger KE, Hong WJ, Tusher VG, Tang J, Tibshirani R, Chu G (2004) Toxicity from radiation therapy associated with abnormal transcriptional responses to DNA damage. *Proc Natl Acad Sci U S A* 101:6635–6640
44. Foray N, Randrianarison V, Marot D, Perricaudet M, Lenoir G, Feunteun J (1999) Gamma-rays-induced death of human cells carrying mutations of BRCA1 or BRCA2. *Oncogene* 18:7334–7342
45. Salmena L, Narod S (2012) BRCA1 haploinsufficiency: consequences for breast cancer. *Womens Health (Lond Engl)* 8:127–9
46. Perrin-vidoz L, Sinilnikova OM, Stoppa-lyonnet D, Lenoir GM, Mazoyer S (2002) The nonsense-mediated mRNA decay pathway triggers degradation of most BRCA1 mRNAs bearing premature termination codons. *Hum Mol Genet* 11:2805–2814
47. Anczuków O, Ware MD, Buisson M, Zetoune AB, Stoppa-lyonnet D, Sinilnikova OM, Mazoyer S, Ą SM, Umr C (2008) Does the nonsense-mediated mRNA decay mechanism prevent the synthesis of truncated BRCA1, CHK2, and p53 proteins? *Hum Mutat* 29:65–73
48. Sedic M, Skibinski A, Brown N, et al (2015) Haploinsufficiency for BRCA1 leads to cell-type-specific genomic instability and premature senescence. *Nat Commun* 6:7505
49. Nikjoo H, O'Neill P, Wilson WE, Goodhead DT (2001) Computational approach for determining the spectrum of DNA damage induced by ionizing radiation. *Radiat Res* 156:577–83
50. Hagen U (1986) Current aspects on the radiation induced base damage in DNA. *Radiat Environ Biophys* 25:261–71
51. Dextraze ME, Gantchev T, Girouard S, Hunting D (2010) DNA interstrand cross-links induced by ionizing radiation: An unsung lesion. *Mutat Res - Rev Mutat Res* 704:101–107
52. Guo Z, Shu Y, Zhou H, Zhang W, Wang H (2015) Radiogenomics helps to achieve personalized therapy by evaluating patient responses to radiation treatment. *Carcinogenesis* 36:307–317
53. Popanda O, Marquardt JU, Chang-Claude J, Schmezer P (2009) Genetic variation in normal tissue toxicity induced by ionizing radiation. *Mutat Res* 667:58–69
54. Vral A, Willems P, Claes K, Poppe B, Perletti G, Thierens H (2011) Combined effect of polymorphisms in Rad51 and Xrcc3 on breast cancer risk and chromosomal radiosensitivity. *Mol Med Rep* 4:901–912
55. Willems P, Claes K, Baeyens A, et al (2008) Polymorphisms in nonhomologous end-joining genes associated with breast cancer risk and chromosomal radiosensitivity. *Genes Chromosomes Cancer* 47:137–148

Additional File 1: Primers

The primer sequences (both forward and reverse)

Amplicon (exon)	Forward	Reverse
c.1A>G (E2)	TCTGCTCTGGGTAAAGGTAGTAGA	GAAGGCCCTTTCTTCTGGTT
c.1961del (E11)	GGAAGTCTTCTACCAGGC	TTAACTTCAGCTCTGGGAAAG
c.2311T>C (E11) = SNP	CCTAGCCTTCCAAGAGAAG	CCATGAATTAGTCCCTTGG
c.2359dup (E11)	CCTAGCCTTCCAAGAGAAG	CCATGAATTAGTCCCTTGG
c.3331_3334del (E11)	GTAGGTTCCAGTACTAATGAAG	CTGAAATCAGATATGGAGAGAAATC
c.3481_3491del (E11)	CCATATCTGATTTTCAGATAACTTA	GATAAGTTCTCTTCTGAGGACTC
c.3661G>T (E11)	GCAGGAGTCCTAGCCCTTTC	GGTTACTGCAGTCATTTAAGCTATTC
c.4327C>T (E13)	GACTGCTCAGGGCTATCCTC	CAGACACCTCAAACCTTGTCAGC
c.4391_4393delinsTT (E14)	GACTCTTCTGCCCTTGAGGA	AAGGGGATGACCTTTCCACT

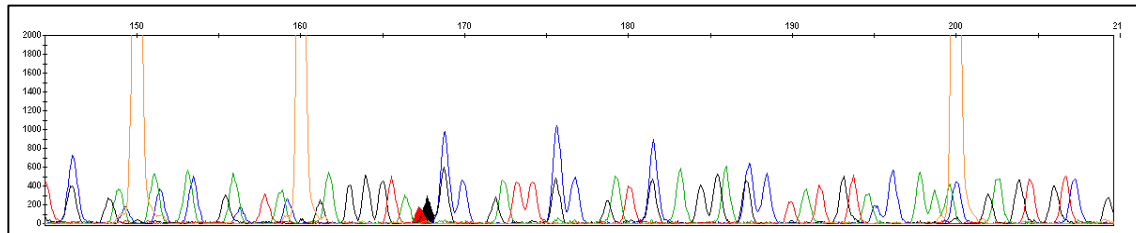
Additional File 2: Results of the fragment analysis

Illustration of fragment analysis data of a SNP without loss of the mutant allele

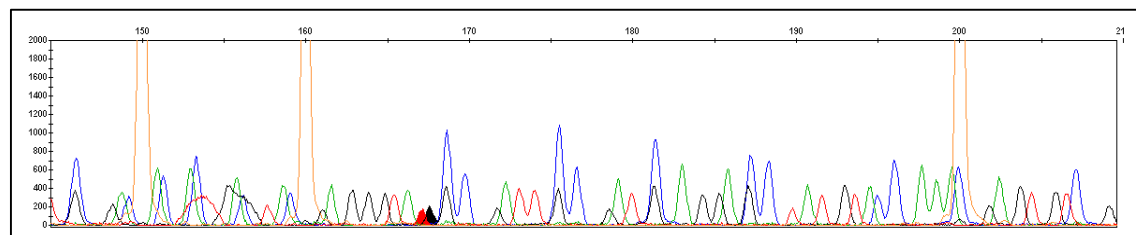
Fragment analysis of c.2311T>C in BC01 (forward)

Limited loss of mutant mRNA could be detected (mean ratio = 0.7). This is in agreement with the MiSeq data with a VAF of approximately 50%.

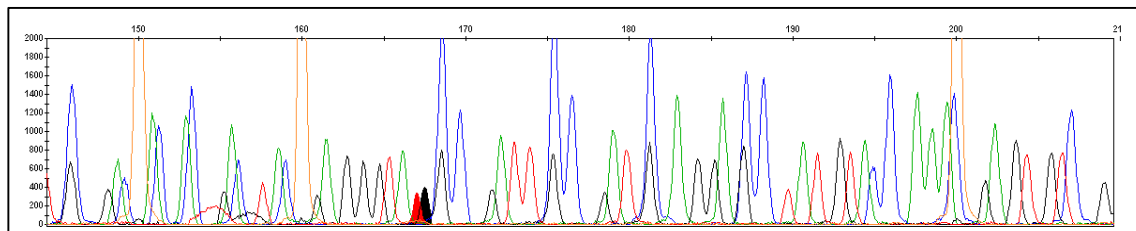
a. cDNA



b. cDNA with puromycin



c. genomic DNA

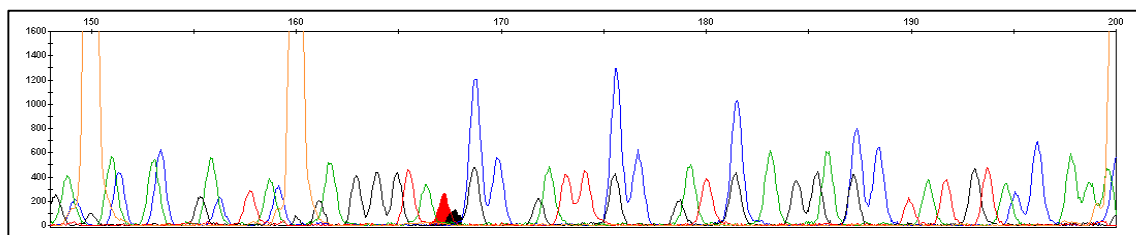
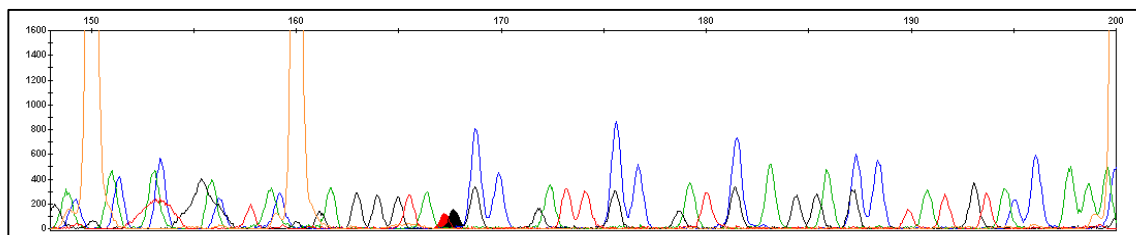
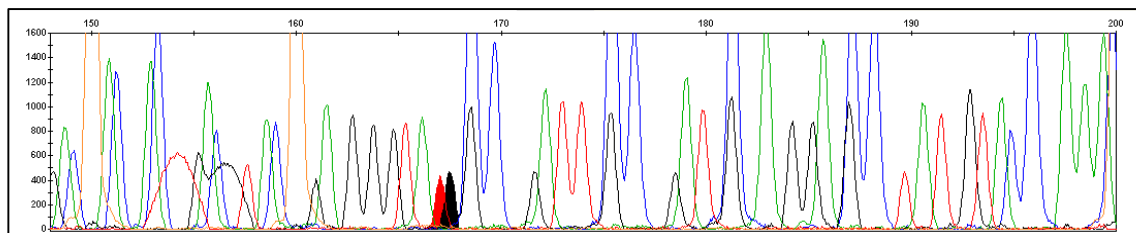


Additional File 3: Results of the fragment analysis

Illustration of fragment analysis data of a SNP with loss of the mutant allele

Fragment analysis of c.2311T>C in BC17 (forward)

A loss of the mutant allele could be detected. In this patient, the T (black) represents the mutant allele. This loss of allelic imbalance is in agreement with the MiSeq data. The VAF for cDNA is 26%, or only half of the frequency on gDNA. This is reflected in the ratio of 0.48 for fragm. analysis in this particularly example.

a. cDNA**b. cDNA with puromycin****c. genomic DNA**

PAPER III: Analysis of chromosomal radiosensitivity of healthy *BRCA2* mutation carriers and non-carriers in *BRCA* families with the G2 micronucleus assay.

Annelot Baert¹, Julie Depuydt¹, Tom Van Maerken², Bruce Poppe³, Fransiska Malfait³, Tim Van Damme³, Sylvia De Nobele³, Gianpaolo Perletti^{1,4}, Kim De Leeneer³, Kathleen B.M. Claes^{3*} and Anne Vral^{1*°}.

¹Department of Basic Medical Sciences, Ghent University, Ghent, Belgium, ²Department of Pediatrics and Medical Genetics, Ghent University, Belgium, ³Center for Medical Genetics, Ghent University Hospital, Belgium, ⁴Department of Biotechnology and Life Sciences, University of Insubria, Busto A, Italy

* Equal contribution

Key words:

BRCA2 mutation carriers, non-carrier relatives, ionizing radiation, micronucleus assay, chromosomal radiosensitivity

Running Title:

Baert et al.: Evaluation of chromosomal radiosensitivity in *BRCA2* mutation carriers and non-carriers

Oncology reports 2017; 37, 1379-1386

Doi: 10.3892/or.2017.5407

Abstract

Breast cancer risk increases drastically in individuals with a heterozygous germline *BRCA1* or *BRCA2* mutation, while it is estimated to equal the population risk for relatives without the familial mutation (non-carriers). The aim of this study is to use a G2 phase specific micronucleus assay to investigate whether lymphocytes of healthy *BRCA2* mutation carriers are characterized by increased radiosensitivity compared to controls without a family history of breast/ovarian cancer and how this relates to healthy non-carrier relatives. *BRCA2* is active in HR, a DNA damage repair pathway, specifically active in the late S/G2 phase of the cell cycle. We found a significantly increased radiosensitivity in a cohort of healthy *BRCA2* mutation carriers compared to individuals without a familial history of breast cancer ($p=0.046$, Mann Whitney test). At the individual level, 50% of healthy *BRCA2* mutation carriers showed a radiosensitive phenotype (radiosensitivity score of 1 or 2), whereas 83% of the controls showed no radiosensitivity ($p=0.038$, one-tailed Fisher Exact test). An odds ratio of 5 (95%CI: 1.07-23.47) indicates an association between the *BRCA2* mutation and radiosensitivity in healthy mutation carriers. These results indicate the need for the gentle use of ionizing radiation for either diagnostic or therapeutic use in *BRCA2* mutation carriers. We detected no increased radiosensitivity in the non-carrier relatives.

Introduction

BRCA1 and *BRCA2* heterozygous mutation carriers have a strongly increased risk to develop breast (BC) and ovarian cancer (OC). The lifetime risk to develop BC is 70-80% for *BRCA1* mutation carriers and 50-60% for *BRCA2* mutation carriers (1). For relatives who did not inherit the germline *BRCA1/2* mutation segregating in the family (non-carrier relatives), the risk of BC occurrence is generally estimated to be as low as the risk assessed in the general population. This might imply that intensified BC detection screening, using - amongst others - mammography screening and MRI, as applied in individuals at high risk is unnecessary in non-carriers (2–7). However, one study reported a 2-5 fold increase of BC occurrence in non-carriers of families with either *BRCA1* or *BRCA2* mutations (8). Another study reported a younger than expected age at diagnosis of BC for non-carriers, that was most evident in *BRCA1* families (9). Moreover, one study by Evans and coworkers detected a possible higher relative risk for BC in non-carrier relatives of *BRCA2* families, compared to non-carriers in *BRCA1* families (10). In summary, these studies suggest that DNA alterations (for example SNPs) in other genes may modify the relative risk for the development of BC in non-carriers, compared to the general population. Moreover, the authors of these studies recommended targeted BC detection screening using for example mammography in non-carriers at a frequency comparable to the intensive BC screening performed in individuals at high risk.

Both *BRCA1* and *BRCA2* are caretaker genes playing different roles in the repair of DSB (DSB), induced by exposure to genotoxic agents like ionizing radiation (IR). While *BRCA1* has a more general function in the detection and signaling of a DSB and in the activation of the G2/M cell cycle checkpoint, *BRCA2* exerts a specific function in the recruitment of RAD51 recombinase to the DSB site. This latter event is essential for the activation of the HR (HR) pathway, that relies on the undamaged sister chromatid as template for resynthesis of the damaged strand. This occurs in the late S and G2 phase of the cell cycle and leads to error-free repair of DSB (1).

Knowing that both *BRCA1* and *BRCA2* are important in the repair of DSB, exposure of mutation carriers to IR - a potent inducer of DSB - for either diagnostic or therapeutic purposes appears to be counterintuitive, as mutation carriers may be more prone to develop radiation-induced BC (11).

Radiosensitivity of *BRCA1* mutation carriers has previously been reported in the literature and was investigated and confirmed by our research group by means of the G2 micronucleus (MN) assay in combination with an evaluation of the G2/M checkpoint efficiency in peripheral blood lymphocytes of healthy *BRCA1* mutation carriers compared to healthy volunteers (12). However, the impact of IR on heterozygous cells of healthy *BRCA2* mutation carriers remains to be elucidated.

So far, several cohort studies were able to prove a positive correlation between exposure to diagnostic X-rays and BC risk in *BRCA2* mutation carriers (11,13,14). Others however, could not detect a similar correlation (15–18). Furthermore, Bernstein et al. detected no increased induction of contralateral BC upon exposure to radiotherapy in *BRCA2* mutation carriers (19). Such discrepancies are likely due to differences in inclusion criteria, data-acquisition and other issues of the studies. It is however difficult and unethical to setup long-term unbiased studies to evaluate the relationship between *BRCA2* mutations, the exposure to diagnostic or therapeutic radiation and BC risk. *In vitro* chromosomal assays are effective tools to investigate radiosensitivity. Chromosomal radiosensitivity testing on lymphocytes from *BRCA2* mutation carriers has been performed with techniques such as the G0 micronucleus (MN) assay and the G2 assay for chromatid breaks, occasionally enhanced with a whole chromosome paint FISH (20–25). However, for several of these studies, it was unclear if the *BRCA2* heterozygotes were healthy individuals or BC patients, which was previously broached by Baeyens et al. (20). Furthermore, differences in experimental setup make comparisons between studies difficult (26). Despite these differences, all but one study were able to detect an elevated chromosomal radiosensitivity in BC patients with a *BRCA2* mutation (20–25). However, no comparison was made with sporadic BC patients. The study of Baeyens et al. previously demonstrated enhanced radiosensitivity in both BC patients with a *BRCA1/2* mutation and sporadic BC patients, suggesting that the enhanced sensitivity might not be the result of the mutation (20). No univocal results were achieved for healthy *BRCA2* mutation carriers. Radiosensitivity in non-carrier relatives has not been studied extensively, only one study reported no increased radiosensitivity measured with the G0 MN and G2 chromatid break assay in a small cohort (n=10) of relatives of both *BRCA1* and *BRCA2* families without the familial mutation when compared to a population cohort (20).

In the present study we aimed to investigate the chromosomal radiosensitivity in healthy *BRCA2* mutation carriers by means of the G2 micronucleus assay. We previously used this assay and confirmed radiosensitivity in healthy *BRCA1* mutation carriers (n=18) compared to healthy controls without a family history of BC or OC (n=20) (12), and in ataxia-telangiectasia patients and family members (27). In addition, we also included healthy relatives not carrying the familial germline *BRCA1* or *BRCA2* mutation in the present study. This cohort of non-carriers was included to evaluate radiosensitivity in individuals with a comparable genetic background, but without the familial *BRCA1* or *BRCA2* mutation.

Materials and methods

Sample collection

Blood samples were collected from individuals consulting the Centre for Medical Genetics of the Ghent University Hospital (Ghent, Belgium) (CMGG), in the context of predictive testing for hereditary BC. Heparin blood samples were collected for the G2 MN assay. In addition, EDTA samples were collected for mutation analysis. We collected blood samples from 18 *BRCA2* mutation carriers and 17 subjects from both *BRCA1* (n=9) and *BRCA2* families (n=8) not showing the familial mutation (non-carriers). None of the individuals selected for this study had developed cancer at time of blood sample collection. We also selected 18 blood samples from a historical cohort of healthy volunteers without a personal or familial history of BC for optimal age and gender match, to determine the normal distribution of micronucleus yields in unaffected individuals from the general population (12).

The study was approved by the ethical committee of the Ghent University Hospital (B67020111641 d.d. 20/09/2011) and all participants signed an informed consent.

Molecular analysis

All healthy individuals selected for this study had a family history of BC or OC and a mutation in either *BRCA1* or *BRCA2* was identified in each proband. All *BRCA2* mutations carriers are heterozygous for an unequivocal deleterious mutation. This was confirmed by Sanger sequencing of the relevant amplicon. Sanger sequencing was performed on the ABI3730XL instrument using the BigDye® Terminator Cycle Sequencing Kit (Life Technologies, USA), according to manufacturer's instructions; sequences were analyzed using the SeqPilot software (JSI medical systems, Germany).

Molecular analyses were not performed in healthy volunteers because of the absence of a personal or familial anamnesis for BC or OC.

The G2 micronucleus assay

The G2 MN assay was performed as previously described (12). In brief, heparinized blood was cultured in the presence of phytohaemagglutinin (PHA, 2%v/v, Gibco) to stimulate T-lymphocyte division. After 3 days, a population of cycling lymphocytes was obtained and the culture was irradiated with a 2 Gy dose of ^{60}Co γ rays. We opted to use a dose of 2 Gy as this is a well-accepted dose for chromosomal radiosensitivity testing in lymphocytes (20–22,24). Immediately after irradiation, cytochalasin B (cyto B, 6 $\mu\text{g}/\text{ml}$, Sigma Aldrich) was added to all cultures, including a non-irradiated culture. Cyto B blocks the cytokinesis and allows the identification of first division cells as a binucleated (BN) cell. After an incubation period of 8 h, all cultures were fixed with the sequential addition of KCl (75 mM), a solution of methanol, acetic acid and Ringer (4:1:5) and a combination of methanol and acetic acid (4:1) to pelleted cells. Finally, the cell suspension was concentrated and spread on slides. Slides were stained with 4',6-diamidino-2-phenylindole (DAPI) and scanned with a Metafer 4 platform and MN search software (Metasystems, Germany). The automated image analysis system selects BN cells and determines the number of MN per BN cell. BN cells and MN selection are manually checked for false positives or false negatives. For each condition, two cultures were prepared and two slides per culture were analyzed. A minimum of 600 BN cells was scored per coded slide. To assess individual radiosensitivity, a radiosensitivity score (RS score) was determined. The mean and SD of the MN yield of the group of healthy volunteers (HV) was set as cut-off value to determine the RS score of healthy volunteers, *BRCA2* mutation carriers and non-carrier relatives. A MN yield higher than the $\text{mean}_{\text{HV}} + 1\text{SD}_{\text{HV}}$ was scored as 1, indicating a milder radiosensitive phenotype, whereas a result higher than the $\text{mean}_{\text{HV}} + 2\text{SD}_{\text{HV}}$ was scored as 2, and indicated a more severe radiosensitive phenotype. If the individual value was lower than $\text{mean}_{\text{HV}} + 1\text{SD}_{\text{HV}}$, a score of 0 was attributed to the tested subject.

Statistical analysis

Age and gender differences across the three groups were judged by means of a one-way anova and Chi square test respectively. The median, interquartile range, average and standard deviation of micronuclei yields (number of MN per 1000 BN cells) were assessed in

each group of subjects. Intergroup differences of MN yields between healthy volunteers, *BRCA2* mutation carriers and non-carrier relatives of *BRCA1* and *BRCA2* pedigrees were analyzed by the Mann-Whitney Wilcoxon test. A one-tailed Fisher exact test was performed to compare unpaired, independent proportions of patients showing a radiosensitive phenotype, evaluated by RS scoring. For both assays a 5% alpha error was set as the boundary for statistical significance. The odds ratio (OR) was calculated, based on the RS scores in healthy individuals and *BRCA2* mutation carriers, to assess the association between the presence of a *BRCA2* mutation and radiosensitivity according to the following formula:

$$OR = \frac{\# \text{BRCA2 mutation carriers with an RS} > 0 \times \# \text{healthy volunteers with an RS} = 0}{\# \text{BRCA2 mutation carriers with an RS} = 0 \times \# \text{healthy volunteers with an RS} > 0}$$

The 95% confidence interval (CI) was used as a proxy for significance. The VassarStats platform and the SPSS software (IBM, version 23) were used to perform statistical analysis.

Results

The mean age does not differ significantly for the healthy volunteers (35.3 years), the *BRCA2* mutation carriers (40.9 years) and the non-carrier relatives (40.0 years) (p-value=0.56, one-way anova). Also, no significant difference in gender distribution was observed for these three groups (68%, 61% and 71% of individuals are female respectively) (p-value=0.84, Chi square test). The number of spontaneously-occurring micronuclei (MN yields in non-irradiated samples) was not significantly different among the three groups of enrolled subjects (Table I and Figure 1).

Table I. Overview of the median, interquartile range, mean and SD of the micronucleus yield (#MN/1000BN).

		0 Gy	2 Gy
Healthy volunteers (HV)	median	12	56
	Interquartile range	9.75	27.5
	mean	14.33	61.22
	SD	8.85	21.73
BRCA2 mutation carriers (MC)	median	14	74
	Interquartile range	7.75	54.75
	mean	16.11	86.11
	SD	6.91	41.87
p value vs. healthy volunteers (Mann-Whitney)		0.177	0.046
Relatives who did not inherit the familial <i>BRCA1/2</i> mutation	median	16	69
	Interquartile range	8	26
	mean	17.23	68.11
	SD	7.74	22.30
p value vs. healthy volunteers (Mann-Whitney)		0.116	0.400

SD standard deviation, MN micronucleus, BN binucleated cells

Compared to healthy volunteers without a family history of BC/OC, *BRCA2* mutation carriers showed a significant increase in mean MN yields after exposure to 2 Gy IR (p-value=0.046, Mann Whitney). Conversely, the radiation-induced MN yields were similar in relatives who did not inherit the familial *BRCA1/2* mutation and healthy volunteers without a family history of BC/OC. The mean MN yield in *BRCA2* mutation carriers was higher compared to the mean yield in non-carriers (86.11 vs. 68.11 MN/1000 BN cells respectively). This difference was however not significant (p-value=0.298, Mann Whitney), probably due to the small cohort and the high SD (Table I and Figure 1). Furthermore, MN yields did not differ between non-carrier relatives from *BRCA1* or *BRCA2* pedigrees (Table II).

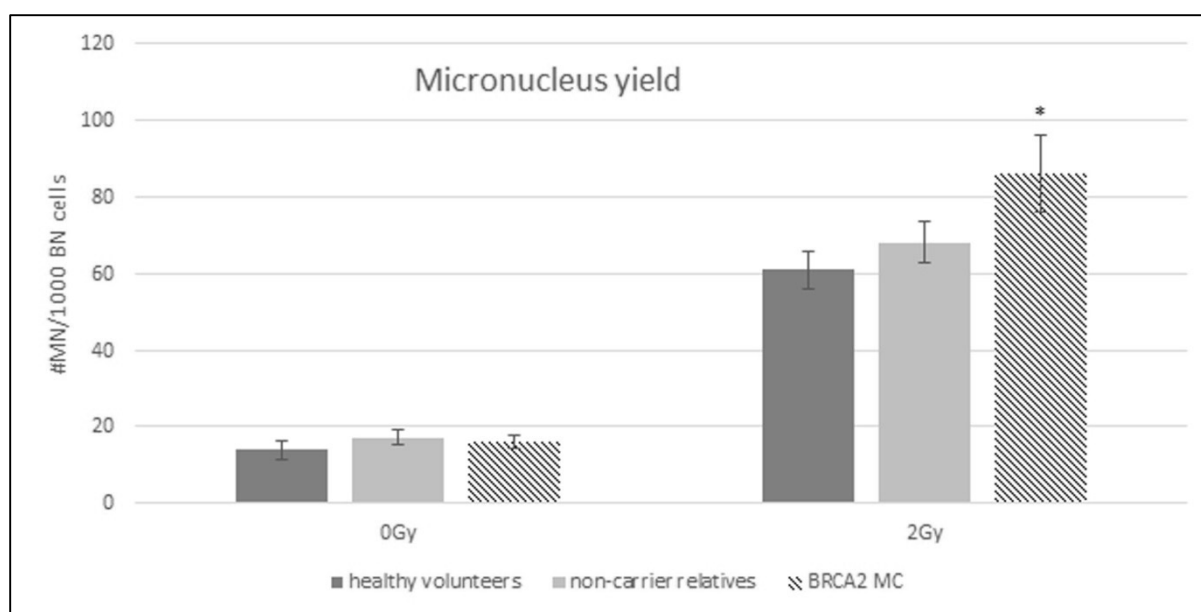


Figure 1 Mean G2 micronucleus yield

Mean MN yield for healthy volunteers, healthy relatives who did not inherit the familial *BRCA1/2* mutation and healthy *BRCA2* mutation carriers. * indicates a significant difference (p -value<0,05) compared to the healthy volunteers determined by Mann Whitney U test. Error bars represent the standard error of the mean. MN micronucleus, BN binucleated, MC mutation carriers

Table II. Overview of median, interquartile range, mean and SD of the micronucleus yield (#MN/1000BN) for healthy relatives who did not inherit the familial germline *BRCA1/2* mutation.

	0 Gy	2 Gy
Relatives who did not inherit the familial <i>BRCA1</i> mutation (n=9)		
median	14	66
Interquartile range	12	57
mean	16.44	69.04
SD	6.88	27.45
Relatives who did not inherit the familial <i>BRCA2</i> mutation (n=8)		
median	16	70
Interquartile range	12.75	51.71
mean	18.11	66.98
SD	9.18	16.59
p value vs. <i>BRCA1</i> non-carriers (Mann-Whitney)	0.7339	0.9601

SD standard deviation, MN micronucleus, BN binucleated cells

The individual MN yields after exposure to 2 Gy and the radiosensitivity score (RS score) for each *BRCA2* mutation carrier, non-carrier relative and healthy volunteer are listed in Table III.

Furthermore, Table III shows mutational data (both nucleotide and protein nomenclature) and individuals with the same family ID are related. Figure 2 shows the distribution of the three groups for the different RS scores. A significant higher number of *BRCA2* mutation carriers (n=9/18; 50%) showed increased RS scores (score 1 or 2) compared to healthy volunteers (n=3/18; 17%) (P=0.038, one-tailed Fisher exact test). For the relatives who did not inherit the familial germline mutation only 24% (n=4/17) showed an elevated radiosensitivity at the individual level. RS scoring in related individuals (see Family ID in Table III) however shows some variation. An OR of 5 (95% CI: 1.07 – 23.46) for *BRCA2* mutation carriers vs. healthy volunteers, indicates a significant association between the presence of a *BRCA2* mutation and radiosensitivity according to our criteria.

All but one of the 18 mutation carriers enrolled in the present study are heterozygous for a mutation predicted to result in a premature termination codon (PTC). The patient with the deleterious missense mutation (*BRCA2* c.8167G>C; p.(Asp2723His) obtained a RS score of 2.

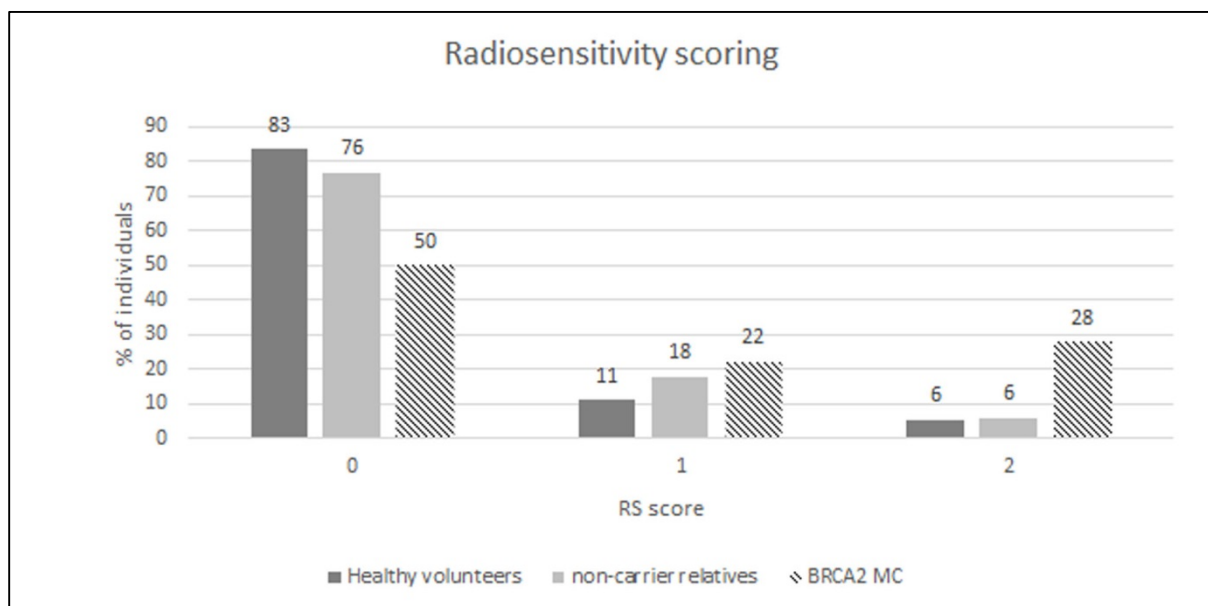


Figure 2 Radiosensitivity scoring

Distribution (%) of healthy volunteers, healthy relatives who did not inherit the familial *BRCA1/2* mutation and healthy *BRCA2* mutation carriers over the different RS scores. RS score 0 correlates to no increased radiosensitivity, RS score 1 indicates a milder radiosensitive phenotype and RS score 2 reflects a more severe radiosensitive phenotype. RS Radiosensitivity, MC mutation carriers

Table III. Germline mutation, Family ID, micronucleus yields (#MN/1000BN) and RS score for *BRCA2* mutation carriers, relatives who did not inherit the familial mutation (non-carrier relatives) and healthy volunteers (numbering of the nucleotides according to RefSeq nr. NM_000059.3; A of ATG start codon = nucleotide +1)

BRCA2 mutation carriers							Non-carrier relatives						Healthy volunteers			
ID	Family ID	Mutation: nucleotide	Mutation: protein	0 Gy	2 Gy	RS score	ID	Family ID	Family gene	0 Gy	2 Gy	RS score	ID	0 Gy	2 Gy	RS score
M2.01	BR-32-2170	c.658_659delGT	p.(Val220fs*4)	14	119	2	NM.06	BR-32-0156	BRCA2	17	51	0	D01	19	83	1
M2.02	BR-32-1748	c.1389_1390del	p.(Val464fs*3)	15	91	1	NM.17	BR-32-0342	BRCA1	8	29	0	D12	10	52	0
M2.03	BR-32-1748	c.1389_1390del	p.(Val464fs*3)	19	83	1	NM.01	BR-32-0645	BRCA1	20	63	0	D13	7	47	0
M2.04	BR-32-1748	c.1389_1390del	p.(Val464fs*3)	12	58	0	NM.10	BR-32-1134	BRCA1	14	74	0	D15	12	55	0
M2.05	BR-32-1748	c.1389_1390del	p.(Val464fs*3)	16	56	0	NM.13	BR-32-1225	BRCA1	18	43	0	D16	17	44	0
M2.06	BR-32-1758	c.1989del	p.(Phe663fs*5)	12	163	2	NM.12	BR-32-1225	BRCA1	11	57	0	D17	7	58	0
M2.07	BR-32-0884	c.4171del	p.(Glu1391fs*19)	37	65	0	NM.07	BR-32-1444	BRCA1	12	66	0	D21	13	48	0
M2.08	BR-32-0884	c.4171del	p.(Glu1391fs*19)	20	90	1	NM.08	BR-32-1444	BRCA1	12	78	0	D04	12	40	0
M2.09	BR-32-1759	c.4936_4939del	p.(Glu1646fs*23)	20	65	0	NM.02	BR-32-1494	BRCA1	24	87	1	D05	6	30	0
M2.10	BR-32-1759	c.4936_4939del	p.(Glu1646fs*23)	18	53	0	NM.16	BR-32-1967	BRCA1	29	125	2	D06	15	74	0
M2.11	BR-32-0156	c.6275_6276del	p.(Leu2092Profs*7)	12	63	0	NM.03	BR-32-0884	BRCA2	20	91	1	D29	9	29	0
M2.12	BR-32-1565	c.6275_6276del	p.(Leu2092Profs*7)	8	44	0	NM.04	BR-32-0884	BRCA2	16	73	0	D30	30	109	2
M2.13	BR-32-1930	c.6275_6276del	p.(Leu2092Profs*7)	23	183	2	NM.09	BR-32-1748	BRCA2	21	70	0	D32	7	96	1
M2.14	BR-32-1930	c.6275_6276del	p.(Leu2092Profs*7)	12	86	1	NM.11	BR-32-1758	BRCA2	8	45	0	D31	26	73	0
M2.15	BR-32-1920	c.8167G>C	p.(Asp2723His)	10	118	2	NM.05	BR-32-1759	BRCA2	38	85	1	D35	37	76	0
M2.16	BR-32-1628	c.8332-?_8487-?del	p.(Ile2778Lysfs*40)	22	29	0	NM.14	BR-32-1759	BRCA2	12	69	0	D37	6	75	0
M2.17	BR-32-0937	c.8904delC	p.(Val2969fs*7)	10	131	2	NM.15	BR-32-2170	BRCA2	13	52	0	D38	17	52	0
M2.18	BR-32-0082	c.9256+1G>C	r.9118_9256del; p.(Val3040Aspfs*18)	10	53	0							D39	8	61	0
Median				14	74					16	69					
Interquartile range				7.75	54.75					8	26					
Mean				16.11	86.11					17.23	68.11					
SD				6.91	41.87					7.74	22.30					

The splice site mutation present in M2.18 was previously described by Claes et al. (39), where it was erroneously defined as IVS24G>A.

SD standard deviation, MN micronucleus, BN binucleated cells, RS radiosensitivity

Discussion

Results of the G2 micronucleus assay performed after exposure to 2 Gy γ -rays showed a significantly increased radiosensitivity in healthy *BRCA2* mutation carriers compared to healthy controls. Previous studies with a large number of different techniques were able to demonstrate enhanced radiosensitivity in BC patients with a *BRCA2* mutation, however, no univocal results were achieved for healthy *BRCA2* mutation carriers (20–25). Non-carrier relatives of either *BRCA1* or *BRCA2* families did not show an increased radiosensitive phenotype compared to the cohort of healthy volunteers, which is in agreement with the study of Baeyens et al. (20). We previously performed the G2 MN assay in a group of 18 healthy *BRCA1* mutation carriers, and found a significantly increased MN yield after exposure to 2 Gy γ -rays (12). These findings are analogous to the results of the present study, performed in healthy carriers of pathogenic *BRCA2* mutations. Figure 3 shows the integration of the data from healthy *BRCA1* mutation carriers in the present study. The detection of an increased mean MN yield in both *BRCA1* and *BRCA2* mutation carriers after exposure to ionizing radiation can be explained by their mutual role in DNA double strand break repair (reviewed by Roy et al. (1)).

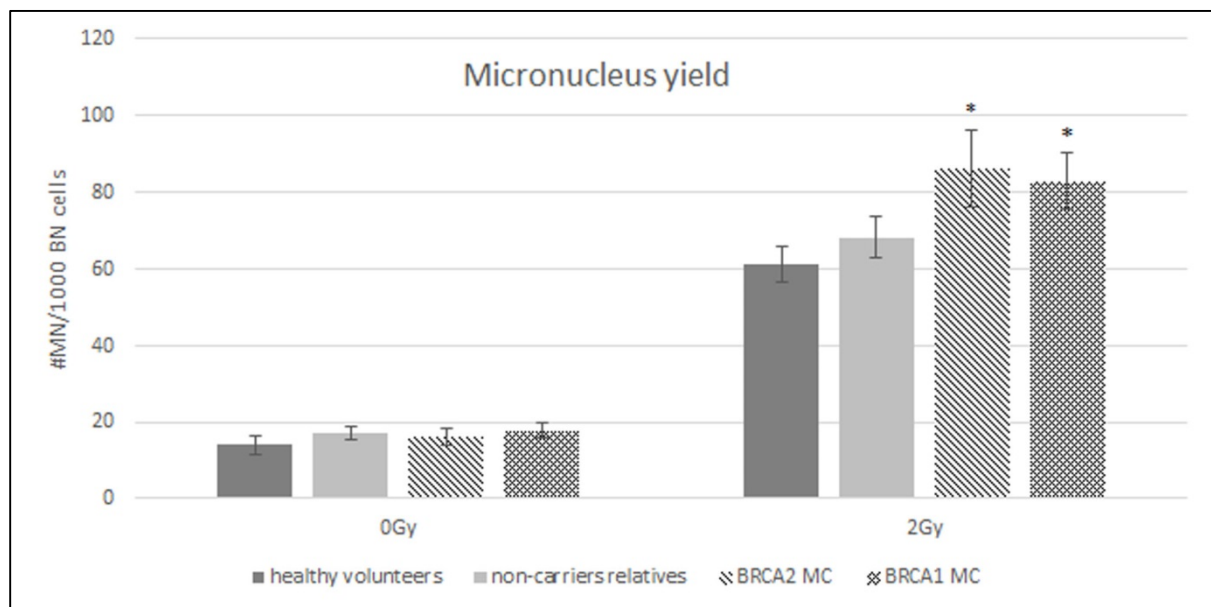


Figure 3 Mean G2 micronucleus yield

Mean MN yield for healthy volunteers, healthy relatives who did not inherit the familial *BRCA1/2* mutation, healthy *BRCA2* and healthy *BRCA1* mutation carriers. * indicates a significant difference (p -value<0,05) compared to the healthy volunteers determined by Mann Whitney U test. Error bars represent the standard error of the mean. MN micronucleus, BN binucleated, MC mutation carriers

In our previous study we also analyzed the G2/M checkpoint activity by the addition of caffeine, an agent abrogating the G2/M checkpoint, to the irradiated cultures and demonstrated a significantly impaired checkpoint activation in *BRCA1* mutation carriers compared to healthy volunteers (12). Analysis of the G2/M checkpoint activation in the current *BRCA2* cohort did not reveal a significant difference (data not shown). This result is in agreement with the fact that *BRCA2* is not activated in this particular checkpoint pathway as reviewed by Roy et al. (1), but does not support the data obtained by Menzel et al. (28), suggesting a role for *BRCA2* as regulator of G2 checkpoint maintenance following DNA damage introduced in a human osteosarcoma cell line (U2OS) expressing dominant-negative p53 by a high dose of ionizing radiation (6 Gy).

The role of *BRCA2* in the HR pathway, a DNA repair pathway active in S and G2 phase of the cell cycle, is extensively reported in literature (for a review: (1)). Our study, focusing on radiosensitivity testing of lymphocytes in these phases of the cell cycle, shows an OR of 5 (95%CI: 1.07-23.47) for healthy individuals with a heterozygous *BRCA2* mutation compared to healthy controls. This indicates a positive association between the presence of a *BRCA2* mutation and radiosensitivity that could be attributed to deficient HR capacity in heterozygous cells.

Two independent research groups have reported a decreased DSB repair capacity in *BRCA2* heterozygous cells. Keimling et al. used an enhanced green fluorescent protein (EGFP)-based assay to report impaired HR capacity in lymphoblastoid cells with a *BRCA2* monoallelic truncating frameshift mutation. They confirmed this decrease in HR capacity in a *BRCA2* knockdown Hela cell line (29). Arnold et al. demonstrated distinct defects in DNA DSB repair in lymphoblastoid cell lines (LCL) from heterozygous *BRCA2* mutation carriers through analysis of γ H2AX repair kinetics (30). Although the latter study did not focus on DNA repair by HR, it indicates a malfunction of DSB repair in LCL from *BRCA2* mutation carriers that could be attributed to diminished HR activity.

Most mutation carriers enrolled in the present study (n=17/18, 94%) had a mutation resulting in a premature termination codon (PTC). The presence of a PTC mutation is expected to activate NMD of the gene transcript. Previous research from various groups including ours, demonstrated a reduction of mutant mRNA to approximately half of the WT mRNA levels in lymphocytes of individuals with a PTC mutation in *BRCA1* (12,31,32). Arnold et al. (30) detected a similar mutant mRNA reduction for *BRCA2* mutations leading to a PTC.

Furthermore, Arnold et al. (30) and Keimling et al. (29) report distinct reduced protein levels in lymphoblastoid cell lines from heterozygous *BRCA2* mutation carriers, though quantitative analysis of this variation was not performed. Previously, haploinsufficiency has been suggested as the mechanism for hereditary BC development in *BRCA1* and *BRCA2* mutation carriers (33). In the present study, a higher than expected number of radiosensitive individuals in the *BRCA2* mutation carriers indicates that haploinsufficiency might also be responsible for the radiosensitive phenotype in carriers of a mutation generating a PTC. In this study, only one individual with a deleterious missense mutation was included. This substitution results in an amino acid change at position p.2723 and impairs protein functionality as shown by a homology-directed DNA break repair functional assay (34). For this individual, we obtained a high RS score of 2. Further research in larger patient cohorts with different types of mutations is needed to evaluate if the type of mutation influences the radiosensitive phenotype or if there are additional parameters determining this phenotype.

Results of the G2 MN assay show no increased radiosensitivity in the group of non-carrier relatives of both *BRCA1* and *BRCA2* families compared to a group of healthy volunteers. Furthermore, only 24% of non-carriers showed an elevated radiosensitivity at the individual level (RS score 1 or 2). This was not significantly different from the fraction of healthy volunteers (17%) that was found to have an increased RS score. In addition, no difference was observed between non-carriers from *BRCA1* (RS score=0 in 7/9 investigated relatives) or *BRCA2* families (RS score=0 in 6/8 investigated relatives). However, we observed some variation within the different groups. We hypothesize that modifiers may play a role: indeed, selected SNPs in DNA damage repair genes and other common variants have been associated with an increased radiosensitivity (35–37) and increased BC risk (35,38). Much larger studies are needed to evaluate the subtle influence of possible modifying factors on BC risk and radiosensitivity.

Conclusion

The present study demonstrated higher radiosensitivity in healthy *BRCA2* mutation carriers compared to healthy volunteers by means of the G2 MN assay after exposure of peripheral blood lymphocytes to a dose of 2 Gy γ -rays. No increased radiosensitivity was observed in non-carrier relatives of *BRCA1* and *BRCA2* families. When evaluating radiosensitivity at the individual level, a significantly higher proportion of *BRCA2* mutation carriers (50%) showed a mild or more severe radiosensitivity compared to healthy volunteers (17%) and non-carriers (24%). Furthermore, an OR of 5 indicates a positive association between the *BRCA2* mutation and an increased radiosensitivity in healthy mutation carriers. These results indicate that care should be taken when applying ionizing radiation for either diagnostic or therapeutic purposes in *BRCA2* mutation carriers. However, a study including larger populations of subjects carrying different types of *BRCA2* mutations and non-carriers, will be performed to further elucidate the effect of each single mutation on the radiosensitive phenotype and the influence of possible underlying factors.

Acknowledgements

The authors thank all participants who donated a blood sample for this assay. They thank Céline De Brock, Brecht Crombez, Ilse Coene, Johanna Aernoudt, Toke Thiron, Greet De Smet and Leen Pieters for their technical assistance. Prof. Dr. Thierens is thanked for the use of the irradiation facility.

This study was funded by the Belgian Foundation against Cancer (project 2012-216).

Conflict of interest statement

The authors declare that they have no competing interest

Informed consent statement

The study was approved by the ethical committee of the Ghent University Hospital (B67020111641 d.d. 20/09/2011) and all participants signed an informed consent.

References

1. Roy R, Chun J and Powell SN: BRCA1 and BRCA2: different roles in a common pathway of genome protection. *Nat Rev Cancer* 12: 68–78, 2012.
2. Bernholtz S, Laitman Y, Kaufman B, Shimon-Paluch S and Friedman E: Phenocopy breast cancer rates in Israeli BRCA1 BRCA2 mutation carrier families: Is the risk increased in non-carriers? *Breast Cancer Res Treat* 132: 669–673, 2012.
3. Domchek SM, Gaudet MM, Stopfer JE, *et al.*: Breast cancer risks in individuals testing negative for a known family mutation in BRCA1 or BRCA2. *Breast Cancer Res Treat* 119: 409–414, 2010.
4. Harvey SL, Milne RL, McLachlan SA, *et al.*: Prospective study of breast cancer risk for mutation negative women from BRCA1 or BRCA2 mutation positive families. *Breast Cancer Res Treat* 130: 1057–1061, 2011.
5. Korde LA, Mueller CM, Loud JT, Struewing JP, Nichols K, Greene MH and Mai PL: No evidence of excess breast cancer risk among mutation-negative women from BRCA mutation-positive families. *Breast Cancer Res Treat* 125: 169–173, 2011.
6. Kurian AW, Gong GD, John EM, *et al.*: Breast cancer risk for noncarriers of family-specific BRCA1 and BRCA2 mutations: Findings from the breast cancer family registry. *J Clin Oncol* 29: 4505–4509, 2011.
7. Nielsen HR, Petersen J, Krogh L, Nilbert M and Skytte A-B: No evidence of increased breast cancer risk for proven noncarriers from BRCA1 and BRCA2 families. *Fam Cancer*: 4–9, 2016.
8. Smith a, Moran a, Boyd MC, *et al.*: Phenocopies in BRCA1 and BRCA2 families: evidence for modifier genes and implications for screening. *J Med Genet* 44: 10–15, 2007.
9. Vos JR, De Bock GH, Teixeira N, Van Der Kolk DM, Jansen L, Mourits MJE and Oosterwijk JC: Proven non-carriers in BRCA families have an earlier age of onset of breast cancer. *Eur J Cancer* 49: 2101–2106, 2013.
10. Evans DGR, Ingham SL, Buchan I, *et al.*: Increased rate of phenocopies in all age groups in BRCA1/BRCA2 mutation kindred, but increased prospective breast cancer risk is confined to BRCA2 mutation carriers. *Cancer Epidemiol Biomarkers Prev* 22: 2269–2276, 2013.
11. Pijpe A, Andrieu N, Easton DF, *et al.*: Exposure to diagnostic radiation and risk of breast cancer among carriers of BRCA1/2 mutations: retrospective cohort study (GENE-RAD-RISK). *BMJ* 345: e5660, 2012.
12. Baert A, Depuydt J, Van Maerken T, *et al.*: Increased chromosomal radiosensitivity in asymptomatic carriers of a heterozygous BRCA1 mutation. *Breast Cancer Res* 18: 52, 2016.
13. Andrieu N, Easton DF, Chang-claude J, Rookus MA, Brohet R and Cardis E: Effect of Chest X-Rays on the Risk of Breast Cancer Among BRCA1 / 2 Mutation Carriers in the International BRCA1 / 2 Carrier Cohort Study : A Report from the EMBRACE , GENEPSO , GEO-HEBON , and IBCCS Collaborators ' Group. *J Clin Oncol* 24: 3361–3366, 2006.
14. Lecarpentier J, Noguès C, Mouret-Fourme E, *et al.*: Variation in breast cancer risk with mutation position , smoking , alcohol , and chest X-ray history , in the French National BRCA1 / 2 carrier cohort (GENEPSO). *Breast Cancer Res Treat* 130: 927–938, 2011.
15. Narod SA, Lubinski J, Ghadirian P, *et al.*: Screening mammography and risk of breast cancer in BRCA1 and BRCA2 mutation carriers: a case-control study. *Lancet Oncol* 7:

- 402–6, 2006.
16. Giannakeas V, Lubinski J, Gronwald J, *et al.*: Mammography screening and the risk of breast cancer in BRCA1 and BRCA2 mutation carriers: a prospective study. *Breast Cancer Res Treat* 147: 113–8, 2014.
17. Goldfrank D, Chuai S, Bernstein JL, *et al.*: Effect of mammography on breast cancer risk in women with mutations in BRCA1 or BRCA2. *Cancer Epidemiol Biomarkers Prev* 15: 2311–2313, 2006.
18. John EM, Mcguire V, Thomas D, *et al.*: Diagnostic chest X-rays and breast cancer risk before age 50 years for BRCA1 and BRCA2 mutation carriers. *Cancer Epidemiol Biomarkers Prev* 22: 1547–56, 2013.
19. Bernstein JL, Thomas DC, Shore RE, *et al.*: Contralateral breast cancer after radiotherapy among BRCA1 and BRCA2 mutation carriers: a WECARE study report. *Eur J Cancer* 49: 2979–85, 2013.
20. Baeyens A, Thierens H, Claes K, Poppe B, de Ridder L and Vral A: Chromosomal radiosensitivity in BRCA1 and BRCA2 mutation carriers. *Int J Radiat Biol* 80: 745–756, 2004.
21. Gutiérrez-Enríquez S, Ramón Y Cajal T, Alonso C, *et al.*: Ionizing radiation or mitomycin-induced micronuclei in lymphocytes of BRCA1 or BRCA2 mutation carriers. *Breast Cancer Res Treat* 127: 611–22, 2011.
22. Trenz K, Rothfuss A, Schütz P and Speit G: Mutagen sensitivity of peripheral blood from women carrying a BRCA1 or BRCA2 mutation. *Mutat Res* 500: 89–96, 2002.
23. Ernestos B, Nikolaos P, Koulis G, Eleni R, Konstantinos B, Alexandra G and Michael K: Increased chromosomal radiosensitivity in women carrying BRCA1/BRCA2 mutations assessed with the G2 assay. *Int J Radiat Oncol Biol Phys* 76: 1199–205, 2010.
24. Becker AA, Graeser MK, Landwehr C, *et al.*: A 24-color metaphase-based radiation assay discriminates heterozygous BRCA2 mutation carriers from controls by chromosomal radiosensitivity. *Breast Cancer Res Treat* 135: 167–175, 2012.
25. Bolognesi C, Bruzzi P, Gismondi V, Volpi S, Viassolo V, Pedemonte S and Varesco L: Clinical application of micronucleus test: A case-control study on the prediction of breast cancer risk/susceptibility. *PLoS One* 9: 1–18, 2014.
26. Cardinale F, Bruzzi P and Bolognesi C: Role of micronucleus test in predicting breast cancer susceptibility: a systematic review and meta-analysis. *Br J Cancer* 106: 780–90, 2012.
27. Claes K, Depuydt J, Taylor AMR, *et al.*: Variant Ataxia Telangiectasia: Clinical and Molecular Findings and Evaluation of Radiosensitive Phenotypes in a Patient and Relatives. *Neuromolecular Med* 15: 447–457, 2013.
28. Menzel T, Nähse-Kumpf V, Kousholt AN, *et al.*: A genetic screen identifies BRCA2 and PALB2 as key regulators of G2 checkpoint maintenance. *EMBO Rep* 12: 705–12, 2011.
29. Keimling M, Volcic M, Csernok a., Wieland B, Dork T and Wiesmuller L: Functional characterization connects individual patient mutations in ataxia telangiectasia mutated (ATM) with dysfunction of specific DNA double-strand break-repair signaling pathways. *FASEB J* 25: 3849–3860, 2011.
30. Arnold K, Kim MK, Frerk K, Edler L, Savelyeva L, Schmezer P and Wiedemeyer R: Lower level of BRCA2 protein in heterozygous mutation carriers is correlated with an increase in DSB and an impaired DSB repair. *Cancer Lett* 243: 90–100, 2006.
31. Perrin-vidoz L, Sinilnikova OM, Stoppa-lyonnet D, Lenoir GM and Mazoyer S: The nonsense-mediated mRNA decay pathway triggers degradation of most BRCA1

- mRNAs bearing premature termination codons. 11: 2805–2814, 2002.
32. Anczuków O, Ware MD, Buisson M, *et al.*: Does the nonsense-mediated mRNA decay mechanism prevent the synthesis of truncated BRCA1, CHK2, and p53 proteins? *Hum Mutat* 29: 65–73, 2008.
33. Berger AH, Knudson AG and Pandolfi PP: A continuum model for tumour suppression. *Nature* 476: 163–169, 2011.
34. Guidugli L, Pankratz VS, Singh N, *et al.*: A classification model for BRCA2 DNA binding domain missense variants based on homology-directed repair activity. *Cancer Res* 73: 265–275, 2013.
35. Willems P, Claes K, Baeyens A, *et al.*: Polymorphisms in nonhomologous end-joining genes associated with breast cancer risk and chromosomal radiosensitivity. *Genes Chromosomes Cancer* 47: 137–148, 2008.
36. Guo Z, Shu Y, Zhou H, Zhang W and Wang H: Radiogenomics helps to achieve personalized therapy by evaluating patient responses to radiation treatment. *Carcinogenesis* 36: 307–317, 2015.
37. Popanda O, Marquardt JU, Chang-Claude J and Schmezer P: Genetic variation in normal tissue toxicity induced by ionizing radiation. *Mutat Res* 667: 58–69, 2009.
38. Antoniou AC, Kuchenbaecker KB, Soucy P, *et al.*: Common variants at 12p11, 12q24, 9p21, 9q31.2 and in ZNF365 are associated with breast cancer risk for BRCA1 and/or BRCA2 mutation carriers. *Breast Cancer Res* 14: R33, 2012.
39. Claes K, Poppe B, Machackova E, Coene I, Foretova L, De Paepe A and Messiaen L: Differentiating pathogenic mutations from polymorphic alterations in the splice sites of BRCA1 and BRCA2. *Genes Chromosomes Cancer* 37: 314–320, 2003.

PAPER IV: The RAD51 foci assay for the detection of impaired homologous recombination in synchronized and irradiated MCF10A cells with a BRCA1 or BRCA2 knockdown

Annelot Baert¹, Maria Federica Palermo¹, Julie Depuydt¹, Mattias Van Heetvelde², Bram Verstraete¹, Jan Philippé³, Anna Sablina⁴, Kathleen BM Claes² and Anne Vral¹.

¹Department of Basic Medical Sciences, Ghent University, Ghent, Belgium, ²Center for Medical Genetics, Ghent University Hospital, Belgium, ³Department of Clinical Chemistry, Microbiology and Immunology, Ghent University, Ghent, Belgium, ⁴VIB-KU Leuven Center for Cancer Biology; Department of Oncology, KU Leuven.

In preparation for submission to Plos One

Abstract

Breast cancer predisposition genes *BRCA1* and *BRCA2* play an important role in HR, a DNA double strand break repair pathway active in S and G2 phase of the cell cycle, activated after exposure to ionizing radiation. Impaired double strand break repair might implicate an increased radiation-induced breast cancer risk for individuals with a germline mutation. Several clinical studies and *in vitro* cytogenetic studies could not irrefutably confirm or disprove increased radiosensitivity in germline mutation carriers. An assay specifically evaluating the effect of heterozygous *BRCA1* or *BRCA2* mutations on HR capacity might be more appropriate to determine radiosensitivity of these individuals. In this study, we investigated the suitability of the RAD51 foci assay to evaluate HR capacity in MCF10A cells with reduced protein levels of *BRCA1* and *BRCA2* obtained by RNA interference. After exposure to ionizing radiation, we determined RAD51 foci levels, a hallmark for HR, in S and G2 phase synchronized cells. We demonstrated that in cells with a knockdown for either *BRCA1* or *BRCA2*, the HR pathway is impaired, as observed by the absence of radiation-induced RAD51 foci in synchronized MCF10A cells. We anticipate that this assay can also be applied on synchronized lymphocytes of heterozygous *BRCA1* and *BRCA2* mutation carriers to assess radiosensitivity and HR capacity. It can also be a valuable assay to elucidate pathogenicity of variants of unknown significance in either gene. After thorough validation in a large cohort of *BRCA1/2* mutation carriers, this may open perspectives to a novel functional assay which can be performed in frozen patient material without the need of cloning to distinguish deleterious mutations from neutral *BRCA1/2* variants.

Introduction

Breast cancer risk increases drastically in individuals carrying a germline *BRCA1* or *BRCA2* mutation. *BRCA1* and *BRCA2* are known as caretaker genes and are both active in the DNA damage response pathway. They are both important in HR (HR), a DNA double strand break (DSB) repair pathway, active in S and G2 phase of the cell cycle after exposure to ionizing radiation (IR) (Roy et al. 2012; Mao et al. 2008).

Individuals harboring a germline mutation in either gene might show enhanced radiosensitivity associated with a higher carcinogenic risk after medical exposure to IR. However, studies investigating the impact of exposure to diagnostic or therapeutic X-rays on cancer risk in *BRCA1* and *BRCA2* mutation carriers did not yield univocal results (Pijpe et al. 2012; Lecarpentier et al. 2011; Andrieu et al. 2006; Gronwald et al. 2008; John et al. 2013; Narod et al. 2006; Giannakeas et al. 2014; Goldfrank et al. 2006; Bernstein et al. 2013; Broeks et al. 2007). Currently used techniques to evaluate *in vitro* radiosensitivity in *BRCA1* and *BRCA2* mutation carriers usually focus on chromosomal radiosensitivity (Baeyens et al. 2004; Gutiérrez-Enríquez et al. 2011; Trenz et al. 2002; Ernestos et al. 2010; Becker et al. 2012; Bolognesi et al. 2014; Cardinale et al. 2012; Kote-Jarai et al. 2006; Frankenberg-Schwager & Gregus 2012; Barwell et al. 2007). Also here, results are contradictory, especially when analyzing radiosensitivity in healthy mutation carriers without breast cancer. In our recent studies, we developed an S-G2-phase specific micronucleus (MN) assay to analyze *in vitro* chromosomal radiosensitivity in lymphocytes of healthy *BRCA1* and *BRCA2* mutation carriers compared to healthy controls. We could demonstrate that in general *BRCA1* and *BRCA2* mutation carriers are characterized by a radiosensitive phenotype. However, due to overlap in MN yields between carriers and controls, the G2 micronucleus assay, as all other cytogenic assays, still has limitations when used as a biomarker of individual radiosensitivity in mutation carriers (Baert et al. 2016; Baert et al. 2017). The fact that cytogenetic assays in general are not sensitive enough to detect radiosensitivity in healthy heterozygous *BRCA1/BRCA2* mutation carriers might be due to the fact that radiation-induced DSB, even when induced in S/G2 phase of the cell cycle, are mainly repaired by non-homologous end-joining (NHEJ) and not by HR, the pathway in which *BRCA1* and *BRCA2* play an important role. HR is only involved in the repair of a subset of DSB induced by IR in S and G2 phase of the cell cycle (Mao et al.

2008; Li & Xu 2016; Mladenov et al. 2016; Ceccaldi et al. 2016). So, a better strategy would be to develop an assay that analyses the functionality of HR specifically.

HR relies on RAD51 filament formation which subsequently induces strand invasion for the repair of the DSB. RAD51 protein recruitment to the DSB site is mediated by BRCA1 and BRCA2 and can be detected as nuclear foci upon immunostaining (Mladenov et al. 2016; Rothkamm et al. 2015). Recently, the *ex vivo* RAD51 irradiation-induced foci (IRIF) assay, performed on fresh biopsy samples of cancer patients has shown to be a suitable assay to detect HR deficiency due to defects in proteins involved in the HR pathway such as BRCA1 and BRCA2, a characteristic which renders tumors sensitive to PARP inhibition treatment (Willers et al. 2009; Naipal et al. 2014; AlHilli et al. 2016; Mukhopadhyay et al. 2010; Shah et al. 2014). PARP inhibition treatment is based on the inhibition of single strand break (SSB) repair, resulting in accumulation of SSB which cause collapse of the replication forks and formation of a DSB if encountered during replication in proliferating cells. Repair of these stalled replication fork-induced DSB specifically requires HR. As HR deficient tumor cells cannot repair this type of DSB lesion, cell death will occur (Pommier et al. 2016; Zeman & Cimprich 2014; Lim & Kaldis 2013).

A small number of studies also tested the influence of IR on RAD51 foci formation in non-tumor cells and demonstrated an impaired RAD51 foci formation in *BRCA1/BRCA2* heterozygous cell lines compared to a respective control (Vaclová et al. 2015; Warren et al. 2003; Sioftanos et al. 2010).

The aim of this study was to investigate the suitability of the RAD51 foci assay to evaluate HR capacity in MCF10A cells with reduced protein levels of BRCA1 and BRCA2, which was obtained by RNA interference. DSB were induced by irradiating the cells with a dose of 2 Gy 220 kV X-rays. To achieve a maximum number of cells in S and G2 phase of the cell cycle, the phases in which HR is active, the cells were synchronized by means of aphidicolin, a DNA polymerase inhibitor. In a part of the experiments, we added a PARP inhibitor (PARPi) (Olaparib). The addition of a PARPi in combination with IR will block the repair of radiation-induced single strand breaks. Subsequent replication fork stalling in S-phase transforms the

SSB in a DSB which is exclusively repaired by HR resulting in an extensive activation of this pathway (Urbin et al. 2012).

Materials and methods

Cell lines

MCF10A cells were cultured in monolayers using equal volumes of DMEM-glutamax and F12-glutamax (both Gibco by Life Technologies, USA), supplemented with 5% fetal calf serum (Invitrogen, Belgium), antibiotics (50 U/ml Penicillin (Invitrogen) and 50 µg/ml streptomycin (Invitrogen)) and growth factors (10 µg/ml insulin (Sigma, Belgium), 0.5 µg/ml hydrocortison (Sigma) and 20 ng/ml epidermal growth factor (Peprotech, UK)). Experiments were performed on BRCA1 and BRCA2 knockdown lines (referred to as BRCA1i and BRCA2i), together with a mock-transduced control cell line (here after referred to as control). Knockdown was achieved by stable transduction with lentiviral particles containing DNA sequences encoding short hairpin RNA specific for BRCA1 or BRCA2 RNA interference. In short, lentiviruses were constructed using pLKO.1-puro vectors. The RNA interference sequence for BRCA1 was 5'- CCCTAAGTTTCACTTCTCTAAA - 3' and 5' – TACAATGTACACATGTAA - 3' for BRCA2. For the mock-transduced cell line, an empty vector was used. Furthermore, the vector contained a resistance to puromycin. Transduction of MCF10A cells was achieved by adding 1 µg/ml DNA, TurboFect (1.5 µg/ml) and polybrene (1 µg/ml) to a 30% confluent culture. Two days after transduction, 2 µg/ml puromycin was added to the culture medium and cells were grown in puromycin supplemented medium for another 15 days to obtain stably transduced cell lines.

Sample preparation

Cells were cultured in puromycin (2 µg/ml, Sigma) supplemented medium to select for transduced cells. Cells were switched to puromycin-free culture medium for each experiment. Cells were seeded in a concentration of 200 000 cells in 2 ml culture medium in 6-well plates. Approximately 24h after cell seeding, cells were checked for subconfluency and cell cycle synchronization was initiated.

Synchronization of cell cultures

Cell synchronization was achieved by the addition of aphidicolin (1 µg/ml or 2.857 µM, Sigma) to the culture medium during 24h. Cells were subsequently washed with PBS (1.78 g Na₂HPO₄; 0.42 g KH₂PO₄ and 7.2 g NaCl (all VWR, Belgium) in 1l dH₂O) and incubated with fresh culture medium to restart synthesis.

Irradiation and PARPi treatment.

Three hours after aphidicolin removal, cells were irradiated with 2 Gy 220kV-13mA X-rays, produced by the small animal radiation research platform (SARRP) (Xstrahl, UK). Cells were subsequently incubated at 37°C for another 5 h after irradiation for optimal RAD51 foci formation. To determine this optimal time point, different time points varying between 2 and 8 h were tested (data not shown). To a part of the cultures, a PARP inhibitor (Olaparib) (5 µM, Bio-Connect, The Netherlands) was added 2 h after synchronization, hence one hour before irradiation. RAD51 foci formation was also evaluated in non-treated cell cultures and cultures exposed to PARPi alone. In total, eight repeats were performed for every condition to test for statistically significant differences.

Induction of DNA DSB by IR was verified by means of γH2AX staining according to Depuydt et al. (Depuydt et al. 2013) (supplementary data S1). The inhibition of PARP by Olaparib was confirmed by evaluation of pADPr activity after exposure to H₂O₂ or ionizing radiation in the presence or absence of Olaparib as previously described (Barazzuol et al. 2013) (supplementary data S2).

RAD51 foci assay

Prior to RAD51 foci staining, cells were harvested, cytospinned on polysine slides (VWR) and fixed in 3% paraformaldehyde for 20 min. Slides were washed twice in PBS and antigen retrieval was achieved by incubation (20 min) in a heated (95°C) citrate buffer (0,02% Citric acid (Merck, Germany) in dH₂O, pH=6). Slides were subsequently washed and incubated with a blocking serum containing 1% BSA (Roche, Switzerland); 5% normal goat serum (DAKO, Denmark) and 0,2% Tween 20 (VWR) in PBS. Slides were incubated (overnight, 4°C) with the first antibody RAD51 H-92 (1/2000) (sc-8349, Santa Cruz, USA), washed with PBS and 3% Tween 20, and incubated (30 min, room temperature) with the second antibody (1/1000)

(ThermoScientific, USA). Finally, slides were washed (PBS and 3% Tween 20) and mounted with 200 ng/ml DAPI in fluoromount (both Sigma).

Slides were scanned using the Metacyte software module on the Metafer4 scanning platform (Metasystems, Germany) using a 63X magnification. This software module enables automatic cell detection and foci counting according to set parameters resulting in an objective data acquisition. The number of RAD51 foci was automatically scored in a minimum of 500 cells for every condition per experiment and expressed as the number of RAD51 foci per cell (RAD51 foci/cell).

Cell cycle analysis

MCF10A control cells were harvested at various time points after synchronization to evaluate the percentage of cells in each phase of the cell cycle. Cell permeabilization was achieved by ethanol (95%, -20°C) fixation and DNA was subsequently stained with Propidium Iodide (PI) in a hypotonic staining buffer containing 0.1% Sodium citrate (Merck); 0.3% Triton-X 100 (Sigma); 0.01% PI (Sigma) and Ribonuclease A (0.002%) in dH₂O. Cells and PI content was analyzed on a BD FACSCanto™ (BD Biosciences, USA). Cells of interest were selected based on forward and side scatter area patterns. A non-synchronized sample was used as control.

Western blot analysis

BRCA1 and BRCA2 protein knockdown was evaluated by western blot analysis. Protein extraction was performed in subconfluent cultures of control, BRCA1i and BRCA2i cells using a TE lysis buffer containing 0.1M Tris, 50mM EDTA, 1% NP-40 and 1% protease inhibitor (sigma P8340). Protein concentration was determined by means of the Pierce™ Coomassie protein assay kit (ThermoScientific, USA). For every sample, 50 µg of protein was loaded together with LDS sample buffer (ThermoScientific NP0008; 25%) and dithiothreitol (DDT; Sigma; 43816, 10%) on a 3-8% Tris-Acetate gel (Novac). The gel was run in a Tris-Acetate running buffer supplemented with 2.5% antioxidant during 5 h at 25mA. Proteins were transferred to a methanol pretreated PVDF membrane in a Tris (25mM, Sigma) & glycine (0.2M, VWR) dH₂O blotting buffer enriched with 10% methanol during 16 hour at 30V. Subsequently, the membrane was blocked 1 hour in a tris buffered saline (TBS buffer) with 3% BSA; 5% milk powder and 0.1% Tween 20. After blocking, the membrane was incubated overnight with the primary antibody (rabbit pAb α-BRCA1 (sc-642, diluted 1/1000) or mAb

antibody α -BRCA2 (Millipore OP-95, diluted 1/500), and mouse mAb α -actinin (sc-17829, diluted 1/30 000) as loading control. This incubation was followed by washing and incubation with secondary antibodies, conjugated with hrp (GAR-hrp (Perbio 34160, diluted 1/1000) or GAM-hrp (ThermoScientific 31450, diluted 1/1000)). Visualization was achieved via chemoluminescence kit (ThermoScientific) and images were obtained by the Chemidoc-it imaging system (UVP, Canada) and Vision Works LS software (UVP).

Statistical analysis of the data

The mean number of RAD51 foci/cell, standard deviation (SD) and standard error on the mean (SEM) were determined for the four different conditions (non-treated, PARPi, IR and PARPi + IR) in the three cell lines (control, BRCA1i and BRCA2i). Furthermore, a fold change was calculated to quantify the change of RAD51 foci in comparison to the control cell line. A fold change < 1 indicates a reduction of RAD51 foci induction in the cell line for a certain condition. To evaluate changes in RAD51 foci formation, statistical analysis was performed using the Mann-Whitney test for unpaired analysis of non-parametric data. A 5% alpha error as boundary ($p\text{-value} \leq 0.05$) was applied and calculations were performed using SPSS software (IBM, version 24).

Results

Western blot analysis

Western blotting revealed a BRCA1 knockdown in BRCA1i cells and a BRCA2 knockdown in BRCA2i cells compared to the control cell line (Figure 1). Quantification of the knockdown via ImageJ revealed an estimated BRCA1 protein reduction of 70% in the BRCA1i cells and an estimated 51% reduction of BRCA2 protein in the BRCA2i cells.

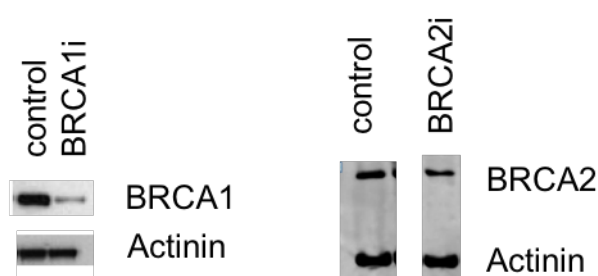


Figure 1. Western Blot analysis

Western blot analysis of BRCA1 and BRCA2 protein levels in the control, BRCA1i and BRCA2i cell lines. Actinin was used as a protein loading control.

Cell cycle analysis

Figure 1a represents the mean percentage of cells in every phase of the cell cycle in a non-synchronized sample and at various time points after aphidicolin removal based on four repeats. As an example, the histogram charts of every time point for one repeat are shown in Figure 2b-f. Synchronization with aphidicolin clearly resulted in an increased number of cells in S phase of the cell cycle. Immediately after aphidicolin synchronization (Figure 2b), about 70% of the cells were at the beginning of S phase. Two (Figure 2c) and three h (Figure 2d) after aphidicolin removal the lowest number of cells in G1 phase of the cell cycle was achieved whilst the number of S phase cells had doubled compared to non-synchronized cultures. Eight h after aphidicolin synchronization, the cells shift towards G2 and M phase of the cell cycle (Figure 2e). As the number of cells in late S phase is at its maximum two and three h after synchronization, these time points were selected for addition of PARPi (2h) and irradiation (3h) to maximize the effect of these agents on RAD51 foci formation.

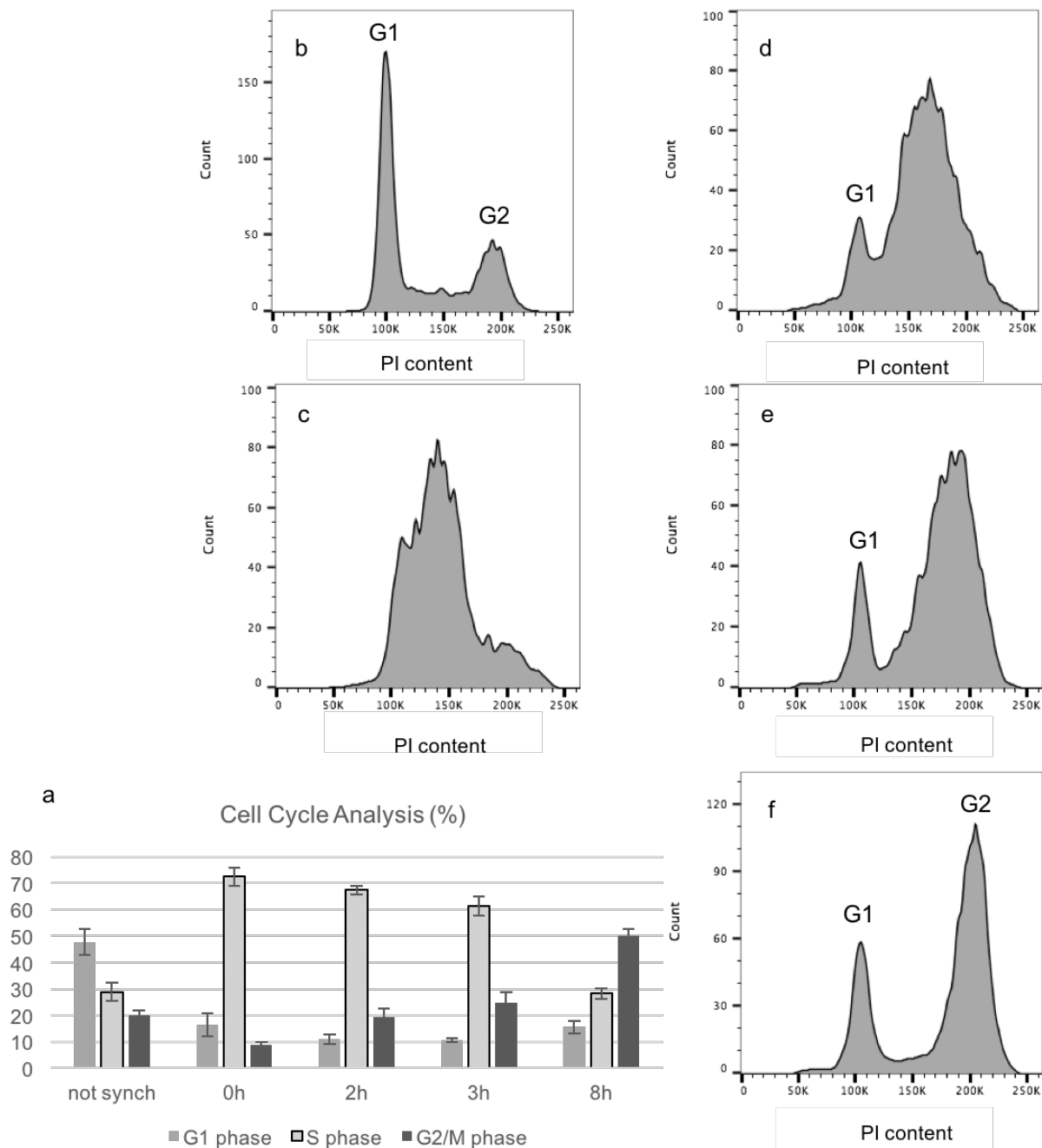


Figure 2. Results of cell cycle analysis

(a) Mean percentage of cells in every phase of the cell cycle before synchronization and at various h after aphidicolin removal. Results are expressed in % and error bars are SEM based on four repeats. (b-f) Histogram tables showing the number of cells in function of the PI content, an indication for DNA content (created with FlowJo™), (b) of a non-synchronized cell culture as control, (c) immediately (0h) after synchronization, (d) 2h after synchronization, (e) 3h after synchronization and (f) 8h after synchronization. PI Propidium Iodide

RAD51 foci formation

Figure 3 shows RAD51 foci in the nuclei of MCF10a control cells. Figure 4 shows the mean number of RAD51 foci in synchronized cell cultures for every cell line for the four tested

conditions. Fold changes are presented in Table 1. We observed a significant lower number of RAD51 foci in both BRCA1i and BRCA2i cells compared to the control cells after exposure to both IR alone and IR with PARPi. Fold changes vary between 0.51 and 0.36. Furthermore, no formation of radiation-induced RAD51 foci could be detected in the knockdown cell lines. The differences in RAD51 foci levels observed when comparing the knockdown and control cell lines in non-treated cell cultures or cell cultures solely exposed to PARPi were not statistically different (Figure 4 and Table 1).

When comparing the different conditions per cell line, only a significant increase in RAD51 foci levels was observed in the control cell line after exposure to IR and combined exposure to IR and PARPi compared to non-treated cells (Figure 4).

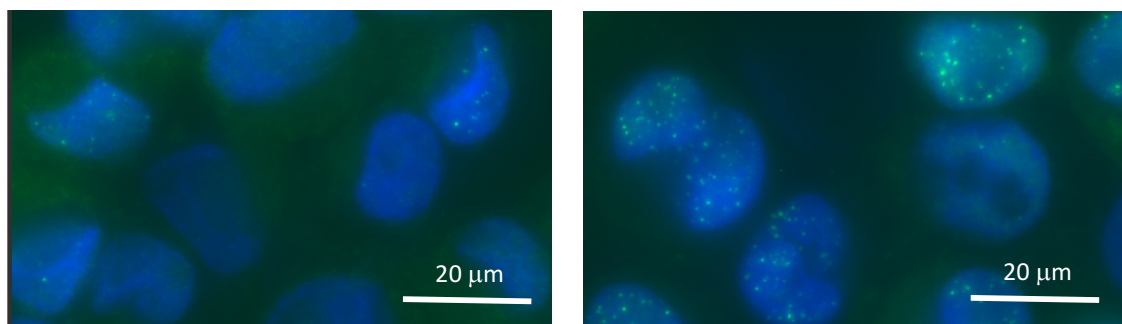


Figure 3. RAD51 foci (green) in control MCF10A DAPI-stained nuclei (blue)

Left panel: synchronized control cells, non-irradiated. Right panel: synchronized control cells, irradiated (2 Gy).

Table 1. Fold changes

	no IR	no IR	IR	IR
	no PARPi	with PARPi	no PARPi	with PARPi
Control	1	1	1	1
BRCA1i	0.91	0.81	0.42 (*)	0,51 (*)
BRCA2i	0.71	0.93	0.36 (*)	0,40 (*)

* indicate significant reductions in RAD51 foci levels compared to the control cell line (p-values<0.05) IR Ionizing radiation, PARPi PARP inhibition

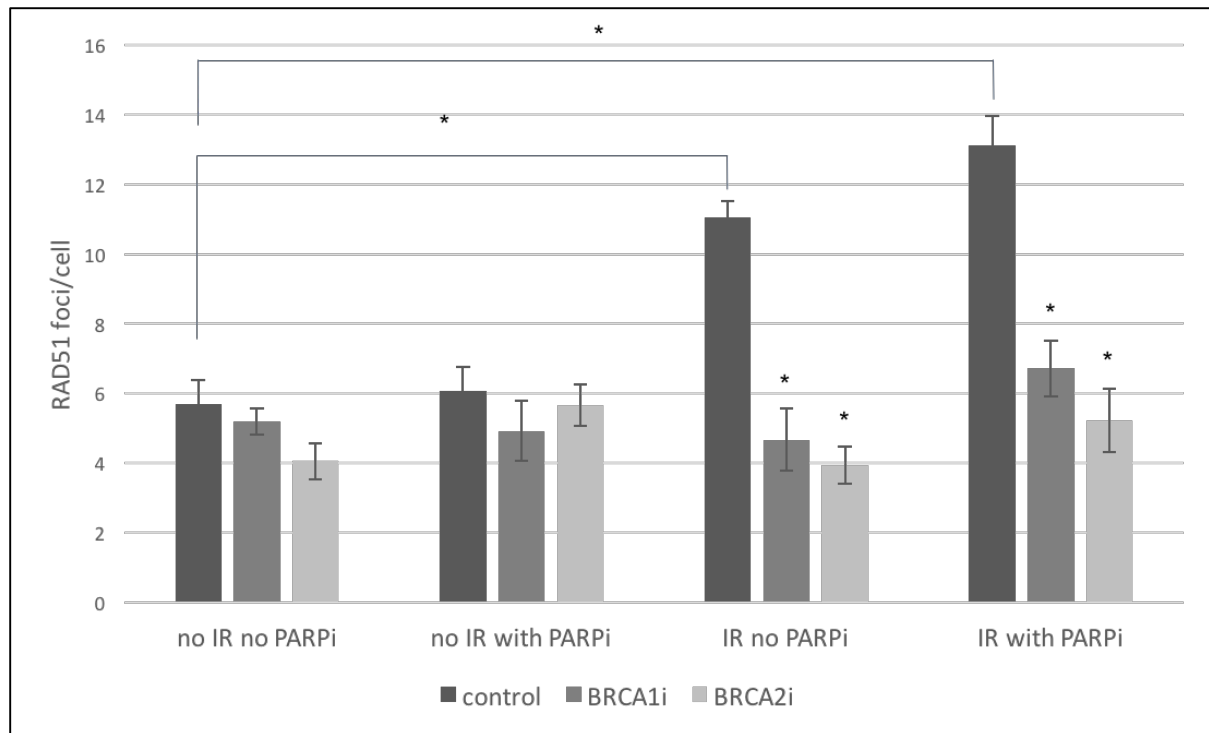


Figure 4. Mean number of RAD51 foci per cell (RAD51 foci/cell) in aphidicolin-synchronized cell cultures for every condition.

Cells were either not treated, exposed to a PARPi, 2 Gy IR or a combination of both. Error bars are SEM based on eight repeats. * indicates significant differences (p -value <0.05) compared to the control cell line within one condition, unless indicated otherwise.

IR Ionizing radiation, PARPi PARP inhibition

Discussion

The aim of this study was to investigate the suitability of the RAD51 foci assay to evaluate HR capacity in MCF10A cells with reduced protein levels of BRCA1 and BRCA2, which was obtained by RNA interference. Cells were synchronized in S and G2 phase for an optimal evaluation of HR capacity. DSB were induced by exposure to IR. To increase the number of DSB, we also used PARPi that transform radiation-induced SSB in DSB during S phase.

We confirmed that HR is involved in repair of radiation-induced DSB in synchronized MCF10A cells. We demonstrated a significant lower number of RAD51 foci in BRCA1i and BRCA2i cell lines compared to the control cell line after exposure to IR alone or a combination of IR and PARPi (Figure 4). Moreover, for BRCA1i and BRCA2i no formation of radiation-induced RAD51 foci was observed. The discrepancy between knockdown and control cells can be explained by the involvement of both proteins in RAD51 microfilament formation and HR initiation for repair of IR-induced DSB. Although direct comparison between the results obtained in the

BRCA1i and BRCA2i cell line is difficult as the remaining protein level for BRCA2 is higher than for BRCA1 (Figure 1), we observed a lower RAD51 foci yield for BRCA2i cells in three of the four tested conditions compared to BRCA1i cells. This lower RAD51 foci yield despite higher protein levels could be attributed to the more specific role that BRCA2 has in RAD51 recruitment and HR, whereas BRCA1 exerts a more pleiotropic role in the DNA damage response (for a review: (Roy et al. 2012)). Further research to evaluate this trend would be necessary.

A number of studies, investigating the influence of BRCA2 on RAD51 foci formation and HR functionality, have been performed using human cell lines, CHO cells, DT40 cells and mice embryonic stem cells. All studies confirmed impaired functionality of HR resulting in a reduction in RAD51 foci formation in heterozygous cells (Kraakman-Van der Zwet et al. 2002; Yuan et al. 1999; Sioftanos et al. 2010; Keimling et al. 2011; Warren et al. 2003).

Conversely, the results of studies focusing on the effect of BRCA1 on RAD51 formation and HR were less univocal. Sioftanos et al. detected a reduction in RAD51 foci formation in *BRCA1* heterozygous mice embryonic stem cells, though less distinct than in *BRCA2* heterozygous cells (Sioftanos et al. 2010). Yuan et al. and Keimling et al., on the other hand, could not demonstrate an effect of *BRCA1* heterozygosity on RAD51 formation or HR capacity (Yuan et al. 1999; Keimling et al. 2011). In a study using lymphoblastoid cell lines of heterozygous *BRCA1* mutation carriers, Vaclova et al. could not directly demonstrate a decrease in RAD51 foci formation compared to a control cell line 4 h after exposure to 10 Gy. However, they did observe a significant increase in γ H2AX intensity in these heterozygous *BRCA1* cells compared to control cells 4 h after irradiation, implicating an increase in number of DSB and argue that this implies a decreased HR activation in mutation carriers (Vaclová et al. 2015). Pathania et al. did not detect a reduction in radiation-induced RAD51 foci in human mammary epithelial cells containing a *BRCA1* mutation exposed to 10 Gy compared to control cells. However, the combined exposure to UV and IR did yield a significant reduction in RAD51 foci (Pathania et al. 2014).

None of these studies took the variation of HR-based DSB repair throughout the different cell cycle phases into account. We demonstrated that 48% of non-synchronized cycling MCF10A cells were in G1 phase of the cell cycle, the cell cycle phase during which HR cannot be

activated due to the absence of the homologous sister chromatid. In our synchronized cell cultures, approximately 90% of the cells were in S or G2 phase of the cell cycle, at time of irradiation. Moreover, more than 60% of cells were in S phase at time of irradiation, the cell cycle phase during which HR activation is maximal for repair of DSB (Mao et al. 2008; Karanam et al. 2012). As aphidicolin induces DNA damage by DNA polymerase inhibition (Kurose et al. 2006; Hanada et al. 2007), caution is needed when analyzing results of aphidicolin synchronized cell cultures. Also other methods for cell cycle synchronization, such as thymidine block or hydroxyurea, induce DNA damage, amongst which DSB (Kurose et al. 2006; Hanada et al. 2007; Saintigny et al. 2001). In our studies, aphidicolin synchronization resulted in the formation of RAD51 foci in non-treated cells, but no significant difference was observed between the control and knockdown cell lines (Figure 4, no IR no PARPi). In non-synchronized cell lines, much lower baseline RAD51 foci (means values ≤ 1) were obtained (data not shown).

In an attempt to activate the HR pathway more extensively, we added PARPi to the cultures prior to irradiation. However, we did not observe a significant increase in the number of RAD51 foci effect compared to IR alone. As a consequence, the combined treatment did not result in a better discrimination between the knockdown cell lines and the control cell line. This might be due to an exhaustion of HR capacity by aphidicolin synchronization and exposure to IR. Furthermore, we should consider the many different functions PARP fulfills in the DNA damage response, including detection and signaling of DSB and stabilization of stalled replication forks (Pommier et al. 2016; Khodyreva & Lavrik 2016). The complex PARP network is not fully understood and inhibition might impair additional HR activation and RAD51 foci formation in our assay. We hypothesize that PARP trapping, initiated by Olaparib at the SSB site (Murai et al. 2012; Pommier et al. 2016), might impair HR activation once the SSB is transformed in a DSB due to replication fork collapse. This would also explain why no increased RAD51 formation is observed in synchronized cells after PARPi treatment alone compared to non-treated cells.

In conclusion, we demonstrated that in cells containing a knockdown for either BRCA1 or BRCA2, the HR pathway is impaired, which results in the absence of radiation-induced formation of RAD51 foci in synchronized cells. As in both cell lines $\leq 50\%$ of the wild type activity is retained after lentiviral knockdown, the results obtained in the MCF10A cell line

may mimic the situation in healthy carriers of a germline *BRCA1/2* mutation. Therefore, applying this assay on synchronized fibroblasts/breast epithelial cells/lymphocytes of heterozygous *BRCA1* and *BRCA2* mutation carriers might be a useful strategy to assess radiosensitivity and HR capacity for these patients. This should be thoroughly evaluated in a large cohort of patients with known deleterious mutations located in different functional domains of both genes. In case heterozygous mutation carriers can be clearly distinguished from controls, such an assay can be very valuable to determine the functional effect of variants of unknown clinical significance in either gene, which aids adequate genetic counseling of carriers of such variants.

Competing interests

The authors have no competing interest to declare.

Acknowledgement

This research was funded by the Belgian Foundation against Cancer (project 2012-216).

References

- AlHilli, M.M. et al., 2016. In vivo anti-tumor activity of the PARP inhibitor niraparib in homologous recombination deficient and proficient ovarian carcinoma. *Gynecologic Oncology*, pp.1–10.
- Andrieu, N. et al., 2006. Effect of Chest X-Rays on the Risk of Breast Cancer Among BRCA1 / 2 Mutation Carriers in the International BRCA1 / 2 Carrier Cohort Study : A Report from the EMBRACE , GENEPSO , GEO-HEBON , and IBCCS Collaborators ' Group. *Journal of Clinical Oncology*, 24(21), pp.3361–3366.
- Baert, A. et al., 2017. Analysis of chromosomal radiosensitivity of healthy BRCA2 mutation carriers and non-carriers in BRCA families with the G2 micronucleus assay. *Oncology reports*, p.In press.
- Baert, A. et al., 2016. Increased chromosomal radiosensitivity in asymptomatic carriers of a heterozygous BRCA1 mutation. *Breast Cancer Research*, 18(1), p.52.
- Baeyens, A. et al., 2004. Chromosomal radiosensitivity in BRCA1 and BRCA2 mutation carriers. *International journal of radiation biology*, 80(10), pp.745–756.
- Barazzuol, L. et al., 2013. Evaluation of poly (ADP-ribose) polymerase inhibitor ABT-888 combined with radiotherapy and temozolomide in glioblastoma. *Radiation Oncology*, 8(1), p.65.
- Barwell, J. et al., 2007. Lymphocyte radiosensitivity in BRCA1 and BRCA2 mutation carriers and implications for breast cancer susceptibility. *International journal of cancer. Journal international du cancer*, 121(7), pp.1631–6.
- Becker, A.A. et al., 2012. A 24-color metaphase-based radiation assay discriminates heterozygous BRCA2 mutation carriers from controls by chromosomal radiosensitivity. *Breast Cancer Research and Treatment*, 135(1), pp.167–175.
- Bernstein, J.L. et al., 2013. Contralateral breast cancer after radiotherapy among BRCA1 and BRCA2 mutation carriers: a WECARE study report. *European journal of cancer (Oxford, England : 1990)*, 49(14), pp.2979–85.
- Bolognesi, C. et al., 2014. Clinical application of micronucleus test: A case-control study on the prediction of breast cancer risk/susceptibility. *PLoS ONE*, 9(11), pp.1–18.
- Broeks, A. et al., 2007. Identification of women with an increased risk of developing radiation-induced breast cancer: a case only study. *Breast cancer research : BCR*, 9(2), p.R26.
- Cardinale, F., Bruzzi, P. & Bolognesi, C., 2012. Role of micronucleus test in predicting breast cancer susceptibility: a systematic review and meta-analysis. *British journal of cancer*, 106(4), pp.780–90.
- Ceccaldi, R., Rondinelli, B. & D'Andrea, A.D., 2016. Repair Pathway Choices and Consequences at the Double-Strand Break. *Trends in Cell Biology*, 26(1), pp.52–64.
- Depuydt, J. et al., 2013. Relative biological effectiveness of mammography X-rays at the level of DNA and chromosomes in lymphocytes. *International journal of radiation biology*, 89(7), pp.532–8.
- Ernestos, B. et al., 2010. Increased chromosomal radiosensitivity in women carrying BRCA1/BRCA2 mutations assessed with the G2 assay. *International journal of radiation oncology, biology, physics*, 76(4), pp.1199–205.
- Frankenberg-Schwager, M. & Gregus, A., 2012. Chromosomal instability induced by mammography X-rays in primary human fibroblasts from BRCA1 and BRCA2 mutation carriers. *International Journal of Radiation Biology*, 88(11), pp.846–857.
- Giannakeas, V. et al., 2014. Mammography screening and the risk of breast cancer in BRCA1

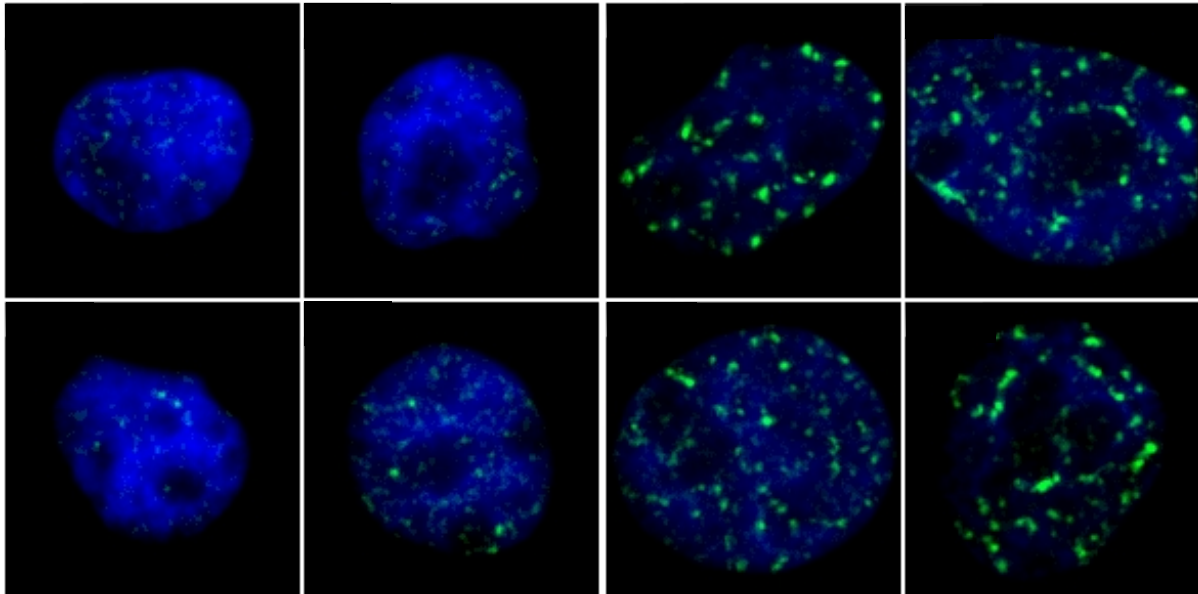
- and BRCA2 mutation carriers: a prospective study. *Breast cancer research and treatment*, 147(1), pp.113–8.
- Goldfrank, D. et al., 2006. Effect of mammography on breast cancer risk in women with mutations in BRCA1 or BRCA2. *Cancer epidemiology, biomarkers & prevention : a publication of the American Association for Cancer Research, cosponsored by the American Society of Preventive Oncology*, 15(11), pp.2311–2313.
- Gronwald, J. et al., 2008. Early radiation exposures and BRCA1-associated breast cancer in young women from Poland. *Breast cancer research and treatment*, 112(3), pp.581–4.
- Gutiérrez-Enríquez, S. et al., 2011. Ionizing radiation or mitomycin-induced micronuclei in lymphocytes of BRCA1 or BRCA2 mutation carriers. *Breast cancer research and treatment*, 127(3), pp.611–22.
- Hanada, K. et al., 2007. The structure-specific endonuclease Mus81 contributes to replication restart by generating double-strand DNA breaks. *Nature structural & molecular biology*, 14(11), pp.1096–104.
- John, E.M. et al., 2013. Diagnostic chest X-rays and breast cancer risk before age 50 years for BRCA1 and BRCA2 mutation carriers. *Cancer epidemiology, biomarkers & prevention : a publication of the American Association for Cancer Research, cosponsored by the American Society of Preventive Oncology*, 22(9), pp.1547–56.
- Karanam, K. et al., 2012. Quantitative Live Cell Imaging Reveals a Gradual Shift between DNA Repair Mechanisms and a Maximal Use of HR in Mid S Phase. *Molecular Cell*, 47(2), pp.320–329.
- Keimling, M. et al., 2011. Functional characterization connects individual patient mutations in ataxia telangiectasia mutated (ATM) with dysfunction of specific DNA double-strand break-repair signaling pathways. *The FASEB Journal*, 25(11), pp.3849–3860.
- Khodyreva, S.N. & Lavrik, O.I., 2016. Poly(ADP-Ribose) polymerase 1 as a key regulator of DNA repair. *Molecular Biology*, 50(4), pp.580–595.
- Kote-Jarai, Z. et al., 2006. Increased level of chromosomal damage after irradiation of lymphocytes from BRCA1 mutation carriers. *British journal of cancer*, 94(2), pp.308–310.
- Kraakman-Van der Zwet, M. et al., 2002. Brca2 (XRCC11) Deficiency Results in Radioresistant DNA Synthesis and a Higher Frequency of Spontaneous Deletions Brca2 (XRCC11) Deficiency Results in Radioresistant DNA Synthesis and a Higher Frequency of Spontaneous Deletions. , 2(2), pp.669–679.
- Kurose, A. et al., 2006. Effects of Hydroxyurea and Aphidicolin on Phosphorylation of Ataxia Telangiectasia Mutated on Ser 1981 and Histone H2AX on Ser 139 in Relation to Cell Cycle Phase and Induction of Apoptosis. , 221(March), pp.212–221.
- Lecarpentier, J. et al., 2011. Variation in breast cancer risk with mutation position , smoking , alcohol , and chest X-ray history , in the French National BRCA1 / 2 carrier cohort (GENEPSO). *Breast cancer research and treatment*, 130(3), pp.927–938.
- Li, J. & Xu, X., 2016. DNA double-strand break repair: a tale of pathway choices. *Acta Biochim Biophys Sin*, 48(7), pp.641–646.
- Lim, S. & Kaldis, P., 2013. Cdks, cyclins and CKIs: roles beyond cell cycle regulation. *Development*, 140(15), pp.3079–93.
- Mao, Z. et al., 2008. DNA repair by nonhomologous end joining and homologous recombination during cell cycle in human cells. *Cell Cycle*, 7(18), pp.2902–2906.
- Mladenov, E. et al., 2016. DNA double-strand-break repair in higher eukaryotes and its role in genomic instability and cancer: Cell cycle and proliferation-dependent regulation.

- Seminars in Cancer Biology*, 37–38(2016), pp.51–64.
- Mukhopadhyay, A. et al., 2010. Development of a functional assay for homologous recombination status in primary cultures of epithelial ovarian tumor and correlation with sensitivity to poly(ADP-ribose) polymerase inhibitors. *Clinical Cancer Research*, 16(8), pp.2344–2351.
- Murai, J. et al., 2012. Trapping of PARP1 and PARP2 by clinical PARP inhibitors. *Cancer Research*, 72(21), pp.5588–5599.
- Naipal, K. a. T. et al., 2014. Functional ex vivo assay to select Homologous Recombination deficient breast tumors for PARP inhibitor treatment. *Clinical cancer research : an official journal of the American Association for Cancer Research*, 20(18), pp.4816–4826.
- Narod, S.A. et al., 2006. Screening mammography and risk of breast cancer in BRCA1 and BRCA2 mutation carriers: a case-control study. *The Lancet. Oncology*, 7(5), pp.402–6.
- Pathania, S. et al., 2014. BRCA1 haploinsufficiency for replication stress suppression in primary cells. *Nature communications*, 5, p.5496.
- Pijpe, A. et al., 2012. Exposure to diagnostic radiation and risk of breast cancer among carriers of BRCA1/2 mutations: retrospective cohort study (GENE-RAD-RISK). *BMJ*, 345, p.e5660.
- Pommier, Y., O'Connor, M.J. & de Bono, J., 2016. Laying a trap to kill cancer cells: PARP inhibitors and their mechanisms of action. *Science Translational Medicine*, 8(362), pp.1–8.
- Rothkamm, K. et al., 2015. DNA Damga Foci: Meaning and Significance. *Environmental and molecular mutagenesis*, 56, pp.491–504.
- Roy, R., Chun, J. & Powell, S.N., 2012. BRCA1 and BRCA2: different roles in a common pathway of genome protection. *Nature reviews. Cancer*, 12(1), pp.68–78.
- Saintigny, Y. et al., 2001. Characterization of homologous recombination induced by replication inhibition in mammalian cells. *EMBO Journal*, 20(14), pp.3861–3870.
- Shah, M.M. et al., 2014. An ex vivo assay of XRT-induced Rad51 foci formation predicts response to PARP-inhibition in ovarian cancer. *Gynecologic Oncology*, 134(2), pp.331-7.
- Sioftanos, G. et al., 2010. BRCA1 and BRCA2 heterozygosity in embryonic stem cells reduces radiation-induced Rad51 focus formation but is not associated with radiosensitivity. *International journal of radiation biology*, 86(12), pp.1095–105.
- Trenz, K. et al., 2002. Mutagen sensitivity of peripheral blood from women carrying a BRCA1 or BRCA2 mutation. *Mutation research*, 500(1–2), pp.89–96.
- Urbini, S.S. et al., 2012. Uncoupling of RAD51Focus Formation and Cell SurvivalAfter Replication Fork Stalling in RAD51D Null CHOCells Salustra. *Environmental and molecular mutagenesis*, 53, pp.114–124.
- Vaclová, T. et al., 2015. DNA repair capacity is impaired in healthy BRCA1 heterozygous mutation carriers. *Breast Cancer Research and Treatment*.
- Warren, M. et al., 2003. Phenotypic effects of heterozygosity for a BRCA2 mutation. *Human Molecular Genetics*, 12(20), pp.2645–2656.
- Willers, H. et al., 2009. Utility of DNA repair protein foci for the detection of putative BRCA1 pathway defects in breast cancer biopsies. *Molecular cancer research : MCR*, 7(8), pp.1304–9.
- Yuan, S.S.F. et al., 1999. BRCA2 is required for ionizing radiation-induced assembly of Rad51 complex in vivo. *Cancer Research*, 59(15), pp.3547–3551.
- Zeman, M.K. & Cimprich, K.A., 2014. Causes and consequences of replication stress. *Nature cell biology*, 16(1), pp.2–9.

Supplementary data

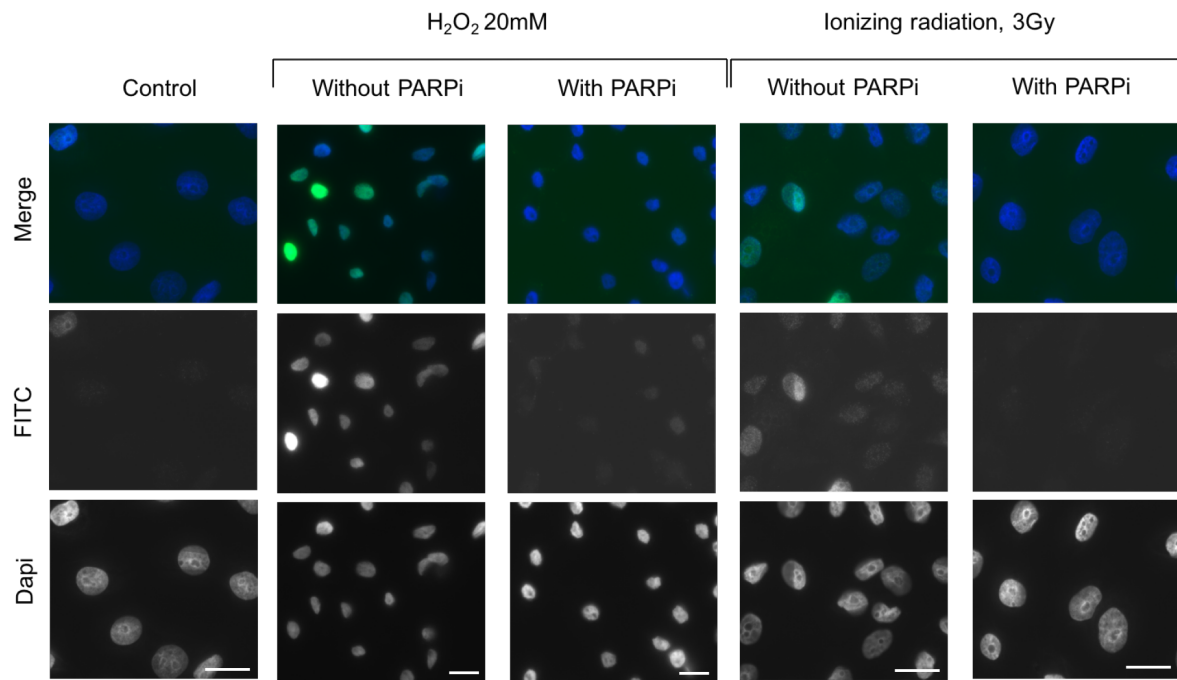
non-irradiated (0 Gy)

irradiated (2 Gy)



S1: γH2AX foci staining after exposure of control MCF10A cells to ionizing radiation.

Induction of γH2AX foci was assessed 30 min after exposure to ionizing radiation (2 Gy) or mock irradiation (0 Gy). Immunostaining was performed by means of a monoclonal anti-γH2AX antibody (biolegend cat 613402) (Depuydt et al. 2013). Image gallery showing four cells for each condition taken with Metafer 4 (Metasystems).



S2: Evaluation of PARP inhibition by Olaparib.

Immunodetection for poly (ADP-ribose) activity was performed according to Barazzuol et al. (Barazzuol et al. 2013) in synchronized control MCF10A cells. PARP activation was induced by H₂O₂ treatment (20mM, 10 min) or exposure to ionizing radiation (3 Gy) and visualized by anti-pADPr immunostaining with FITC signal (green). Addition of Olaparib (PARPi) (5 μ M) 1 hour before H₂O₂ treatment or exposure to ionizing radiation, resulted in an absence of PARP activity. MCF10A nuclei were counterstained with DAPI (blue). Images taken with Metafer 4 (Metasystems). Scale bar indicates 20 μ m.

Paper V: Thorough *in silico* and *in vitro* cDNA analysis of 21 putative *BRCA1/2* splice variants and identification of activated cryptic splice donor sites in exon 11 of *BRCA2*

Annelot Baert (1,2), Eva Machackova (3), Ilse Coene (2), Carol Cremin (4), Kristin Turner (4), Cheryl Portigal-Todd (4), Marie Jill Asrat (4), Jennifer Nuk (4), Allison Mindlin (4), Young Sean (5), Andree MacMillan (6), Tom Van Maerken (2), Martin Trbusek (7), Wendy C McKinnon (8), Marie E Wood (8), William D Foulkes (9), Marta Santamariña (10), Miguel de la Hoya (11), Lenka Foretova (3), Bruce Poppe (2), Toon Rosseel (2), Kim De Leeneer (2), Anne Vral (1), Ana Vega (10), Kathleen BM Claes (2)

1 Department of Basic Medical Sciences, Ghent University, Ghent, Belgium

2 Center for Medical Genetics, Ghent University Hospital, Ghent, Belgium

3 Department of Cancer Epidemiology and Genetics, Masaryk Memorial Cancer Institute, Brno, Czech Republic

4 Hereditary Cancer Program, BC Cancer Agency, Vancouver, British Columbia, Canada.

5 Cancer Genetics Laboratory, BC Cancer Agency, Vancouver, British Columbia, Canada.

6 Provincial Medical Genetics Program, Eastern Health, St. John's, NL, Canada

7 Department of Internal Medicine - Hematology and Oncology, University Hospital Brno, Brno, Czech Republic

8 Familial Cancer Program, University of Vermont Medical Center, Burlington, VT, Canada

9 Department of Medicine, Division of Medical Genetics, Faculty of Medicine, McGill University, Montreal, Quebec, Canada

10 Fundación Pública Galega de Medicina Xenómica-SERGAS, Grupo de Medicina Xenómica, CIBERER, IDIS, Santiago de Compostela, Spain.

11 Molecular Oncology Laboratory, Hospital Clínico San Carlos, Madrid, Spain

In preparation for submission to Human Mutation

Abstract

For 21 putative *BRCA1/2* splice site variants the concordance between mRNA analysis and predictions by *in silico* programs was evaluated. Aberrant splicing was confirmed for 12 alterations. *In silico* prediction tools were helpful to determine for which variants cDNA analysis is warranted, however, predictions for variants in the Cartegni consensus region but outside the canonical sites, were less reliable. Learning algorithms like Adaboost and Random Forest outperformed the classical tools. Further validations are warranted prior to implement these novel tools in clinical settings.

Additionally, we report here for the first time activated cryptic donor sites in the large exon 11 of *BRCA2* by evaluating the effect at the cDNA level of a novel tandem duplication (5' breakpoint in intron 4; 3' breakpoint in exon 11) and of a variant disrupting the splice donor site of exon 11 (c.6841+1G>C). Additional sites were predicted, but not activated. These sites warrant further research to increase our knowledge on *cis* and *trans* acting factors involved in the conservation of correct transcription of this large exon. This may contribute to adequate design of ASOs (antisense oligonucleotides), an emerging therapy to render cancer cells sensitive to PARP inhibitor and platinum therapies.

Introduction

The risk of breast and ovarian cancer increases drastically in individuals carrying a germline *BRCA1* or *BRCA2* mutation. Heterozygous pathogenic mutations are associated with a lifetime risk of 50-80% for breast cancer and 30-50% for ovarian cancer (Roy et al. 2012). However, due to an evolution in sequencing technologies, the number of individuals undergoing screening drastically increased and this led to a significant rise in the number of variants of unknown clinical significance (VUS). The detection of a VUS is a challenge for health care providers as the impact on the risk for breast or ovarian cancer risk is unclear (Goldgar et al. 2004). For missense variants, a number of functional tests have been proposed (e.g. (Millot et al. 2012; Hendriks et al. 2014), but the implementation on a large scale in a clinical diagnostic setting is not feasible. In contrast, mRNA analyses to investigate intronic and exonic variants that might impair proper RNA splicing, are more widely used. The effect of putative splice site variants can be evaluated *in silico* as a wide variety of tools have been developed (Jian et al. 2014b). Indeed, pre-mRNA splicing is highly regulated and variants in the highly conserved dinucleotides at the splice site donor/acceptor sites at the intron boundaries, in the conserved adjacent sequences or variants in the branchpoints and exonic splicing enhancers (ESE) might lead to aberrant splicing (Strachan & Read 2010; Houdayer et al. 2012; Spurdle et al. 2008). Several guidelines have been formulated to assist the decision-making process (Caminsky et al. 2014; Tang et al. 2016; Houdayer et al. 2008). Accurate prediction by these tools is dependent on the ability to detect the wild type (WT) splice site or define regions such as the branchpoints or ESE. Furthermore, it depends on the degree of conservation of the region in which the variant is situated (Caminsky et al. 2014). *In silico* prediction tools such as MaxEntScan (MES) (Yeo & Burge 2004), Alternative Splice Site Predictor (ASSP) (Wang & Marín 2006) and human splicing finder (HSF) (Desmet et al. 2009) have previously been extensively validated for the prediction of aberrant splicing (Caminsky et al. 2014; Tang et al. 2016; Houdayer et al. 2008). The major problem that prohibits the use of these tools in diagnostic labs is the difficulty in interpreting the output (Jian et al. 2014b). One reason for this difficulty is that there is no unified standard to measure how splicing signals change when one allele is substituted by another because most tools only output prediction scores for potential splice sites given an input DNA sequence. Due to complex dependencies existing among the bases around splice sites, all of the abovementioned programs show some limitations and none of these was shown to perfectly predict the impact

on pre-mRNA splicing. Learning algorithms such as AdaBoost (Pashaei et al. 2016) and Random Forest (Meher et al. 2016) are now emerging and need to be validated for the use in research and clinical practice.

Furthermore, for the evaluation of the effect of exonic variants on splicing, ESE-specific *in silico* prediction tools such as ESEfinder (Cartegni et al. 2003), RESCUE-ESE (Fairbrother et al. 2002) and the quantitative evaluation of hexamers as exonic splicing elements (Ke et al. 2011) can be applied.

In this study we evaluated the concordance between the “classic prediction tools” and more recently developed algorithms (AdaBoost and Random Forest) for 21 BRCA1/2 variants. Especially for variants outside the canonical splice sites (+/-1, +/-2), currently frequently applied prediction tools are less adequate (Spurdle et al. 2008). We compared the *in silico* output with data of *in vitro* RNA splicing assays.

We tested the effect of 21 variants of unknown clinical significance in *BRCA1* (n=11) and *BRCA2* (n=10) on mRNA splicing in short term cultured peripheral blood lymphocytes. We investigated the concordance between mRNA analysis outcome and *in silico* predictions for all variants.

In addition we evaluated the effect at the cDNA level of a novel large tandem duplication spanning exons 5 to a large part of exon 11 in *BRCA2*. We found that besides a skip of the exon, two cryptic splice sites were activated within exon 11. We confirmed that these were also activated in a patient with an interrupted donor site due to a G>C substitution at position +1 of intron 11.

Materials and Methods

Variant selection

We selected 21 DNA alterations in *BRCA1* (n=11) and *BRCA2* (n=10) to test for aberrant splicing (Table 1). These include besides intronic variants, also missense and silent variants - both within and outside the Cartegni consensus region. In addition, we investigated the effect of a large duplication in *BRCA2* at the cDNA level. Online repositories such as ClinVar (Landrum et al. 2015) LOVD (<http://databases.lovd.nl/shared/variants/BRCA1/unique> and <http://databases.lovd.nl/shared/variants/BRCA2>) and the literature were checked for available information of these variants. Some variants have entries in the ClinVar or LOVD databases, but no assays to elucidate splicing effects were previously reported and their pathogenicity remained unclear.

In silico prediction

Five prediction tools integrated in Alamut® Visual 2.8.1 (Interactive Biosoftware, France), were used to assess the impact of the variants on splice sites *in silico*. These programs are also freely available online: MaxEntScan (MES) (http://genes.mit.edu/burgelab/maxent/Xmaxentscan_scoreseq.html) (Yeo & Burge 2004); Human Splicing Finder (HSF) (Desmet et al. 2009) and Splice Site Finder (SSF) (Shapiro & Scnaphthy 1987), both accessible on the HSF website (<http://www.umd.be/HSF3/>); Splice Site Prediction by Neural Network (NNSplice) (http://www.fruitfly.org/seq_tools/splice.html) (Reese et al. 1994) and GeneSplicer (Pertea et al. 2001) (http://www.cbcb.umd.edu/software/GeneSplicer/gene_spl.shtml).

Previous evaluation of these *in silico* tools resulted in a cut-off value of 5% for SSF and NNSplice (Houdayer et al. 2012; Tang et al. 2016). The cut-off for MES varies between 10% (Tang et al. 2016) and 15% (Houdayer et al. 2012; Jian et al. 2014a) depending on the study. The cut-off for HSF was set at 2% (Tang et al. 2016) and for GeneSplicer, no cut-off value was reported to our knowledge.

Furthermore, we consulted the dbSNP v1.1 database for Adaboost and Random Forest scores. A score higher than 0.6 is indicative for aberrant splicing (Jian et al. 2014a).

All variants located in the coding regions, were also evaluated for their effect on exonic splicing enhancers (ESE). Disruptions of these six bp motifs can result in improper splicing and can be predicted by tools such as ESEFinder (Cartegni et al. 2003) and RESCUE-ESE (Fairbrother et al. 2002). Both tools are also integrated in Alamut® Visual 2.8.1. The quantitative evaluation of all RNA hexamers as potential exonic splicing elements (Ke et al. 2011) was used to calculate total exonic splicing regulatory sequence (ESRseq) score change (Δ ESRseq scores) for every exonic variant, as stipulated by (Di Giacomo et al. 2013). The cut-off was experimentally determined to be -0.663 by analysis of variants in exon 7 of the *BRCA2* gene (Di Giacomo et al. 2013).

Finally, for variants in the coding regions the effect of amino acid substitution itself should also be taken into account. Therefore, Priors, an online tool combining amino acid substitution severity and spliceogenecity-based probability for pathogenicity of *BRCA1* and *BRCA2* point mutations was also consulted (Vallée et al. 2016).

Sample collection, cell cultures, RNA isolation and cDNA preparation

Individuals with variants of interest donated a blood sample in EDTA tubes and signed an informed consent. From these blood samples, peripheral blood lymphocytes (PBL) were isolated using Lymphoprep™ (STEMCELL Technologies, Canada) according to the manufacturer's guidelines. These PBL were cultured in RPMI (completed with 1 %L-glutamine and 0.5 % penicillin/streptomycin), foetal calf serum (10 %), 2-mercaptoethanol (0.1 %; all Gibco, USA) and sodium pyruvate (1 %, Life Technologies, USA). Phytohaemagglutinin (10 µl/ml, Gibco) was added to stimulate cell division. At day 7, puromycin (200µg/ml, Sigma Aldrich, USA) was added to the cultures to avoid nonsense-mediated decay (NMD). Four to six hours later, whole RNA was extracted using the QIAamp® RNeasy Mini Kit (QIAGEN, USA) according to the manufacturer's instructions. The total RNA and purity was measured using the DropSense96 reader (TRINEAN, Belgium). The RNA was converted to complementary DNA (cDNA) using either the iScript™ cDNA Synthesis Kit (Bio-Rad Laboratories, USA) or the Superscript® II Reverse Transcriptase Kit (Life Technologies, USA).

RT-PCR and sequencing

Splicing aberrations were assessed by means of RT-PCR using either primers in separate exons or primers situated at the exon boundaries (supplementary file S1) to avoid genomic DNA

interference. Fragment sizes were checked on the Labchip GX (Caliper Life Sciences, USA) or on agarose gel. Sanger sequencing was performed using the BigDye® Terminator Cycle Sequencing Kit (Life Technologies). Transcripts from carriers were compared to at least three controls for RT-PCR and at least one control was included for sequencing analysis. For the analysis of *BRCA1* variant c.4675+3A>T, cloning was performed using the TA Cloning™ kit (ThermoFisher Scientific) to characterize the various aberrant transcripts revealed by RT-PCR.

Nomenclature

Nucleotide and exon numbering for cDNA is based on NCBI entries NM_007294.3 (*BRCA1*) and NM_000059.3 (*BRCA2*). Nucleotide +1 corresponds to A of AUG translation initiation codon (according to HGVS guidelines). NM_007294.3 omits the historical exon 4 and rennumbers the remaining exon sequentially (Ensembl transcript: ENST00000357654.7). In Table 1, the “legacy numbering” is also provided.

Results

An overview of the *BRCA1* and *BRCA2* variants evaluated can be found in Table 1. For this study, we only included variants for which no unequivocal conclusions on pathogenicity and/or mRNA splicing data were available. If relevant, ClinVar IDs are provided. Table 1 summarizes *in silico* prediction data as well as the results of cDNA analysis in short-term cultured lymphocytes in the presence of puromycin. Out of 21 tested DNA alterations, 12 DNA alterations (seven *BRCA1* and five *BRCA2* variants) resulted in one or more aberrant mRNA transcripts. Furthermore, the *BRCA2* duplication c.425+415_4780dup{ins GATCGCAGTGA}, spanning exons 5, 6, 7, 8, 9, 10 and a large part of exon 11, was shown to result in a complex splicing pattern.

1. cDNA analysis results for four variants in canonical splice sites

BRCA1 c.5468-1G>A, is located in the splice acceptor site of the last coding exon 23. Loss of the WT splice site, unanimously predicted by all prediction tools (Table 1), results in an out of frame deletion of the first 11 bp of exon 23 as a cryptic splice site acceptor was activated 11 bp downstream of the wild type acceptor site. This resulted in an aberrant transcript (r.5468_5478del), leading to a premature termination codon (PTC) (p.(Ala1823Valfs*2)) (Figure 1a). We cannot rule out that this variant also leads to skipping of exon 23, the last exon of *BRCA1*, as we have no means to design primers in the next exon.

Loss of the WT donor splice site by *BRCA1* c.4986+1G>C, results in the activation of a cryptic splice site at c.4986+65. This leads to an aberrant transcript in which the first 65 intronic nucleotides of intron 15 are retained: r.4986_4987ins4986+1_486+65, p.(1662Phefs*14) (Figure 1b).

BRCA1 c.5152+2dup inactivates the splice donor site of exon 17, resulting in an aberrant transcript lacking exon 17 (r.5075_5152del; p.(Asp1692_Trp1718delinsGly)) (Figure 1c).

BRCA2 c.6841+1G>C results in the abolishment of the WT splice donor site of exon 11, accurately predicted by all tools. This leads to multiple aberrant transcripts of which a skip of exon 11 (r.1910_6841del, p.(Leu638_Gly2281del)) is the most abundant (Figure 2a & 2b). However, additional isoforms are obvious from Figure 2a. These are further described under point 4.

Table 1. Overview of tested *BRCA1* and *BRCA2* variants, in silico predictions and mRNA analysis results (continued)

gene	mutation	exon/ intron	legacy numbering (BRCA1 "exon 4" included in the numbering)	ClinVar ID	Splicing prediction							
					affected splice site	SSF (0-100)	MES (0-16)	NNSPLICE (0-1)	gene splicer (0-15)	HSF (0-100)	adaboost	random forest
BRCA1	c.80>5G>A	intron 2	intron 2	125520	donor	91.49 ⇒ 79.34 (-13.3%)	10.65 ⇒ 6.06 (-43.1%)	1.00 ⇒ 0.94 (-5.7%)	1.93 ⇒ —	95.25 ⇒ 83.08 (-12.8%)	1	0.90
	c.134+5G>T	intron 3	intron 3	96899	donor	87.86 ⇒ 75.47 (-14.1%)	10.08 ⇒ 3.86 (-61.7%)	0.89 ⇒ — (-85.7%)	2.61 ⇒ —	89.42 ⇒ 77.10 (-13.8%)	1	0.93
	c.1878A>G; (p=)	exon 11	exon 11	231250	cryptic donor (c.1878)	— ⇒ 78.55	— ⇒ 4.85	— ⇒ 0.60	/	77.89 ⇒ 88.46 (+13.6%)	/	/
	c.4115G>A; p.(Cys1372Tyr)	exon 10	exon 12	55105	cryptic donor (c.4112)	— ⇒ 71.41	0.35 ⇒ 5.85 (+1563.7%)	— ⇒ 0.68	/	80.86 ⇒ 82.02 (+1.4%)	/	/
	c.4186-10G>A	intron 11	intron 12	69800	acceptor	= 78.64	4.57 ⇒ 3.76 (-17.7%)	/	1.83 ⇒ —	78.45 ⇒ 78.33 (-0.2%)	0	0
	c.4674A>G; (p=)	exon 14	exon 15	no entry	donor	78.15 ⇒ —	6.84 ⇒ 4.95 (-27.7%)	0.44 ⇒ —	0.75 ⇒ —	83.37 ⇒ 78.51 (-5.8%)	0.83	0.63
					cryptic donor (c.4664)	= 91.56	/	/	/	/		
	c.4675+3A>T	intron 14	intron 15	125722	donor	78.15 ⇒ —	6.84 ⇒ —	0.44 ⇒ —	0.75 ⇒ —	95.95 ⇒ 77.95 (-18.8%)	1	0.97
					cryptic donor (c.4664)	= 91.56	/	/	/	/		
	c.4986+1G>C	intron 15	intron 16	no entry	donor	70.38 ⇒ —	5.91 ⇒ —	0.66 ⇒ —	/	81.24 ⇒ —	1	0.95
BRCA2	c.5152+2dup	intron 17	intron 18	55424	cryptic donor (c.4986+65)	= 73.18	/	/	/	= 78.81	/	/
	c.5278-22C>G	intron 19	intron 20	no entry	donor	74.34 ⇒ —	7.96 ⇒ —	0.95 ⇒ —	2.25 ⇒ —	78.04 ⇒ —	/	/
	c.5468-1G>A	intron 22	intron 23	125856	acceptor	= 90.05	= 13.07	= 0.99	14.41 ⇒ 13.72 (-4.8%)	= 93.64	/	/
					acceptor	87.91 ⇒ —	9.53 ⇒ —	0.76 ⇒ —	8.87 ⇒ —	90.15 ⇒ —	1	0.95
					cryptic acceptor (c.5479)	/	— ⇒ 3.89	/	/	76.68 ⇒ 76.49 (-0.2%)	/	/
	c.425+415_4780dup[ins GATCGAGTGA]			no entry	/	/	/	/	/	/	/	/
	c.517G>C; p.(Gly173Arg)	exon 7	/	182177	acceptor	94.42 ⇒ 88.67 (-6.1%)	10.00 ⇒ 8.79 (-12.1%)	0.98 ⇒ 0.92 (-6.1%)	8.28 ⇒ 4.40 (-46.9%)	96.60 ⇒ 92.44 (-4.3%)	1	0.88
	c.3326C>T; p.(Ala1109Val)	exon11	/	51450	cryptic donor (c.3324)	— ⇒ 72.13	— ⇒ 6.33	— ⇒ 0.88	/	— ⇒ 76.20	/	/
	c.4899C>G; p.(Ile1633Met)	exon 11	/	no entry	cryptic donor (c.4894)	— ⇒ 77.38	1.30 ⇒ 6.93 (+431.3%)	— ⇒ 0.88	/	67.65 ⇒ 79.66 (+17.8%)	/	/
	c.6313A>G; p.(Ile2105Val)	exon 11	/	38034	cryptic acceptor (c.4910)	77.69 ⇒ 75.36 (-3.0%)	0.51 ⇒ —	/	/	78.60 ⇒ 76.79 (-2.3%)	/	/
BRCA2					cryptic donor (c.6312)	/	— ⇒ 1.73	/	/	— ⇒ 67.35	/	/
					cryptic acceptor (c.6314)	/	/	/	/	— ⇒ 71.98	/	/
	c.6841+1G>C	intron 11	/	no entry	donor	86.91 ⇒ —	10.24 ⇒ —	0.99 ⇒ —	/	93.16 ⇒ —	1	0.82
	c.7618-6G>T	intron 15	/	no entry	acceptor	86.07 ⇒ 86.78 (+0.8%)	7.11 ⇒ 8.46 (+18.9%)	0.69 ⇒ 0.98 (+41.6%)	3.17 ⇒ 5.76 (+81.9%)	79.10 ⇒ 81.94 (+3.6%)	0	0.01
	c.8488-9T>G	intron 19	/	no entry	acceptor	74.35 ⇒ —	3.30 ⇒ —	/	/	82.32 ⇒ 79.22 (-3.8%)	1	0.97
	c.8488-12A>G	intron 19	/	no entry	cryptic acceptor (c.8488-8)	— ⇒ 72.17	— ⇒ 3.78	/	— ⇒ 2.68	— ⇒ 80.12	0	0.06
	c.8488-14A>G	intron 19	/	no entry	acceptor	= 74.35	3.30 ⇒ 2.85 (-13.7%)	/	/	82.32 ⇒ 82.51 (+0.2%)	/	/
					acceptor	74.35 ⇒ 74.57 (+0.3%)	3.30 ⇒ 0.84 (-74.5%)	/	/	= 82.32	/	/
BRCA2					cryptic acceptor (c.8488-13)	— ⇒ 74.99	— ⇒ 6.20	/	— ⇒ 1.67	— ⇒ 73.58	/	/
	c.8954-5A>G	intron 22	/	no entry	acceptor	82.36 ⇒ —	10.35 ⇒ 5.82 (-43.7%)	0.53 ⇒ 0.49 (-8.2%)	3.75 ⇒ —	87.47 ⇒ 87.40 (-0.1%)	1	0.96
BRCA2					cryptic acceptor (c.8954-4)	— ⇒ 89.17	— ⇒ 10.19	— ⇒ 0.89	— ⇒ 5.64	— ⇒ 90.94	/	/

Table 1. Overview of tested <i>BRCA1</i> and <i>BRCA2</i> variants, in silico predictions and mRNA analysis results (continued)										
gene	mutation	exon/ intron	legacy numbering (<i>BRCA1</i> "exon 4" included in the numbering)	ClinVar ID	ESE finder	RESCU-ESE	hexamers ΔESRseq score	PRIORS	Effect on mRNA splicing	Protein effect
<i>BRCA1</i>	c.80-15G>A	intron 2	intron 2	125520	/	/	/	/	r.-19_80del (skip exon 2)	p.?
	c.134+5G>T	intron 3	intron 3	96899	/	/	/	/	r.81_134del (skip exon 3)	p.(Cys27*)
	c.1878A>G; (p.=)	exon 10	exon 11	231250	2 new sites (SC35)	no changes	2.4758	N/A	no effect on splicing	no effect on splicing
	c.4115G>A; p.(Cys1372Tyr)	exon 12	exon 12	55105	1 new site (SRp55)	1 ESE activated	-1.3814	0.02	no effect on splicing	no effect on splicing
	c.4186-10G>A	intron 11	intron 12	69800	/	/	/	/	no effect on splicing	no effect on splicing
	c.4674A>G; (p.=)	exon 14	exon 15	no entry	1 new site (SRp55)	no changes	2.4475	0.02	r.4665_4675del	p.(Gln1556Glyfs*14)
	c.4675+3A>T	intron 14	intron 15	125722	/	/	/	/	complex effect on splicing, see Table 2 and Figure 3	
	c.4986+1G>C	intron 15	intron 16	no entry	/	/	/	/	r.4986_4987ins4986+1_486+65	p.(1662Phefs*14)
	c.5152+2dup	intron 17	intron 18	55424	/	/	/	/	r.5075_5152del (skip exon 17)	p.(Asp1692_Trp1718delinsGly)
	c.5278-22C>G	intron 19	intron 20	no entry	/	/	/	/	no effect on splicing	no effect on splicing
	c.5468-1G>A	intron 22	intron 23	125856	/	/	/	/	r.5468_5478del	p.(Ala1823Valfs*2)
	c.425+415_4780dup (ins GATCGACGTGA)			no entry	/	/	/	/	effect on splicing, see Figure 5	
	c.517G>C; p.(Gly173Arg)	exon 7	/	182177	disruption of 4 ESE and 1 new ESE	no changes	2.1849	0.02	r.517_631del (skip exon 7)	p.(Gly173Serfs*19)
	c.3326C>T; p.(Ala1109Val)	exon11	/	51450	no changes	2 ESE disrupted	-2.9402	0.02	no effect on splicing	no effect on splicing
<i>BRCA2</i>	c.4899C>G; p.(Ile1633Met)	exon 11	/	no entry	no changes	no changes	0.1009	0.02	no effect on splicing	no effect on splicing
	c.6313A>G; p.(Ile2105Val)	exon 11	/	38034	1 new site (SRp40)	1 ESE disrupted	0.8822	0.02	no effect on splicing	no effect on splicing
	c.6841+1G>C	intron 11	/	no entry	/	/	/	/	effect on splicing, see Figure 2	
	c.7618-6G>T	intron 15	/	no entry	/	/	/	/	no effect on splicing	no effect on splicing
	c.8488-9T>G	intron 19	/	no entry	/	/	/	/	r.8487_8488ins8488-8_8488-1	p.(Trp2830Tyrfs*36)
	c.8488-12A>G	intron 19	/	no entry	/	/	/	/	no effect on splicing	no effect on splicing
	c.8488-14A>G	intron 19	/	no entry	/	/	/	/	r.8487_8488ins8488-13_8488-1	p.(Trp2830Hisfs*19)
	c.8954-5A>G	intron 22	/	no entry	/	/	/	/	r.8953_8954ins8954-4_8954-1	p.(Val2985Aspfs*34)

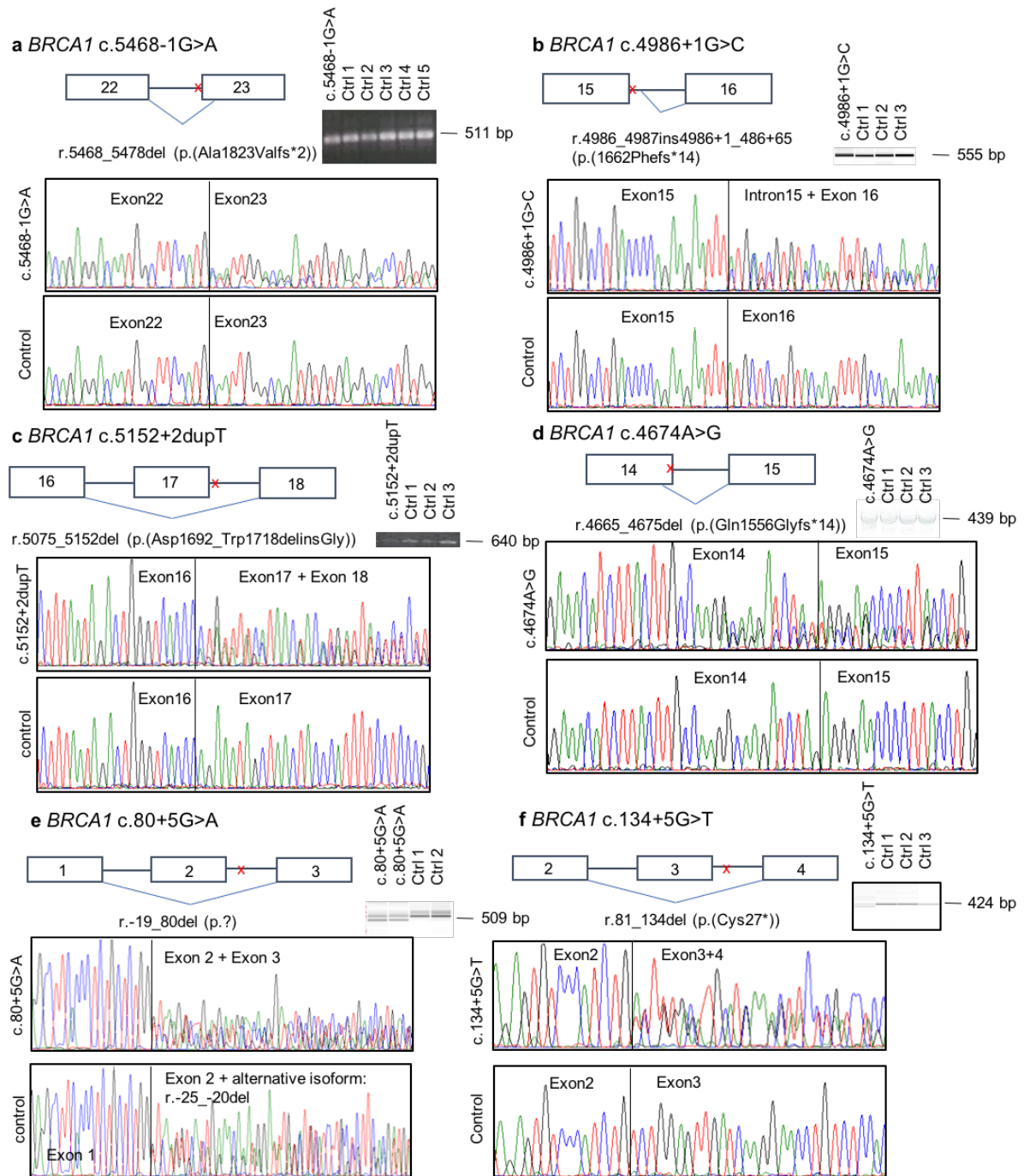


Figure 1. Results of *in vitro* mRNA analysis of six *BRCA1* variants leading to aberrant splicing

Schematic representation of six *BRCA1* variants leading to aberrant splicing with the red x illustrating the position of the variant. RT-PCR results on agarose gel or Labchip GX and sequencing results are shown for the patient with the mutation and a negative control. From panel (e) it is clear that r.-25_-20del represents a major alternative splicing event, observed in both the patient and controls (Colombo et al. 2014; Menéndez et al. 2012).

Nucleotide and exon numbering for cDNA is based on NCBI entry NM_007294.3.

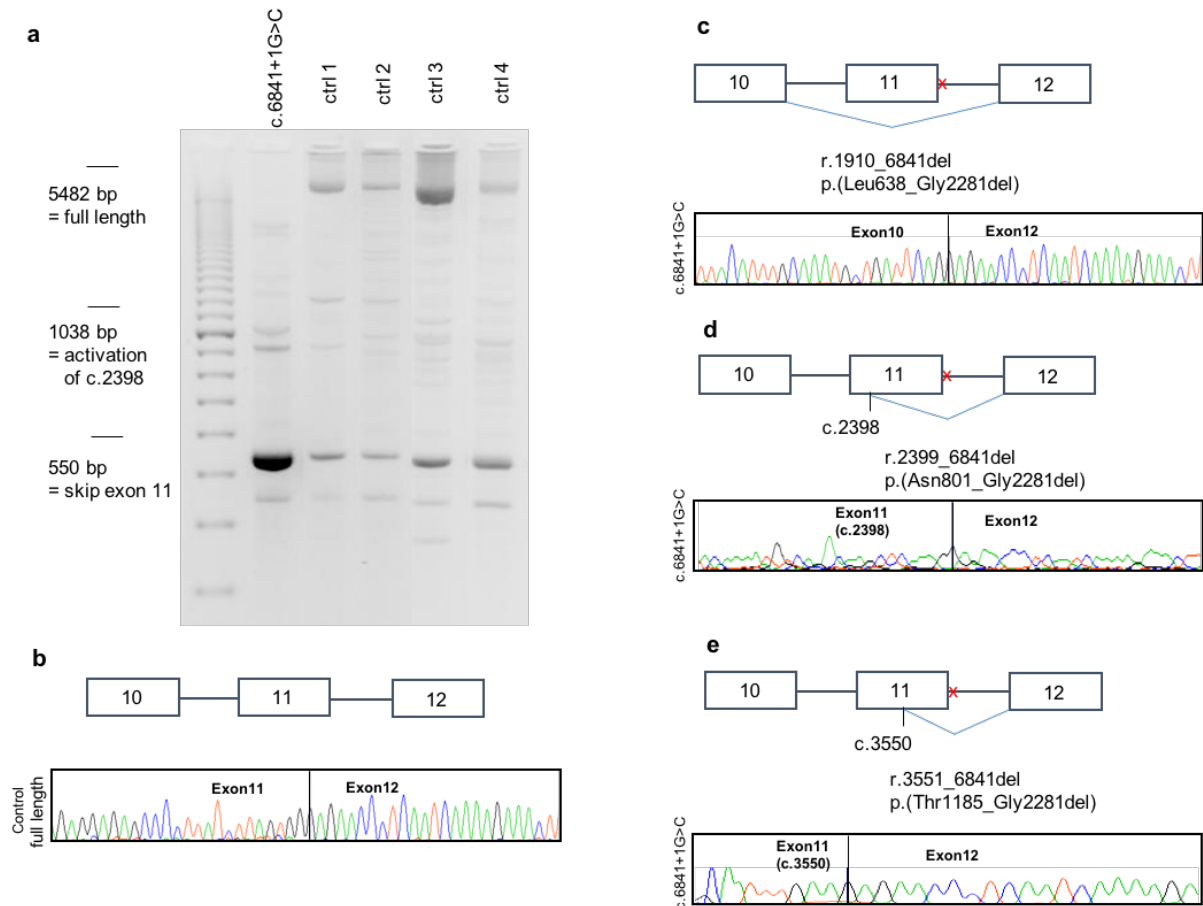


Figure 2. Schematic representation of the results of *in vitro* mRNA analysis for the *BRCA2* variant c.6841+1G>C.

(a) RT-PCR products of the c.6841+1G>C variant and controls in agarose gel; (b-e) splicing structural representation (up) and representative sequences (down) from one control (b) and the different splicing alternative events. Nucleotide and exon numbering for cDNA is based on NCBI entry NM_000059.3.

2. cDNA analysis results for ten variants outside the canonical splice sites but in the Cartegni consensus region

The Cartegni consensus region encompasses 11 bases of the 5' splice site (from the three last exonic to the eight first intronic bases) and 14 bases of the 3' site (from the 12 last intronic to the first two exonic bases) (Cartegni et al. 2002).

Two exonic variants in this region both result in aberrant splicing. The substitution c.4674A>G, affecting the second last nucleotide of exon 14 in *BRCA1*, leads to the abolishment of the natural splice donor site as predicted by all *in silico* tools. The lack of a natural splice donor site resulted in the activation of a cryptic splice site at position c.4664, only predicted by SSF

(score = 91.56), leading to a deletion of the last 11 nucleotides of exon 14: r.4665_4675del; p.(Gln1556Glyfs*14) (Table 1 and Figure 1d).

BRCA2 c.517G>C, located in the first nucleotide of exon 7 leads to an aberrant transcript containing an out of frame skip of exon 7 (r.517_631del; p.(Gly173Serfs*19)) due to the inactivation of the WT splice donor (Table 1 and Figure 4a). Only a small reduction in scores was provided by the different programs (for MES this was lower than the 15% cut-off proposed by (Houdayer et al. 2012; Jian et al. 2014a)) but higher than the 10% cut-off more recently proposed by (Tang et al. 2016). Priors calculated a greater change of pathogenicity through splicing defects (probability = 0.34) than as to be expected from the missense variant itself (probability = 0.02). Only AdaBoost en Random Forest provided high scores indicative for aberrant splicing.

Five out of eight intronic variants in the Cartegni consensus region resulted in aberrant splicing and *in silico* predictions for these variants were accurate: *BRCA1* c.80+5G>A, c.134+5G>T & c.4675+3A>T and *BRCA2* c.8488-9T>G & c.8954-5A>G.

RT-PCR with primers located in exons 11-16 resulted in a smear of PCR products on agarose gel for patient with the *BRCA1* variant c.4675+3A>T, where in the two tested controls only a single band of the expected length was observed (Figure 3). To analyze the products of different lengths, cloning followed by sequencing was performed for 57 clones. Two heterozygous SNPs (*c.4308T/C* and *c.4837A/G*) allowed to determine if the transcript originated from the WT or the mutant allele. An overview of the aberrant mRNA transcripts is shown in Figure 3 and Table 2. The major effect of this mutation is the activation of a cryptic donor site, 11 nucleotides upstream of the wild type donor site of exon 14, similar as for the patient with c.4674A>G. In addition, increased expression of the naturally occurring isoform lacking exon 14 (out of frame) was observed. Interestingly, we have no evidence that this represents a major splice event in the patient with c.4674A>G. However, for analysis of this patient a different primer set to generate a shorter fragment was used (cfr. Supplementary Table) and cloning was not performed in that case.

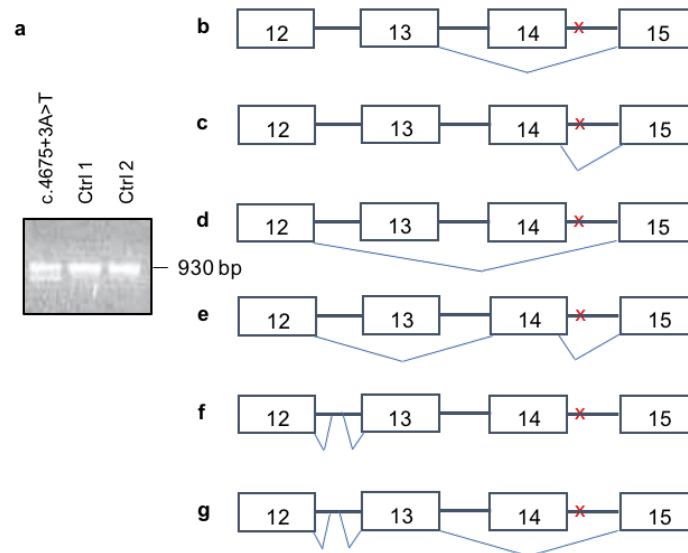


Figure 3. Schematic representation of RT-PCR and sequencing results obtained by primers located in exons 11 and 16 for *BRCA1* c.4675+3A>T

(a) RT-PCR results on agarose gel revealed a smear of bands, (b-g) cloning of the cDNA fragment revealed several different isoforms transcribed both from the mutant as well as from the wild type allele.

Table 2. Overview of aberrant transcripts detected for *BRCA1* c.4675+3A>T

transcript	RNA	Protein	% (number of clones/total sequenced)	% from the WT allele	Fig 2
full length	/	/	43,90% (25/57)	96% (24/25)	/
out of frame skip of exon 14	r.4485_4675del	p.Ser1496Glyfs*14	24,60% (14/57)	7% (1/14)	b
out of frame deletion of last 11 nucleotides of exon 14	r.4665_4675del	p.Gln1556Glyfs*14	17,50% (10/57)	0% (0/10)	c
in frame skip of exon 13 and 14	r.4358_4675del	p.Ala1453_Leu1558 del	3,50% (2/57)	0% (0/2)	d
out of frame skip of exon 13 and the last 11 nucleotides of exon 14	c.4385_4484del	p.Ala1453Gyfs*10	3,50% (2/57)	0% (0/2)	e
full length and insertion of 66 nucleotides from intron 12	r.4357_4358ins(6 6)	p.Lys1452_Ala1453ins(22)	3,50% (2/57)	100% (2/2)	f
full length and insertion of 63 nucleotides from intron 12	r.4357_4358ins(6 3)	p.Lys1452_Ala1453ins(21)	1,70% (1/57)	100% (1/1)	f
insertion of 66 nucleotides from intron 12 and skip of exon 14	r.4357_4358ins(6 6) + r.4485_4675del	p.Lys1452_Ala1453ins(22) + p.Ser1496Glyfs*14	1,70% (1/57)	100% (1/1)	g

BRCA1 c.80+5G>A abolishes the WT donor site of exon 2. With primers located in the non-coding exon 1 and exon 7, we found that this variant leads to out of frame skipping of exon 2 (r.-19_80del; p.?) leading to loss of the translation initiation codon (Table 1 and Figure 1). In addition, we found both in the controls and the patient carrying the mutation an abundant alternative transcript (r.-25_-20del: skip of the last six nucleotides of exon 1), which has previously been described as naturally occurring isoform.

BRCA1 c.134+5G>T inactivates the donor of exon 3 leading to an out of frame skip of exon 3, resulting a PTC: r.81_134del; p.(Cys27*) (Figure 1f). Skipping of exon 3 has previously been described as a naturally occurring isoform (Colombo et al. 2014) , but from Figure 1f it becomes clear that this isoform is hardly detectable in controls compared to the patient with the c.134+5G>T substitution.

BRCA2 c.8954-5A>G (Figure 4b) was found to generate a cryptic splice site, resulting in an out of frame insertion of four nucleotides from intron 22 (r.8953_8954ins8954-4_8954-1; p.(Val2985Aspfs*34)). As this is an out of frame transcript, inducing a premature stop codon, it is expected to be prone to NMD.

The outcome of two variants in the Cartegni site of *BRCA2* intron 19 was different. *BRCA2* c.8488-9T>G creates a cryptic acceptor site, leading to an aberrant transcript with an *out of frame* insertion of the last eight nucleotides of intron 19 (r.8487_8488ins8488-8_8488-1; p.(Trp2830Tyrf*36)) (Table 1 and Figure 4c). In contrast, *BRCA2* c.8488-12A>G was not found to induce aberrant splicing. This was accurately predicted by all *in silico* prediction tools (Table 1).

Also three other intronic variants in the Cartegni consensus region (*BRCA1* c.4186-10G>A and *BRCA2* c.7618-6G>T; c.8488-12A>G) did not result in aberrant splicing. Based on the MES predictions, aberrant splicing for *BRCA1* c.4186-10G>A (-17.7%) and *BRCA2* c.8488-12A>G (-13.7%) could be expected based on the cut-off of -10% proposed by (Tang et al. 2016). Even with the more severe -15% cut-off proposed by (Houdayer et al. 2012) aberrant splicing was expected for *BRCA1* c.4186-10G>A.

For *BRCA2* c.7618-6G>T the classic splice prediction tools showed increased scores for the acceptor site, compatible with normal splicing.

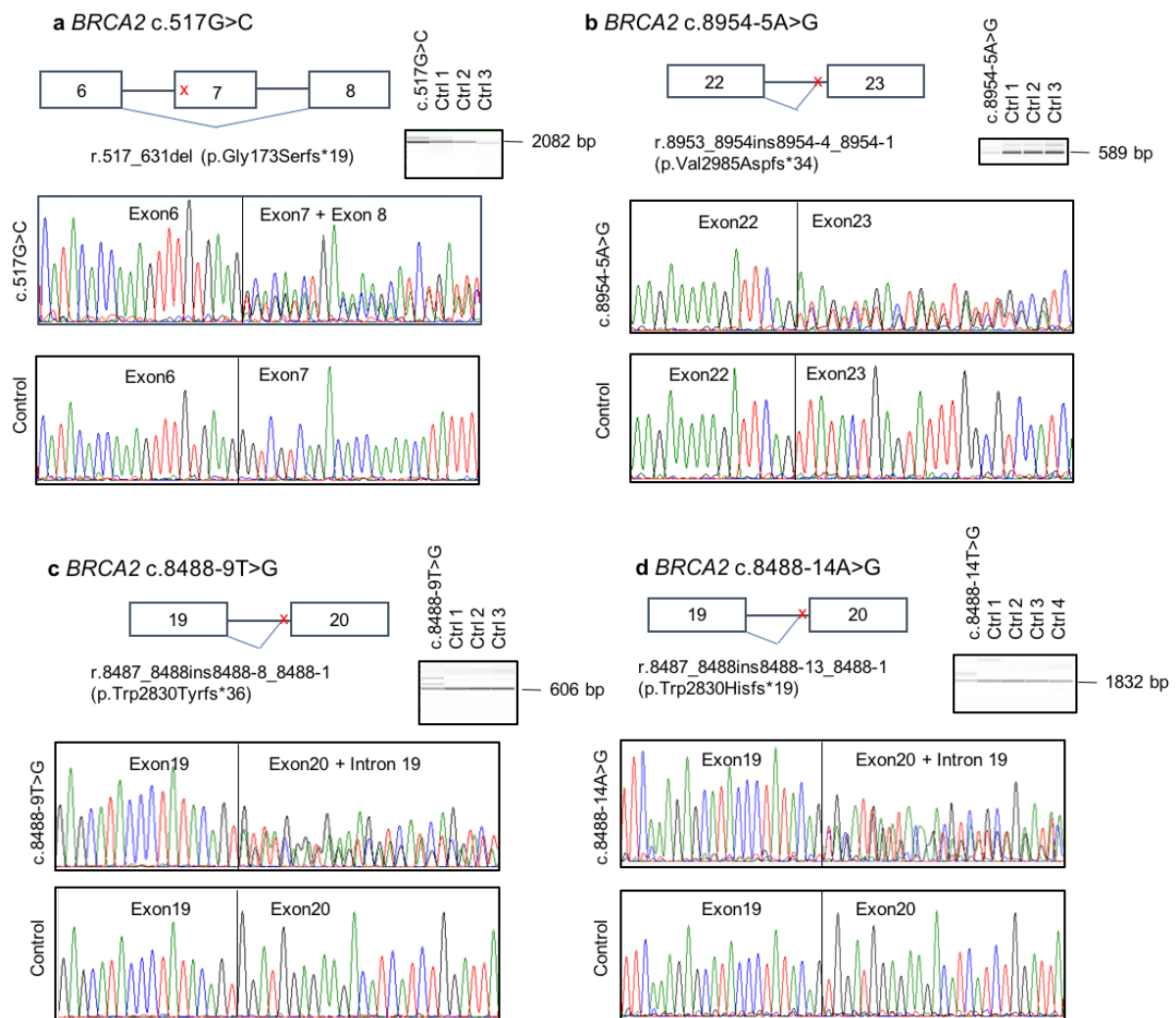


Figure 4. Results of *in vitro* mRNA analysis of four *BRCA2* variants

Schematic representation of four *BRCA2* variants leading to aberrant splicing with the red x illustrating the position of the variant. RT-PCR results on agarose gel or Labchip GX and sequencing results are shown. Nucleotide and exon numbering for cDNA is based on NCBI entry NM_000059.3.

3. cDNA analysis results for seven variants outside the Cartegni consensus region

We evaluated the effect at the mRNA level of two intronic variants outside the Cartegni consensus region: *BRCA1* c.5278-22C>G and *BRCA2* c.8488-14A>G. *BRCA2* c.8488-14A>G leads to aberrant splicing. This results from the creation of a cryptic splice site, predicted by all tools consulted, and a reduction in strength of the WT splice site, only predicted by MES. The aberrant transcript contains an out of frame insertion of the last 13 nucleotides of intron 19: r.8432_8433ins8433-13_8433-1; p.(Trp2830Hisfs*19) (Table 1, Figure 4d).

BRCA1 c.5278-22C>G did not result in aberrant splicing, which was correctly predicted by all consulted *in silico* prediction tools (Table 1).

None of the five tested exonic variants outside the Cartegni consensus region [two in *BRCA1*: c.1878A>G (p.=) & c.4115G>A; p.(Cys1372Tyr) and three in *BRCA2*: c.3326C>T; p.(Ala1109Val), c.4899C>G; p.(Ile1633Met) & c.6313A>G; p.(Ile2105Val)] affected mRNA splicing. However, the prediction tool Priors, classified three variants [*BRCA1* c.1878A>G (p.=) & c.4115G>A; p.(Cys1372Tyr); *BRCA2* c.3326C>T; p.(Ala1109Val)] as “moderate probability of pathogenicity from the creation of a de novo splice donor” (score 0.3, see Table 1). ΔESRseq scoring predicted a splicing effect for *BRCA2* c.3326C>T and *BRCA1* c.4115G>A (ΔESRseq scores below -0.663, see table 1). ESEfinder and RESCUE-ESE predicted both disruption and/or creation of a new ESE for every variant except for *BRCA2* c.4899C>G (Table 1). Furthermore, *BRCA1* c.4115G>A was predicted to activate of a cryptic donor site at position c.4112. However, this cryptic donor site was not strong enough to compete with the WT splice site (Table 1). None of the variants were predicted to have an effect due to an altered protein structure (Prior missense score 0.02 in Table 1).

4. Identification of multiple cryptic donor sites within the large exon 11 of *BRCA2* in case of interruption of the wild type exon 11 donor site

cDNA analysis in lymphocytes of a patient heterozygous for the *BRCA2* variant c.426-415_4780dup{ins GATCGCAGTGA} (Figure 5a) revealed a complex splicing pattern. RT-PCR combining a forward primer in exon 11 and a reverse primer in exon 10, did not result in a PCR product in controls but resulted in two fragments (Fig 5c and 5d) in the patient with the duplication. A similar approach with a forward primer in exon 10 and a reverse primer in exon 7 resulted in the identification of an additional two PCR products (Fig 5e and 5f). We conclude

from these results that this duplication leads to a mix of different transcripts. The major effects are the inclusion of a cryptic exon in intron 4 (r.425+415 to c.426-209), skipping of exon 11 and aberrant transcripts due to the activation of two cryptic donor sites within exon 11: c.2398 and c.3550. All combinations observed are out of frame.

We evaluated if the cryptic donor sites at c.2398 and c.3550 were also activated in a patient with the *BRCA2* c.6841+1G>C mutation. Besides skipping of exon 11, several other aberrant transcripts were observed. Also in this patient, the cryptic splice donor sites at c.2398 and c.3550 are activated, resulting in the skip of respectively 4443 and 3291 nucleotides of the 3' part of exon 11: r.2399_6841del; p.(Asn801_Gly2281del) (Figure 2c) and r.3551_6841del; p.(Thr1185_Gly2281del) (Figure 2d) respectively. The activation of c.2398 leads to a band of 1038 bp, visible on the gel (Figure 2a), which was confirmed by means of direct sequencing. No band in concordance with activation of c.3550 was observed in the initial RT-PCR. However, by means of allele specific primers (supplementary file S1), we could confirm the activation of this particular cryptic splice site.

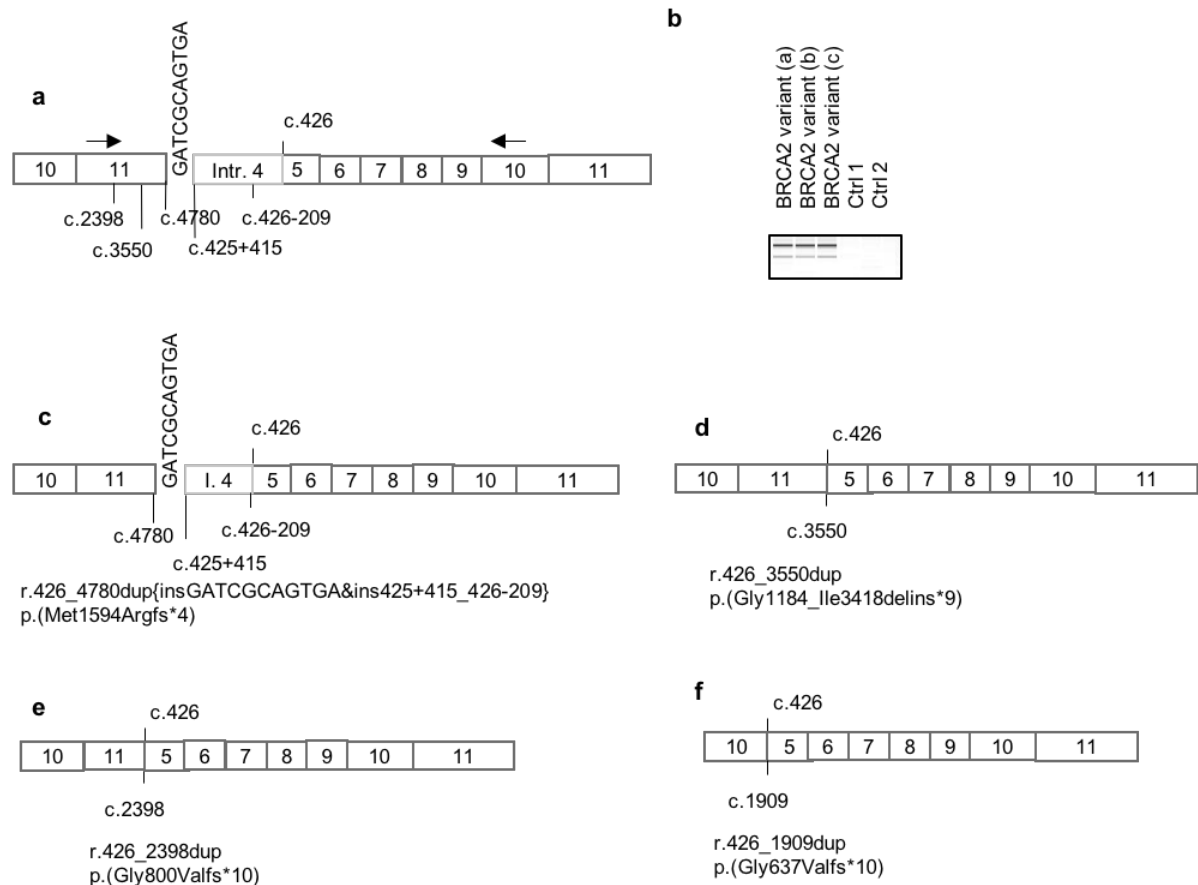


Figure 5. Results of RT-PCR with a forward primer located in exon 10 or 11 and a reverse in exon 10 for the patient heterozygous for *BRCA2* c.426-415_4780dup{ins GATCGCAGTGA} Schematic representation of the complex tandem duplication, (b) Result of aberrant transcript specific PCR analyzed by Labchip GX), (c-f) Schematic representation of the different aberrant transcripts:

- (c) The largest PCR product contained all nucleotides from the start of the primer till c.4780 (the presumed breakpoint in exon 11), an insertion of 11 nucleotides (GATCGCAGTGA), followed by 293 nucleotides from intron 4 (from c.425+415 to c.426-209) and continued by all nucleotides from exon 5 to position c.4780 in exon 11
- (d) A smaller fragment was produced by the activation of a cryptic splice site donor at nucleotide position c.3550. This fragment does not contain nucleotides c.3551 to c.4780, the 11 bp sequence GATCGCAGTGA nor the 293 nucleotides between c.425+415 to c.426-209 from intron 4
- (e) a smaller fragment was observed by the activation of a cryptic splice site donor at nucleotide position c.2398, followed by the skip of the insertion of 11 nucleotides and the 293 nucleotides of intron 4
- (f) The shortest aberrant fragment was the result of a complete skip of exon 11, and the skip of the insertion of 11 nucleotides and intron 4

All aberrant transcripts are out of frame, ultimately leading to a PTC: (1) p.(Met1594Argfs*4), (2) p.(Gly1184_Ile3418delins*9), (3) p.(Gly800Valfs*10) and (4) p.(Gly637Valfs*10).

Discussion

We evaluated the effect at the cDNA level of 21 variants of unknown clinical significance in *BRCA1* (n=11) and *BRCA2* (n=10) and demonstrated aberrant splicing for 12 variants (*BRCA1* (n=7) and *BRCA2* (n=5)). In addition, we evaluated the effect of a large tandem duplication in *BRCA2*, with breakpoints in intron 4 and exon 11. By incorporating controls in our assays and consulting literature, we verified if the detected transcripts represent naturally occurring alternative transcripts. None of the detected aberrant *BRCA2* transcripts were reported as naturally occurring alternative transcripts (Fackenthal et al. 2016). However, we observed a skip of exon 11 in controls, though be it at very low level (Figure 2). Some of the variants studied in *BRCA1*, lead to a strong upregulation of low abundant naturally occurring transcripts in our patients with specific variants compared to controls: skip of exon 2 (r.-19_80), exon 3 (r.81_134del), exon 13 and 14 (r. 4358_4675del), exon 14 (r.4485_4675del) and exon 17 (r.5075_5152del).

In addition we observed an alternative transcript containing an in frame insertion of 66 nucleotides from intron 13: r.4357_4358ins(66), which has previously been reported by our group in both a control and a patient heterozygous for the *BRCA1* variant 4304G>A (p.=) (Claes et al. 2003). The prevalence of the aberrant transcript was not quantified then, but we now demonstrate that the transcript is present at very low frequency (estimated to be <3.5% of the full length, Table 2 & Figure 2e) and may therefore have been missed by (Colombo et al. 2014).

mRNA splicing assays yield insights in the exact aberrant transcript, which may in turn shed light on the clinical importance of the variant. The majority of the tested splicing variants lead to a frameshift and the creation of a PTC and are therefore expected to be degraded by NMD (Perrin-vidoz et al. 2002; Baert et al. 2016; Ware et al. 2006). Aberrant *BRCA1* transcripts can escape NMD when the PTC is located near the C-terminus or near the translation initiation codon (Perrin-vidoz et al. 2002). Based on this rule, two of our *BRCA1* splice site variants are predicted to escape NMD. *BRCA1* c.134+5G>T, is situated near the translation initiation codon, but as translation would result in only a small protein (p.(Cys27*)), we do not expect any functionality from this aberrant protein and classify this variant as probably pathogenic. The second splicing variant which may evade NMD is *BRCA1* c.5468-1G>A, leading to an

aberrant transcript with a stop codon at amino acid position p.1825, situated in the last exon. Unfortunately, no data from cultured lymphocytes without puromycin are available to check the expression of the aberrant transcript in the absence of NMD inhibition. If this transcript indeed avoids NMD, we still assume a pathogenic effect for this variant as two nonsense mutations resulting in a stop codon downstream of amino acid 1825 (c.5503C>T; p.(Arg1835*)) and c.5559C>A; p.(Tyr1853*)) are also considered as pathogenic mutations (see ClinVar database entries 55601 and 55629) and evasion of NMD was demonstrated for both variants (Perrin-vidoz et al. 2002).

We can expect a pathogenic effect for *BRCA1* c.80+5G>A as the AUG translation initiation codon is lost due to the skip of exon 2. Interruption of the translation initiation codon due to a point mutation has previously been classified as deleterious (ClinVar ID: 54432, 54745, 54746, 55072 and 267523).

BRCA1 c.5152+2dup, leads to an in frame skip of exon 17 (r.5075_5152del; p.(Arg1692_Trp1717delinsGly)). Several naturally occurring transcripts lack exon 17 as reported by (Colombo et al. 2014), besides transcripts lacking exclusively exon 17, also transcripts lacking exons 13-17 and 14-18. We performed RT-PCR with a forward primer located in exon 15 and a reverse in exon 21 and demonstrated the skip of exon 17 was only present in the patient heterozygous for c.5152+2dup (see figure 1b). It is expected that a transcript lacking an in frame exon will avoid NMD. However, skipping this exon leads to the disruption of a large part of the first BRCT domain. The BRCT region consists of two highly conserved repeats (1671 – 1745 and 1779 – 1863) and is required for several functions of the *BRCA1* protein, including recruitment to the DNA damage site, DNA end resection and G2/M checkpoint activation, through binding with numerous interaction partners (Roy et al. 2012). Analysis of several missense variants in these BRCT repeats showed an impaired folding (Lovelock et al. 2006; Lovelock et al. 2007; Glover 2006). We stipulate that loss of 36 amino acids from the 110 amino acids of the first BRCT repeat induced by *BRCA1* c.5152+2dup, may be detrimental for accurate folding of these motifs. Similarly, the *BRCA1* variant c.5468-1G>A; p.(Ala1823Valfs*2) results in loss of the last 30 amino acids of the second BRCT repeat and is therefore expected to cause improper folding of this motif. Binding of several interaction partners might thus be impaired by these two variants, leading to a deleterious effect of these variants. However, to gain more insight in the functional effect western blotting and

functional assays may be performed to further elucidate the effect of these splicing mutations on the expression and various functions of BRCA1.

All aberrant transcripts induced by *BRCA2* c.6841+1G>C are in frame (p.(Thr1185_Gly2281del), p.(Asn801_Gly2281del) and p.(Leu638_Gly2281del)). However, the size of the deletions and the location in the BRC repeat region, necessary for binding of RAD51, an effector of homologous recombination, suggest a pathogenic effect.

mRNA analysis of three variants situated in intron 19 of *BRCA2* revealed different effects. Variants c.8488-9T>G and c.8488-14A>G resulted in aberrant splicing, whereas a variant situated in between those two (c.8488-12A>G) did not impair proper mRNA slicing, which was adequately predicted by the prediction tools consulted. Both c.8488-9T>G and c.8488-14A>G create a novel acceptor site while the natural splice acceptor site is relatively weak, and a naturally occurring skip of exon 20 has been demonstrated (Fackenthal et al. 2016). The variant c.8488-12A>G for which no aberrant splicing was demonstrated, does not result in a de novo “AG” splice acceptor site. To our knowledge, only variants in the canonical splice acceptor site of exon 20 of *BRCA2* (c.8488-1/2) have previously been reported and were shown to result in exon skipping (ClinVar and LOVD)(Fackenthal et al. 2016). We assume that the aberrant transcripts induced by c.8488-9T>G and c.8488-14A>G will be degraded by NMD as NMD was demonstrated for all tested PTC-introducing mutations in *BRCA2*, even when the stop codon is situated towards the C-terminal end (Ware et al. 2006). Therefore, we consider both variants as likely deleterious.

Out of the seven tested exonic variants studied, only two (*BRCA1* c.4674A>G & *BRCA2* c.517G>C) resulted in aberrant splicing.

BRCA1 c.4674A>G, located in the second last nucleotide of exon 14, resulted in aberrant splicing due to an abolished WT splice donor site (Table 1). mRNA analysis revealed the activation of a cryptic donor site upstream at position c.4664, only predicted by SSF, while other possible cryptic splice sites in the area predicted by HSF were not activated. This results in an out of frame skip: r.4665_4675del; p.(Gln1556Glyfs*14) and the formation of a PTC. We therefore classify this variant as likely pathogenic. As the splicing defect is due to loss of the natural splice site, we were not surprised that Δ ESRseq scoring and RESCUE-ESE

demonstrated no effect of the variant on ESE, while ESEfinder predicted the creation of a new ESE.

BRCA2 c.517G>C is located in the first nucleotide of exon 7 and induces aberrant splicing due to loss of the natural splice site. However, splice site prediction tools demonstrate only a marginal decrease in 3' splice site strength (see Table 1). The skip of exon 7 (r.517_631del; p.(Gly173Serfs*19)) is likely to undergo degradation of the transcript by NMD. Δ ESRseq scoring and ESEfinder demonstrated no effect of the variant on ESE as could be expected, while RESCUE-ESE predicted multiple effects on ESE. A variant at the same position (c.517G>T) was previously tested using both minigene and RNA splicing analysis and also resulted in skipping of exon 7 (Gaildrat et al. 2012). Interestingly, a higher than expected presence of splicing mutations affecting potential regulatory elements leading to an exon skip are detected in exon 7 of *BRCA2* (Di Giacomo et al. 2013). Analysis of the influence of ESE in this exon by means of an ESE dependent splicing minigene assay (pcDNA-Dup minigene) has demonstrated that a relatively large region of this exon is characterized by the presence of ESE's. The combination with a relatively weak natural splice sites explains the high number of splicing variants in this exon (Di Giacomo et al. 2013).

In contrast to the large number of substitutions leading to aberrant splicing, both in the coding sequence and the surrounding intronic sequence of exon 7 of *BRCA2*, no such variants have been reported in the large exon 11 of *BRCA2* (Fackenthal et al. 2016), despite the presence of a large number of predicted cryptic acceptor and donor sites in this exon. None of the three variants in exon 11 of *BRCA2* included in this study showed improper splicing. Δ ESRseq scoring was shown to assist the evaluation of regulatory elements in selected exons. The experimentally determined cut-off of -0,6331 for variants in *BRCA2* exon 7 (Di Giacomo et al. 2013), did not result in a good correlation between Δ ESRseq score and mRNA splicing in other exons. For instance, the Δ ESRseq score of respectively -2.9402 and -1.3814 for *BRCA2* c.3326C>T and *BRCA1* c.4115G>A would imply an effect on exonic splice regulation which could not be demonstrated by mRNA analysis. Therefore, the cut-off, experimentally determined for variants in *BRCA2* exon 7, containing a large number of ESE's in combination with weak splice donor and acceptor sites, may not be applicable for variants in other exons. Furthermore, neither the results of ESEfinder nor the results of RESCUE-ESE were concordant with the mRNA results for exonic variants included in this study. This illustrates the limited

predictive value of these tools, although some may be useful for the evaluation of variants in exons enriched for exonic splicing regulators (ESR) like described in *BRCA2* exon 7, *MLH1* exon 10, *BRCA1* exon 6, *CFTR* exon 12 and *NF1* exon 37 (Soukarieh et al. 2016).

To date, no known DNA variations inducing aberrant splicing of *BRCA2* exon 11 have been reported. Here, we detected the activation of two cryptic splice donor sites at c.2398 and c.3550 in the absence of the WT splice site by evaluating the impact on pre-mRNA splicing of a large tandem duplication with a breakpoint 2061 bp upstream of the WT donor site. Activation of both cryptic splice donor sites was confirmed in a patient with substitution abolishing the WT splice donor site of exon 11 (c.6841+1G>C). Scanning of exon 11 with *in silico* prediction tools available through Alamut 2.8.1 revealed several alternative cryptic splice site donors, but none of them were activated in the patient with the variant c.6841+1G>C. The specific activation of the cryptic splice donor sites at positions c.2398 and c.3550 might be due to ESE motifs. We can expect these ESE motifs to lie in the close vicinity to the activated splice sites (Ke et al. 2011; Caceres et al. 2013). The influence of possible ESE's on the cryptic splice site c.3550 and c.2398 should be further experimentally validated (Raponi et al. 2014; Di Giacomo et al. 2013). In Alamut no ESE motifs are predicted. Knowledge on potentially activated splice sites in case of inactivation of the wild type site, may be important to design adequate *BRCA2* ASOs (antisense oligonucleotides), which have been proposed as a promising avenue to prevent resistance to PARP inhibitor therapy in several tumor types (Rytelewski et al. 2016) or as potential therapeutic anti-cancer agent in combination with cisplatin (Rytelewski et al. 2014).

Another aim of this study was to test the performance of *in silico* prediction tools. Our findings confirm that splice site prediction tools accurately predicted the effect of variants in the canonical splice sites. Unfortunately, accuracy of the splice site prediction tools decreases for variants outside these sites. We demonstrated that Adaboost and Random Forest outperformed the classically used tools for variants outside the canonical splice sites. The data from these programs are extracted from dbSNV (Liu et al. 2016) which currently only include data on potential human SNVs within the splicing consensus regions -3 to +8 at the 5' splice site and -12 to +2 at the 3' splice site. For all variants studied and located in these regions the predictions were accurate. However, these programs provide only 1 score. If this

score is higher than 0.6, aberrant splicing is expected but they do not provide an indication on the potential activation/creation of cryptic splice sites; effects need to be studied by cDNA analysis. The 5 prediction tools consulted via Alamut (SSF, MES, NNSplice, gene splicer and HSF), resulted in the misclassification of one or two variants (*BRCA2* c.7618-6G>T & c.8488-12A>G) in the same cohort, dependent on the applied cut-off for MES.

For intronic variants outside the Cartegni consensus region, the classic *in silico* prediction tools were helpful to determine for which variants cDNA analysis would be useful. Our results are in agreement with Théry et al. and Vreeswijk et al. suggesting that cDNA analysis is not required for intronic variants if no effect on splicing is predicted by multiple *in silico* prediction tools (Vreeswijk et al. 2009; Théry et al. 2011).

Priors, a recently published prediction tool, assesses whether pathogenicity of a missense variant is more likely to originate from the amino acid substitution or a splicing defect (Vallée et al. 2016). Of all exonic variants included in this study Priors gave the highest score for impaired splicing (0.34) for *BRCA1* c.4674A>G & *BRCA2* c.517G>C and we showed that both variants lead to aberrant splicing. However, this score is only marginally higher compared to those for other variants [*BRCA1* c.1878A>G (p.=) & c.4115G>A; p.(Cys1372Tyr) and *BRCA2* c.3326C>T; p.(Ala1109Val)] not leading to aberrant splicing (Priors score of 0.3). The marginally higher score for *BRCA2* c.517G>C is supported by the relatively weak splice site score reduction for the natural splice site predicted by all tools for this particular variant and could be expected as Priors integrates MES scoring. This might also explain the relatively low value for *BRCA1* c.4674A>G as MES scoring was not as distinct compared to the other tools for this variant. We only included two variants affecting splicing; a validation study testing a large number of exonic variants for aberrant splicing would allow to gain more insight in a possible threshold above which a strong correlation between *in silico* prediction and aberrant mRNA splicing exists.

To conclude, we confirmed aberrant splicing for 12 out of 21 tested DNA alterations suggesting that these variants may be associated with a pathogenic effect. Further evidence may come from multifactorial likelihood analysis. We demonstrated that *in silico* prediction tools may assist in the evaluation of putative splice site mutations. But the specificity of *in silico* predictions for variants outside the canonical splice sites is lower. Of all consulted tools,

Adaboost and Random Forest scored best in our cohort to indicate which variants in the Cartegni consensus region are expected to lead to aberrant splicing, but can currently not be used for variants outside these regions. Presently, mRNA analysis remains necessary to verify *in silico* predictions and to determine the exact effect and allele specific transcript expression. Our study is the first to reveal actively used cryptic splice donor sites within the large exon 11 of *BRCA2*. This finding opens perspectives for new research on the identification of *cis* and *trans* acting factors involved in correct splicing of this large exon.

Acknowledgements

The authors wish to thank the patients for donating a blood sample.

This study was supported by a grant from “Stichting tegen Kanker” (2012-216). This work was partially founded by a CIBERER grant (ER17P1AC7112/2017), given to A.V.

EM and LF are supported by MH CZ - DRO (MMCI, 00209805) and by the project MEYS - NPS I - LO1413.

References

- Baert, A. et al., 2016. Increased chromosomal radiosensitivity in asymptomatic carriers of a heterozygous *BRCA1* mutation. *Breast Cancer Research*, 18(1), p.52.
- Caceres, E.F. et al., 2013. The evolution, impact and properties of exonic splice enhancers. *Genome Biology*, 14(1465–6914 (Electronic)), p.R143.
- Caminsky, N.G., Mucaki, E.J. & Rogan, P.K., 2014. Interpretation of mRNA splicing mutations in genetic disease: review of the literature and guidelines for information-theoretical analysis. *F1000Research*, 3(May 2016), p.282.
- Cartegni, L. et al., 2003. ESEfinder: A web resource to identify exonic splicing enhancers. *Nucleic Acids Research*, 31(13), pp.3568–3571.
- Cartegni, L., Chew, S.L. & Krainer, A.R., 2002. Listening To Silence and Understanding Nonsense: Exonic Mutations That Affect Splicing. *Nature Reviews Genetics*, 3(4), pp.285–298.
- Claes, K. et al., 2003. Differentiating pathogenic mutations from polymorphic alterations in the splice sites of *BRCA1* and *BRCA2*. *Genes Chromosomes and Cancer*, 37(3), pp.314–320.
- Colombo, M. et al., 2014. Comprehensive annotation of splice junctions supports pervasive alternative splicing at the *BRCA1* locus: A report from the ENIGMA consortium. *Human Molecular Genetics*, 23(14), pp.3666–3680.
- Desmet, F.O. et al., 2009. Human Splicing Finder: An online bioinformatics tool to predict splicing signals. *Nucleic Acids Research*, 37(9), pp.1–14.
- Fackenthal, J.D. et al., 2016. Naturally occurring *BRCA2* alternative mRNA splicing events in clinically relevant samples. *Journal of medical genetics*, 53, pp.1–11.

- Fairbrother, W.G., Yeh, R. & Sharp, P.A., 2002. Predictive Identification of Exonic Splicing Enhancers in Human Genes. *Science*, 297, pp.1007–1013.
- Gaildrat, P. et al., 2012. Multiple sequence variants of BRCA2 exon 7 alter splicing regulation. *Journal of Medical Genetics*, 49(10), pp.609–617.
- Di Giacomo, D. et al., 2013. Functional analysis of a large set of brca2 exon 7 variants highlights the predictive value of hexamer scores in detecting alterations of exonic splicing regulatory elements. *Human Mutation*, 34(11), pp.1547–1557.
- Glover, J.N.M., 2006. Insights into the molecular basis of human hereditary breast cancer from studies of the BRCA1 BRCT domain. *Familial Cancer*, 5(1), pp.89–93.
- Goldgar, D.E. et al., 2004. Integrated evaluation of DNA sequence variants of unknown clinical significance: application to BRCA1 and BRCA2. *American journal of human genetics*, 75(4), pp.535–544.
- Hendriks, G. et al., 2014. An efficient pipeline for the generation and functional analysis of human BRCA2 variants of uncertain significance. *Human Mutation*, 35(11), pp.1382–1391.
- Houdayer, C. et al., 2008. Evaluation of in silico splice tools for decision-making in molecular diagnosis. *Human Mutation*, 29(7), pp.975–982.
- Houdayer, C. et al., 2012. Guidelines for splicing analysis in molecular diagnosis derived from a set of 327 combined in silico/in vitro studies on BRCA1 and BRCA2 variants. *Human Mutation*, 33(8), pp.1228–1238.
- Jian, X., Boerwinkle, E. & Liu, X., 2014a. In silico prediction of splice-altering single nucleotide variants in the human genome. *Nucleic Acids Research*, 42(22), pp.13534–13544.
- Jian, X., Boerwinkle, E. & Liu, X., 2014b. In silico tools for splicing defect prediction: a survey from the viewpoint of end users. *Genetics in medicine : official journal of the American College of Medical Genetics*, 16(7), pp.497–503.
- Ke, S. et al., 2011. Quantitative evaluation of all hexamers as exonic splicing elements. *Genome Research*, 21(8), pp.1360–1374.
- Landrum, M.J. et al., 2015. ClinVar: public archive of interpretations of clinically relevant variants. *Nucleic acids research*, 44(1), pp.862–8.
- Liu, X. et al., 2016. dbNSFP v3.0: A One-Stop Database of Functional Predictions and Annotations for Human Nonsynonymous and Splice-Site SNVs. *Human Mutation*, 37(3), pp.235–241.
- Lovelock, P.K. et al., 2006. Genetic, functional, and histopathological evaluation of two C-terminal BRCA1 missense variants. *Journal of medical genetics*, 43(1), pp.74–83.
- Lovelock, P.K. et al., 2007. Identification of BRCA1 missense substitutions that confer partial functional activity: potential moderate risk variants? *Breast cancer research : BCR*, 9(6), p.R82.
- Meher, P.K., Sahu, T.K. & Rao, A.R., 2016. Prediction of donor splice sites using random forest with a new sequence encoding approach. *BioData mining*, 9, p.4.
- Millot, G. et al., 2012. A guide for Functional Analysis of BRCA1 Variants of Uncertain Significance (VUS). *human mutation*, 33(11), pp.1526–1537.
- Pashaei, E. et al., 2016. A Novel Method for Splice Sites Prediction Using Sequence Component and Hidden Markov Model. , pp.3076–3079.
- Perrin-vidoz, L. et al., 2002. The nonsense-mediated mRNA decay pathway triggers degradation of most BRCA1 mRNAs bearing premature termination codons. , 11(23), pp.2805–2814.

- Pertea, M., Lin, X. & Salzberg, S.L., 2001. GeneSplicer: a new computational method for splice site prediction. *Nucleic acids research*, 29(5), pp.1185–90.
- Raponi, M. et al., 2014. BRCA1 exon 11 a model of long exon splicing regulation © 2014 Landes Bioscience . *RNA biology*, 11(4), pp.351–359.
- Reese, M.G. et al., 1994. Improved Splice Site Detection in Genie. *Journal of Computational Biology*, 4(3), pp.311–323.
- Roy, R., Chun, J. & Powell, S.N., 2012. BRCA1 and BRCA2: different roles in a common pathway of genome protection. *Nature reviews. Cancer*, 12(1), pp.68–78.
- Rytelewski, M. et al., 2014. BRCA2 inhibition enhances cisplatin-mediated alterations in tumor cell proliferation, metabolism, and metastasis. *Molecular Oncology*, 8(8), pp.1429–1440.
- Rytelewski, M. et al., 2016. Reciprocal positive selection for weakness - preventing olaparib resistance by inhibiting BRCA2. *Oncotarget*, 7(15), pp.20825–39.
- Shapiro, M.B. & Scnaphy, P., 1987. RNA splice junctions of different classes of eukaryotes: sequence statistics and functional implications in gene expression. *Nucleic Acids Research*, 15(17), pp.7155–7174.
- Soukarieh, O. et al., 2016. Exonic Splicing Mutations Are More Prevalent than Currently Estimated and Can Be Predicted by Using In Silico Tools. *PLoS Genetics*, 12(1), pp.1–26.
- Spurdle, A.B. et al., 2008. Prediction and assessment of splicing alterations: Implications for clinical testing. *Human Mutation*, 29(11), pp.1304–1313.
- Strachan, T. & Read, A., 2010. Nucleic Acid Structure and Gene Expression. In *Human molecular genetics*. Taylor & Francis Group, pp. 1–27.
- Tang, R., Prosser, D.O. & Love, D.R., 2016. Evaluation of bioinformatic programmes for the analysis of variants within splice site consensus regions. *Advances in Bioinformatics*, 2016.
- Théry, J.C. et al., 2011. Contribution of bioinformatics predictions and functional splicing assays to the interpretation of unclassified variants of the BRCA genes. *European journal of human genetics*, 19(10), pp.1052–8.
- Vallée, M.P. et al., 2016. Adding In Silico Assessment of Potential Splice Aberration to the Integrated Evaluation of BRCA Gene Unclassified Variants. *Human Mutation*, 37(7), pp.627–639.
- Vreeswijk, M.P.G. et al., 2009. Intronic variants in BRCA1 and BRCA2 that affect RNA splicing can be reliably selected by splice-site prediction programs. *Human Mutation*, 30(1), pp.107–114.
- Wang, M. & Marín, A., 2006. Characterization and prediction of alternative splice sites. *Gene*, 366(2), pp.219–227.
- Ware, M.D. et al., 2006. Does nonsense-mediated mRNA decay explain the ovarian cancer cluster region of the BRCA2 gene? *Nature*, 25(2), pp.323–8.
- Yeo, G. & Burge, C.B., 2004. Maximum Entropy Modeling of Short Sequence Motifs with Applications to RNA Splicing Signals. *Journal of Computational Biology*, 11, pp.377–394.

PART III:

GENERAL DISCUSSION

1 RADIOSENSITIVITY TESTING

All high to intermediate risk “breast cancer genes” known to date are involved in the DNA damage response pathway. Therefore, heterozygous mutation carriers may show enhanced radiosensitivity associated with an increased carcinogenic risk after exposure to ionizing radiation. Currently used assays to evaluate enhanced chromosomal radiosensitivity in *BRCA1* or *BRCA2* mutation carriers were unable to univocally confirm this hypothesis and furthermore, they do not allow individual radiosensitivity assessment. Several publications are available in the literature applying different cytogenetic techniques to determine *in vitro* chromosomal radiosensitivity. These tests are generally performed in peripheral blood lymphocytes. In this thesis, we propose an alternative assay, the G2 MN assay, for a better evaluation of chromosomal radiosensitivity in lymphocytes of healthy *BRCA1* and *BRCA2* mutation carriers.

1.1 The G2 micronucleus assay

1.1.1 Development of the G2 micronucleus assay

To date, chromosomal radiosensitivity of *BRCA1* and *BRCA2* mutation carriers has been evaluated extensively with the G0 MN assay or the G2 chromatid break assay. All *in vitro* studies cited in the introduction (chapter 4 of the introduction) were performed in lymphocytes of healthy individuals (the control cohort), breast cancer patients with or without a germline mutation and healthy individuals with a *BRCA1* or *BRCA2* mutation. Generally, *in vitro* chromosomal radiosensitivity studies could demonstrate an enhanced radiosensitivity in breast cancer patients. Although, these assays are suitable to compare radiosensitivity between groups (e.g. breast cancer patients vs non-cancer patients), their use to assess individual radiosensitivity is limited due to overlap of MN distributions between the control and test cohort (see Figure 3.1 a) (Baeyens et al. 2002). Thus, in order to evaluate individual radiosensitivity, an arbitrary cut-off must be determined.

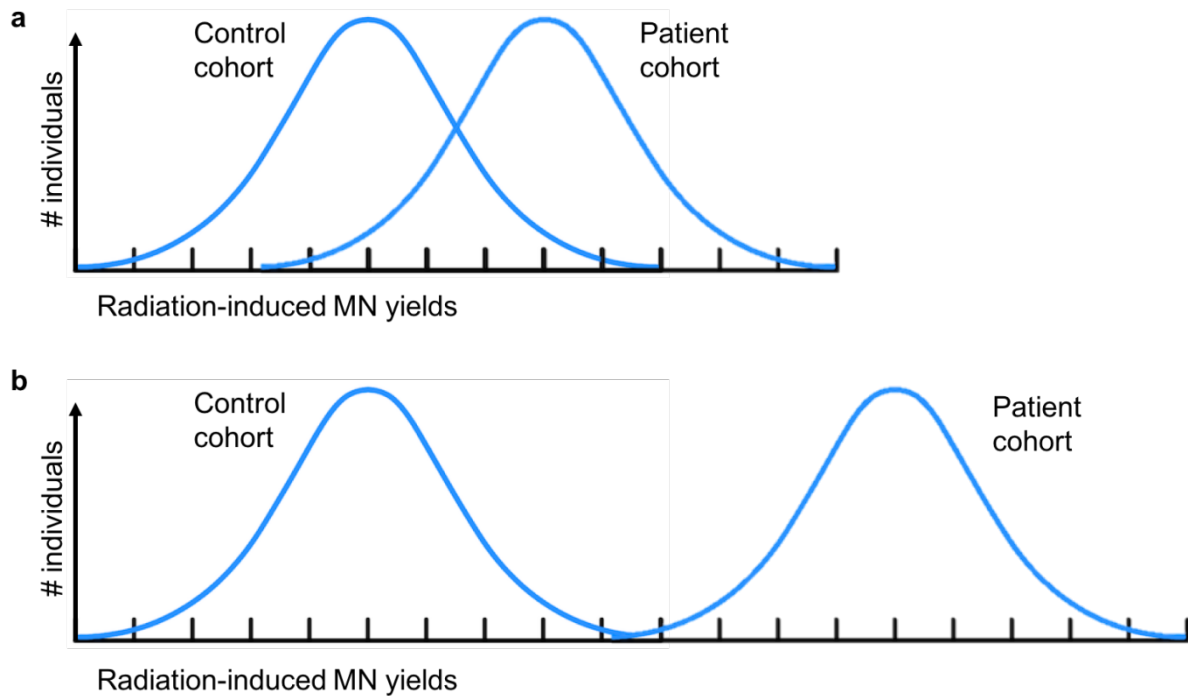


Figure 3.1: simulated representation of the distribution of patient (or test) cohort results compared to control cohort results. (a) two cohort with overlapping radiation-induced MN yields and (b) two cohorts of which the radiation-induced MN yields do not overlap

Studies investigating the effect of a *BRCA1* or *BRCA2* mutation on radiosensitivity either in healthy individuals or breast cancer patients did not yield consistent results (Barwell et al. 2007; Becker et al. 2012; Gutiérrez-Enríquez et al. 2011; Ernestos et al. 2010; Baeyens et al. 2004; Baeyens et al. 2002).

A major limitation of the G0 MN assay to evaluate radiosensitivity in *BRCA1* and *BRCA2* mutation carriers, is the fact that lymphocytes are exposed to ionizing radiation during G0 phase of the cell cycle, while, *BRCA1* and *BRCA2* are mainly active in DNA damage response pathways activated during S and G2 phase of the cell cycle (Roy et al. 2012). The G0 MN assay might thus not be the appropriate assay to evaluate the effect of mutations in *BRCA1* and *BRCA2* on chromosomal radiosensitivity. From this point of view, the G2 chromatid break assay may be better suited. In the G2 chromatid break assay, lymphocytes are cultured 3 days prior to exposure to ionizing radiation and a short post-irradiation incubation time of one hour and a half, is applied. Colcemid is added during the last hour of the post-irradiation incubation in order to stop cells in metaphase for analysis of chromatid breaks. Given the short post-irradiation incubation period, cells trapped in mitosis must have been irradiated in

G2 phase of the cell cycle. Nonetheless, studies applying this assay for the evaluation of radiosensitivity in *BRCA1* and *BRCA2* mutation carriers did not yield univocal results (Buchholz et al. 2002; Barwell et al. 2007; Baeyens et al. 2004; Ernestos et al. 2010). Bryant et al. proposed the 'signal' model to explain the formation of chromatid breaks. In this model, a chromatid break is generated by one DSB initiating a recombinational exchange. This exchange forms a chromatid break when incomplete (Bryant 2004). It is not known if *BRCA1* and *BRCA2* are involved in this mechanism. Furthermore, HR capacity declines when progressing through G2 phase of the cell cycle (Karanam et al. 2012) and as lymphocytes are irradiated in late G2 phase for the G2 chromatid break assay, HR-mediated DSB repair might be minimal.

To optimally evaluate the radiosensitivity phenotype of *BRCA1* and *BRCA2* mutation carriers, we designed a modified MN assay focusing on the S and G2 phases of the cell cycle. With the G2 MN assay, two distinct endpoints: (1) the radiation-induced MN yield and (2) the G2/M checkpoint efficiency ratio (or IRP in paper I), are measured. The first endpoint reflects the DSB repair capacity in these phases of the cell cycle, while the second endpoint allows evaluation of the G2 arrest capacity. The G2 MN assay is described in detail in chapter 5.1.3 of the introduction and the main differences between the G2 and the G0 MN protocol are presented in Figure 3.2.

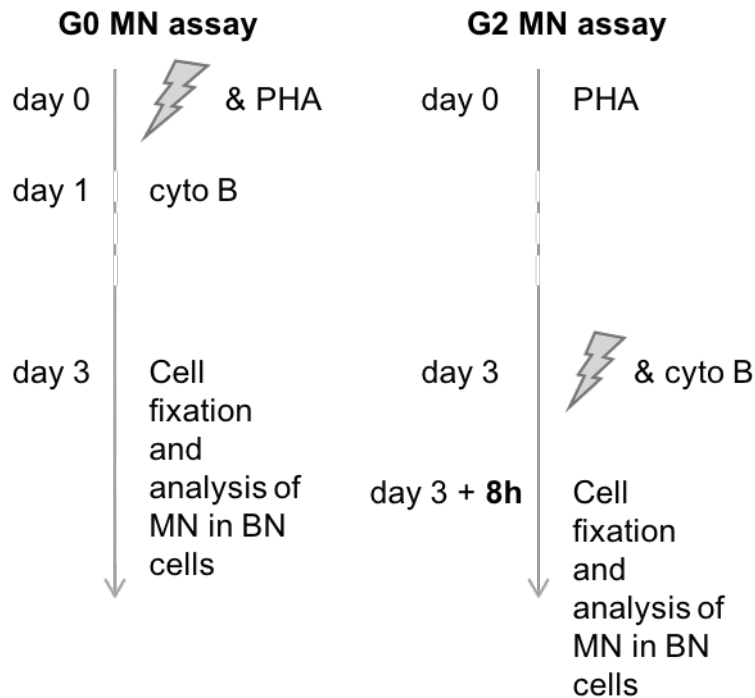


Figure 3.2: schematic overview of the G0 and G2 micronucleus assay protocol

For the determination of the optimal irradiation dose and post-irradiation incubation time, we consulted the literature and performed preliminary experiments in a small control cohort. The cited studies applied doses ranging between 1 and 8 Gy for chromosomal radiosensitivity analysis with 2 Gy as most often used dose point. We selected two dose points, being 2 and 4 Gy ^{60}Co γ -rays.

We stimulated the lymphocytes to proliferate during 3 days by which we obtain a culture with cells in all phases of the cell cycle. After exposure to ionizing radiation and addition of cyto B, we apply a short post-irradiation incubation period of 8 h to allow DSB repair and formation of BN cells (see Figure 3.2). We evaluated the effect of the chosen doses and the short post-irradiation incubation time on the analyzed BN cells by means of a BrdU staining (see Figure 3.3). We were able to establish that 80 – 90% of BN cells were in the G2 phase at time of irradiation (results after exposure to 4 Gy, paper II).

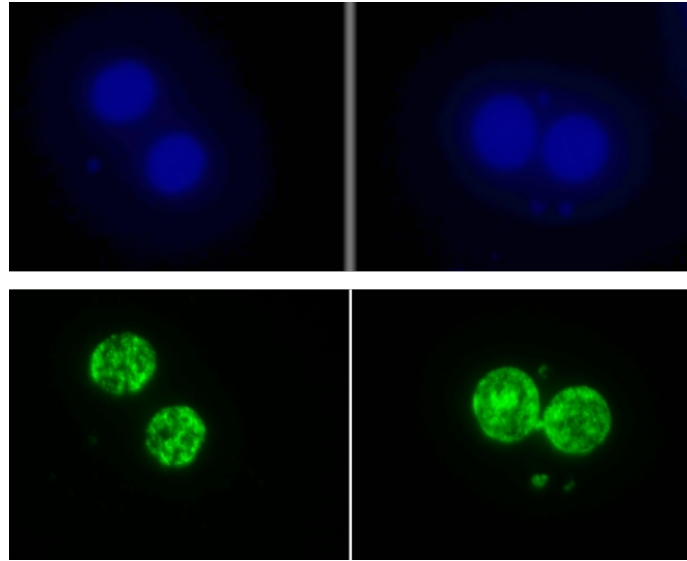


Figure 3.3: Results of the BrdU assay. Cells going through S phase, while BrdU is present in the culture medium, will incorporate the thymidine analog. BrdU incorporation in the DNA can subsequently be evaluated by means of an immunostaining with a BrdU specific antibody. DAPI staining of the nuclei (blue) is shown in the top panel. In the bottom panel, immunostaining for BrdU with a green fluorescent label is visualized (images by Metafer4, Metasystems).

To measure the second endpoint, the G2/M checkpoint efficiency ratio, we added an ATM kinase inhibitor to part of our cultures to abrogate the G2/M checkpoint as ATM inhibition impedes cyclin/Cdk inhibition, required for G2 arrest. Caffeine was selected based on the studies by Terzoudi and colleagues, where the G2 chromatid break assay was combined with caffeine to assess G2 arrest capacity. So far, this approach was successful in AT patients and *ATM* heterozygous mutation carriers (Pantelias & Terzoudi 2011; Terzoudi 2009).

Before applying the assay on a cohort of *BRCA1* and *BRCA2* mutation carriers, we validated the G2 MN assay on lymphocytes of a variant AT patient as AT patients are known to be very radiosensitive and ATM has a role in both HR and G2/M checkpoint arrest. Furthermore, we applied the assay on the patients relatives harboring a heterozygous *ATM* mutation. We compared the performance of the G2-MN assay with the G0 MN assay in parallel cultures and on multiple samplings to evaluate the robustness of the assays.

1.1.2 Validation of the G2 MN assay in an AT patient and its application in heterozygous ATM mutation carriers

Chromosomal radiosensitivity has been demonstrated repeatedly in AT patients as ATM, a key activator of the DNA damage response pathway, is absent or impaired in these individuals (George et al. 2009; Kiuru et al. 2014; Distel et al. 2006; Kühne et al. 2004; Vral et al. 1996). Moreover, AT patients are characterized by such an increased radiosensitivity, that no overlap in MN yields with the control cohort is observed (see Figure 3.1 b). Therefore, the G0 MN assay can be used to evaluate individual radiosensitivity in these patients.

We had access to a variant AT patient, compound heterozygous for two deleterious *ATM* mutations, to evaluate the performance of the G2 micronucleus assay compared to the G0 MN assay (paper I). This variant AT case is atypical as residual ATM kinase activity was demonstrated, which is not the case in classic AT patients. The atypical phenotype of this AT patient was furthermore illustrated by the relatively old age (early twenties) at the time of diagnosis. While radiosensitivity is well documented for classic AT patients, as discussed above, and can be used as a functional assay to phenotypically complement the diagnosis of AT in these patients, only scant data are available on the suitability/sensitivity of radiosensitivity assays to support a diagnosis of AT in patients showing “milder or atypical” forms of the disease (Jongmans et al. 1998; Gilad et al. 1998; Bartsch et al. 2012).

Performing the G0 MN assay on lymphocytes of this variant AT patient, an enhanced radiosensitivity could be demonstrated by a 1.8-fold increased MN yield compared to our control cohort. However, this increase is lower than the 3- to 4-fold increase typically observed in classic AT patients. Evaluation of the first endpoint with the G2 MN assay on three independent samplings demonstrated a 4-fold increase in MN yield for the AT patient compared to the experimental control. Assessment of the G2/M checkpoint efficiency ratio (2nd endpoint) with the G2 MN assay revealed a severely impaired G2 arrest capacity, which is in agreement with the studies by Terzoudi et al., evaluating G2 arrest capacity with the G2 chromatid break assay (Pantelias & Terzoudi 2011; Terzoudi et al. 2011). However, in case of a classical AT patient with no functional ATM, a checkpoint ratio of one is expected which implies a complete disruption of the G2 arrest capacity. The mean ratio observed in our variant AT patient is somewhat higher (1.85), pointing to remaining functionality of this particular checkpoint.

Additionally, we had access to three relatives of the variant AT patient who were heterozygous ATM mutation carriers. Chromosomal radiosensitivity in heterozygous ATM mutation carriers has also been studied extensively. Current studies, evaluating chromosomal radiosensitivity by means of the G2 chromatid break assay, show that these individuals are more radiosensitive compared to a control cohort, though be it less pronounced compared to AT patients. Furthermore, overlap between the patient and control cohort is observed (see Figure 3.1 a) (Pantelias & Terzoudi 2011; Terzoudi et al. 2011; Tchirkov et al. 1997; Sanford et al. 1990; Chen et al. 1994).

Evaluation of G0 MN yields in these heterozygous relatives demonstrated no enhanced chromosomal radiosensitivity. When applying the G2 MN assay, on the other hand, all heterozygous mutation carriers showed increased MN yields and impaired G2 arrest capacity intermediate between our controls and the patient.

A clear difference was noticed between the mother, carrier of the splice site mutation c.8851-1G>T and the father and niece with the missense mutation c.8122G>A (p.Asp2708Asn) as the former was characterized by a higher MN yield and a more pronounced impairment of the G2/M checkpoint. This could be attributed to the fact that no full-length mRNA transcript is transcribed from the allele with the splice site mutation identified in the mother, and no residual kinase activity was derived from the c.8851-1G>T allele in contrast to the c.8122G>A allele. A larger study including a wide range of different ATM mutations would allow a better insight in this phenomenon.

1.1.3 Chromosomal radiosensitivity measured by the G2 MN assay in a cohort of BRCA1 and BRCA2 mutation carriers

Since the G2 MN assay performed well in heterozygous ATM mutation carriers (paper I), and because ATM and BRCA1 and BRCA2 are active in the same DNA damage response pathway, we applied the same test to evaluate chromosomal radiosensitivity in blood samples of healthy BRCA1 and BRCA2 mutation carriers and non-carrier relatives (paper II & paper III). Blood samples of healthy, age and gender matched volunteers without a personal or familial history of breast and ovarian cancer were used to determine the normal distribution of the MN yield and G2/M checkpoint ratio in the general population.

BRCA1

With regard to the first endpoint studied with the G2 MN assay a significant increased radiosensitivity was observed in the cohort of *BRCA1* mutation carriers. Mean radiation-induced MN yields after exposure to both 2 and 4 Gy ionizing radiation are shown in Figure 3.4 (paper II).

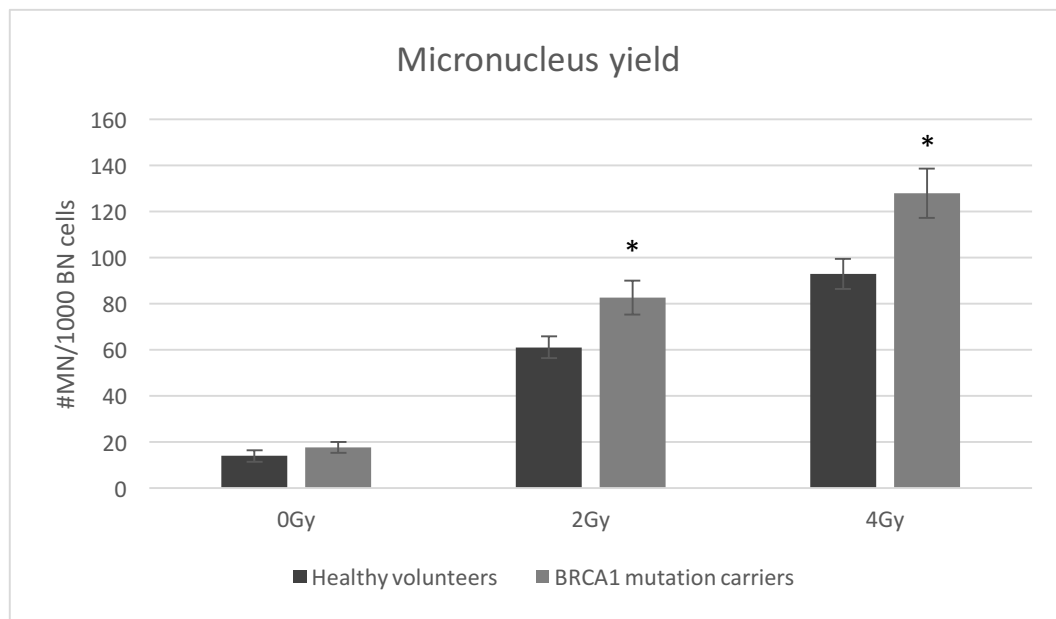


Figure 3.4: MN yields after exposure to 2 or 4 Gy ⁶⁰Co γ-rays. Significant differences compared to the control cohort (p<0.05) are indicated with * (figure from paper II).

Evaluation of the G2/M checkpoint efficiency ratio, the second endpoint, in the cohort of *BRCA1* mutation carriers demonstrated an impaired G2 arrest capacity compared to the control group (paper II).

BRCA2

The radiation-induced MN yield in the cohort of *BRCA2* mutation carriers was significantly increased compared to control individuals after exposure to 2 Gy (see Figure 3.5) (results paper III). Evaluation of the G2 arrest capacity in this test cohort showed no significant difference in the activation of the G2/M checkpoint compared to the controls (e.g. G2/M checkpoint ratio equals 1.8 versus 2.1 respectively after exposure to 2 Gy). These results were anticipated as *BRCA2*, unlike *BRCA1*, is not involved in the G2/M checkpoint activation (reviewed by: (Roy et al. 2012)). Our data do not support the results of Menzel et al. (2011),

to our knowledge the only study suggesting a role for BRCA2 in the G2/M checkpoint (Menzel et al. 2011).

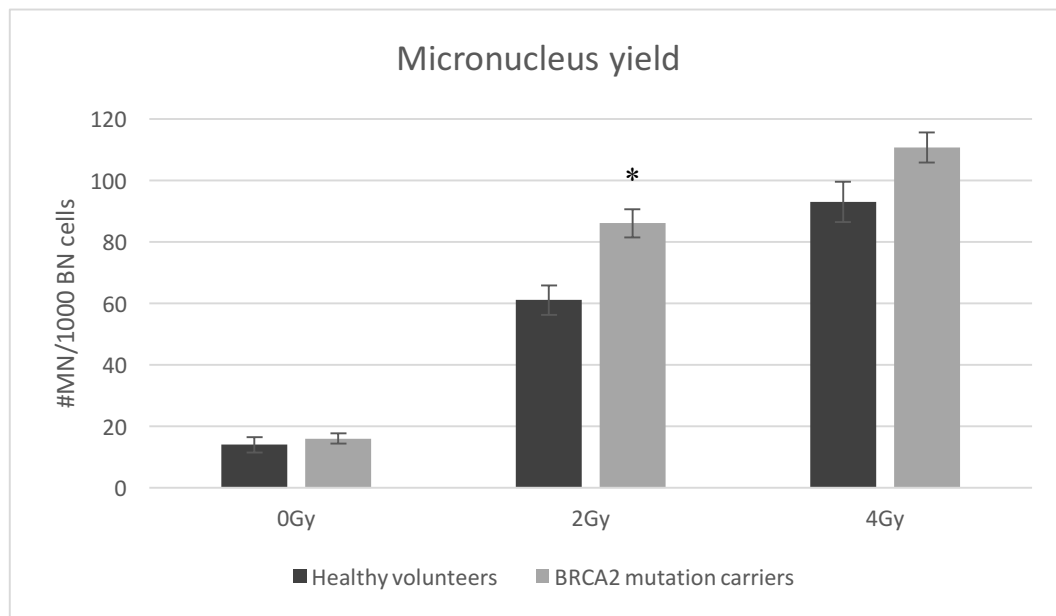


Figure 3.5: MN yields after exposure to 2 and 4 Gy ^{60}Co γ -rays. Significant differences compared to the control cohort ($p < 0.05$) are indicated with * (figure adapted from paper III).

The increase in radiation-induced MN yields after exposure to 4 Gy was not significant in the cohort of *BRCA2* mutation carriers compared to the control cohort and this dose point was therefore not included in paper III. We speculate that the higher dose resulted in a prolonged or irreversible G2 arrest of heavily damaged lymphocytes of *BRCA2* mutation carriers. In *BRCA1* mutation carriers on the other hand, heavily damaged cells are more likely to go through mitosis and become BN due to an impaired G2 arrest. This is illustrated by the observation that out of the eight *BRCA1* mutation carriers for whom an increased radiation-induced MN yield was observed, six also demonstrated an impaired G2 arrest.

The impact of cell cycle delay, and more specifically prolonged G2 arrest, was previously discussed by Nasonova and Ritter as they observed an increase in aberration yields with increasing culture time as more damaged lymphocytes were able to overcome G2 arrest (Nasonova & Ritter 2004). Landsverk et al. demonstrated the existence of a secondary, late activation of G2 arrest capacity, only observed after exposure to doses as high as 4 Gy in B-lymphocyte cancer cell lines. Persistent phosphorylation of Chk1 is proposed to mediate the prolonged G2 arrest (Landsverk et al. 2011). The difference between *BRCA1* and *BRCA2* mutation carriers observed in our cohort, might be inherent to the fact that *BRCA1* is involved

in Chk1 activation upon detection of DNA damage to initiate G2 arrest capacity (Yarden et al. 2002). Furthermore, this late activation of G2 arrest could be overruled by addition of an ATM inhibitor (Landsverk et al. 2011). Interestingly, after exposure to caffeine, mean radiation-induced MN yield for *BRCA2* mutation carriers were comparable to those of *BRCA1* mutation carriers (data not shown).

Taken together, we provide evidence of an enhanced radiosensitivity for both healthy *BRCA1* and *BRCA2* mutation carriers as demonstrated by increased radiation-induced MN yields in the lymphocytes. Furthermore, we speculate that the observed increase in MN yields in healthy mutation carriers, whereas previously G0 studies failed to prove a similar correlation (Gutiérrez-Enríquez et al. 2011; Baeyens et al. 2004), is inherent to our study design. Indeed, several studies evaluating BRCA1 protein levels throughout the cell cycle could demonstrate an absence of BRCA1 in G0 phase of the cell cycle, followed by a modest incline during G1 phase (compared to G0 phase), a major increase during S phase and a maximum protein level during the G2 phase. The cell cycle dependent increase in protein level is based on an induction of mRNA transcription and subsequent translation during G1/S transition. After reaching a peak in G2 phase, BRCA1 protein levels decrease again. This decrease upon entering of the G1 phase is mediated by a decline in mRNA transcription and protein degradation by proteases and ubiquitination (Choudhury et al. 2004; Liu et al. 2010; Okada & Ouchi 2003). Several papers also evaluated BRCA1 stability after exposure to ionizing radiation independent of the cell cycle. These papers describe that exposure to high doses resulted in degradation of BRCA1, presumably to facilitate radiation-induced apoptosis. Exposure to doses below 5 Gy did not influence protein levels, which is important information in respect to our experimental set-up (Liu et al. 2010; Okada & Ouchi 2003).

In addition to variation in expression of BRCA1 protein levels inherent to the cell cycle, posttranslational modifications, in function of the cell cycle, further enhance the cell cycle dependent activation of this protein. The principal posttranslational modification of BRCA1 is phosphorylation, which occurs at several amino acid sites (see Figure 3.6). Current working hypothesis is that in its hypo-phosphorylated form, found in G1 phase of the cell cycle, BRCA1 is involved in the activation of c-NHEJ, while its hyper-phosphorylated isoform, induced by cell cycle transition and/or in response to DNA damage, mediates HR during S and G2 phase

of the cell cycle (see Figure 3.7) (Zhang et al. 2004; Saha & Davis 2016). Key proteins responsible for phosphorylation of BRCA1 are ATM and checkpoint kinase 2 (chk2) (Zannini et al. 2014; Zhang et al. 2004; Summers et al. 2011).

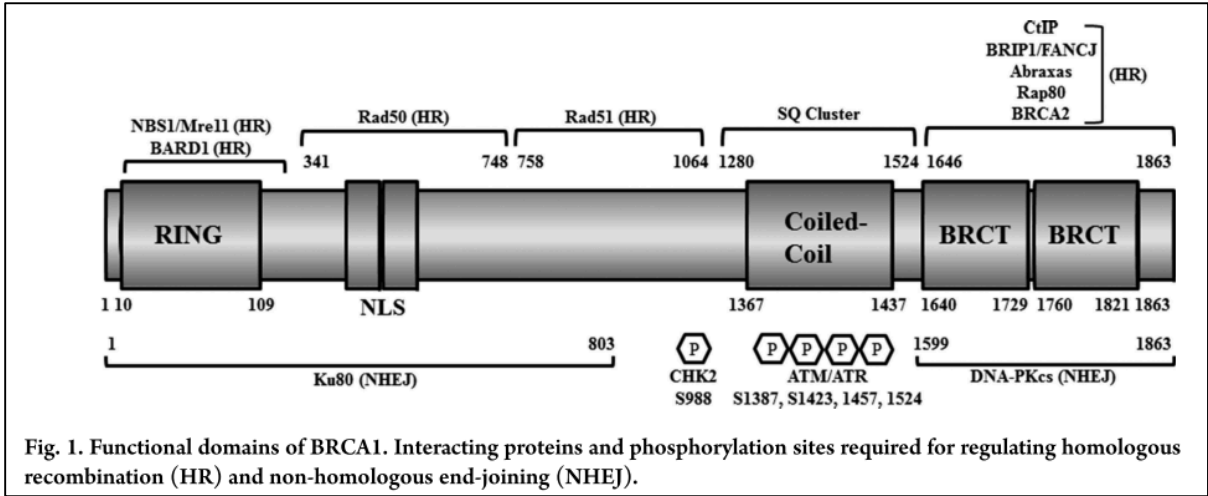


Figure 3.6: Overview of the functional domains, the interacting proteins and phosphorylation sites of BRCA1 (Saha & Davis 2016).

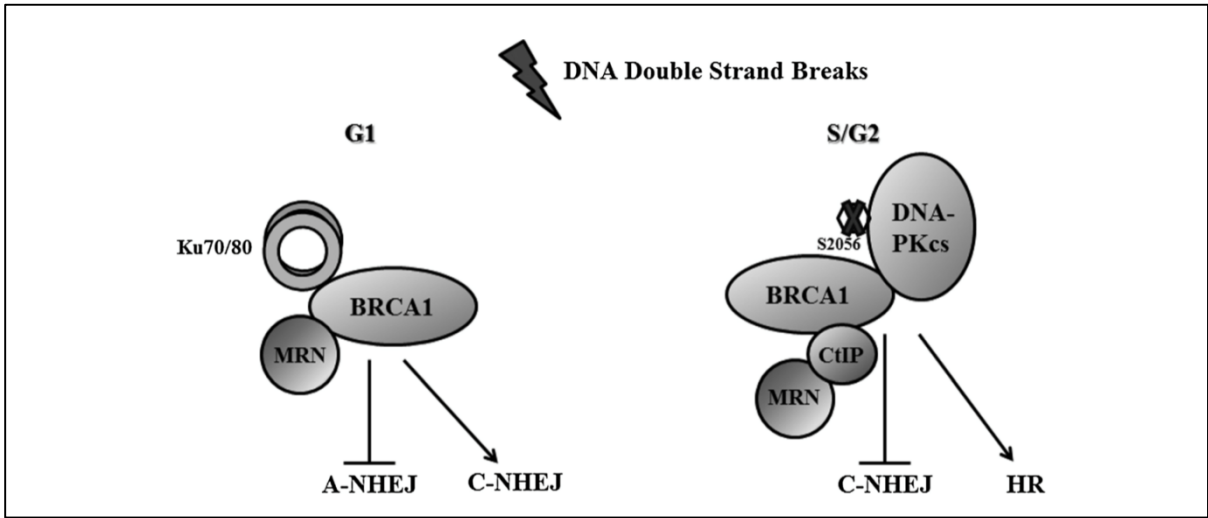


Figure 3.7: BRCA1 interactions during G1 and S/G2 phase for repair of radiation-induced DSB. In the absence of HR (during G1 phase), interaction of BRCA1 with Ku80 and the MRN complex promotes the C-NHEJ pathway, while downregulating mutagenic A-NHEJ. In S phase, the interaction of BRCA1 with DNA-PKcs inhibits C-NHEJ, thereby redirecting the pathway choice towards HR pathway. Either way, BRCA1 induces the activation of the least error prone pathway throughout all stages of the cell cycle (Saha & Davis 2016).

Concerning BRCA2 protein expression, less data are available. One study demonstrated a more or less steady expression in cycling cells for all phases of the cell cycle (Esashi et al. 2005), but no data for G0 cells are available in literature. Although steady levels of BRCA2

protein are detected throughout all phases of cycling cells, BRCA2 activity, like BRCA1, is regulated by posttranslational modifications. Current studies suggest a role for cyclin-dependent kinases (Cdk), checkpoint kinases (Chk1 and Chk2) and Plk1 (Polo-like kinase 1) in response to DNA damage and cell cycle progression for phosphorylation of BRCA2 at various amino acid sites (see Figure 3.8) (Esashi et al. 2005; Lee et al. 2004). The Cdk and Plk1-mediated phosphorylation seems to be upregulated in G2 phase of the cell cycle and is maximal during M phase where it impairs RAD51 interaction, directing BRCA2 towards a different role in this phase of the cell cycle. This alternate function in mitosis mediates chromosome condensation and stabilization and/or segregation (Lee 2014; Esashi et al. 2005; Lee et al. 2004). Induction of DNA damage impairs Plk1 and CDK-dependent phosphorylation of BRCA2, enhancing the DNA damage response function of BRCA2. This is mediated by Chk1 and Chk2 phosphorylation of the C-terminus of BRCA2 in response to ionizing radiation, crucial for RAD51 recruitment and interaction (Zannini et al. 2014).

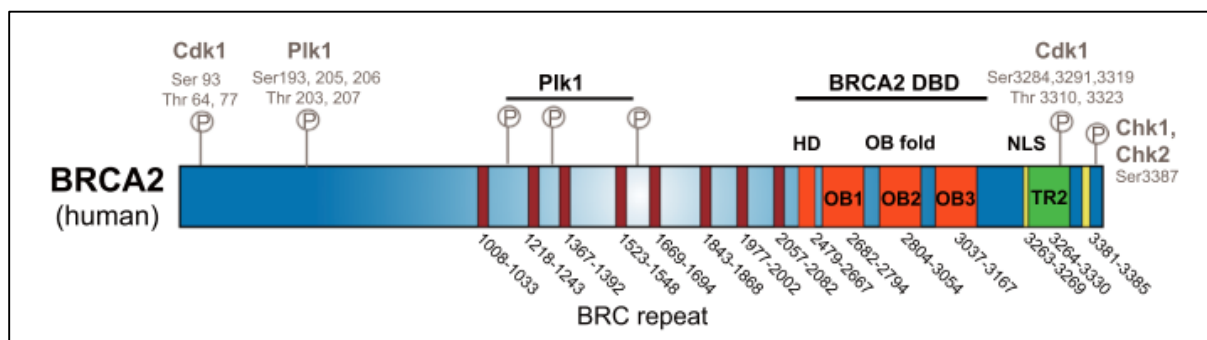


Figure 3.8: Overview of the functional domains, interaction partners and phosphorylation sites of BRCA2 (Lee 2014).

Several studies discussed in this chapter demonstrate BRCA1 and BRCA2 activation and HR mediated DSB repair upon induction of complex DSB by ionizing radiation. We therefore speculate that the enhanced radiosensitivity, observed by increased MN yields detected with the G2 MN assay in mutation carriers, is indeed due to an impaired HR capacity resulting in less efficient repair of DSB and – as a consequence – an increased MN yield. The enhanced radiosensitivity phenotype of *BRCA1* mutation carriers can furthermore be attributed to an impaired G2 arrest capacity as demonstrated by a significantly decreased G2/M checkpoint efficiency ratio. This cell cycle dependent activation of both proteins not only strengthens our theory that the G2 MN is a better suited assay to evaluate radiosensitivity in healthy *BRCA1* and *BRCA2* mutation carriers compared to the G0 MN assay, it also indicates that the

radiosensitive phenotype observed with the G0 MN assay in breast cancer patients with a *BRCA1* or *BRCA2* mutation is not due to the mutation status, but might be inherent to the cancer status (Baeyens et al. 2004).

However, caution is needed when interpreting the results of the studies cited above with respect to our studies in lymphocytes as most experiments were conducted in cancer cell lines (e.g. breast cancer cell line MCF7 and cervical cancer cell line Hela). As far as we are aware no such studies were conducted in non-cancerous breast epithelial cell lines or lymphocytes.

1.1.4 Chromosomal radiosensitivity measured by the G2 MN assay in non-carriers

In paper III, *in vitro* chromosomal radiosensitivity of a group non-carrier relatives of both *BRCA1* (n=9) and *BRCA2* (n=8) families was investigated to evaluate whether the observed increase in radiation-induced MN yields in mutation carriers is linked to the mutation status. No significantly increased radiation-induced MN yields were observed compared to healthy individuals without a personal or familial history of breast or ovarian cancer ($MN_{2Gy}=68$ versus $MN_{2Gy}=61$). Radiosensitivity in non-carrier relatives was previously only evaluated in one study. This study reported no increased radiosensitivity measured with the G0 MN and G2 chromatid break assay in a small cohort (n=10) of relatives of both *BRCA1* and *BRCA2* families without the familial mutation when compared to a population cohort (Baeyens et al. 2004) and is in agreement with our results.

The mean radiation-induced MN yield was higher for *BRCA2* mutation carriers than for non-carrier relatives, but this difference was not significant because of the relatively large inter-individual variation. The relatively high inter-individual variation was observed in all tested cohorts and could be inherent to the assay (see chapter 1.1.4 of the general discussion) or may be the result of genetic modifiers influencing radiosensitivity given that MN formation can be the result of defects in various DNA damage response pathways. Previous research has demonstrated that selected SNPs in DNA damage repair genes and other common variants may be associated with an increased radiosensitivity. For example, data from Willems et al. demonstrated that specific SNPs in Ku70 and Ku80, involved in c-NHEJ, result in an increased breast cancer risk and an enhanced chromosomal radiosensitivity, observed by an increase in G0 MN yields (Willems et al. 2008). Furthermore, Popanda et al. demonstrates, in

his review, a clear influence of certain SNPs in *ATM* and other numerous DNA damage response genes on radiosensitivity. In these studies, radiosensitivity is demonstrated by an increase in adverse side effects of radiotherapy in carriers (Popanda et al. 2009). Furthermore, a limited number of studies demonstrated an increased breast cancer incidence in these non-carriers compared to a control cohort (Smith et al. 2007; Vos et al. 2013; Evans et al. 2013), which might also be attributed to the presence of modifiers such as SNPS or other genetic alterations.

1.1.5 *G2 MN assay for individual assessment of radiosensitivity*

In addition to the evaluation of chromosomal radiosensitivity on a cohort-level, we aimed to develop an assay applicable in a clinical setting for the individual assessment of radiosensitivity. Unfortunately, MN distribution of mutation carriers and controls overlap (see Figure 3.1 a), so to define an individual radiosensitivity phenotype, a radiosensitivity scoring system was developed.

In *BRCA1* mutation carriers, individual radiosensitivity assessment (Radiosensitivity INDicator (RIND) scoring) is based on both endpoints of the G2 MN assay taking into account DNA repair and G2 arrest capacity after exposure to 4 Gy. This RIND score varies between 0 and 4 whereby a RIND score of 0 correlates with no increased radiosensitivity and a RIND score of 4 equals a severely increased radiosensitivity. Scores varying between 1 and 3 correlate to different grades of mild or moderate increased radiosensitivity. Applying this scoring system, 72% of *BRCA1* mutation carriers show some degree of radiosensitivity (RIND score 1-4). Furthermore, 28% *BRCA1* mutation carriers demonstrated RIND scores of 3 and 4, scores which were never observed in healthy individuals (see Figure 3.9, paper II).

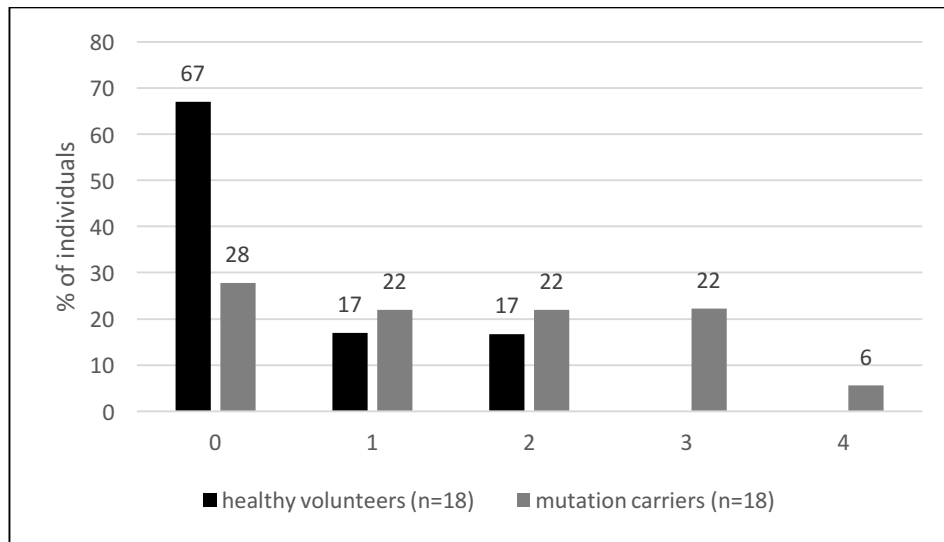


Figure 3.9: Individual radiosensitivity scoring based on RIND scores after exposure to 4 Gy ^{60}Co γ -rays for healthy volunteers and *BRCA1* mutation carriers (paper II).

For *BRCA2* mutation carriers and non-carriers, individual radiosensitivity scoring (RS score) is based on the results of the radiation-induced MN yields after exposure to 2 Gy (see Figure 3.10). An RS score of 0 correlates to no increased radiosensitivity, an RS score of 1 indicates a milder radiosensitive phenotype and an RS score of 2 reflects a more severe radiosensitive phenotype. *BRCA2* mutation carriers are characterized by an increased RS score compared to the controls demonstrated by 50% of mutation carriers showing an RS score of 1 or 2, whereas 83% of controls are not radiosensitive (RS-score=0). RS scores of non-carriers do not significantly differ from scores observed in the control cohort. This scoring system can be valuable in assisting physicians in their decision-making regarding the diagnostic and therapeutic exposure to ionizing radiation at the individual level.

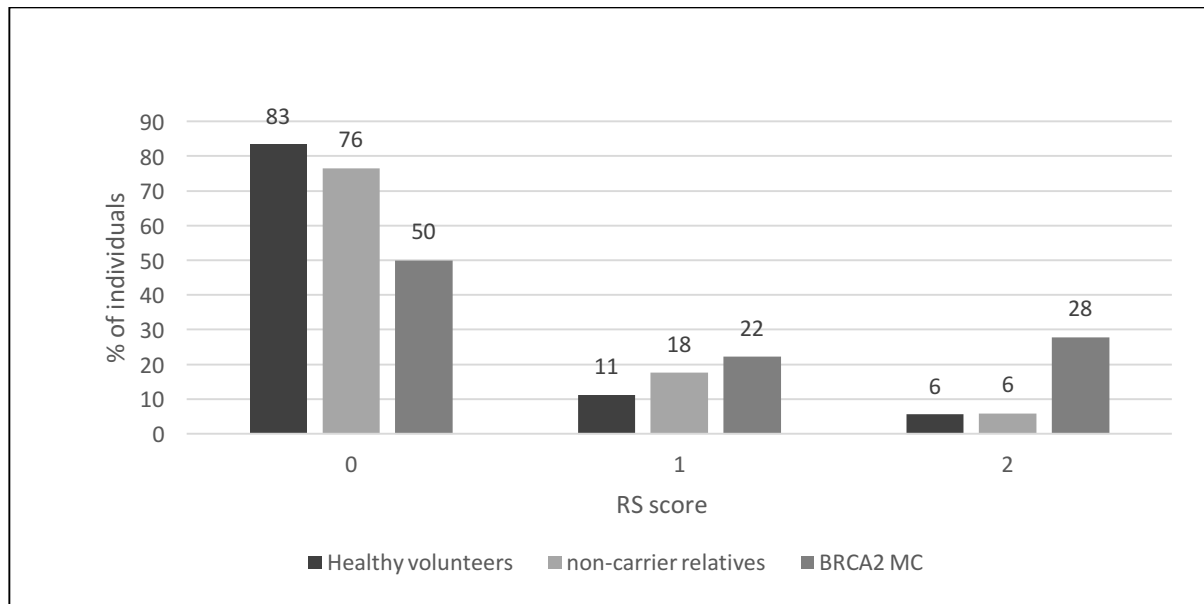


Figure 3.10: Individual radiosensitivity (RS) scoring for healthy volunteers, non-carriers and *BRCA2* mutation carriers (paper III).

Overlapping MN distribution have also been observed in the past with the G0 MN assay when comparing RS in breast cancer patients with healthy controls. In these studies, an arbitrary cut-off, typically the 90th percentile of the MN distribution from the healthy control cohort, was determined to assess individual radiosensitivity (e.g. (Baeyens et al. 2002)).

Vral and colleagues previously demonstrated that a major – but intrinsic – problem of the G0 MN assay is its high intra-individual variability, which determines the reproducibility of the assay (Vral et al. 2002; Vral et al. 2004). The observed intra-individual variation can be attributed to different factors such as the cell/serum balance in blood samples, influenced by immune status and diet (Fenech 1999; Roberts et al. 1997). These factors may also contribute to intra-individual variation observed with the G2 MN assay. Intra-individual variation can be reduced by evaluating the results in multiple blood samples from a single individual. To assess intra-individual variation for the G2 MN assay, we performed multiple testing of seven healthy volunteers and four *BRCA1* mutation carriers. Despite variations observed in the radiation-induced MN yields and G2/M checkpoint ratios between multiple samplings, no significant differences in RIND scores were observed when comparing all repeats. To reduce random variation, our MN values were always based on results obtained in two parallel cultures set up for every blood sample, as was previously suggested by Vral et al. (Vral et al. 2002).

Furthermore, variations in genetic background will also contribute to differences in radiosensitivity (see chapter 1.1.3 of the discussion), complicating individual assessment of radiosensitivity related to a specific *BRCA1* or *BRCA2* mutation. In paper II and III, we demonstrated that non-related individuals with the same mutation can exhibit different RIND/RS phenotype. Furthermore, related mutation carriers do not necessarily show an identical RS/RIND score. Given the numerous pathways involved in the formation of MN, ideally a very large study is required on mutation carriers, non-carrier relatives and unrelated controls, to link the results of a radiosensitivity assay with whole genome/transcriptome/epigenome data to identify potential genetic modifiers influencing the radiosensitive phenotype. However, the statistical processing of the vast amount of data will be challenging.

As shown in this discussion, the G2 MN assay has some limitations. Therefore, we decided that a test evaluating more directly the HR capacity in lymphocytes of mutation carriers could be useful.

1.2 The RAD51 foci assay to assess radiosensitivity in cells with reduced *BRCA1* and *BRCA2* protein levels

Activation of HR upon exposure to ionizing radiation and the impact of *BRCA1* and *BRCA2* has been discussed in chapter 3.3.2.2 of the introduction and in chapter 1.1.3 of the general discussion. Recently, a RAD51 foci assay has been developed to allow evaluation of HR activity. Performed on tumor biopsies irradiated *ex-vivo*, the RAD51 foci assay allows to identify HR deficient tumors. This may facilitate the selection of patients eligible for PARP inhibition treatment, a cancer treatment strategy based on synthetic lethality in HR deficient tumor cells (Willers et al. 2015). Furthermore, in a small number of studies, the assay was used to evaluate radiation-induced RAD51 foci formation in heterozygous *BRCA1/2* cell lines (Vaclová et al. 2015; Warren et al. 2003; Sioftanos et al. 2010).

In paper IV, we investigated the suitability of the RAD51 foci assay to evaluate HR capacity in MCF10A cells with reduced protein levels of *BRCA1* and *BRCA2*, obtained by RNA interference. Cells were synchronized in S phase of the cell cycle prior to exposure to ionizing radiation by means of aphidicolin as HR activation for repair of DSB is maximal in this cell cycle phase (Mao

et al. 2008; Karanam et al. 2012). We demonstrated that BRCA1 and BRCA2 knockdown cell lines are characterized by a diminished HR activity after exposure of synchronized cells to ionizing radiation. Moreover, whereas a doubling in RAD51 foci after exposure to ionizing radiation can be detected for the control cells, no radiation-induced foci were observed for the knockdown cell lines (see Figure 3.11). We also showed that synchronization of the MCF10A cells resulted in an increase of RAD51 foci compared to non-synchronized cells. This can be attributed to a higher number of S phase cells applying HR for repair of endogenous and aphidicolin-induced DSB.

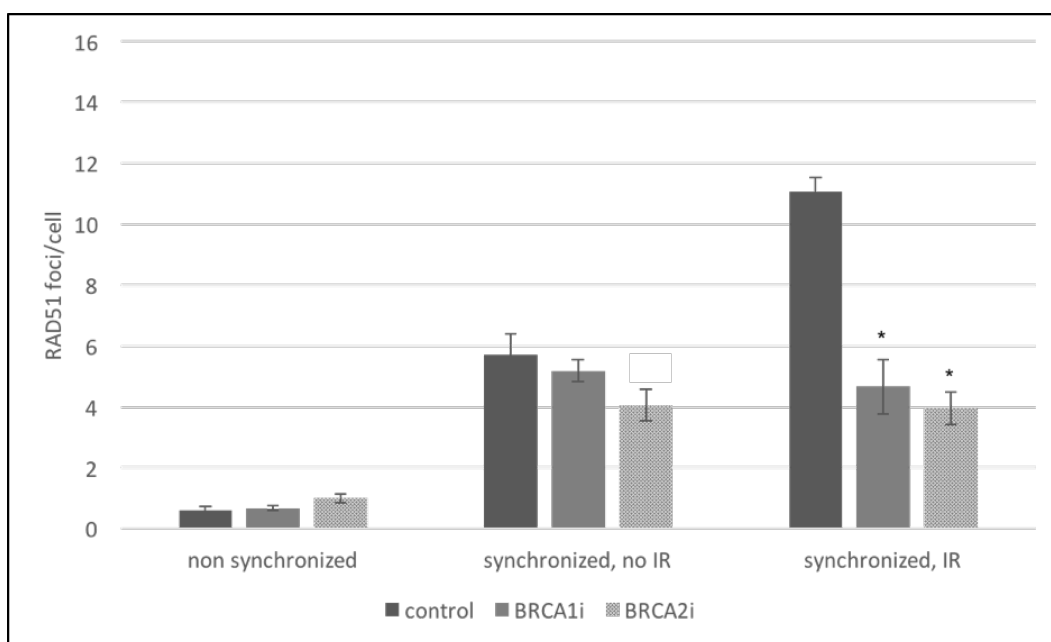


Figure 3.11: results of the RAD51 foci assay. Significant differences, compared to the control cell line ($p < 0.05$), are indicated with * (figure adapted from paper IV). IR: Ionizing radiation

Our data obtained in MCF10A cells support the hypothesis that application of the RAD51 foci assay on synchronized lymphocytes of heterozygous *BRCA1* and *BRCA2* mutation carriers might be promising to evaluate HR functionality and radiosensitivity. Additionally, the absence of overlap between the results of the control versus the BRCA knockdown cells, shown in Figure 3.12, implies that this assay might be better suited for individual radiosensitivity assessment. Furthermore, this assay could be applied for the evaluation of HR capacity in individuals with mutations in other genes involved in HR such as PALB2. The evaluation of HR activation in lymphocytes with the RAD51 foci assay after exposure to ionizing radiation might also shed light on their sensitivity for PARP inhibitor treatment as

these individuals might develop breast tumors characterized by HR deficiency and PARP inhibitor sensitivity.

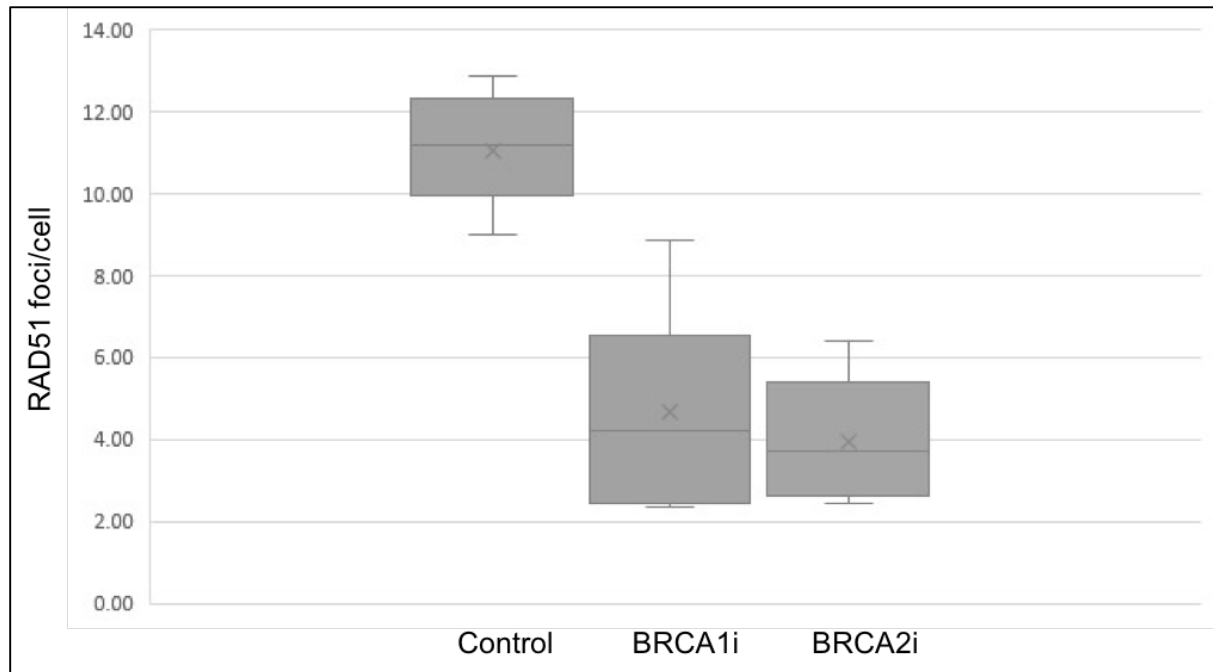


Figure 3.12: Boxplot of all results of the RAD51 foci assay (synchronized and exposed to 2 Gy) based on eight repeats per cell line. No overlap is observed in RAD51 foci yields for the control versus the knockdown cell lines. (results used for this boxplot come from paper IV)

Attempts to discriminate even better between BRCA knockdown cell lines and control cell lines by specifically inducing HR activation through PARP inhibition were unsuccessful as no significant increase in RAD51 foci were obtained after combined treatment with a PARP inhibitor and ionizing radiation compared to ionizing radiation alone (paper IV). This might be attributed to exhaustion of HR activation due to protein depletion after aphidicolin synchronization and exposure to ionizing radiation. Moreover, in BRCA knockdown cell lines and not for the control cell line, synchronization alone seems to be sufficient for exhaustion of the HR pathway. We speculate that BRCA1 or BRCA2 protein levels might be the limiting factors in the activation of HR in this particular setting. A number of studies describe BRCA1 and BRCA2 protein levels throughout the cell cycle (Esashi et al. 2005; Choudhury et al. 2004; Liu et al. 2010; Okada & Ouchi 2003). However, evaluation of BRCA1 and BRCA2 protein levels in MCF10A cells and lymphocytes in response to ionizing radiation would need to be conducted for further investigation.

The absence of a significant induction of RAD51 foci when comparing synchronized cells with synchronized cells exposed to a PARP inhibitor (paper IV) may point towards another possible explanation, inherent to the inhibition itself. As discussed in the introduction (chapter 3.3.2.4), PARP is involved in numerous pathways. The effect of PARP inhibition treatment predominantly relies on the inhibition of BER and the failure to repair SSB. These SSB subsequently result in stalled replication forks during synthesis and the formation of single-ended DSB, that are exclusively repaired by HR (see Figure 3.13 (1)) (Murai et al. 2012; Pommier et al. 2016). However, PARP is also important in the stabilization of replication damage repair and DSB repair. Unfortunately, the complex network mediating these PARP functions is not completely understood and inhibition of PARP might interfere with initiation of HR and RAD51 foci formation (Pommier et al. 2016; Khodyreva & Lavrik 2016). Furthermore, we must consider PARP trapping during inhibition. Application of several PARP inhibitors, including Olaparib, results in PARP trapping (see Figure 3.13 (2)) (Murai et al. 2012; Pommier et al. 2016). PARP trapping does not only result in the inhibition of PARP function, but also retains PARP at the site of the DNA damage (single strand break, double strand break or replication damage) (Murai et al. 2012; Murai et al. 2013). This might be caused by binding of the inhibitor at the NAD⁺ site, necessary for the parylation activity of PARP and/or allosteric conformational changes resulting in a stabilized DNA-PARP complex (Murai et al. 2012). Although studies demonstrated that PARP trapping might be more deleterious than the mere inhibition of its function, this is not fully understood (Murai et al. 2012; Pommier et al. 2016). One possibility is the replication fork collision with the PARP-DNA complexes, resulting in a collapse and single ended DSB. However, as the net effect is not different than that of inhibition alone, it does not explain the additional cytotoxicity granted to PARP trapping. Another possibility is the inclusion of other proteins in the PARP-DNA complexes which might render these complexes difficult to remove (Pommier et al. 2016; Murai et al. 2012). We stipulate that the presence of such a complex at the stalled replication fork would impede repair of the induced single ended DSB. However, limited information regarding repair and repair kinetics of PARP-DNA complexes has been published. Murai et al. proposes a repair model based on different mechanisms including, besides HR, the Fanconi Anemia pathway (FA), template switching (TS) and proteins such as ATM, FAN1 and Polymerase β (POLB) (see Figure 3.13 (2)) (Murai et al. 2012).

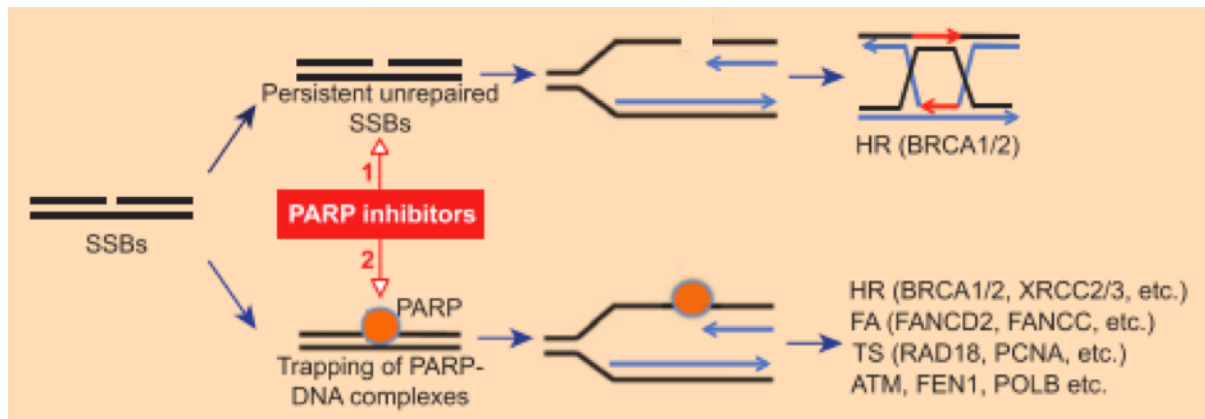


Figure 3.13: PARP inhibition: (1) inhibition by inactivation of PARP function and BER (see text) and (2) inhibition by PARP-trapping (see text).

Finally, we must consider the effect of aphidicolin synchronization on PARP inhibitor treatment. Although aphidicolin is washed away from the culture medium at the time the cells are exposed to a PARP inhibitor and/or ionizing radiation, their respective effect on a mutual target, being the replication fork, should be considered. Aphidicolin impairs replication fork functionality by inhibition of DNA polymerase while PARP stabilizes the replication fork. Inhibition of PARP then results in the inhibition of single strand break repair, which leads to replication fork collapse during synthesis.

The absence of a PARP inhibitor specific effect on HR may also be inherent to our assay set-up, in which we apply the RAD51 foci assay in control and BRCA1/2 knockdown breast epithelial cells with residual protein expression. Up to now, all literature referring to the RAD51 foci assay and PARP inhibition is limited to tumor biopsies from patients with germline BRCA1 mutation. The loss of functional BRCA1 or BRCA2 in the tumor cells results in HR-deficiency which renders the tumor cells sensitive to PARP inhibitors due to synthetic lethality (Pommier et al. 2016).

1.3 The carcinogenic risk of medical exposure to IR of *BRCA1* and *BRCA2* mutation carriers
Pathogenic mutations in DNA damage response genes such as *BRCA1* and *BRCA2*, resulting in impaired DNA damage response may contribute to genomic instability and carcinogenesis (Aparicio et al. 2014). By means of the G2 MN assay, we provided evidence that pathogenic *BRCA1* and *BRCA2* mutations result in an increased radiosensitivity.

In these papers, doses of 2 and 4 Gy ^{60}Co γ -rays were used. These doses are considerably higher than those received by diagnostic exposure to ionizing radiation (see introduction, doses varying between 1 and 30 mSv), by which direct extrapolation of our results to the risks of diagnostic exposure is not possible. Nevertheless, such high doses are necessary to induce sufficient DNA damage to obtain a measurable impact with the assays used in this study in our control and test cohort. Furthermore, this fits in our original scope to develop a biomarker for the evaluation of “individual” radiosensitivity. Although we did not evaluate the response of doses lower than 2 Gy, it has been shown that even at the very low doses used in diagnostic settings, DNA damage in the form of DSB is induced. Rothkamm and Löbrich demonstrated that doses as low as 1 mGy of 90 kV X-rays induce DSB in primary fibroblast cultures, observed by γH2AX foci staining (Rothkamm & Löbrich 2003).

A major contributor of exposure to ionizing radiation in a diagnostic setting in woman at high risk of breast cancer is mammography screening. Mammography screening is offered to individuals at high risk and starts at young ages (see chapter 1.5.2 of the introduction) as they are at risk of early onset breast cancer. Despite the relatively low mean glandular dose of one mammography screening (± 4 mGy per breast), its carcinogenic risk cannot be discarded as the repetitive nature of this screening method results in a considerable cumulative dose in individuals starting mammography screening at young age. Furthermore, breasts of younger women are also denser which complicates proper screening, indicated by a decreased sensitivity (Carney et al. 2003). Taking additional images for a better screening evaluation or the application of a higher dose for a higher resolution image will increase the total glandular dose (personal communication).

Additionally, we should consider the fact that 30 kV X-rays used in mammography screening have a higher RBE than ^{60}Co γ -rays, typically used to perform risk assessments. As mammography X-rays are characterized by a higher RBE, they induce more complex DSB compared to ^{60}Co γ -rays, demonstrated by Depuydt et al. (see Figure 3.14) (Depuydt et al. 2013).

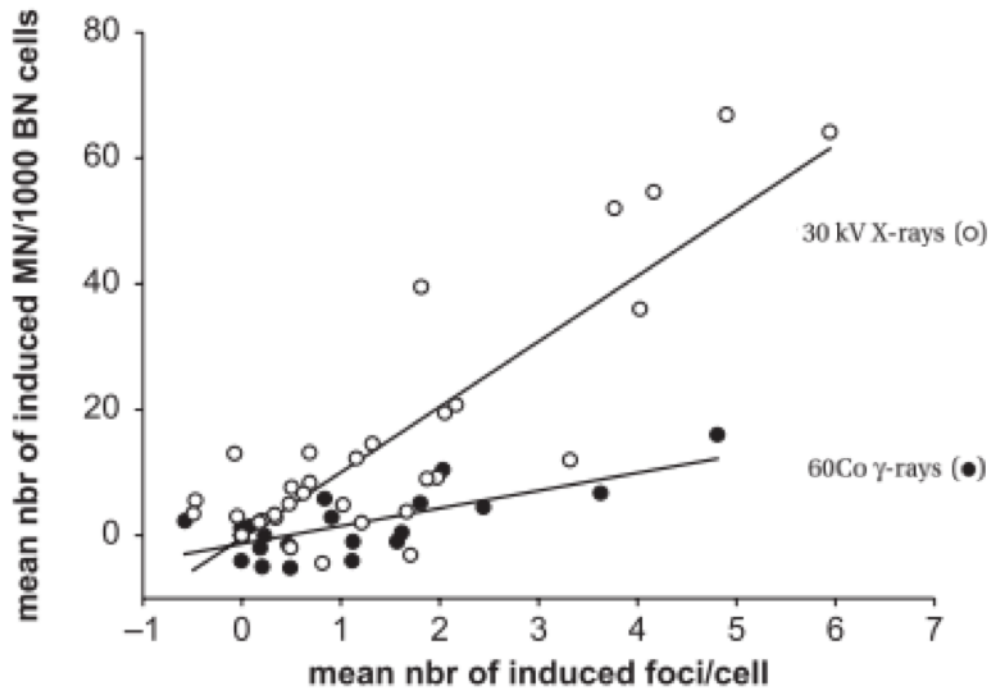


Figure 3.14: Mean number of MN/1000 BN cells in function of the mean number of foci/cell in lymphocytes for both radiation qualities. Mammography-induced DSB, quantified by means of the γ H2AX foci assay, were reported to yield a higher number of MN, compared to an equal amount of induced γ H2AX foci by ^{60}Co γ -rays (doses vary from 5 to 2000 mGy) (Depuydt et al. 2013).

Finally, we have to take into account that current risk evaluations are based on a linear no threshold hypothesis and do not take into account a possible bystander effect which could lead to a low-dose hypersensitivity in breast glandular tissue (Averbeck 2009). Breast epithelial cells are highly organized and are characterized by gap junction-mediate cell-cell communication which might leave these cells prone to bystander effects (Defamie et al. 2014). Indeed, recent research by our group demonstrated that breast epithelial cells lining the duct are characterized by a low dose hypersensitivity (see Figure 3.15) (Depuydt et al. n.d.). This would imply an underestimation of the carcinogenic risk of low doses of 30 kV mammography X-rays.

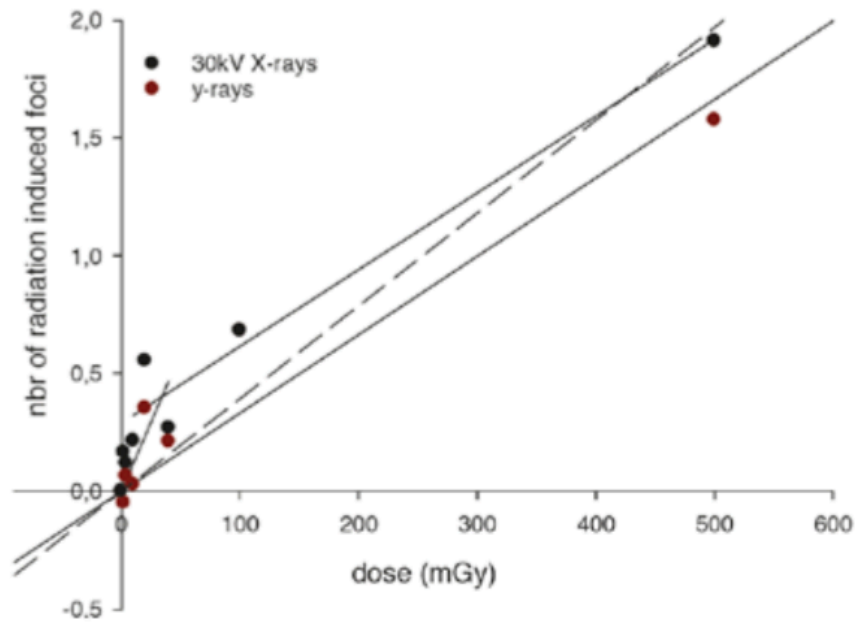


Figure 3.15: dose-response curve for γ H2AX foci-induction after exposure of breast tissue to ^{60}Co γ -rays and 30 kV X-rays. The dose-response curve for each quality is visualized in full lines and demonstrates a biphasic nature for 30 kV X-rays. The dashed line demonstrates the linear regression for 30 kV X-rays omitting the 2 to 40 mGy dose points. The regression in the low dose area (0-40 mGy) is 8.7 times steeper than in the higher dose range (20 to 100 mGy) (Depuydt et al. n.d.).

Limited data are available concerning the radiation-induced carcinogenic risk in *BRCA1* and *BRCA2* mutation carriers. Whereas some clinical studies reported an absence of increased breast cancer incidence in *BRCA* mutation carriers after exposure to ionizing radiation in a diagnostic setting, others could not exclude an increased breast cancer risk for mutation carriers younger than 30 or 40 years (Drooger et al. 2015; Pijpe et al. 2012; Andrieu et al. 2006; Gronwald et al. 2008; Narod et al. 2006). Several EU guidelines foresee mammography screening, for women at high risk, starting at the age of 30 (The Netherlands (www.hebon.nl) and Belgium (Gillet et al. 2011)) or 40 (UK (gov.uk)). The US screening guidelines provide the opportunity to start mammography screening from 25 years onwards (NCCN 2016). However, risk estimates by Berrington de Gonzalez et al. in young *BRCA* mutation carriers provide no evidence of a net benefit of mammography screening between the ages of 30-34 years (Berrington de Gonzalez et al. 2009). A net benefit was only observed at the age of 35 years and older. These calculated risk estimates are based on several assumptions including an increased risk of radiation-induced breast cancer in mutation carriers, which is supported by our experimental data.

The results obtained in our studies, although performed at higher doses of ionizing radiation, suggest caution when exposing healthy tissues of BRCA mutation carriers to ionizing radiation for diagnostic purposes. Especially mammography screening in mutation carriers at young ages (25 to 35 years) should be avoided as the net gain is small and the detrimental effects could outweigh the benefits of screening. Current screening settings at UZ Gent avoid exposure to ionizing radiation of young individuals at high risk (not solely mutation carriers) and use MRI screening. A first mammography screening is conducted at the age of 40, followed by routine screening from 50 years onwards (personal communication). However, this cautious screening plan is not implemented at the national level. We plea for a general gentle use of mammography screening in individuals at high risk due to a germline mutation in *BRCA1* or *BRCA2*. Techniques such as MRI seem to be better suited to screen these individuals. Indeed, despite reports concerning a lower specificity and/or sensitivity (Enriquez & Listinsky 2009; Pataky et al. 2013; Ahern et al. 2014), MRI screening is useful in high risk cohorts, even when considering the higher cost compared to mammography screening (Obdeijn et al. 2014; Ahern et al. 2014).

The implications of our results on radiotherapy treatment for *BRCA1* and *BRCA2* mutation carriers who developed breast cancer are difficult to assess. The main aim of radiotherapy is to eradicate the (breast) tumor while preserving the healthy, surrounding tissues. Our results suggest that the healthy breast tissue might be more prone to health consequences associated with an impaired DNA damage response capacity such as radiation-induced carcinogenesis and adverse effects. Unfortunately, only a limited number of studies evaluated the carcinogenic risk of adjuvant radiotherapy in BRCA mutation carriers and results are not univocal. In their review, Drooger et al. specifically warn against the exposure of young individuals (<30 years) to ionizing radiation for therapeutic purposes as a carcinogenic effect could not be excluded (Drooger et al. 2015).

Nevertheless, we also must consider the fact that tumors in these individuals might be more radiosensitive due to failed DNA damage responses, including failed HR-mediated repair of DSB, which may be a benefit in treatment of these individuals. The application of our assays on breast tumor tissue in mutation carriers would allow the evaluation of the possible treatment benefit in these individuals. Furthermore, targeted therapies such as a PARP

inhibitor, exploiting failed HR-mediated DSB repair in tumor cells, could be applied. Currently, an array of PARP inhibitors are being tested in various clinical trials for their effectiveness in breast cancer treatment (Livraghi & Garber 2015) and one, Olaparib (Lynparza, AstraZeneca), has been approved for ovarian cancer treatment in patients with a deleterious germline *BRCA1/2* mutation (Kim et al. 2015). PARP inhibitor treatment allows a more direct targeting of the tumor, whilst damage to the surrounding tissue is expected to be smaller, resulting in fewer side effects compared to radiotherapy. Nonetheless, adverse effects occur and appear to be similar to those observed after systemic treatment with chemotherapy. Furthermore, the inhibition of DNA damage response mechanisms may result in the induction of cancer due to an accumulation of DSB in normal tissue (Livraghi & Garber 2015). A small number of cases of acute myeloid leukemia and myelodysplastic syndrome were reported (incidence <1%), but most individuals developing new primary malignancies were also treated with DNA-damaging chemotherapeutics (Sonnenblick et al. 2014). Further research to elucidate the long-term effects of PARP inhibitor treatment are warranted.

1.4 Choosing the appropriate assay to evaluate individual radiosensitivity

The choice of the radiosensitivity assay will be inherent to the gene that is mutated. When a mutation has been detected or is presumed in a gene involved in c-NHEJ, radiosensitivity analysis by means of the G0 MN is advisable. In case of a mutation in a gene involved in HR, the G2 MN is the more appropriate assay to evaluate individual radiosensitivity. Additionally, the G2 MN assay can be applied if mutations are present in genes involved in the G2/M checkpoint. If a mutation is detected or presumed in a gene that affects both pathways or if little information is known about the genetic background, it would be advisable to apply both assays.

For example, in our study performed on a patient with a variant form of AT with residual kinase activity, we obtained an enhanced radiosensitivity with both the G0 and the G2 MN assay, this as ATM is involved in both pathways. The most discriminative result was obtained with the G2 MN assay, which may point to the fact that ATM is more important in the DNA damage response when cells are in S or G2 phase of the cell cycle (Claes et al. 2013).

For *BRCA1* and *BRCA2* heterozygous mutation carriers, we demonstrated that the G2 MN assay is the more appropriate tool to evaluate radiosensitivity. This is in line with the expectations as both *BRCA1* and *BRCA2* are mainly involved in DNA damage response pathways active in S and G2 phase of the cell cycle. In addition, the role of *BRCA1* in the G2/M checkpoint results in the applicability of the second endpoint (G2 arrest capacity), analyzed in the G2 MN assay.

Besides the G2 MN assay, we optimized a second biomarker, the RAD51 foci assay. This assay allows a more direct evaluation of the HR pathway and might prove valuable for individual assessment of HR efficiency and radiosensitivity in *BRCA1* and *BRCA2* mutation carriers. This assay might also be useful for individuals carrying a mutation in other genes that affect HR, such as *ATM* and *PALB2*.

Whereas the RAD51 foci assay could prove a valuable addition to or alternative for the G2 MN assay, a similar approach could be considered for the G0 MN assay. Evaluation of key c-NHEJ proteins such as *Artemis* could shed light on the functionality of this particular pathway.

In general, it would be advisable to perform a panel of assays for thorough evaluation of the radiosensitivity phenotype of an individual. The results may be used to refine diagnosis if a mutation is presumed or to tailor diagnostic and therapeutic exposure to ionizing radiation of individuals characterized by a genomic instability and high cancer risk.

1.5 Limitation of the use of lymphocytes for analysis of individual radiosensitivity

Radiosensitivity tests are generally performed in peripheral blood lymphocytes as they are an easy-accessible source of patient-own material. They are a valuable cell type to evaluate how individuals with a different genetic background (e.g. mutation carriers versus controls) respond to ionizing radiation and therefore, an appropriate cell source to develop a clinically useful biomarker to assess of the overall individual radiosensitivity (Kote-Jarai et al. 2006; Rieger et al. 2004; Foray et al. 1999).

Nevertheless, lymphocytes are not the most appropriate cell type to study the mechanisms underlying the formation of radiation-induced breast cancer. Cancer risk in *BRCA1* and

BRCA2 mutation carriers is predominantly associated with breast and ovarian cancer (van Asperen et al. 2005; Thompson et al. 2002). Several theories, such as the involvement of the XIST RNA (Sirchia et al. 2009) or hormones (Santen et al. 2009), have been proposed to explain this phenomenon. None of these theories seem to adequately explain the cell type specific cancer development in *BRCA1* or *BRCA2* mutation carriers.

Another possible explanation is the difference in DNA DSB repair pathways utilized by breast and ovarian epithelial cells compared to other cell types. While not thoroughly investigated, it is known that different cell types use the repair pathways to a different extent (D'Errico et al. 2007). One could suggest that breast and ovarian epithelial cells in S and G2 phase mainly rely on the HR-pathway to repair DNA DSB, while other cell types, including fibroblasts and other epithelial cells, rely on the c-NHEJ pathway. A reduced level of *BRCA1* or *BRCA2* due to a mutation would render the HR-pathway inefficient while the c-NHEJ pathway remains proficient (Sedic & Kuperwasser 2016). This theory is supported by results obtained by Sedic et al. (2015) as they demonstrated an increased genomic instability in human breast epithelial cells but not in skin fibroblast with pathogenic mutations of *BRCA1* (Sedic et al. 2015).

Further research evaluating the difference in pathway use between different cell types, including breast epithelial cells, fibroblasts and lymphocytes, could shed light on this phenomenon. This could be achieved by evaluating the induction of DSB by means of γ H2AX foci, combined with the RAD51 foci assay to measure HR activation and a Artemis foci assay to quantify c-NHEJ activation. As cell cycle phase is a key factor in this experimental setup, incorporation of a geminin staining, indicative for cells in S and G2 phase, would be advisable (Wohlschlegel et al. 2002).

2 cDNA ANALYSIS OF PUTATIVE SPLICE SITE VARIANTS

Besides assays evaluating the effect of radiation, also other tests may be helpful for the determination of a functional effect of variants in BRCA1/2. Therefore, a final aim of this thesis focusses on the determination of the functional effect of putative splice site variants by cDNA analysis in lymphocytes. The identification of VUS is a major issue for labs offering diagnostic testing and is reflected in the large number of VUS reported in the ClinVar database (NCBI). VUS are a true challenge for health care providers as the impact of these variants on breast/ovarian cancer risk is unclear. mRNA analysis to investigate intronic and exonic variants that might impair proper RNA splicing, a highly regulated process, are widely used. In paper V, we evaluated the outcome of 19 VUS at the cDNA level and assessed the performance of multiple *in silico* prediction tools (discussed in chapter 2.1). We demonstrated aberrant splicing for nine variants, suggesting that these variants are likely pathogenic (discussed in chapter 2.2). Improper mRNA splicing was due to the loss of wild type splice sites leading to a skip of an entire exon or originated from the activation of cryptic splice sites leading to aberrant transcripts. By studying the effect at the cDNA level of a novel tandem duplication with a 5' breakpoint in intron 4 and a 3' breakpoint in exon 11 of the *BRCA2* gene, we identified an actively used cryptic donor site within the large exon 11. To our knowledge, this is the first report on an activated cryptic donor site in the large exon 11 of *BRCA2*. Many more strong sites were predicted *in silico*, but not activated. The identification of this site warrants further research to gain more insight in *cis* and *trans* acting factors playing a role in the conservation of correct transcription of this large exon in which to date no mutations have been reported associated with aberrant splicing.

2.1 Aberrant splicing and accuracy of *in silico* prediction tools

We evaluated the performance of a wide array of *in silico* prediction tools for their sensitivity and specificity (paper V). The power of these tools to accurately predict the effect of splice site variants is dependent on the degree of conservation of the region in which the variant is located, the ability to accurately predict the wild type splice site, and the ability to define important regions such as the branchpoints or ESE (Caminsky et al. 2014; Houdayer et al. 2012). Therefore, the efficiency of these splicing tools largely depends on the location of the variant. In total, three different regions are defined. The first highly defined region is the

canonical splice site. This region comprises the two intronic nucleotides flanking each exon and are always GT at the splice donor site and AG at the splice acceptor site. Variants located in this region are expected to disrupt proper mRNA splicing and prediction tools perform well. The effect of variants outside this splice site consensus region is more difficult to assess. For variants in the cartegni consensus region (see Figure 3.16), but outside the canonical splice site, *in silico* prediction lacks specificity. However, the *in silico* prediction tools performed well for our intronic variants outside the Cartegni consensus region. We found that neither of the three *in silico* tools for evaluation of exonic variants (ESEfinder, ESE-RESCUE and Δ ESRseq) performed well. Additional optimization and validation could improve these prediction tools, but for now, mRNA analysis remains necessary to verify the *in silico* prediction result and to determine the exact aberrant transcript for pathogenicity evaluation of putative splice site mutations.



Figure 3.16: The Cartegni consensus region encompasses 11 bases of the 5' splice site (from the three last exonic to the eight first intronic bases) and 14 bases of the 3' site (from the 12 last intronic to the first two exonic bases) (Cartegni et al. 2002).

2.2 Aberrant splicing, pathogenicity assessment and functional analysis

Classification of VUS is based on a multifactorial approach including familial segregation, frequency in cases versus controls and functional analysis (Table IV). However, each piece of this puzzle has its limitations (Couch et al. 2008; Goldgar et al. 2008).

Table IV. Data relevant for multifactorial likelihood analysis for variant classification (Goldgar et al. 2008)

Line of Evidence	Advantages	Disadvantages
Frequency in cases and controls	Provides direct estimate of associated cancer risk.	Variants are rare, so such studies would need to be prohibitively large (10,000+).
Co-occurrence (in <i>trans</i>) with deleterious mutations	If homozygotes and compound heterozygotes are assumed to be embryonic lethal (or vanishingly rare), can often classify a variant as neutral based on a single observation. If homozygote has distinct phenotype can classify variant as pathogenic.	Much less power to show causality. Quantification dependent on the assumed fitness of homozygous, which is not known with precision.
Cosegregation with disease in pedigrees	Easy quantifiable, directly related to disease risk. Not susceptible to uncertainties in mutation frequencies or population stratification.	Requires sampling of additional individuals in the pedigrees (particularly additional cases) which may be difficult to achieve.
Family history	Is usually available for most variants without additional data or sample collection. Potentially very powerful.	Dependent on family ascertainment scheme. Could be biased in stratified populations with heterogeneous ascertainment, so not as robust as cosegregation. Power may be low for infrequent variants.
Species conservation/AA change severity/splice predictions	Can be applied to every possible missense change in the relevant genes (or potential intronic splice variant). Could be highly predictive if enough evolutionary time sequence is available and validated models are used.	Only indirectly related to disease risk. Magnitude of odds ratios typically not sufficient to classify variants without additional information.
Functional studies	Can biologically evaluate the effect the variant has on the ability of the protein to perform some of the key cellular functions.	May only be relevant for variants in certain domains of the protein. The function tested may not be related to cancer causation.
Pathological classification	Potentially quantifiable. In some cases can be highly predictive.	Prediction using routine pathology data weak. Systematic evaluation requires tumor material. Assumes missense and null mutations have similar tumor characteristics.

In paper V, we evaluated the effect at the cDNA level for 21 putative splice site variants and found that 12 of them lead to aberrant splicing. One limitation of our study is that we were not able to evaluate for all variants allele-specific assessment of aberrant splicing. For several variants sequencing data clearly showed equal expression of the aberrant and full length transcript and complete absence of the aberrant transcript in controls. For these variants our data provide a reasonable suggestion regarding pathogenicity. However, allele-specific assessment of aberrant splicing in combination with a multifactorial likelihood analysis is necessary to definitively classify a variant as deleterious (Spurdle et al. 2008).

For most of the tested variants, aberrant splicing led to the formation of a premature termination codon. Based on previous experimental work and literature, we can expect the activation of NMD, resulting in a degradation of the mRNA and a reduction in protein level (Baert et al. 2016; Perrin-vidoz et al. 2002; Ware et al. 2006). In that case, pathogenicity is to be expected as a similar net result is obtained compared to deleterious frameshift mutations for which pathogenicity is established.

Certain aberrant transcripts may evade NMD because of the location of the premature termination codon at the C or N-terminus of BRCA1 or because an *in frame* deletion/insertion

does not result in the formation of a premature termination codon. For these variants, the impact must be assessed at multiple levels. Initially, the aberrant transcript abundance must be evaluated in function of the full-length transcript. Furthermore, translation of the aberrant transcript can be verified by means of a Western blot analysis. If an aberrant protein is detected, an evaluation of its impact on proper protein functionality must be assessed by means of a functional assay.

For two splice site variants in *BRCA1* (c.5152+2dupT (p.Asp1692_Trp1718delinsGly) & c.5468-1G>A (p.Ala1823Valfs*2)), evaluated in paper V, pathogenicity classification was less straightforward due to the in frame deletion of exon 18 and a premature termination codon predicted to evade NMD respectively. Although presently aberrant transcript abundance has not been evaluated, pathogenicity might be expected given the disruption of the functional BRCT domain and based on pathogenicity classification of other variants in the region. The disrupted BRCT domain is important for, amongst others, *BRCA1* recruitment to the DNA damage site and DNA end resection. As two main functions of the DNA damage response activity of *BRCA1* might be disrupted, subsequent activation of HR might be impaired. This could be evaluated by means of the G2 MN assay or a HR-specific functional assay such as the RAD51 foci assay. As proposed in chapter 1.2 of the general discussion, the application of the RAD51 foci assay on synchronized lymphocytes of individuals with pathogenic *BRCA1* or *BRCA2* mutations might be promising to evaluate HR functionality and radiosensitivity. Once validated, this assay could be applied for pathogenicity assessment of splice site variants leading to various types of aberrant transcripts.

In paper II, we evaluated the effect of different types of aberrant transcripts on radiosensitivity, measured by the G2 MN assay in *BRCA1* mutation carriers. Therefore, we compared the effect of aberrant transcripts sensitive to NMD and aberrant transcripts escaping NMD due to the absence or the 5' location of a PTC on the individual RIND scores. Haploinsufficiency is the main mechanism suggested for breast carcinogenesis (Salmena & Narod 2012) and seems to be the underlying mechanism for radiosensitivity in individuals with an NMD-sensitive mutation. However, we demonstrated a higher median RIND score for individuals carrying a mutation in the 5' part of the gene, for which no NMD could be detected, compared to individuals with aberrant transcripts susceptible for NMD, which may

point towards another mechanism, such as dominant negative effect, in these individuals (paper II). As indicated in paper II, our data suggest the need for larger studies involving different types of mutations and the RAD51 foci assay appears to be well suited to evaluate the effect of different types of mutations on HR and radiosensitivity.

3 GENERAL CONCLUSION

We demonstrated that the G2 MN assay is a valuable assay to assess radiosensitivity in cohorts of *ATM*, *BRCA1* and *BRCA2* heterozygous mutation carriers.

Unfortunately, intra-individual variation of the assay, and inter-individual variation which might be caused by the influence of other DNA damage response pathways on MN formation, complicate individual radiosensitivity assessment due to overlap in MN yields between the test and control cohort. Therefore, an arbitrary scoring system was set up which allows a “graded” assessment of the individual radiosensitive phenotype. In search of an assay to allow a better individual assessment of HR capacity in heterozygous *BRCA1* and *BRCA2* mutation carriers, we evaluated the use of the RAD51 foci assay in S phase synchronized breast epithelial cells with reduced *BRCA1* or *BRCA2* protein levels and demonstrated impaired RAD51 foci formation, and thus HR capacity, in response to radiation-induced DSB. Both the G2 MN assay and the RAD51 foci assays can be applied for the assessment of radiosensitivity evaluation and/or HR functionality in patients carrying a mutation in an array of genes involved in the DNA damage response active during S and G2 phase of the cell cycle, or more specifically, engaged in HR activation.

The results obtained in these papers indicate that care should be taken when applying ionizing radiation for diagnostic or therapeutic purposes in (young) individuals at high risk of breast cancer due to a mutation in *BRCA1* or *BRCA2* as they may be at higher risk of developing radiation-induced breast cancer.

These results refer to individuals heterozygous for an unequivocal deleterious *BRCA1* or *BRCA2* mutation. However, a major burden in diagnostic testing of the *BRCA1/2* genes are the identification of VUS. These VUS are a true challenge for health care providers as the impact of these variants on breast/ovarian cancer risk is unclear. We evaluate the effect of 21 variants in *BRCA1* and *BRCA2* by mRNA analysis and demonstrated aberrant splicing for 11 variants suggesting that these are likely pathogenic. Furthermore, we demonstrate that *in silico* prediction tools might assist in the evaluation of these putative splicing variants. However, further optimization is warranted. Finally, we propose the RAD51 foci assay as a functional assay for variants affecting functional domains.

4 References

- Ahern, C.H. et al., 2014. Cost-effectiveness of alternative strategies for integrating MRI into breast cancer screening for women at high risk. *British journal of cancer*, (August), pp.1–10.
- Andrieu, N. et al., 2006. Effect of Chest X-Rays on the Risk of Breast Cancer Among BRCA1 / 2 Mutation Carriers in the International BRCA1 / 2 Carrier Cohort Study : A Report from the EMBRACE , GENEPSO , GEO-HEBON , and IBCCS Collaborators ' Group. *Journal of Clinical Oncology*, 24(21), pp.3361–3366.
- Aparicio, T., Baer, R. & Gautier, J., 2014. DNA double-strand break repair pathway choice and cancer. *DNA Repair*, 19, pp.169–175.
- van Asperen, C.J. et al., 2005. Cancer risks in BRCA2 families: estimates for sites other than breast and ovary. *Journal of medical genetics*, 42(9), pp.711–9.
- Averbeck, D., 2009. Does scientific evidence support a change from the LNT model for low-dose radiation risk extrapolation? *Health physics*, 97(5), pp.493–504.
- Baert, A. et al., 2016. Increased chromosomal radiosensitivity in asymptomatic carriers of a heterozygous BRCA1 mutation. *Breast Cancer Research*, 18(1), p.52.
- Baeyens, A. et al., 2004. Chromosomal radiosensitivity in BRCA1 and BRCA2 mutation carriers. *International journal of radiation biology*, 80(10), pp.745–756.
- Baeyens, A. et al., 2002. Chromosomal radiosensitivity in breast cancer patients with a known or putative genetic predisposition. *British journal of cancer*, 87(12), pp.1379–1385.
- Bartsch, O. et al., 2012. A girl with an atypical form of ataxia telangiectasia and an additional de novo 3.14Mb microduplication in region 19q12. *European Journal of Medical Genetics*, 55(1), pp.49–55.
- Barwell, J. et al., 2007. Lymphocyte radiosensitivity in BRCA1 and BRCA2 mutation carriers and implications for breast cancer susceptibility. *International journal of cancer.*, 121(7), pp.1631–6.
- Becker, A.A. et al., 2012. A 24-color metaphase-based radiation assay discriminates heterozygous BRCA2 mutation carriers from controls by chromosomal radiosensitivity. *Breast Cancer Research and Treatment*, 135(1), pp.167–175.
- Berrington de Gonzalez, A. et al., 2009. Estimated Risk of Radiation-Induced Breast Cancer From Mammographic Screening for Young BRCA Mutation Carriers. *Journal of the National Cancer Institute*, 101(3), pp.205–209.
- Bryant, P.E., 2004. Repair and chromosomal damage. *Radiotherapy and Oncology*, 72(3), pp.251–256.
- Buchholz, T.A. et al., 2002. Evidence of haplotype insufficiency in human cells containing a germline mutation in BRCA1 or BRCA2. *International Journal of Cancer*, 97, pp.557–561.
- Caminsky, N.G., Mucaki, E.J. & Rogan, P.K., 2014. Interpretation of mRNA splicing mutations in genetic disease: review of the literature and guidelines for information-theoretical analysis. *F1000Research*, 3(May 2016), p.282.
- Carney, P.A. et al., 2003. Individual and combined effects of age, breast density, and hormone replacement therapy use on the accuracy of screening mammography. *Ann Intern Med*, 138, pp.168–175.
- Cartegni, L., Chew, S.L. & Krainer, A.R., 2002. Listening To Silence and Understanding Nonsense: Exonic Mutations That Affect Splicing. *Nature Reviews Genetics*, 3(4), pp.285–298.

- Chen, P. et al., 1994. Comparative study of radiation-induced G2 phase delay and chromatid damage in families with ataxia-telangiectasia. *Cancer Genetics and Cytogenetics*, 76(1), pp.43–46.
- Choudhury, A.D., Xu, H. & Baer, R., 2004. Ubiquitination and proteasomal degradation of the BRCA1 tumor suppressor is regulated during cell cycle progression. *Journal of Biological Chemistry*, 279(32), pp.33909–33918.
- Claes, K. et al., 2013. Variant Ataxia Telangiectasia: Clinical and Molecular Findings and Evaluation of Radiosensitive Phenotypes in a Patient and Relatives. *Neuromolecular medicine*, 15(3), pp.447–457.
- Couch, F.J. et al., 2008. Assessment of functional effects of unclassified genetic variants. *Human Mutation*, 29(11), pp.1314–1326.
- D’Errico, M. et al., 2007. Cell type and DNA damage specific response of human skin cells to environmental agents. *Mutation Research - Fundamental and Molecular Mechanisms of Mutagenesis*, 614(1–2), pp.37–47.
- Defamie, N., Chepied, A. & Mesnil, M., 2014. Connexins, gap junctions and tissue invasion. *FEBS Letters*, 588(8), pp.1331–1338.
- Depuydt, J. et al., 2013. Relative biological effectiveness of mammography X-rays at the level of DNA and chromosomes in lymphocytes. *International journal of radiation biology*, 89(7), pp.532–8.
- Depuydt, J. et al., γH2AX foci induced by low dose mammography X-rays in breast tissue. *In preparation*.
- Distel, L.V.R. et al., 2006. Individual differences in chromosomal aberrations after in vitro irradiation of cells from healthy individuals, cancer and cancer susceptibility syndrome patients. *Radiotherapy and Oncology*, 81(3), pp.257–263.
- Drooger, J.C. et al., 2015. Diagnostic and therapeutic ionizing radiation and the risk of a first and second primary breast cancer, with special attention for BRCA1 and BRCA2 mutation carriers: A critical review of the literature. *Cancer Treatment Reviews*, 41(2), pp.187–196.
- Enriquez, L. & Listinsky, J., 2009. Role of MRI in breast cancer management. *Cleveland Clinic Journal of Medicine*, 76(9), pp.525–532.
- Ernestos, B. et al., 2010. Increased chromosomal radiosensitivity in women carrying BRCA1/BRCA2 mutations assessed with the G2 assay. *International journal of radiation oncology, biology, physics*, 76(4), pp.1199–205.
- Esashi, F. et al., 2005. CDK-dependent phosphorylation of BRCA2 as a regulatory mechanism for recombinational repair. *Nature*, 434(March), pp.598–604.
- Evans, D.G.R. et al., 2013. Increased rate of phenocopies in all age groups in BRCA1/BRCA2 mutation kindred, but increased prospective breast cancer risk is confined to BRCA2 mutation carriers. *Cancer Epidemiology Biomarkers and Prevention*, 22(12), pp.2269–2276.
- Fenech, M., 1999. Micronucleus frequency in human lymphocytes is related to plasma vitamin B12 and homocysteine. *Mutation Research - Fundamental and Molecular Mechanisms of Mutagenesis*, 428(1–2), pp.299–304.
- Foray, N. et al., 1999. Gamma-rays-induced death of human cells carrying mutations of BRCA1 or BRCA2. *Oncogene*, 18(51), pp.7334–7342.
- George, K. a et al., 2009. Dose response of gamma rays and iron nuclei for induction of chromosomal aberrations in normal and repair-deficient cell lines. *Radiation research*, 171(6), pp.752–763.

- Gilad, S. et al., 1998. Genotype-phenotype relationships in ataxia-telangiectasia and variants. *American journal of human genetics*, 62(3), pp.551–61.
- Gillet, P. et al., 2011. Borstkanker screening : hoe vrouwen met een verhoogd risico identificeren - welke beeldvorming gebruiken ? Good Clinical Practice (GCP). *Federaal Kenniscentrum voor Gezondheidszorg (KCE)*, KCE Report(D/2011/10.273/90).
- Goldgar, D.E. et al., 2008. Genetic evidence and integration of various data sources for classifying uncertain variants into a single model. *Human Mutation*, 29(11), pp.1265–1272.
- Gronwald, J. et al., 2008. Early radiation exposures and BRCA1-associated breast cancer in young women from Poland. *Breast cancer research and treatment*, 112(3), pp.581–4.
- Gutiérrez-Enríquez, S. et al., 2011. Ionizing radiation or mitomycin-induced micronuclei in lymphocytes of BRCA1 or BRCA2 mutation carriers. *Breast cancer research and treatment*, 127(3), pp.611–22.
- Houdayer, C. et al., 2012. Guidelines for splicing analysis in molecular diagnosis derived from a set of 327 combined in silico/in vitro studies on BRCA1 and BRCA2 variants. *Human Mutation*, 33(8), pp.1228–1238.
- Jongmans, W. et al., 1998. The p53-mediated DNA damage response to ionizing radiation in fibroblasts from ataxia-without-telangiectasia patients. *International journal of radiation biology*, 74(3), pp.287–295.
- Karanam, K. et al., 2012. Quantitative Live Cell Imaging Reveals a Gradual Shift between DNA Repair Mechanisms and a Maximal Use of HR in Mid S Phase. *Molecular Cell*, 47(2), pp.320–329.
- Khodyreva, S.N. & Lavrik, O.I., 2016. Poly(ADP-Ribose) polymerase 1 as a key regulator of DNA repair. *Molecular Biology*, 50(4), pp.580–595.
- Kim, G. et al., 2015. FDA approval summary: Olaparib monotherapy in patients with deleterious germline BRCA-mutated advanced ovarian cancer treated with three or more lines of chemotherapy. *Clinical Cancer Research*, 21(19), pp.4257–4261.
- Kiuru, A. et al., 2014. Assessment of targeted and non-targeted responses in cells deficient in ATM function following exposure to low and high dose X-rays. *PLoS ONE*, 9(3), pp.1–8.
- Kote-Jarai, Z. et al., 2006. Increased level of chromosomal damage after irradiation of lymphocytes from BRCA1 mutation carriers. *British journal of cancer*, 94(2), pp.308–310.
- Kühne, M. et al., 2004. A Double-Strand Break Repair Defect in ATM-Deficient Cells Contributes to Radiosensitivity. *Cancer Research*, 64, pp.500–508.
- Landsverk, K.S. et al., 2011. Three independent mechanisms for arrest in G2 after ionizing radiation. *Cell cycle (Georgetown, Tex.)*, 10(5), pp.819–829.
- Lee, H., 2014. Cycling with BRCA2 from DNA repair to mitosis. *Experimental Cell Research*, 329(1), pp.78–84.
- Lee, M., Daniels, M.J. & Venkitaraman, A.R., 2004. Phosphorylation of BRCA2 by the Polo-like kinase Plk1 is regulated by DNA damage and mitotic progression. *Oncogene*, 23(2004), pp.865–872.
- Liu, W. et al., 2010. Turnover of BRCA1 involves in radiation-induced apoptosis. *PLoS ONE*, 5(12).
- Livraghi, L. & Garber, J.E., 2015. PARP inhibitors in the management of breast cancer: current data and future prospects. *BMC medicine*, 13, p.188.
- Mao, Z. et al., 2008. DNA repair by nonhomologous end joining and homologous

- recombination during cell cycle in human cells. *Cell Cycle*, 7(18), pp.2902–2906.
- Menzel, T. et al., 2011. A genetic screen identifies BRCA2 and PALB2 as key regulators of G2 checkpoint maintenance. *EMBO reports*, 12(7), pp.705–12.
- Murai, J. et al., 2013. Differential trapping of PARP1 and PARP2 by clinical PARP inhibitors. *Cancer Research*, 72(21), pp.5588–5599.
- Murai, J. et al., 2012. Trapping of PARP1 and PARP2 by clinical PARP inhibitors. *Cancer Research*, 72(21), pp.5588–5599.
- Narod, S.A. et al., 2006. Screening mammography and risk of breast cancer in BRCA1 and BRCA2 mutation carriers: a case-control study. *The Lancet. Oncology*, 7(5), pp.402–6.
- Nasonova, E. & Ritter, S., 2004. Cytogenetic effects of densely ionising radiation in human lymphocytes: Impact of cell cycle delays. *Cytogenetic and Genome Research*, 104(1–4), pp.216–220.
- NCCN, 2016. Genetic / Familial High-Risk Assessment : Breast and Ovarian cancer.
- Obdeijn, I.-M. et al., 2014. Should we screen BRCA1 mutation carriers only with MRI? A multicenter study. *Breast cancer research and treatment*, 144(3), pp.577–82.
- Okada, S. & Ouchi, T., 2003. Cell cycle differences in DNA damage-induced BRCA1 phosphorylation affect its subcellular localization. *Journal of Biological Chemistry*, 278(3), pp.2015–2020.
- Pantelias, G.E. & Terzoudi, G.I., 2011. A standardized G2-assay for the prediction of individual radiosensitivity. *Radiotherapy and Oncology*, 101(1), pp.28–34.
- Pataky, R. et al., 2013. Cost-effectiveness of MRI for breast cancer screening in BRCA1 / 2 mutation carriers. *BMC Cancer*, 13(1), p.1.
- Perrin-vidoz, L. et al., 2002. The nonsense-mediated mRNA decay pathway triggers degradation of most BRCA1 mRNAs bearing premature termination codons. , 11(23), pp.2805–2814.
- Pijpe, A. et al., 2012. Exposure to diagnostic radiation and risk of breast cancer among carriers of BRCA1/2 mutations: retrospective cohort study (GENE-RAD-RISK). *BMJ*, 345, p.e5660.
- Pommier, Y., O'Connor, M.J. & de Bono, J., 2016. Laying a trap to kill cancer cells: PARP inhibitors and their mechanisms of action. *Science Translational Medicine*, 8(362), pp.1–8.
- Popanda, O. et al., 2009. Genetic variation in normal tissue toxicity induced by ionizing radiation. *Mutation research*, 667(1–2), pp.58–69.
- Rieger, K.E. et al., 2004. Toxicity from radiation therapy associated with abnormal transcriptional responses to DNA damage. *PNAS*, 101(17), pp.6635–6640.
- Roberts, C.J., Morgan, G.R. & Danford, N., 1997. Effect of hormones on the variation of radiosensitivity in females as measured by induction of chromosomal aberrations. *Environmental Health Perspectives*, 105(SUPPL. 6), pp.1467–1471.
- Rothkamm, K. & Löbrich, M., 2003. Evidence for a lack of DNA double-strand break repair in human cells exposed to very low x-ray doses. *Proceedings of the National Academy of Sciences of the United States of America*, 100(9), pp.5057–62.
- Roy, R., Chun, J. & Powell, S.N., 2012. BRCA1 and BRCA2: different roles in a common pathway of genome protection. *Nature reviews. Cancer*, 12(1), pp.68–78.
- Saha, J. & Davis, A.J., 2016. Unsolved mystery: the role of BRCA1 in DNA end-joining. *Journal of radiation research*, 57(S1), pp.18–24.
- Salmena, L. & Narod, S., 2012. BRCA1 haploinsufficiency: consequences for breast cancer. *Women's health (London, England)*, 8(2), pp.127–9.

- Sanford, K.K. et al., 1990. Enhanced chromatid damage in blood lymphocytes after g2 phase x irradiation, a marker of the ataxia-telangiectasia gene. *Journal of the National Cancer Institute*, 82(12), pp.1050–1054.
- Santen, R. et al., 2009. Estrogen mediation of breast tumor formation involves estrogen receptor-dependent, as well as independent, genotoxic effects. *Annals of the New York Academy of Sciences*, 1155, pp.132–140.
- Sedic, M. et al., 2015. Haploinsufficiency for BRCA1 leads to cell-type-specific genomic instability and premature senescence. *Nature Communications*, 6(May), p.7505.
- Sedic, M. & Kuperwasser, C., 2016. BRCA1-haploinsufficiency: Unraveling the molecular and cellular basis for tissue-specific cancer. *Cell Cycle*, 15(5), pp.621–627.
- Sioftanos, G. et al., 2010. BRCA1 and BRCA2 heterozygosity in embryonic stem cells reduces radiation-induced Rad51 focus formation but is not associated with radiosensitivity. *International journal of radiation biology*, 86(12), pp.1095–105.
- Sirchia, S.M. et al., 2009. Misbehaviour of XIST RNA in breast cancer cells. *PLoS ONE*, 4(5), pp.1–13.
- Smith, a et al., 2007. Phenocopies in BRCA1 and BRCA2 families: evidence for modifier genes and implications for screening. *Journal of medical genetics*, 44(1), pp.10–15.
- Sonnenblick, A. et al., 2014. An update on PARP inhibitors—moving to the adjuvant setting. *Nature Publishing Group*, 12(1), pp.27–41.
- Spurdle, A.B. et al., 2008. Prediction and assessment of splicing alterations: Implications for clinical testing. *Human Mutation*, 29(11), pp.1304–1313.
- Summers, K.C. et al., 2011. Phosphorylation: The Molecular Switch of Double-Strand Break Repair. *International Journal of Proteomics*, 2011, pp.1–8.
- Tchirkov, A. et al., 1997. Detection of heterozygous carriers of the ataxia-telangiectasia (ATM) gene by G2 phase chromosomal radiosensitivity of peripheral blood lymphocytes. *Human Genetics*, 101(3), pp.312–316.
- Terzoudi, 2009. G2-checkpoint abrogation in irradiated lymphocytes: A new cytogenetic approach to assess individual radiosensitivity and predisposition to cancer. *International Journal of Oncology*, 35(5).
- Terzoudi, G.I. et al., 2011. Chromatin dynamics during cell cycle mediate conversion of DNA damage into chromatid breaks and affect formation of chromosomal aberrations: Biological and clinical significance. *Mutation Research - Fundamental and Molecular Mechanisms of Mutagenesis*, 711(1–2), pp.174–186.
- Thompson, D., Easton, D. & the breast cancer linkage consortium, 2002. Cancer Incidence in BRCA1 mutation carriers. *Journal of the National Cancer Institute*, 94(18), pp.1358–1365.
- Vaclová, T. et al., 2015. DNA repair capacity is impaired in healthy BRCA1 heterozygous mutation carriers. *Breast Cancer Research and Treatment*, 152(2), pp.271–282.
- Vos, J.R. et al., 2013. Proven non-carriers in BRCA families have an earlier age of onset of breast cancer. *European Journal of Cancer*, 49(9), pp.2101–2106.
- Vral, A. et al., 2004. Chromosomal aberrations and in vitro radiosensitivity: Intra-individual versus inter-individual variability. *Toxicology Letters*, 149(1–3), pp.345–352.
- Vral, A. et al., 2002. The micronucleus and G2-phase assays for human blood lymphocytes as biomarkers of individual sensitivity to ionizing radiation: limitations imposed by intraindividual variability. *Radiation research*, 157(4), pp.472–477.
- Vral, A., Thierens, H. & De Ridder, L., 1996. Micronucleus induction by 60Co gamma-rays and fast neutrons in ataxia telangiectasia lymphocytes. *International journal of*

- radiation biology*, 70(2), pp.171–176.
- Ware, M.D. et al., 2006. Does nonsense-mediated mRNA decay explain the ovarian cancer cluster region of the BRCA2 gene? *Nature*, 25(2), pp.323–8.
- Warren, M. et al., 2003. Phenotypic effects of heterozygosity for a BRCA2 mutation. *Human Molecular Genetics*, 12(20), pp.2645–2656.
- Willems, P. et al., 2008. Polymorphisms in nonhomologous end-joining genes associated with breast cancer risk and chromosomal radiosensitivity. *Genes, chromosomes & cancer*, 47(2), pp.137–148.
- Willers, H. et al., 2015. DNA Damage Response Assessments in Human Tumor Samples Provide Functional Biomarkers of Radiosensitivity. *Seminars in Radiation Oncology*, 25(4), pp.237–250.
- Wohlschlegel, J. a et al., 2002. Expression of geminin as a marker of cell proliferation in normal tissues and malignancies. *The American journal of pathology*, 161(1), pp.267–273.
- Yarden, R.I. et al., 2002. BRCA1 regulates the G2/M checkpoint by activating Chk1 kinase upon DNA damage. *Nature genetics*, 30(3), pp.285–9.
- Zannini, L., Delia, D. & Buscemi, G., 2014. CHK2 kinase in the DNA damage response and beyond. *Journal of Molecular Cell Biology*, 6(6), pp.442–457.
- Zhang, J. et al., 2004. Chk2 phosphorylation of BRCA1 regulates DNA double-strand break repair. *Molecular and cellular biology*, 24(2), pp.708–718.

Annelot Baert

Fabrieksstraat 27 • 9700 Oudenaarde • Belgium

22/03/1988 • Belgium

0499/32.85.10 • annelot.baert@gmail.com

EXPERIENCE	Research Associate	January 2012 – December 2012 Center for Medical Genetics, Ghent University
	PhD Fellowship	January 2013 – May 2017 Basic Medical Sciences, Ghent University
	Recruitment consultant	April 2017 – Present Pauwels Consulting
INTERNSHIPS	Ghent University	September 2010 – December 2011 Internship in the frame of a master thesis combining genetics and radiobiology. Internship in the preparation of a PhD fellowship
EDUCATION	Sciences and mathematics	Sint Jan Berchmans College, Avelgem Graduated in June 2006
	Bachelor Biomedical Sciences	Ghent University Graduated with distinction in June 2009
	Master Biomedical Sciences – Major Human Genetics	Ghent University Graduated with high distinction in June 2011
SKILLS	Specialist Course Laboratory Animal Science	Ghent University, January 2010
	Specialist Course: from qPCR experiment design to data analysis	Biogazelle, Ghent, October 2014

SCIENTIFIC
OUTPUT
A1 Publications

1. **Annelot Baert**, Maria Federica Palermo, Julie Depuydt, Mattias Van Heetvelde, Bram Verstraete, Jan Phillippé, Anna Sablina, Kathleen Claes and Anne Vral. The RAD51 foci assay for the detection of impaired homologous recombination in irradiated MCF10A cells with a BRCA1 or BRCA2 knockdown.
Article in preparation for submission to Plos One
2. Annelot Baert, Eva Machackova, Ilse Coene, Carol Cremin, Kristin Turner, Cheryl Portigal-Todd, Marie Jill Asrat, Jennifer Nuk, Allison Mindlin, Young Sean, Andree MacMillan, Tom Van Maerken, Martin Trbuse, Wendy C McKinnon, Marie E Wood, William D Foulkes, Marta Santamariña, Miguel de la Hoya, Lenka Foretova, Bruce Poppe, Toon Rosseel, Kim De Leeneer, Anne Vral, Ana Vega, Kathleen BM Claes. Thorough *in silico* and *in vitro* cDNA analysis of 21 putative *BRCA1/2* splice variants and identification of activated cryptic splice donor sites in exon 11 of *BRCA2*.
Article in preparation for submission to Human Mutation
3. **Annelot Baert**, Julie Depuydt, Tom Van Maerken, Bruce Poppe, Fransiska Malfait, Tim Van Damme, Sylvia De Nobele, Gianpaolo Perletti, Kim De Leeneer, Kathleen B.M. Claes and Anne Vral. 2017. Analysis of chromosomal radiosensitivity of *BRCA2* mutation carriers and non-carriers in *BRCA* families with the G2 micronucleus assay. *Oncology Reports* 37: 1379-1386
4. **Annelot Baert**; Julie Depuydt; Tom Van Maerken; Bruce Poppe; Fransiska Malfait; Katrien Storm; Jenneke van den Ende; Tim Van Damme; Sylvia De Nobele; Gianpaolo Perletti; Kim De Leeneer; Kathleen Claes; Anne Vral. 2016. Increased chromosomal radiosensitivity in asymptomatic carriers of a heterozygous *BRCA1* mutation. *Breast Cancer Research* 18 (1): 52
5. Claes, Kathleen, Julie Depuydt, A Malcolm R Taylor, James I Last, **Annelot Baert**, Peter Schietecatte, Veerle Vandersickel, Bruce Poppe, Kim De Leeneer, Marc D’Hooghe, and Anne Vral. 2013. “Variant Ataxia Telangiectasia: Clinical and Molecular Findings and Evaluation of Radiosensitive Phenotypes in a Patient and Relatives.” *Neuromolecular Medicine* 15 (3): 447–457.
6. Vandevoorde, Charlot; Depuydt, Julie; Veldeman, Liv; De Neve, Wilfried; Sebastià, Natividad; Wieme, Greet; **Baert, Annelot**; De Langhe, Sofie; Philippé, Jan; Vral, Anne; Thierens, Hubert. 2016. In vitro cellular radiosensitivity in relationship to late normal tissue reactions in breast cancer patients: a multi-endpoint case-control study. *International Journal of Radiation Biology* 92 (12): 823-836

7. Depuydt, Julie, **Annelot Baert**, Veerle Vandersickel, Hubert Thierens, and Anne Vral. 2013. "Relative Biological Effectiveness of Mammography X-rays at the Level of DNA and Chromosomes in Lymphocytes." *International Journal of Radiation Biology* 89 (7): 532–538.
8. Depuydt, Julie; Beukes, Philip; Vandersickel, Veerle; Verstraete, Bram; Van Heetvelde, Mattias; **Baert, Annelot**; Thierens, Hubert; Slabbert, Jacobus; Vral, Anne. The impact of a *BRCA1* and *BRCA2*-mutation on the radiation response induced by gamma-rays and neutrons in MCF-10A cells. Submitted in *International Journal of Radiation Biology*.
9. Brzozowska, Beata; Ainsbury, Elizabeth; **Baert, Annelot**; Beaton, Lindsay A; Barrios, Leonardo; Barquinero, Joan Francesc; Bassinet, Celine; Beinke, Christina; Benedek, Anett; Beukes, Philip; Bortolin, Emanuela; Buraczewska, Iwona; Burbidge, Christopher; DeAmicis, Andrea; De Angelis, Cinzia; Della Monaca, Sara; Depuydt, Julie; DeSanctis, Stefania; Dobos, Katalin; Domene, Mercedes Moreno; Dominguez, Inmaculada; Facco, Eva; Fattibene, Paola; Frenzel, Monika; Gil, Octavia Monteiro; Gonon, Geraldine; GREGOIRE, ERIC; Gruel, Gaetan; Hadjidekova, Valeria; Hatzi, Vasia; Hristova, Rositsa Petrova; Jaworska, Alicja; Kis, Eniko; Kowalska, Maria; Kulka, Ulrike Marianne; Lista, Florigio; Lumniczky, Katalin; Martinez-Lopez, Wilner; Meschini, Roberta; Moertl, S.; Moquet, Jayne; Noditi, Mihaela; Oestreicher, Ursula; Orta Vazquez, Manuel Luis; Palma, Valentina; Pantelias, G E; Montoro, A.; Patrono, Clarice; Piqueret-Stephan, Laure; Quattrini, Maria Cristina; Regalbuto, Elisa; Ricoul, Michelle; Roch-Lefèvre, Sandrine; Roy, L; Sabatier, L.; Sarchiapone, Lucia; Sebastià, Natividad; Sommer, Sylwester; Sun, Mingzhu; Suto, Yumiko; Terzoudi, G. I.; Trompier, François; Vral, Anne; Wilkins, R. C.; Zafiropoulos, Demetre; Wieser, Albrecht; Woda, Clemens; Wojcik, Andrzej. 2016. RENEB accident simulation exercise. 2017 *International Journal of Radiation Biology* 93 (1): 75-80
10. Mattias Van Heetvelde, Wouter Van Looke, Wim Trypsteen, **Annelot Baert**, Katrien Vanderheyden, Brecht Crombez, Jo Vandesompele, Kim De Leeneer, and Kathleen Claes. 2016. Evaluation of relative quantification of alternatively spliced transcripts using droplet digital PCR. Submitted in *Biochemia Medica*
11. Coppieters, Frauke, Anne Laure Todeschini, Takuro Fujimaki, **Annelot Baert**, Marieke De Bruyne, Caroline Van Cauwenbergh, Hannah Verdin, Miriam Bauwens, Maté Ongenaert, Mineo Kondo, Françoise Meire, Akira Murakami, Reiner A Veitia, Bart Leroy, and Elfride De Baere. 2015. Hidden Genetic Variation in LCA9-associated Congenital Blindness Explained by 5'UTR Mutations and Copy-number Variations of NMNAT1. *Human Mutation* 36 (12): 1188–1196.

SCIENTIFIC
OUTPUT
Conferences

1. Borstkanker: van Onderzoek tot Hoop
Ghent (Belgium), 8/10/2016 (*Attendance*)
2. 42nd Annual Meeting of the European Radiation Research Society
Amsterdam (The Netherlands), 4-9/09/2016
Poster presentation: The use of an optimised RAD51 foci assay to evaluate radiosensitivity and homologous recombination capacity in a BRCA2 knockdown cell line.
3. 15th International Congress of Radiation Research
Kyoto (Japan), 25 – 29/05/2015
Poster presentation: The G2 micronucleus-assay for the analysis of in vitro chromosomal radiosensitivity in individuals carrying a BRCA1 mutation.
4. 15th Annual meeting of the Belgian Society of Human Genetics
Liège (Belgium), 06/03/2015 (*Attendance*)
5. 41st Annual Meeting of the European Radiation Research Society
Rhodes (Greece), 14 – 19/09/2014
Oral presentation: The G2 micronucleus assay for the analysis of in vitro chromosomal radiosensitivity in individuals carrying a BRCA1 or BRCA2 mutation.
6. 5th International Symposium on Hereditary Breast and Ovarium Cancer
Montréal (Canada), 23 – 25/04/2014
Poster presentation: Development of an S-G2 micronucleus assay for the detection of *in vitro* chromosomal radiosensitivity in BRCA1 and BRCA2 mutation carriers.
7. 14th Annual meeting of the Belgian Society of Human Genetics
Antwerp (Belgium), 07/02/2014
Oral presentation: Development of an S-G2 micronucleus assay for the detection of in vitro chromosomal radiosensitivity in BRCA1 and BRCA2 mutation carriers.
8. Science day of the Faculty of Medicine and Health Sciences
Ghent (Belgium), 07/02/2014
Short oral presentation: Development of an S-G2 micronucleus assay for the detection of in vitro chromosomal radiosensitivity in BRCA1 and BRCA2 mutation carriers.
9. 2nd Oncopoint
Ghent (Belgium), 06/02/2014

Short oral presentation: Development of an S-G2 micronucleus assay for the detection of in vitro chromosomal radiosensitivity in *BRCA1* and *BRCA2* mutation carriers.

10. 7th PhD Day of the Department of Basic Medical Sciences
Ghent (Belgium), 05/02/2014

Oral presentation: Development of an S-G2 micronucleus assay for the detection of in vitro chromosomal radiosensitivity in *BRCA1* and *BRCA2* mutation carriers.

11. 10th Annual meeting of the Belgian Society of Human Genetics
Ghent (Belgium), 26/02/2010 (*Attendance*)